Identification and Characterization of Novel Factors that Influence Minisatellite Stability in Stationary Phase Yeast Cells

A Dissertation
SUBMITTED TO THE FACULTY OF
UNIVERSITY OF MINNESOTA
BY

Bonnie Maureen Alver

IN PARTIAL FULFILLMENT OF THE REQUIREMENTS
FOR THE DEGREE OF
DOCTOR OF PHILOSOPHY

Dr. David Kirkpatrick, Advisor

November 2012

Acknowledgements

Unending thanks to my advisor, Dr. David Kirkpatrick, for his continuous guidance, patience, advice and support and for introducing me to the world of Dr. Who.

To the Kirkpatrick lab past and present (and Kelaine Haas), thank you for making the lab a great place to work at and for providing your support these past four years. Thank you to Pete Jauert for being a fantastic teacher, science guru and friend.

Many thanks and praises to my undergraduates, Melissa O'Hehir and Laura Brosnan. You knocked my socks off with your unerring dedication to your projects and your lab technique finesse.

A special thank you to all of the labs at the U of M who helped me with techniques, lent me reagents or allowed me to use equipment. This includes: The Berman Lab, The Bielinsky Lab, The Clarke Lab, The Gale Lab, The Koepp Lab and The Wright Lab.

Finally, I thank my family (Fedors, Oleskows and Alvers). Your love and support has kept me motivated and excited to have chosen a career in science.

Dedication

This thesis is dedicated to Bob Alver. Somehow we made it through grad school together.

Table of Contents

Acknowledgements....i
Dedication....ii
Table of Contents....iii
List of Tables....v
List of Figures....vi

Chapter I: Introduction....1
Chapter II: Genome-Wide Identification of Factors that Influence Minisatellite Stability in Stationary Phase Yeast....19
Chapter Summary....21
Introduction....20
Results....24
Discussion....35
Data Contribution....41
Figures/Tables....43
Chapter III: Novel Checkpoint Pathway Organization Promotes Genome Stability in Stationary Phase Yeast Cells....57
Chapter Summary....58
Introduction....59
Results....62
Discussion....77
Data Contribution....86
Figures/Tables....87
Chapter IV: The Mechanism of Stationary Phase Minisatellite Alteration in Replication Checkpoint Mutants is Dependent upon Recombination and Nucleotide Availability....100
Chapter Summary....101
Introduction....102
Results....104
Discussion....114
Data Contribution....119
Figures/Tables....121

Chapter V: The Influence of Replication Checkpoint Components on the Stability of the Human *HRAS1* Oncogene - associated Minisatellite....129
Chapter Summary....130
Introduction....131
Results....133
Discussion....137
Data Contribution....141
Figures/Tables....142
Chapter VI: Final Discussion....148
Chapter VII: Materials and Methods....169
Chapter VIII: References....197
Chapter IX: Appendices....214
The Effect of DNA Damaging Agents and UV on Stationary Phase Minisatellite Stability....215

List of Tables

Chapter I

Table 1-1: Comparison of Microsatellites and Minisatellites…….....18

Chapter II

Table 2-1: Summary of Hits from the *ade2-min3* SGA Analysis of the Yeast Nonessential and Essential Strain Sets…….....51

Table 2-2: Summary of Hits from the *ade2-h7.5* SGA Analysis of the Yeast Nonessential Strain Set…….....52

Table 2-3: Enriched GO Terms of Hits from the *ade2-min3* SGA Analysis of the Yeast Nonessential and Essential Strain Sets ……...54

Table 2-4: Enriched GO Terms of Hits from the *ade2-min3* SGA Analysis of the Yeast Nonessential and Essential Strain Sets and the *ade2-h7.5* SGA Analysis of the Yeast Nonessential Strain Set……..56

Chapter III

Table 3-1: Blebbing Phenotypes of Checkpoint-Annotated Genes…….....98

Chapter VIII

Table 8-1: Plasmids and Yeast Strains…….....183

Table 8-2: Primers……..192

.

List of Figures

Chapter I

Figure 1-1: A Color Segregation Assay to Detect Minisatellite Instability in Yeast……....15

Chapter II

Figure 2-1: Synthetic Genetic Array (SGA) Analysis to Screen for Minisatellite Instability….....43

Figure 2-2: Summary of Overlapping Hits from the *ade2-min3* and *ade2-h7.5* SGA Screens.....46

Figure 2-3: Specific Mismatch Repair Components Stabilize Minisatellites in Stationary Phase.....48

Chapter III

Figure 3-1: Summary of the Arrangement of Checkpoint-Associated Factors in Mitotic and Stationary Phase Pathways…….....……....87

Figure 3-2: Colony Morphology of Strains Bearing the *ade2-min3* Allele…….....88

Figure 3-3: Several Checkpoint Components Stabilize Minisatellites During Stationary Phase….....89

Figure 3-4: Minisatellite Alterations Occur in Quiescent Cells in Checkpoint Mutants….....91

Figure 3-5: Independent Pathways Regulate Minisatellite Stability During Stationary Phase….....92

Figure 3-6: Blebbing Characteristics Differ Among Strains Bearing the *ade-min3* Allele…….....95

Figure 3-7: Characterization of the Role of Mrc1p in Stationary Phase Cells…….....97

Chapter IV

Figure 4-1: Protein Expression in Quiescent Yeast Cells Bearing the *ade2-min3* Minisatellite Allele…….....…121

Figure 4-2: Minisatellite Tract Alterations in an *mrc1*Δ Strain are Mediated by Homologous Recombination…….....125

Figure 4-3: Minisatellite Alterations in an *mrc1*Δ Strain are Partially Dependent Upon Single Strand Annealing and Non-Homologous End Joining…….....126

Figure 4-4: Nucleotide Pool Availability Affects the Stability of the *ade2-min3* Minisatellite…….....127

Figure 4-5: Summary of Pathways that Mediate Minisatellite Stability in Stationary Phase Yeast…….....128

Chapter V

Figure 5-1: The *ade2-h7.5* Minisatellite Allele…….....142

Figure 5-2: Replication Checkpoint Components are Required for *ade2-h7.5* Minisatellite Stability….....…….....143

Figure 5-3: Summary of the *ade2-h7.5* Tract Alterations Observed in Replication Checkpoint Strains….....…….....144

Figure 5-4: Minisatellite Alterations in an *mrc1*Δ Strain are Mediated by Recombination Factors…….....…147

Chapter VI

Figure 6-1: Model of Minisatellite Tract Alterations in Mitotic and Stationary Phase Cells…….....167

.

Chapter I

Introduction

An Introduction to Non-Dividing Cells

Stationary phase is a state in which cells have exited active growth associated with the cell cycle in response to starvation and have entered into a non-dividing state. This state is reversible upon the creation of favorable environment conditions. Stationary phase has been well studied in the single-celled organism *Escherichia coli* (reviewed in (Rosenberg, 2001)). Despite existing in non-dividing state, stationary phase *E. coli* cells exhibit a high degree of mutability. These mutations, referred to as 'adaptive mutations,' occur in response to environment stress. Double strand break repair featuring recombination and DNA replication polymerase slippage events have been shown to play an active role in driving adaptive mutation (Harris et al., 1994, Harris et al., 1997a). Correspondingly, a decrease in mismatch repair components in *E. coli* stationary phase cells results in an increase in adaptive mutation rates (Harris et al., 1997b). These studies indicate that stationary phase is a survival mechanism that allows cells to adjust to and respond to various environment cues thereby allowing them to escape cell death. Mechanisms associated with *E. coli* stationary phase mutations have enormous implications for genomic mutability within human cells, the majority of which are non-dividing.

Human Quiescent Cells

Human somatic cells and stem cells exist in a state known as G_0 or quiescence. Similar to stationary phase *E. coli* cells, quiescent cells are non-dividing and retain the ability to re-enter the cell cycle. Within the human body, quiescence is important for

maintaining the supply of adult stem cells within stem cell niches (Reya et al., 2001). This allows stem cells to be poised for re-entry into the cell cycle in response to environmental stress such as blood loss or tissue damage (Arai et al., 2004, Abou-Khalil and Brack, 2010).

The preservation of such important cellular populations is essential in preventing permanent damage and disease. However, the regulatory mechanisms associated with quiescent hematopoietic stem cells and neural stem cells are not well understood. Recent studies have suggested that DNA damage and repair pathways have a role in maintaining quiescence. For example, the maintenance of stem cell quiescence is largely promoted by the tumor suppressor gene p53 (Liu et al., 2009a, Liu et al., 2009b). Furthermore, mutations in double strand break repair pathways, such as mismatch repair (MMR) or nucleotide excision repair (NER), have been shown to result in defects in the maintenance of stem cell pools (Kenyon and Gerson, 2007).

Mis-regulation of the quiescent cell state can have a dramatic influence on human disease. Cancer formation in eukaryotic organisms begins with an initial oncogenic event that can result in genome instability occurring within a quiescent cell population. These mutations could promote uncontrolled re-entry into the cell cycle, resulting in tumorigenesis (Kim et al., 2005, Suda et al., 2005, Jin et al., 2009b). At present, little is known about the pathogenic events that allow eukaryotic cells to transition out of a quiescent state and become proliferative. This has primarily been due to the difficulty in studying mutagenic events in a mammalian quiescent cell system.

Stationary Phase in Yeast - a Model for Quiescence

Stationary phase cells of the yeast *Saccharomyces cerevisiae* display several characteristics that recapitulate the phenotypes of quiescent cells found within humans (Werner-Washburne et al., 1993, Gray et al., 2004). Like human quiescent cells, yeast stationary phase cells retain the ability to re-enter the cell cycle and resume active growth when environmental conditions become favorable. Yeast stationary phase cells also share the characteristics of condensed, unreplicated chromosomes, a significant decrease in the overall level of gene expression, and an increase in cellular autophagy. Thus, the more genetically tractable yeast provides an excellent model organism in which to study cells that have exited the cell cycle.

Further investigation into the composition of cultures of yeast stationary phase cells revealed that they consist of slowly dividing (nonquiescent) cells as well as true non-dividing (quiescent) cells (Allen et al., 2006, Aragon et al., 2008). Each subpopulation is defined by a distinct set of traits. Quiescent cells are dense, unbudded and are able to survive for extended periods of time. These cells also contain soluble mRNAs that encode stress response proteins thereby allowing cells to respond to a variety of environmental conditions. Nonquiescent cells are less dense, produce cell buds and become apoptotic or senescent after several days. They also accumulate a high level of reactive oxygen species. These studies highlight the complexity of stationary phase and suggest that additional unidentified factors as well as regulatory mechanisms govern the maintenance of cells that have exited the cell cycle.

Repetitive Elements and Genome Mutability

After the discovery of DNA, the majority of research focused on understanding the concept of the "central dogma." It was believed that the sole purpose of DNA was to encode for RNA which in turn encoded for the expression of protein. Since that time, it was discovered that the human genome is largely composed of non-coding DNA. Once deemed 'useless' or 'parasitic' these non-coding regions were found to consist of tandem repetitive elements (Orgel and Crick, 1980). Categorized by repeat unit size, repetitive elements are comprised of units of sequences that can range from one to hundreds of nucleotides in length (reviewed in (Debrauwere et al., 1997).

Microsatellites (also known as Short Tandem Repeats) are a well-known class of tandem repeats that are composed of units 1 - 14bp in length (Table 1-1) (Tautz and Renz, 1984, Sia et al., 1997). These repeat units are typically composed of non-variable mono-, di- or tri-nucleotide sequences. A second class of tandem repetitive elements is known as a minisatellite. Minisatellites (also known as Variable Number of Tandem Repeats) are classically defined as repetitive tracts of DNA consisting of repeat units that are specifically 15 - 100bp in size (Vergnaud and Denoeud, 2000). Furthermore, the sequences comprising each repeat unit within a minisatellite are often highly variable from unit to unit. The genomic location of each class of tandem repeat differs as well. Microsatellites composed of mono- or di- nucleotide repeats are primarily localized at intergenic regions while those composed of tri-nucleotide repeats are located within or adjacent to coding sequences (Debrauwere et al., 1997). In contrast, minisatellites are found within the sub-telomeric regions of chromosomes (Royle et al., 1988).

Microsatellite instability has long been connected with human disease, the most well studied being those associated with tri-nucleotide repeats. Expansions of tri-nucleotide repeat sequences through replication polymerase slippage results in an increase in microsatellite mutability (Schlotterer and Tautz, 1992, Richards and Sutherland, 1994). The expansion of a microsatellite repeat sequence can directly impact the expression of nearby genes. For example, a CTG microsatellite located at the 3'UTR of the gene *DMPK* (dystrophia myotonica protein kinase) has been shown to give rise to myotonic dystrophy (Brook et al., 1992). Myotonic dystrophy is an RNA gain-of-function disease in which the transcribed *DMPK*/(CUG)n RNA is sequestered within cell nuclei and binds to the splicing protein MBNL1 (muscleblind-like 1) (Davis et al., 1997, Napierala and Krzyzosiak, 1997, Miller et al., 2000). This results in the aberrant splicing of the skeletal muscle gene *ClC-1* (chloride channel 1) and myotonia (Mankodi et al., 2002, Kanadia et al., 2006).

Aberrant mismatch repair also increases microsatellite mutability. Individuals with hereditary non-polyposis colorectal cancer (HNPCC) have an increased risk of cancer due to mutations in the mismatch repair genes *MLH1*, *MSH2*, *MSH6* or *PMS2* (Fishel et al., 1993, Bronner et al., 1994, Nicolaides et al., 1994, Bonadona et al., 2011). Mutations within mismatch repair genes give rise to a high incidence of microsatellite instability (Umar, 2004, Sheng et al., 2006, Geiersbach and Samowitz, 2011). Alterations within microsatellites can affect the expression of neighboring genes, such as those involved in cell proliferation, thereby contributing to the formation of disease (reviewed in (Boland and Goel, 2010)). While the mechanisms associated with microsatellite

instability and disease formation has been well studied, how alterations within minisatellite repetitive tracts impact various human diseases remains to be fully elucidated.

Genomic Functions of Minisatellites and Human Disease

Several clues have shed light on determining the potential association of minisatellite instability and human disease. For example, minisatellites have been shown to serve numerous important biological functions. These functions include regulating gene transcription (Cohen et al., 1987, Spandidos and Holmes, 1987, Krontiris, 1995), interfering with gene splicing (Turri et al., 1995), acting as chromosomal fragile sites (Yu et al., 1997, Lukusa and Fryns, 2008), and influencing chromosomal pairing during meiosis (Chandley, 1989, Ashley, 1994). A well characterized example of minisatellite genomic function is that associated with the *HRAS1* oncogene (Capon et al., 1983). This minisatellite is composed of repeat units that are 28bp in length and vary in C or G content at nucleotides located at +7nt and +15nt. The *HRAS1* minisatellite is located 3' of the *HRAS1* open reading frame and has been shown to act as a binding site for the family of rel/NF-κB transcription factors (Trepicchio and Krontiris, 1992)**.** Similar to the formation of microsatellite-associated HNPCC, altered alleles of the *HRAS1* minisatellite can result in the enhancement of *HRAS1* transcription thereby promoting cell proliferation – a hallmark of cancer (Spandidos and Holmes, 1987, Krontiris, 1995).

In support of this model, rare alleles of the *HRAS1* minisatellite have been correlated with tumors of the lung, bladder, ovaries, and brain and have been isolated

from the primary tumors of breast cancer patients (Devlin et al., 1993, Ding et al., 1999, Rosell et al., 1999, Weitzel et al., 2000, Vega et al., 2001). Rare altered alleles of additional human minisatellites are linked to an increased risk of variety of different types of disease. These include myoclonus epilepsy (Lafreniere et al., 1997, Virtaneva et al., 1997), diabetes mellitus (Kennedy et al., 1995), asthma (Kirkbride et al., 2001), ADHD (Faraone et al., 2001, Yang et al., 2007) and several different forms of cancer (Krontiris, 1995, Calvo et al., 1998, Rosell et al., 1999, Weitzel et al., 2000, Vega et al., 2001). Despite the association between altered minisatellites and disease, little is known about the factors that regulate minisatellite stability or how minisatellites undergo alterations in specific cell populations to become pathogenic alleles.

Known Mechanisms of Minisatellite Alteration

Additional characterization of minisatellites revealed that these repetitive elements are predominantly stable in actively dividing cells yet change in repeat length as well as in composition during meiosis (Jauert et al., 2002, Richard et al., 2008). Further investigation into hypermutable human germline minisatellites showed that the repeat tract alterations consisted of complex inter-allelic rearrangements (Buard and Vergnaud, 1994, Jeffreys et al., 1994). These findings have implicated homologous recombination as the primary mechanism for minisatellite germline mutation. Interestingly, the nature of the tract alterations were highly polar in nature suggesting that surrounding cis-acting elements, or DNA sequences, affected the location of alterations (Armour et al., 1993, Jeffreys et al., 1994, Jeffreys et al., 1998, Vergnaud and Denoeud, 2000). These cis-

acting sequences located within the human germline have since been referred to as recombination hotspots.

Minisatellite alterations within somatic cells occur at a much lower frequency than those within the germline. The majority of somatic tract alterations consist of randomly dispersed deletions or insertions (Jeffreys and Neumann, 1997). Unlike germline mutations, somatic minisatellite alterations are thought to arise from aberrant DNA replication such as those associated with polymerase slippage events. This was supported by studies in which human minisatellites, integrated into the genome of the yeast *S. cerevisiae*, were found to become unstable in mitotic cells bearing mutations in the flap endonuclease *RAD27* or the replication factor *DNA2* (Lopes et al., 2002, Maleki et al., 2002).

As discussed above, the majority of human cells exist in a quiescent state. Mutations that occur within this distinct cellular population can result in the loss of cell growth inhibition resulting in the formation of tumors and cancer progression Due to the correlation between minisatellite instability and cancer, it is tempting to speculate that minisatellite alterations within quiescent cells could contribute to the formation of proliferative cells that give rise to cancer. However, studying minisatellite instability in quiescent cells has been difficult due to the lack of an appropriate assay system.

Detecting Minisatellite Instability in Stationary Phase Cells

Yeast as a Model Organism

Over the past several years, the yeast *S. cerevisiae* has proven to be a formidable model organism in which to investigate minisatellite alterations. Similar to humans, minisatellites in yeast are located at sub-telomeric regions of chromosomes. This is in contrast to mouse and rat models in which minisatellites are primarily localized at interstitial chromosomal sites (reviewed in (Bois, 2003)). A key characteristic of some human germline minisatellites is they are hypermutable. In contrast, minisatellites with a high mutation rate have not been found within the germline of higher order eukaryotic systems such as mice. One explanation for this difference is that minisatellites in humans, unlike mice, are localized next to recombination hotspots which are known to correlate with high rates of repeat instability.

S. cerevisiae utilizes homologous recombination as a primary mechanism for genomic alteration. Our laboratory and others have demonstrated that the integration of a human-derived minisatellite next to recombination hotspots within the yeast genome recapitulates the increased rate of meiotic minisatellite mutation found within human germline cells (Bois and Jeffreys, 1999, Jauert et al., 2002). We demonstrated that, like in human cells, meiotic minisatellite alterations in yeast resulted in tract expansions as well as contractions. Finally, we showed that the minisatellite tract was stable in mitotic cells thereby mimicking the level of minisatellite stability found within human somatic cells. Thus, the genetically tractable yeast provides an excellent model system in which to study the mechanisms that regulate minisatellite stability.

An Assay System for Detecting Minisatellite Alterations in Quiescent Yeast

To understand what factors, specifically gene products, may be involved in maintaining minisatellite stability, we developed a color segregation assay that allows us to directly monitor minisatellite alterations that occur within *S. cerevisiae*. For this assay, we constructed the *ade2-min3* allele in which a minisatellite consisting of three identical 20bp repeat units plus a 5bp linker was inserted into the *Xba*I site of the adenine biosynthesis gene, *ADE2* (Figure 1-1a) (Kelly et al., 2007). Integration of the minisatellite allele within the genome of white haploid cells results in the disruption of the *ADE2* open reading frame rendering cells Ade^- and red in color. This red pigment is produced as a byproduct of the disruption of the adenine biosynthetic pathway (Smirnov et al., 1967). Alterations that occur within the minisatellite, such as the loss of one repeat or the gain of two repeats, can result in the restoration of the *ADE2* open reading frame resulting in Ade^+ cells that are white. The most common alteration that we have detected within the *ade2-min3* allele is the loss of one whole repeat unit. Together, our assay allows us to easily detect minisatellite alterations in yeast by monitoring yeast colonies for a red to white color change (Figure 1-1b).

We previously utilized this assay to take a forward genetics approach to identify factors that when mutated, resulted in minisatellite instability within the *ade2-min3* allele (Kelly et al., 2007). Through this UV mutagenesis screen, we identified a specific class of mutants which gave rise to a novel color segregation phenotype. This phenotype, which we termed 'blebbing,' is characterized by white microcolonies, or papillations, that have formed on the surface of an overall red colony (Figure 1-1b). The blebbing phenotype is in stark contrast to the well-characterized sectoring phenotype in which colonies consist

of alternating red and white pie-shaped wedges. Sectoring is a phenotype associated with tract alterations that have occurred in mitotic cells. Further characterization of blebbing strains revealed that this phenotype was specific to minisatellite alterations that did not occur until cells within the colony had reached stationary phase. These strains did not produce a sectoring phenotype. As discussed above, stationary phase yeast cells mimic several key characteristics associated with human quiescent cells. Thus, we now have an effective assay system that allows us to identify mutations that gave rise to minisatellite alterations in cells that are in a non-proliferative cell state.

Complementation analyses of the mutant strains giving rise to the blebbing phenotype revealed that mutations in the genes *ZRT1* and *ZAP1* resulted in minisatellite instability in stationary phase cells (Kelly et al., 2007). Each gene is involved in maintaining intracellular zinc levels; *ZRT1* encodes for a high-affinity zinc transporter and *ZAP1* encodes for zinc-dependent transcription factor that induces *ZRT1* expression when zinc levels within the cells are low (Zhao and Eide, 1996, Zhao and Eide, 1997). Therefore, we hypothesize that maintaining proper zinc homeostasis within cells is important for preventing minisatellite alterations in stationary phase.

Characterization of a strain bearing a deletion of *ZRT1* revealed the blebbing phenotype was primarily due to the loss of one repeat unit from the minisatellite tract (Kelly et al., 2007). We further demonstrated that these tract alterations were specific to the non-dividing or quiescent subpopulation of stationary phase. Importantly, we showed that the blebbing phenotype was independent of adenine auxotrophy or the chromosomal location of the *ade2-min3* allele. Our results suggest that blebbing is specific to mutations

within trans-acting acting factors, or gene products, rather than potential cis-acting elements that could be within the vicinity of the *ADE2* locus.

Comparison of the repeat tract within the *ade2-min3* allele to those found within human minisatellites reveals striking differences. For example, the *ade2-min3* minisatellite is comprised of identical repeats while human-associated minisatellites are often longer and composed of repeat units variable in sequence (Vergnaud and Denoeud, 2000). Secondly, only approximately 50% of the *ade2-min3* allele consists of C and G nucleotides, while in human minisatellites these bases are greatly enriched (Bois, 2003). To study the stability of a human minisatellite, we constructed a second allele in which a minisatellite composed of seven-and-a-half variable repeats of the *HRAS1*-associated minisatellite was inserted into the *ADE2* gene of *S. cerevisiae* (the *ade2-h7.5* allele) (Figure 1-1c) (Kelly et al., 2011). This minisatellite consists of four different repeat units which vary in C or G content at positions +14nt and +22nt. We previously demonstrated that *ade2-h7.5* alterations occurring within stationary phase cells also give rise to the blebbing phenotype and that the deletion of *ZRT1* or *ZAP1* resulted in strains that produced a high level of blebbing (Kelly et al., 2011). We are therefore able to monitor tract alterations within a human-derived minisatellite in stationary phase cells providing a direct association to human cell minisatellite tract alterations.

As discussed above, a common mechanism for germline minisatellite instability in human cells is that of homologous recombination. Our laboratory has since demonstrated that tract alterations occurring within meiotic yeast cells are also mediated by a recombination based mechanism (Jauert et al., 2002). Because stationary phase tract

alterations consisted of the gain or the loss of whole repeat units, we predicted that minisatellite alterations within stationary phase cells were mediated primarily by homologous recombination (Kelly et al, 2007). Deleting the key recombination factor genes *RAD50*, *RAD51* or *RAD52* in a *zrt1*Δ strain bearing the *ade2-min3* or the *ade2-h7.5* alleles suppressed minisatellite alterations (Chapter 9: Appendices) (Kelly et al., 2011). Therefore, similar to meiotic minisatellite instability, minisatellite alterations occurring in stationary phase cells are dependent upon homologous recombination pathways.

Through our intense characterization of the blebbing phenotype in yeast, we have shown that our assay system allows us to readily identify minisatellite alterations in quiescent cells. Currently, little is known about what factors, besides zinc, stabilize minisatellite alterations within this specific population. To address this issue, the primary goals of the Kirkpatrick laboratory include: identifying and characterizing additional factors that regulate stationary phase minisatellite stability, comparing the factors that stabilize the *ade2-min3* allele to the factors that stabilize the human-associated *ade2-h7.5* allele, and analyzing the mechanisms that mediate stationary phase minisatellite alterations.

For this thesis work, my goal was to identify and characterize additional factors that maintain minisatellite stability in stationary phase yeast cells. In Chapter 2, I begin by introducing a modified version of a whole-genome screen known as the Synthetic Genetic Array analysis (SGA) (Tong et al., 2001, Tong and Boone, 2006, Li et al., 2011) that I performed to screen for mutant strains that produced a high level of stationary phase minisatellite instability. I discuss the significance of the hits obtained from this

screen as well as how the composition of the minisatellite affects the factors that regulate repeat stability. In Chapter 3, I discuss my findings associated with characterizing several hits identified in the SGA screen. These hits included genes that were primarily associated with checkpoint signaling pathways in actively dividing cells. My results show that a specific subset of checkpoint components stabilizes minisatellites in stationary phase and that well-characterized checkpoint pathways established in actively dividing cells are not conserved in stationary phase cells. In Chapter 4, I explore the mechanisms that give rise to minisatellite alterations in stationary phase cells, and in Chapter 5, I establish that several checkpoint components are associated with the stability of the *HRAS1*-derived *ade2-h7.5* allele. Together, my work greatly expands our knowledge of the regulatory mechanisms associated with minisatellites in a quiescent cell system and provides an explanation of how minisatellites can undergo alterations to become potential pathogenic alleles.

Figure 1-1.

A Color Segregation Assay to Detect Minisatellite Stability in Yeast.

(a) The *ade2-min3* Minisatellite Allele**.** A minisatellite consisting of three identical 20bp repeats plus a 5bp linker is inserted into the *Xba*I site of *ADE2* in the yeast *S. cerevisiae*. **(b)** An Assay for Detecting Minisatellite Alterations. Insertion of the *ade2-min3* minisatellite allele disrupts the *ADE2* open reading frame resulting in red cells that are auxotrophic for adenine. The loss of one repeat unit or the gain of two repeat units restores the *ADE2* reading frame. These alterations result in white Ade^{+} cells. Using this assay, we have identified two color-segregation colony phenotypes. Sectoring colonies consist of alternating white and red wedges and is specific to alterations in mitotic cells. The blebbing phenotype consists of white microcolonies on the surface of a red colony and is indicative of minisatellite alterations in stationary phase cells. **(c)** The *HRAS1*-associated *ade2-h7.5* Minisatellite Allele. The *ade2-h7.5* minisatellite allele consists of seven-and-a-half 28bp repeats of the *HRAS1* oncogene - associated minisatellite sequence. Each repeat type (numbered 1-4) differ at positions +14nt and + 22nt with either a C or G. The specific nucleotides at these positions are indicated in the table for each repeat type. The minisatellite as well as flanking sequence unique to the *HRAS1* locus is inserted at the *Xba*I site of *ADE2*, throwing the gene out of frame. Loss of one repeat unit restores the open reading frame.

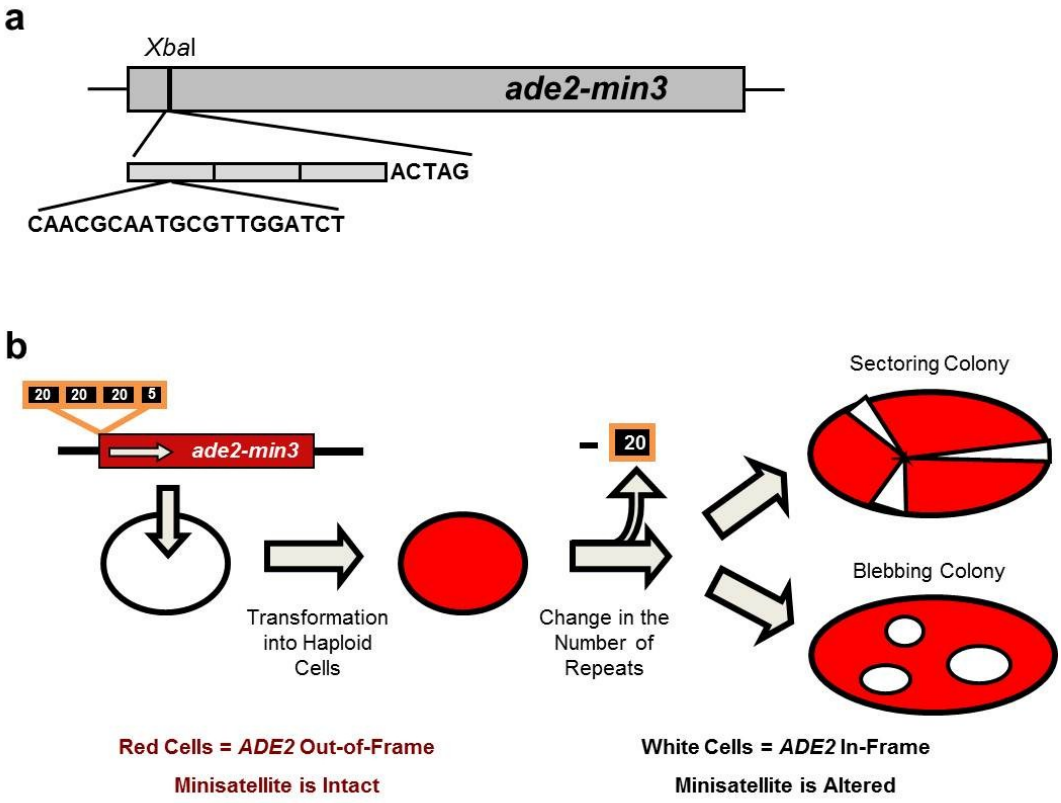

c

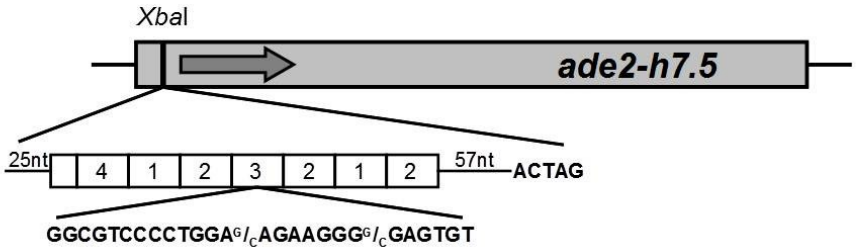

Repeat Type	Base at +14nt	Base at +22nt
1	G	C
2	G	G
3	C	G
4	C	C

Table 1-1. Comparison of Microsatellites and Minisatellites

	Microsatellite	Minisatellite
Repeat Size	1-14bp	15-100bp
Repeat Composition	Non-Variable (mono-, di-, tri-)	Variable
Genomic Location	Intergenic (mono-, di-) Coding Sequence (tri-)	Sub-telomeric
Primary Instability	Mitosis	Meiosis
Mechanisms of Alteration	Polymerase Slippage	Recombination
Associated Diseases	Huntington's Disease, Muscular Dystrophy, Spinocerebellar Ataxia	Cancer, Epilepsy, Diabetes, Cardiovascular Disease, ADHD

Chapter II

Genome-Wide Identification of Factors that Influence Minisatellite Stability in Stationary Phase Yeast

Chapter Summary

The eukaryotic genome is comprised of a variety of repetitive elements. Minisatellites are a type of repetitive element composed of repeat units 15 - 100bp in length. Alterations occurring within minisatellites have been correlated to a variety of diseases; however, little is known about what factors prevent minisatellite alterations from occurring. Previously, our lab developed a unique color segregation assay in which a minisatellite was inserted into the *ADE2* gene in the yeast *Saccharomyces cerevisiae* to monitor alteration events. Minisatellite alterations occurring within stationary phase cells give rise to a specific phenotype referred to as blebbing. Here, we performed a modified version of the Synthetic Genetic Array (SGA) analysis to screen for mutants that produced a blebbing phenotype in strains bearing either a minisatellite consisting of three identical repeats (*ade2-min3* allele) or a minisatellite consisting of variable repeat units (*ade2-h7.5* allele). From our screens, we identified 102 genes that affect the stability of the *ade2-min3* allele and 157 genes that affect *ade2-h7.5* minisatellite stability. Only seven hits overlapped both screens, indicating that different factors regulate repeat stability depending upon the minisatellite size and composition. Importantly, we demonstrate that mismatch repair is associated with the stability of the *ade2-h7.5* allele, indicating that this type of DNA repair stabilizes complex minisatellites in stationary phase cells. Thus, our work adds insight into what novel factors regulate minisatellite stability.

Introduction

Various types of repetitive DNA exist in abundance within eukaryotic genomes. Minisatellites are a specific class of tandem repetitive DNA composed of repeat units that are specifically 15 - 100bp in size and variable in nature (Vergnaud and Denoeud, 2000). Despite being entirely composed of non-coding sequences, minisatellites are associated with several biological functions. For example, minisatellites located at 5' or 3' untranslated regions of genes have been shown to regulate gene expression (Cohen et al., 1987, Spandidos and Holmes, 1987, Krontiris, 1995). Minisatellite alleles located in intronic regions of genes were shown to mediate gene splicing (Turri et al., 1995), and minisatellites at chromosome ends can act as chromosomal fragile sites directly contributing to genomic instability (Yu et al., 1997, Lukusa and Fryns, 2008). Several connections have been established that link altered minisatellite alleles to human disease (Lafreniere et al., 1997, Kennedy et al., 1995, Kirkbride et al., 2001, Krontiris, 1995, Weitzel et al., 2000, Vega et al., 2001). It is currently thought that aberrant function associated with rare minisatellite alleles contributes to the formation of disease. How minisatellites undergo alterations in specific cellular populations and become pathogenic alleles is an ongoing question.

A common mechanism of cancer formation in eukaryotic organisms begins with an initial oncogenic event that can result in mutations that promote uncontrolled re-entry into the cell cycle, resulting in tumorigenesis (Kim et al., 2005, Suda et al., 2005, Jin et al., 2009b). At present, little is known about how these genomic instability events, specifically those related to minisatellite alterations, can occur within non-dividing cells.

We previously developed a color segregation assay that allows us to monitor repeat alterations in stationary phase cells of the yeast *S. cerevisiae* (Kelly et al., 2007, Kelly et al., 2011, Kelly et al., 2012). In brief, we inserted a either a minisatellite consisting of three 20bp repeat units and a 5bp linker (the *ade2-min3* allele) or a minisatellite consisting of seven-and-a-half variable repeats of the *HRAS1*-associated minisatellite (the *ade2-h7.5* allele) into the open reading frame of the gene *ADE2* rendering cells red and Ade^- (Figure 2-1a & b). Minisatellite alterations that have occurred in stationary phase, or quiescent cells, give rise to white Ade^+ microcolonies known as blebs.

Previously, we performed a UV mutagenesis screen to isolate mutants affecting the stability of the *ade2-min3* minisatellite tract. Using this screen, we identified and characterized several mutations in the zinc homeostasis genes *ZRT1* and *ZAP1* which gave rise to a blebbing phenotype (Kelly et al., 2007). We also demonstrated that the deletion of *ZRT1* in a strain bearing the human *HRAS1* minisatellite allele (*ade2-h7.5*) resulted in a blebbing phenotype (Kelly et al., 2011). These results directly linked zinc homeostasis to the maintenance of minisatellite stability during stationary phase

Here, we used a modified version of the Synthetic Genetic Array (SGA) analysis (Tong et al., 2001, Tong and Boone, 2006, Li et al., 2011) in an effort to: 1) determine what factors are involved in regulating minisatellite stability in stationary phase cells and 2) determine if minisatellites varying in repeat composition and size are regulated by different factors in stationary phase cells. We performed two independent SGA analyses which utilized a query strain containing either the *ade2-min3* or the *ade2-h7.5* minisatellite allele. We identified 102 candidate genes in the *ade2-min3* screen and 157

genes in the *ade2-h7.5* screen that are involved in minisatellite stability in stationary phase cells. Only seven hits were identified in both SGA analyses indicating that minisatellites are largely regulated by different factors depending upon the repeat composition and size of the minisatellite. These included the dubious open reading frames *BUD28* (Ni and Snyder, 2001) and YGL217C, the uncharacterized gene YLR125W, the vacuolar transport gene *MON1* (Meiling-Wesse et al., 2002) and the previously characterized zinc-transport genes *COT1*, *ZAP1* and *ZRT1* (Kelly et al., 2007, Kelly et al., 2011). We hypothesize that proper regulation of zinc levels within the cells is important for preventing genomic instability regardless of minisatellite composition.

One of the blebbing hits detected in our *ade2-h7.5* screen was a deletion of the mismatch repair gene *PMS1* (reviewed (Marti et al., 2002)). Further characterization of several nonessential mismatch repair mutants revealed that *MLH1*, *MSH2* and *MSH6* are also involved in maintaining the stability of the *ade2-h7.5* allele in stationary phase. Thus, our work directly implicates mismatch repair in preventing minisatellite alterations from occurring within the *HRAS1* minisatellite in a stationary phase cell population, but not the *ade2-min3* minisatellite which does not exhibit sequence variation. Together, our data suggest new characteristics to add to the definition of what defines a minisatellite and lends support to the idea that factors that regulate minisatellite stability largely depend upon the composition of the minisatellite itself.

Results

Genome-wide Identification of Factors Required for Maintaining ade2-min3 *Minisatellite Stability in Stationary Phase Cells*

We previously reported a unique color segregation assay that allows us to monitor minisatellite instability occurring within the yeast *S. cerevisiae* (Kelly et al., 2007, Kelly et al., 2011, Kelly et al., 2012). This assay employs the *ade2-min3* allele, which consists of a minisatellite featuring three identical 20bp repeat units inserted into the gene *ADE2* (Figure 2-1a). Stationary phase minisatellite alterations can be monitored by detecting colonies for the presence of a blebbing phenotype.

Since our initial UV screen was not saturating, we took a whole-genome approach to identify additional factors involved in regulating minisatellite stability in stationary phase cells. We performed a modified version of the SGA analysis to screen for mutants that produced a blebbing phenotype (Figure 2-1c) (Tong et al., 2001, Tong and Boone, 2006, Li et al., 2011). For this assay, we mated a query strain containing the *ade2-min3* allele to the entire yeast nonessential deletion haploid set or a haploid set of strains bearing temperature-sensitive (ts) alleles of essential genes. Double mutants containing the minisatellite were isolated and assessed for a blebbing phenotype on a qualitative scale of + (low level of blebbing) to ++++ (high level of blebbing) (Figure 2-1d). The high level of blebbing (++++) was equivalent to that of our positive control, *zrt1*Δ (Kelly et al., 2007, Kelly et al., 2011). Hits were characterized as mutations that produced a level of blebbing ranked as +++ to ++++ for at least two out of the three independent screens that were performed.

Through our screen, we identified 102 candidate genes that, when mutated, resulted in a strong blebbing phenotype (Table 2-1). These included the zinc homeostasis genes *ZRT1* and *ZAP1* identified in our original UV mutagenesis screen (Kelly et al., 2007), thus demonstrating that our SGA analysis was working correctly and also reiterating the importance of maintaining zinc homeostasis in stationary phase cells. Also included were the genes *PKC1*, an essential gene that encodes for a serine/threonine kinase that regulates cell wall modifications (Levin et al., 1990), and *RAD27*, which encodes for a nuclease that processes Okazaki fragments (reviewed in (Liu et al., 2004b)). Both genes were previously shown by our lab to be important for maintaining minisatellite stability in stationary phase cells (Kelly et al., 2012).

To determine if any enriched gene ontology (GO) terms were represented within the 102 candidate hits, we performed GO Term analysis using the following databases: Generic Gene Ontology Term Finder (http://go.princeton.edu/cgi-bin/GOTermFinder), Funcassociate 2.0 (http://llama.mshri.on.ca/func associate _client/html/), Fun Spec (http://funspec.med.utoronto. ca/), Profiling of Complex Functionality (ProfCom) (http://webclu.bio.wzw. tum.de/profcom/) and Database for Annotation, Visualization and Integrated Discovery v6.7 (DAVID) (http://david.abcc. ncifcrf. gov/). Enriched GO terms were characterized as those that were represented in at least three out of the five databases. We find that genes associated with GO terms representing chromosomal maintenance, intracellular protein transport and DNA replication are overrepresented within our list of 102 hits (Table 2-3). Based upon this result, we conclude that these

cellular processes are important for regulating the stability of the *ade2-min3* minisatellite allele in stationary phase yeast cells.

Of note were three hits from the *ade2-min3* SGA analyses that were represented in both the nonessential and the essential mutant strain sets. These hits included the stress response kinase gene *DBF2* (Johnston and Thomas, 1982), the checkpoint gene *SLI15* (Ruchaud et al., 2007)and the SNARE complex gene *SEC22* (Liu and Barlowe, 2002). Deletion of *DBF2* and *SLI15* in the nonessential strain set resulted in strains that produced a low level of blebbing. However, ts alleles of both strains were identified as hits in our screen. Our results suggest that aberrant alleles of either gene are more detrimental to minisatellite stability than complete loss of the gene itself. We found the opposite effect for the gene *SEC22*, which was identified as a hit when deleted but not as a ts allele. Therefore, variations in gene product expression appear to differentially affect *ade2-min3* minisatellite stability.

Of the 102 genes identified in our screen, only three produced a high level of blebbing (++++) for at least two out of the three independent analyses that were performed (Table 2-1). These included the zinc transporter gene *ZRT1* (Zhao and Eide, 1996), the mitochondrial transport gene *ODC1* (Palmieri et al., 2001) and *SAC1*, a gene encoding for a lipid phosphatase involved in protein trafficking and cell wall maintenance (reviewed in (Strahl and Thorner, 2007)). Based on our results, we predict that aberrant cellular trafficking, such as that involved in regulating intracellular protein and zinc levels, drastically affects the stability of a minisatellite allele in stationary phase yeast cells.

Identification of Factors that Maintain the Stability of the ade2-h7.5 HRAS1 - *associated Minisatellite Allele in Stationary Phase Yeast Cells*

While the *ade2-min3* allele allows us to readily assess mutant strains for minisatellite instability, the tandem repeats comprising the minisatellite do not mimic those found within human cells. For example, most human minisatellites are significantly enriched for GC content whereas only 50% of the *ade2-min3* minisatellite is comprised of GC bases (Vergnaud and Denoeud, 2000). Human minisatellites are also composed of long repeat units that are variable in sequence composition. Because of these differences, human minisatellites may be regulated by different factors than those associated with the *ade2-min3* allele - a short minisatellite consisting of identical repeat units.

Previously, we demonstrated that our reporter assay system can be used to monitor the stability of a complex minisatellite associated with the human *HRAS1* oncogene (Kelly et al., 2007, Kelly et al., 2011). The assay incorporates a portion of the *HRAS1* minisatellite into the *ADE2* gene resulting in the *ade2-h7.5* allele (Figure 2-1b). This minisatellite is composed of 7.5 repeat units that are 28bp in size and variable in GC content at positions +14nt and +22nt (Capon et al., 1983). Similar to the *ade2-min3* assay system, insertion of the intact minisatellite disrupts the *ADE2* open reading frame which renders cells red in color and auxotrophic for adenine. Minisatellite alterations can restore the correct reading frame generating white Ade^+ cells. Alterations occurring in stationary phase cells are monitored by assessing colonies for the presence of a blebbing color segregation phenotype.

To identify the factors involved in regulating the stability of a complex human-associated minisatellite during stationary phase, we employed the same SGA methodology described above, screening the strain set three independent times. For this analysis, we mated a query strain bearing the *ade2-h7.5* allele to the yeast nonessential deletion haploid set and assessed the resulting double mutants for a blebbing phenotype. Hits were characterized as mutations that resulted in a level of blebbing ranked as +++ to ++++ on a scale of + to ++++. A caveat to using the *ade2-h7.5* allele as a query strain for this screen is that the overall level of blebbing associated with this allele is approximately 4-fold lower than that produced by *ade2-min3* strains (Kelly et al., 2011), thus making phenotypic scoring more difficult.

Using this analysis, we identified 157 candidate hits that result in high level of blebbing when mutated (Table 2-2). To determine if any enriched GO terms were represented in this set of hits, we performed GO term analysis as described above. Intriguingly, no enriched GO terms were associated with this data set. However, a large number of uncharacterized open reading frames were included in this set of hits which could skew the results of our GO term analysis. A lack of significant GO terms representing the hits from the screen could also be due to the possibility that many cellular processes and components rather than a distinct set are involved in regulating the stability of the *ade2-h7.5* minisatellite allele in stationary phase yeast cells.

Within this particular set of 157 hits, we found that four mutant strains maintained a very high level of blebbing throughout our *ade2-h7.5* SGA analyses (++++ for at least two out of the three screens performed) (Table 2-2). These hits included the previously

characterized zinc transporter genes *ZRT1* and *ZAP1* (Zhao and Eide, 1996, Zhao and Eide, 1997, Kelly et al., 2007, Kelly et al., 2011). Also included was the uncharacterized gene encoded by the open reading frame YHR022C and the mismatch repair associated gene, *PMS1* (Prolla et al., 1994a, Prolla et al., 1994b). We conclude that maintaining proper cellular zinc homeostasis is also important in preventing *ade2-h7.5* minisatellite instability in stationary phase cells and that mismatch repair is involved in regulating minisatellite stability within this population of cells.

Analysis of Factors Involved in Maintaining the Stability of Both the ade2-min3 *and* ade2-h7.5 *Minisatellite Alleles in Stationary Phase Cells*

Interestingly, only seven genes were identified as hits in both the *ade2-min3* and *ade2-h7.5* SGA screens (Figure 2-2a). These included the genes *BUD28*, *COT1*, *MON1*, YGL217C, YLR125W, *ZAP1* and *ZRT1*. *BUB28* and YGL217C are both dubious open reading frames that are unlikely to code for a protein. Each open reading frame, however, overlaps the coding sequence of a nearby characterized gene. *BUD28* overlaps 98% of the ribosomal subunit gene *RPL22A* (Planta and Mager, 1998) while YGL217C overlaps only approximately 10% of *KIP3*, a gene that encodes for a kinesin-like protein involved in mitotic spindle positioning (Cottingham and Hoyt, 1997). *RPL22A* was identified as a hit in our *ade2-min3* SGA screen but not in the *ade2-h7.5* screen. Nevertheless, it is possible that this gene was not identified in the *ade2-h7.5* screen due to the difficulty in scoring each strain. Deletion of the open reading frame YGL217C is represented twice in the nonessential deletion haploid set; one deletion strain was identified as a hit in both

screens and the second was not. No other hits were duplicated within our strain sets. PCR analysis revealed that both of the YGL217C isolates from the strain collection and our SGA analyses are correct deletion mutants. Therefore, one or both isolates could contain a secondary mutation that enhances or suppresses the blebbing phenotype.

PCR analysis of the YLR125W deletion mutant from the nonessential haploid strain set as well as of the *ade2-min3* YLR125W mutant from the final step of the SGA analysis revealed that each strain was wild-type at the YLR125W locus. As both strains are $G418^R$, we predict that the *KANMX* PCR product used to construct the deletion collection parental strain is located elsewhere in the genome, likely at an area of homology to the YLR125W locus. Future analysis to determine the genomic location of the deletion will give insight into the source of blebbing observed in this strain.

The remaining genes overlapping each data set are associated with intracellular transport. Included is the vacuolar transport gene *MON1* and the zinc-mediating vacuolar transport gene *COT1* (Conklin et al., 1992, MacDiarmid et al., 2000, Meiling-Wesse et al., 2002, Wang et al., 2002). The final two overlapping hits are the zinc homeostasis genes *ZAP1* and *ZRT1* (Zhao and Eide, 1996, Zhao and Eide, 1997) that were previously shown by our lab to be important in minisatellite stability (Kelly et al., 2007, Kelly et al., 2011). From this data, we conclude that the disruption of cellular transport within stationary phase cells, particularly that associated with zinc transport, results in the destabilization of a minisatellite regardless of tract length or repeat unit sequence composition.

To determine if any sets of genes were overrepresented in both the *ade2-min3* and *ade2-h7.5* hit lists, we performed GO term analyses on the combined results of each screen. Predictably, only seven general GO terms were associated with this set of hits (Table 2-4). These included chromosome, centromeric region (GO:0000775), condensed chromosome kinetochore (GO:0000777), endosome (GO:0005768), kinetochore (GO:0000776), leading strand elongation (GO:0006272), plasma membrane (GO:0005886) and spindle (GO:0005819). Each term is associated primarily with genes identified in the *ade2-min3* screen rather than those of the *ade2-h7.5* screen. Based upon the low number of overlapping hits between each screen and the results from our GO term analysis, we conclude that each minisatellite allele is regulated by a distinct set of genes that do not share many overlapping functions or processes.

To verify the results of the SGA analysis and characterize the genes involved in regulating both minisatellites, we deleted each gene in our well-characterized *ade2-min3* (DTK271) and *ade2-7.5* (DTK1188) strain backgrounds and assessed the resulting mutants for a blebbing phenotype (Kelly et al., 2007, Kelly et al., 2011). The level of blebbing was quantified for each mutant by plating individual strains onto enriched media and allowing colonies to grow into stationary phase. We then counted the number of blebs on the surface of 100 colonies for each strain. The level of blebbing was considered to be significantly different when compared to the wild-type parental strain if the 95% confidence intervals of the mean did not overlap.

We previously analyzed the effect of a *COT1* deletion on the stability of the *ade2-min3* minisatellite in the DTK271 strain background and did not find a significant

increase in the level of blebbing compared to the wild-type (WT) parental strain (Kelly et al., 2007). However, this conclusion was drawn after only four days of colony growth at room temperature. We have since found that this does not provide enough time to capture additional events that might occur at later timepoints in stationary phase. Here, we revisit the level of blebbing of each strain using a modified quantification assay in which blebs are counted after six days at room temperature.

As previously reported, deletion of *ZAP1* and *ZRT1* in both *ade2-min3* and *ade2-h7.5* strain backgrounds resulted in a high level of blebbing compared to the WT parental strains (Figure 2-2b and 2-2c) (Kelly et al., 2007, Kelly et al., 2011). However, unlike the results from the SGA analyses, strains bearing a deletion of *COT1*, *MON1* or *BUD28* (*RPL22A*) did not result in a dramatic increase in blebbing in either strain background. The deletion of *COT1* (DTK1082), *MON1* (DTK1699) or *RPL22A* (DTK1991) in a strain bearing the *ade2-min3* allele produced a level of blebbing that, while significantly greater than that of the WT strain (DTK271), was only 30% of that displayed by the *zrt1*Δ (DTK878) strain (DTK1082 at 8.8 blebs/colony; DTK1699 at 9.7 blebs/colony; DTK1991 at 6.7 blebs/colony vs. DTK271 at 4.7 blebs/colony and DTK878 at 24.5 blebs/colony). An *ade2-h7.5* strain bearing a deletion of *COT1* (DTK1973), *MON1* (DTK1990) or *RPL22A* (DTK1992) did not produce a significant increase in blebbing compared to the WT strain (DTK1188) (DTK1973 at 2.6 blebs/colony; DTK1990 at 2.6 blebs/colony; DTK1992 at 0.3 blebs/colony vs. DTK1188 at 2.0 blebs/colony). We suspect that these results could be due to a secondary mutation in the SGA strain

background or the DTK271/DTK1188 strain background which could act as an enhancer or a suppressor of the blebbing phenotype.

Mismatch Repair Regulates ade2-h7.5 *Minisatellite Stability in Stationary Phase Cells*

Previous work in mitotic cells has suggested that mismatch repair is associated with preventing microsatellite rather than minisatellite alterations (Sia et al., 1997). From our screen however, we discovered that the deletion of *PMS1* in a strain bearing the *ade2-h7.5* minisatellite allele resulted in a strong blebbing phenotype, indicating a potential role for mismatch repair in stationary phase cells (Table 2-2). *PMS1* encodes for a mismatch repair protein that, together with Mlh1p, repairs multiple forms of damaged DNA (Prolla et al., 1994a, Prolla et al., 1994b). To verify the results of our screen, we deleted *PMS1* in the DTK1188 strain background (Kelly et al., 2011) and quantified the average number of blebs/colony. Deletion of *PMS1* (DTK1902) confirmed the results from the SGA analysis as DTK1902 produced a significantly higher level of blebbing (13.4 blebs/colony) compared to the wild-type strain (DTK1188; 2.0 blebs/colony) (Figure 2-3a).

To determine if other well-characterized mismatch repair genes (genes reviewed (Marti et al., 2002)), were involved in maintaining stationary phase minisatellite stability, we quantified the level of blebbing in several mismatch repair mutant strains bearing the *ade2-h7.5* allele (Figure 2-3a). Strains bearing a deletion of *MLH1* (DTK1900; 10.0 blebs/colony), *MSH2* (DTK1903; 13.8 blebs/colony) and *MSH6* (DTK1907; 14.1 blebs/colony) produced notably higher levels of blebbing compared to the WT strain.

Deletion of *EXO1*, *MLH2*, *MLH3* or *MSH3* did not result in a level of blebbing significantly different from that of the WT strain. Together our results indicate that a specific subset of mismatch repair genes is involved in minisatellite stability. Our results further demonstrate that mismatch repair has a role in maintaining minisatellite stability, specifically that of the *HRAS1*- associated minisatellite, in stationary phase.

Finally, we examined the tract alterations occurring with the *ade2-h7.5* allele of the *MLH1*, *PMS1*, *MSH2* and *MSH6* mutant strains. We performed whole-cell PCR across the minisatellite of at least 100 independent blebs per strain. The majority of minisatellite alterations for each mutant consisted of a tract contraction in which one repeat unit was lost (DTK1900 (*mlh1*Δ) = 112/121, 93%; DTK1902 (*pms1*Δ) = 116/121, 95%; DTK1903 (*msh2*Δ) = 119/121, 98%; DTK1907 (*msh6*Δ) = 107/113, 95%). We also observed a loss of four repeat units in all strains except the *MSH2* deletion mutant (DTK1900 (*mlh1*Δ) = 6/121, 5%; DTK1902 (*pms1*Δ) = 3/121, 3%; DTK1907 (*msh6*Δ) = 5/113, 4%). An allele expansion of two repeat units was the only tract expansion observed and was specific to the deletion of *PMS1* (1/121, 1%). The remaining alleles for each strain did not show any change in tract length size suggesting that the minisatellite alteration was due to the loss of a single nucleotide (DTK1900 (*mlh1*Δ) = 3/121, 2%; DTK1902 (*pms1*Δ) = 1/121, 1%; DTK1903 (*msh2*Δ) = 2/121, 2%; DTK1907 (*msh6*Δ) = 1/113, 1%).

To characterize the alterations occurring within the *HRAS1* minisatellite, we sequenced the minisatellite tract of 20 individual blebs for the four mismatch repair mutants discussed above (Figure 2-3b). The majority of repeat losses observed in each

strain occurred within the center of the minisatellite specifically, at the fourth or fifth repeat unit. Interestingly, deletion of *PMS1* resulted in tract alterations that were not observed within the other strains. These included the loss of a single nucleotide within the fourth repeat and a gene conversion event at the second repeat. Together, our work demonstrates the importance of mismatch repair in regulating *ade2-h7.5* minisatellite stability as well as characterizes the types of tract alterations associated with the mutations of specific mismatch repair components.

Discussion

For this chapter, we performed a modified version of the SGA analysis (Tong et al., 2001, Tong and Boone, 2006, Li et al., 2011) to identify genes involved in maintaining minisatellite stability in stationary phase cells. We performed two individual screens; the first screen utilized a query strain bearing a minisatellite consisting of three identical 20bp repeats (*ade2-min3* allele) (Kelly et al., 2007, Kelly et al., 2011, Kelly et al., 2012) while the second screen utilized a query strain containing a minisatellite consisting of seven-and-a-half 28bp repeats of the *HRAS1*-associated minisatellite allele (*ade2-h7.5* allele) (Kelly et al., 2007, Kelly et al., 2011). Each screen incorporated analysis of approximately 4,800 nonessential genes with an additional 450 essential genes screened using the *ade2-min3* allele. Using this approach, we discovered 102 genes that are involved in regulating the stability of the *ade2-min3* minisatellite and 157 genes that regulate the stability of the *ade2-h7.5* minisatellite in stationary phase cells. Only seven hits overlapped both screens. Finally, we demonstrated that mismatch repair genes

regulate *ade2-h7.5* minisatellite stability indicating that DNA repair mechanisms are active in stationary phase cells.

We investigated the hits of each screen independently to characterize candidate genes associated with each individual minisatellite. GO term analysis of the 102 hits from the *ade2-min3* screen revealed that the majority of enriched GO terms were associated with chromosomal regulation and DNA replication. We were surprised to find such strong evidence of DNA replication in stationary phase cells since bulk DNA synthesis does not take place within this population. However, previous work has shown that discrete areas of DNA replication do occur, possibly at regions of localized DNA repair (de Morgan et al., 2010). Therefore, our results suggest that DNA replication is involved in preventing minisatellite alterations in stationary phase, potentially at sites of genomic repair.

In support of this hypothesis, several hits identified in the *ade2-min3* screen were genes associated with DNA replication and repair. These included *POL31*, a subunit of Polδ (Sugimoto et al., 1995, Giot et al., 1997, Hashimoto et al., 1998) and the Polε subunits *DPB3* or *DPB4* (Araki et al., 1991, Araki, 1994, Lou et al., 2008) (Table 1-3). Also included were the *RFC2* and *RFC4* subunits of Replication Factor C (RF-C) (Noskov et al., 1994, Cullmann et al., 1995, Yao et al., 2003). RF-C is a clamp loader of the proliferating cell nuclear antigen (PCNA), a sliding clamp for Polδ and Polε (Chilkova et al., 2007). Both Polδ and Polε have been implicated in DNA repair mechanisms. Polδ has been shown to be involved in base excision repair (Blank et al., 1994), repair of UV-damaged DNA (Torres-Ramos et al., 1997) and template switching

after DNA damage occurs (Vanoli et al., 2010). Polε has been implicated in nucleotide excision repair (Shivji et al., 1995), base excision repair (Wang et al., 1993) and double strand break repair (Holmes and Haber, 1999).

Additional replication and repair genes identified in our screen included the sumo-ligase gene *MMS21* (Prakash and Prakash, 1977, Montelone and Koelliker, 1995) and *RAD27*, a flap endonuclease involved in base excision repair and double strand break repair (Wu et al., 1999, Tseng and Tomkinson, 2004). Our lab as well as others has previously implicated *RAD27* in minisatellite stability (Lopes et al., 2002, Kelly et al., 2012). Together, our data suggest that components of DNA replication and repair mechanisms prevent *ade2-min3* minisatellite alterations in stationary phase cells.

GO term analysis of candidate hits from the *ade2-h7.5* SGA analysis did not produce any overrepresented GO term attributes. This finding could be a consequence of factors that regulate the stability of the *ade2-h7.5* minisatellite representing a wide range of cellular functions, or that the inherent low level of blebbing associated with the *ade2-h7.5* allele (Kelly et al., 2011) complicated the accuracy of scoring this screen. A third possibility is that the high number of uncharacterized open reading frames identified as hits could have compromised any clearly defined enriched GO term from being detected in this data set. It would be of interest to determine if any of these uncharacterized open reading frames are expressed predominantly in stationary phase cells, which could help clarify why many of these genes were identified in our screen.

Interestingly, only seven gene hits overlapped between the *ade2-min3* and *ade2-h7.5* screens (Figure 2-2a). These included *BUD28*, *COT1*, *MON1*, YGL217C,

YLR125W, *ZAP1* and *ZRT1*. The genes *ZRT1* and *ZAP1* were previously characterized by our lab as having a role in minisatellite stability (Kelly et al., 2007, Kelly et al., 2011). To verify the results of our screens, we constructed mutant strains of the overlapping hits in the DTK271 (*ade2-min3*) or DTK1188 (*ade2-h7.5*) strain backgrounds (Figure 2-2b and 2-2c) (Kelly et al., 2007, Kelly et al., 2011). Our results revealed that, like the SGA analyses, deletion of *ZRT1* or *ZAP1* in the DTK271 or DTK1188 strain backgrounds resulted in a dramatic increase in minisatellite instability in both the *ade2-min3* and *ade2-h7.5* alleles. Deletion of *COT1*, *MON1* or *RPL22A* (*BUD28*) however, resulted in only a moderate increase in *ade2-min3* instability. The deletion of each of these genes did not result in a significant increase in *ade2-h7.5* instability. We predict that differences in strain backgrounds, such as the presence of a secondary enhancer or suppressor mutation, affects the level of minisatellite stability.

With the discovery that very few factors regulate the *ade2-min3* and *ade2-h7.5* minisatellite, our work suggests that the actual differences in the make-up of the minisatellite govern repeat tract stability and alteration. This is further supported by the differences in GO term analysis results between the *ade2-min3* and the *ade2-h7.5* screens. Our laboratory, as well as others, has previously shown that tract length and sequence variability within a minisatellite allele can greatly affect repeat stability (Denoeud et al., 2003, Jauert and Kirkpatrick, 2005, Legendre et al., 2007). Our current study supports these findings and suggests that the composition and size of the minisatellite affect which cellular components and mechanisms govern tract stability.

Therefore, our work provides a mechanistic explanation for the tract alteration variability observed in previous minisatellite experiments.

Surprisingly, a strong candidate hit identified in the *ade2-h7.5* screen was the mismatch repair gene *PMS1* (Prolla et al., 1994a, Prolla et al., 1994b). Blebbing quantification of a *PMS1* deletion mutation in our DTK1188 strain background confirmed the results of our SGA analysis (Figure 2-3a). Until now, microsatellites, not minisatellites have been characterized by their association with components of the mismatch repair system (Strand et al., 1993, Strand et al., 1995, Johnson et al., 1996). Work comparing the rate of tract alterations of microsatellites and a minisatellite in yeast demonstrated that minisatellite instability was not significantly affected by mutations in mismatch repair mutant strains (Sia et al., 1997). However, the minisatellite tract utilized in this previous study was identical to that used to construct our *ade2-min3* allele, and the assay was performed in actively dividing cells. Our work has revealed that deletion of *PMS1* affects the stability of the *ade2-h7.5* minisatellite allele rather than the *ade2-min3* allele. Thus, as discussed above, the composition of a minisatellite may dictate which factors are involved with preventing tract alterations within stationary phase cells.

Interestingly, the depletion of mismatch repair components in stationary phase cells of *Escherichia coli* has been shown to result in enhanced genomic mutations, presumably as a mechanism of adaptation (Longerich et al., 1995, Harris et al., 1997b). Because the deletion of *PMS1* resulted in an enhanced blebbing phenotype indicating stationary phase specificity, we quantified the level of blebbing in strains bearing the *ade2-h7.5* minisatellite as well as a deletion of other well characterized nonessential

mismatch repair genes *EXO1*, *MLH1*, *MLH2*, *MLH3*, *MSH2*, *MSH3* or *MSH6* (Figure 2-3a) (genes reviewed (Marti et al., 2002)). These genes and mechanisms are highly conserved in humans (reviewed in (Harfe and Jinks-Robertson, 2000)). Our results indicate that a specific subset of mismatch repair genes are involved in stationary phase minisatellite stability and includes the genes *PMS1*, *MLH1*, *MSH2* and *MSH6*.

Previous work demonstrated that mutating the mismatch repair genes *MLH1*, *MSH2* or *PMS1* resulted in a high degree of microsatellite instability, while mutating *MSH3* or *MSH6* had a less drastic effect (Strand et al., 1993, Strand et al., 1995, Johnson et al., 1996, Sia et al., 1997). This and other work suggested that yeast contain two mismatch repair complexes; the first complex contains *MLH1*, *MSH2*, *PMS1* and *MSH6* while the second incorporates *MLH1*, *MSH2*, *PMS1* and *MSH3* and (Johnson et al., 1996, Marsischky et al., 1996). Each complex has been implicated in the repair of different substrates; Msh2p together with Msh6p recognizes base:base mismatches as well as small loops generated by insertion or deletion mispairing (Alani, 1996, Marsischky et al., 1996) while Msh2p/Msh3p primarily targets large loops (Habraken et al., 1996, Marsischky et al., 1996). Based upon our data, we predict that the Mlh1p, Msh2p, Msh6p and Pms1p complex prevents the instability of the *ade2-h7.5* minisatellite by targeting and repairing mismatches associated with polymerase slippage. Misalignment of repeat units can occur due to the high degree of similarity between each unit (Figure 2-1b). Future pathway analysis utilizing the strains discussed above will help to dissect the relationships between each of the mismatch repair genes.

In summation, we have conducted the first whole-genome screen to identify factors that regulate minisatellite stability in stationary phase cells. Through our work we have discovered several pieces of data that shed light on how minisatellite alterations could occur within a stationary phase population. This includes the finding that disruption of DNA replication and repair components result in a dramatic increase in minisatellite instability. Finally, we found evidence establishing that factors involved in regulating minisatellite stability are affected by minisatellite repeat length and sequence. Thus, our work lends support to the argument that the composition of the repeat tract within a minisatellite greatly affects minisatellite stability and regulatory mechanisms.

Data Contribution

We are grateful to Dr. Robin Wright and Dr. Charlie Boone for the nonessential and essential yeast haploid strain sets, respectively. We thank Dr. Duncan Clarke for the plasmid pDC369 and the yeast strains DCY2556 and DCY2557.

We thank Dr. Katy Kelly for constructing the strains DTK271, DTK878, DTK902 and DTK1082. The strain DTK1188 was constructed by Dr. Katy Kelly and Laura Brosnan. The query strains used for the *ade2-min3* SGA screen were constructed by Pete Jauert. We are grateful to Pete Jauert and Laura Brosnan for performing the *ade2-h7.5* SGA analysis. We thank Melissa O'Hehir for constructing and performing bleb quantification on the strains DTK1699, DTK1973 and DTK1975. Analysis of the *ade2-h7.5* minisatellite tract (PCR and sequencing) was a joint effort with Melissa O'Hehir.

The construction of each SGA hit list and the comparison of the results from each screen were performed in cooperation with Pete Jauert and Benjamin VanderSluis.

Figure 2-1.

Synthetic Genetic Array (SGA) Analysis to Screen for Minisatellite Instability.

(a) The *ade2-min3* allele consists of three identical 20bp repeats plus one additional base pair inserted into the *Xba*I site of *ADE2* resulting in a 5bp overhang. Insertion of the minisatellite disrupts the *ADE2* open reading frame. A gain of two repeats or loss of one repeat restores the *ADE2* reading frame. **(b)** The *ade2-h7.5* allele contains seven-and-a-half 28bp repeats that differ at positions +14nt and + 22nt with a C or a G as well as flanking sequence unique to the *HRAS1* locus. The minisatellite is inserted at the *Xba*I site of *ADE2* and shifts the gene out of frame. Loss of a repeat restores the open reading frame. **(c)** Summary of the modified SGA screen. A query strain bearing the *ade2-min3* or *ade2-h7.5* allele was mated to the entire *S. cerevisiae* non-essential deletion collection or the essential strain collection containing temperature sensitive mutant alleles. At different steps, strains were pinned to various selective media to isolate the desired mutant strains. Final haploid strains bearing the minisatellite allele plus a deletion mutation or ts allele were assessed for a blebbing phenotype. **(d)** Each screen was performed using a 96-well format. Strains on plates from the final double mutant selection step were scored for a blebbing phenotype on a qualitative scale of + to ++++ (++++ = level of blebbing produced by the zrt1Δ positive control).

a

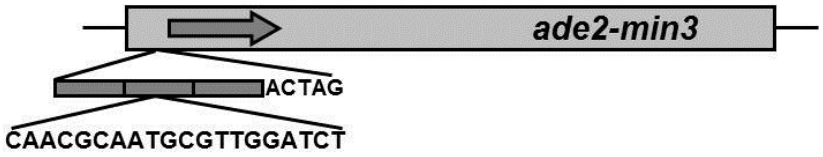
ade2-min3
ACTAG
CAACGCAATGCGTTGGATCT

b

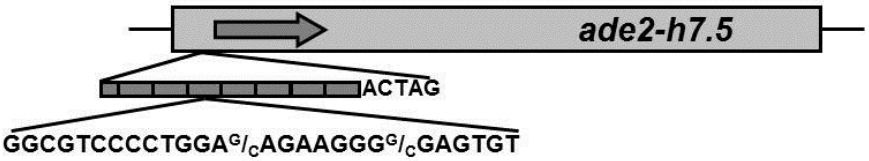
ade2-h7.5
ACTAG
GGCGTCCCCTGGA G/C AGAAGGG G/C GAGTGT

c

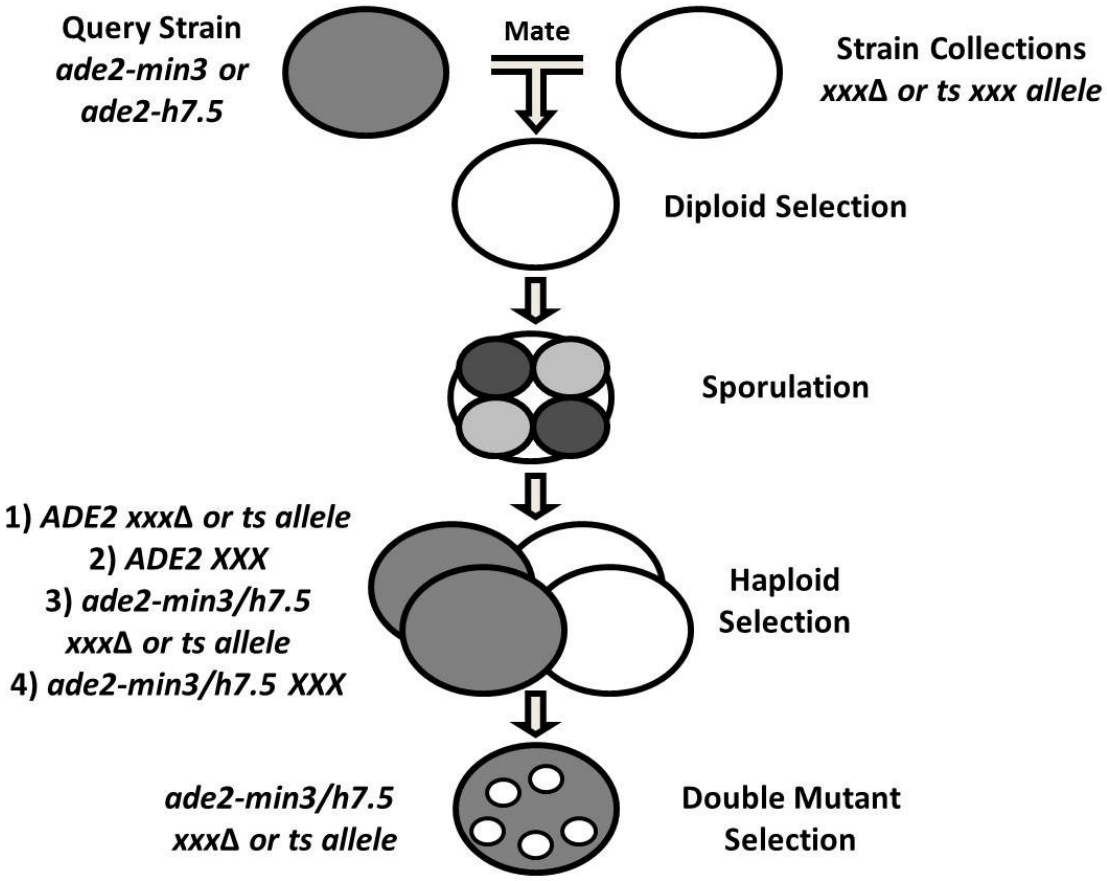
Query Strain
ade2-min3 or
ade2-h7.5
Mate
Strain Collections
xxxΔ or ts xxx allele
Diploid Selection
Sporulation
1) ADE2 xxxΔ or ts allele
2) ADE2 XXX
3) ade2-min3/h7.5
xxxΔ or ts allele
4) ade2-min3/h7.5 XXX
Haploid
Selection
ade2-min3/h7.5
xxxΔ or ts allele
Double Mutant
Selection

d

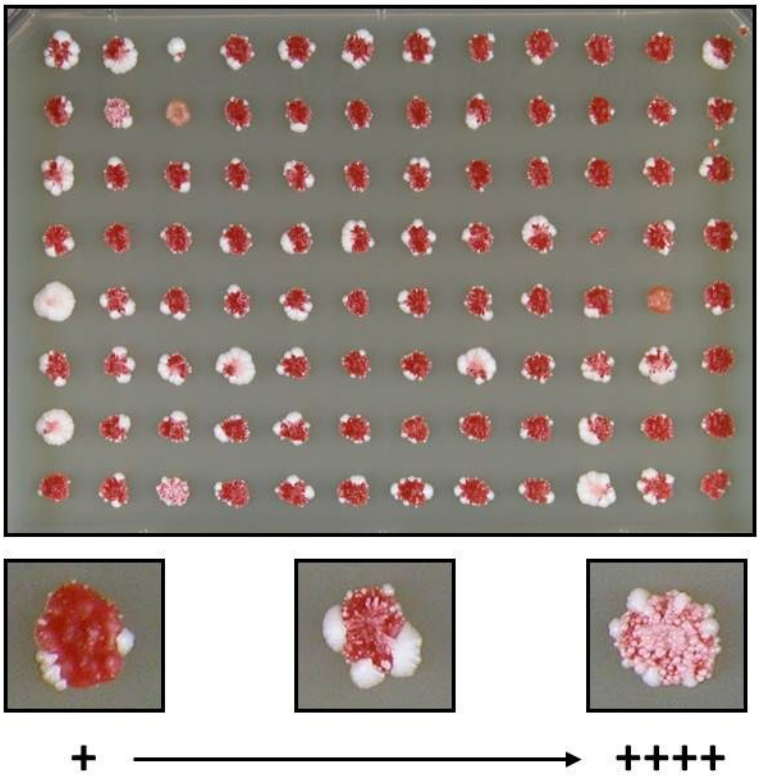

Figure 2-2.

Summary of Overlapping Hits from the *ade2-min3* and *ade2-h7.5* SGA Screens. **(a)** Of the 102 hits obtained from the *ade2-min3* SGA analysis and 157 hits obtained from the *ade2-h7.5* SGA analysis, seven hits overlapped both screens. **(b)** Blebbing quantification of strains bearing the *ade2-min3* allele. YPD cultures were inoculated with a single red colony and grown for four hours at 30°C. Each culture was diluted and plated onto solid YPD media. Strains were incubated at 30°C for two days and then at RT for six days. Blebs were counted on 100 colonies. The average number of blebs +/- the 95% confidence interval was calculated for each strain. This experiment was repeated three independent times. The black horizontal line indicates the average number of blebs/colony of the WT strain. **(c)** Blebbing quantification of strains bearing the *ade2-h7.5* allele was performed as in (b).

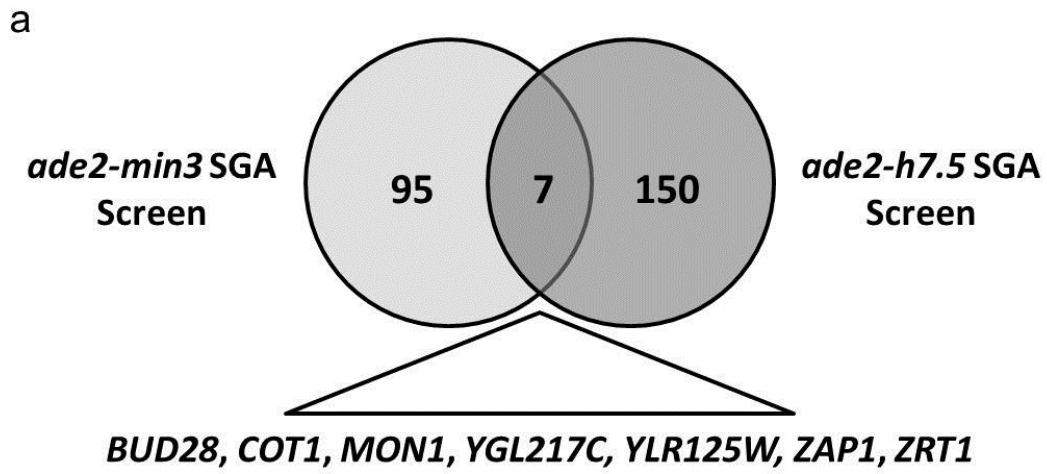

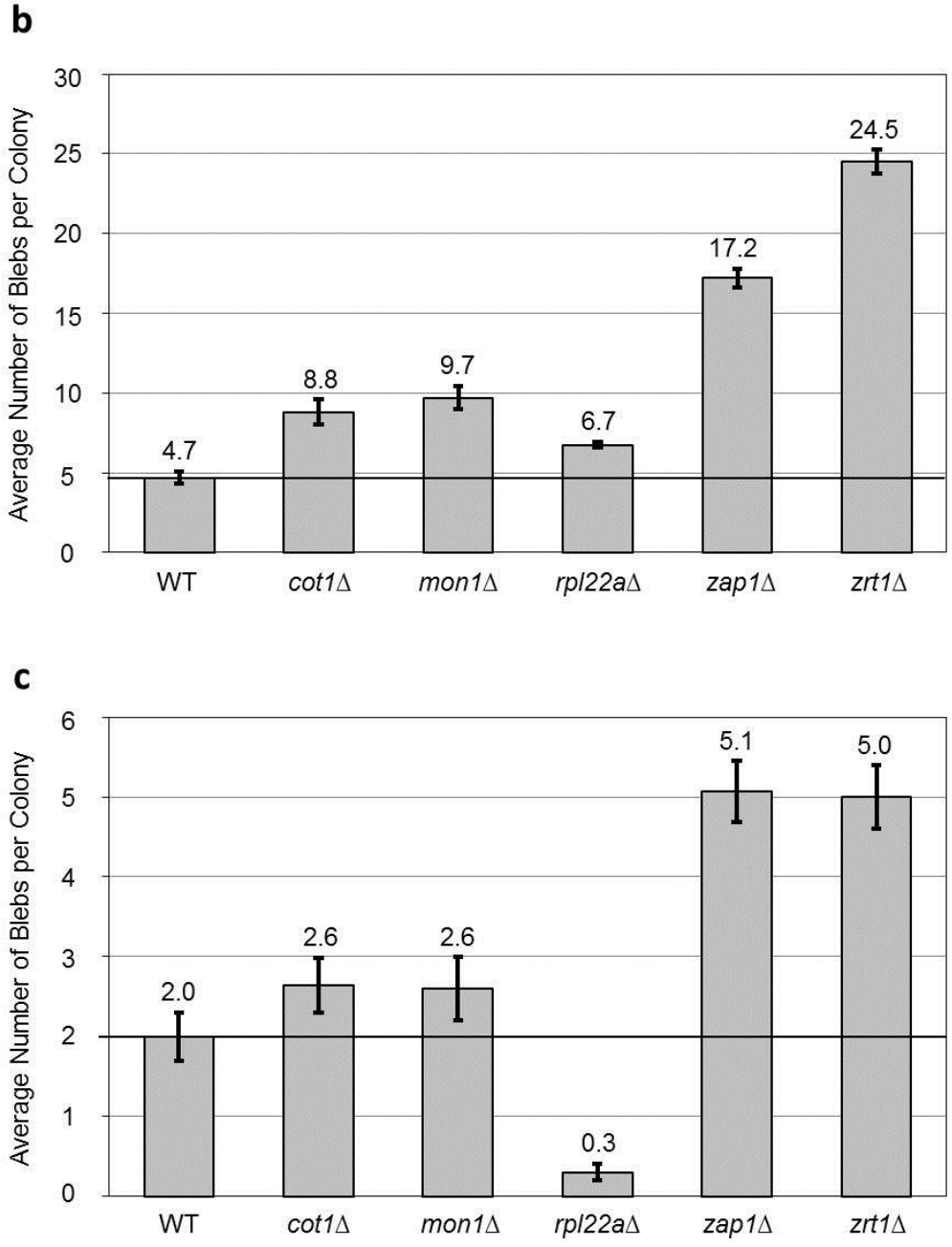
b
Average Number of Blebs per Colony
30
25
20
15
10
5
0
4.7
8.8
9.7
6.7
17.2
24.5
WT
cot1Δ
mon1Δ
rpl22aΔ
zap1Δ
zrt1Δ
c
Average Number of Blebs per Colony
6
5
4
3
2
1
0
2.0
2.6
2.6
0.3
5.1
5.0
WT
cot1Δ
mon1Δ
rpl22aΔ
zap1Δ
zrt1Δ

Figure 2-3.

Specific Mismatch Repair Components Stabilize Minisatellites in Stationary Phase. **(a)** Blebbing quantification for *ade2-h7.5* strains bearing a deletion of a nonessential mismatch repair gene was performed as described in Figure 1-2b and in Chapter VII: Materials and Methods. **(b)** Summary of *ade2-h7.5* mismatch repair mutant alterations. Sequencing across the minisatellite tract was performed on genomic DNA isolated from 20 individual blebs for each strain. The parental allele is given as a reference. The location of a lost repeat unit is indicated by a break within the minisatellite tract. Added repeat units are indicated in grey and loss of nucleotides are indicated by the symbol (*).

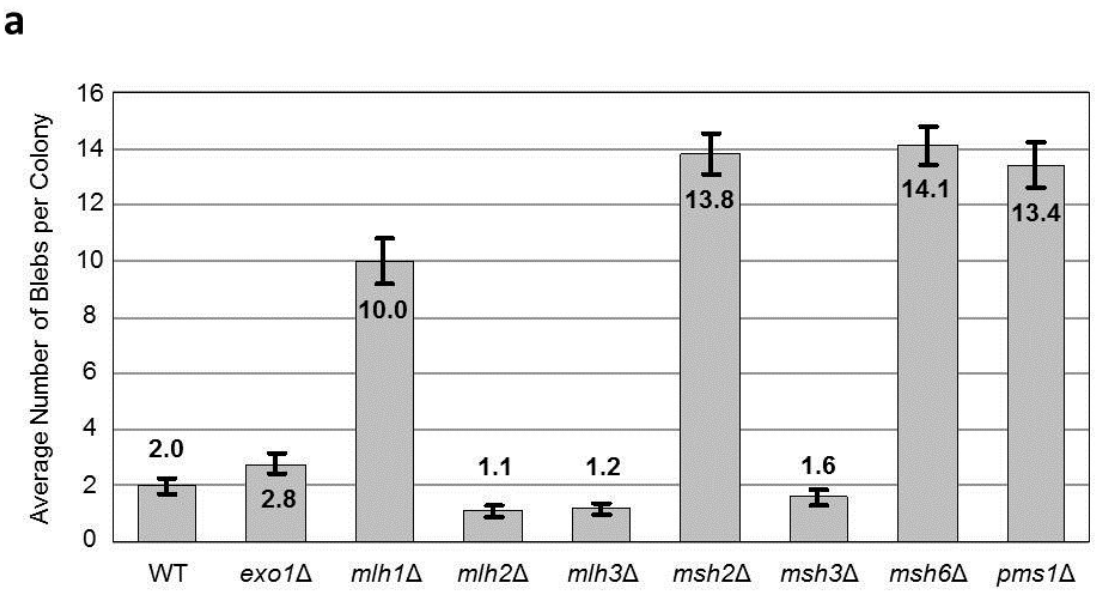

b

DTK1900 (*mlh1*Δ)

Class	# of alleles identified	*ade2-h7.5* allele structure
Parental		4 1 2 3 2 1 3
Loss: 1 Repeat	6	4 1 2 3 1 3
	4	4 1 2 2 1 3
	4	4 1 2 3 2 3
	3	4 2 3 2 1 3
Loss: 4 Repeats	3	4 1 3

DTK1902 (*pms1*Δ)

Class	# of alleles identified	*ade2-h7.5* allele structure
Parental		4 1 2 3 2 1 3
Loss: 1 Nucleotide	1	4 1 2 3* 2 1 3
Gene Conversion Loss: 1 Repeat	1	4 2 2 3 2 3
Loss: 1 Repeat	5	4 1 2 2 1 3
	5	4 1 2 3 1 3
	3	4 2 3 2 1 3
	2	4 1 2 3 2 3
	1	4 1 3 2 1 3
Loss: 4 Repeats	2	4 1 3

DTK1903 (*msh2*Δ)

Class	# of alleles identified	*ade2-h7.5* allele structure
Parental		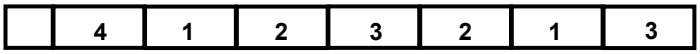
Loss: 1 Repeat	7	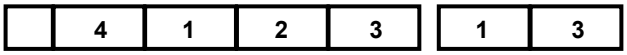
	5	
	3	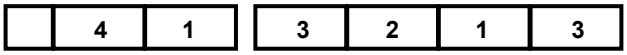
	2	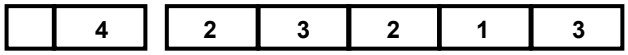
	2	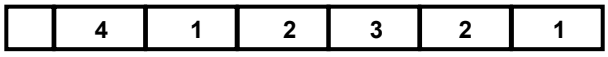
	1	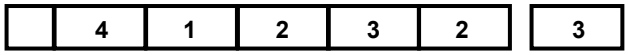

DTK1907 (*msh6*Δ)

Class	# of alleles identified	*ade2-h7.5* allele structure
Parental		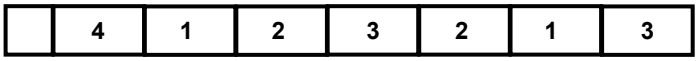
Loss: 1 Repeat	9	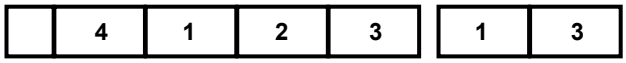
	3	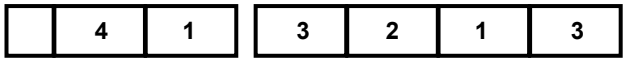
	3	
Loss: 4 Repeats	4	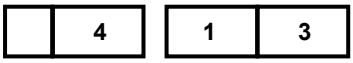
	1	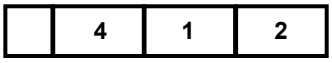

Table 2-1: Summary of Hits from the *ade2-min3* SGA Analysis of the Yeast Nonessential and Essential Strain Sets

Gene	ORF	Gene	ORF	Gene	ORF	Gene	ORF	Gene	ORF
*ABD1**	YBR236C	*ERG10**	YPL028W	*ORC2**	YBR060C	*RRS1**	YOR294W	*TOF1*	YNL273W
ADE12	YNL220W	*FAL1**	YDR021W	*ORC3**	YLL004W	*RSP5**	YER125W	*TSC11**	YER093C
*APC11**	YDL008W	*GAS2*	YLR343W	*PAC10*	YGR078C	***SAC1***	**YKL212W**	*UPS2*	YLR168C
ARL1	YBR164C	*HBT1*	YDL223C	*PDS1**	YDR113C	*SEC17**	YBL050W	*URA7*	YBL039C
*ASK1**	YKL052C	*IPL1**	YPL209C	*PEP5*	YMR231W	*SEC22**	YLR268W	*USO1**	YDL058W
ATG3	YNR007C	*KAP122*	YGL016W	*PKC1**	YBL105C	*SEC59**	YMR013C	*VPS41*	YDR080W
BAP3	YDR046C	*LCB1**	YMR296C	*POB3**	YML069W	*SLA1*	YBL007C	*YCF1*	YDR135C
BUB3	YOR026W	*MAK10*	YEL053C	*POL31**	YJR006W	*SLI15**	YBR156C	YCL060C	YCL060C
BUD28	YLR062C	*MCD1**	YDL003W	*POL32*	YJR043C	*SMC5**	YOL034W	YCL075W	YCL075W
*CBF2**	YGR140W	*MCM5**	YLR274W	*PSE1**	YMR308C	*SNU114**	YKL173W	YGL114W	YGL114W
CCZ1	YBR131W	*MET30**	YIL046W	*RAD27*	YKL113C	*SPC29**	YPL124W	YGL217C	YGL217C
*CEP3**	YMR168C	*MFA1*	YDR461W	*RAV1*	YJR033C	*SSA1*	YAL005C	YGR291C	YGR291C
*COF1**	YLL050C	*MGA2*	YIR033W	*RFC2**	YJR068W	*SSD1*	YDR293C	YKR035C	YKR035C
*COP1**	YDL145C	*MMR1*	YLR190W	*RFC4**	YOL094C	*STT4**	YLR305C	YLR125W	YLR125W
COT1	YOR316C	*MMS21**	YEL019C	*RIC1*	YLR039C	*STU1**	YBL034C	YOR008C*	YOR008C
CSM3	YMR048W	*MOB2**	YFL034C-B	*RMD1*	YDL001W	*SWH1*	YAR042W	*YPT31*	YER031C
DBF2	YGR092W	*MON1*	YGL124C	*RPB3**	YIL021W	*TAF12**	YDR145W	*ZAP1*	YJL056C
DCG1	YIR030C	*MRC1*	YCL061C	*RPL22A*	YLR061W	*TEC1*	YBR083W	***ZRT1***	**YGL255W**
DPB3	YBR278W	*MUP1*	YGR055W	*RPT4**	YOR259C	*TEM1**	YML064C		
DPB4	YDR121W	*NNF1**	YJR112W	*RPT6**	YGL048C	*TIM22**	YDL217C		
*ERG8**	YMR220W	***ODC1***	**YPL134C**	*RRI1*	YDL216C	*TLG2*	YOL018C		

a. Genes appearing in bold typeface are the strongest hits from the *ade2-min3* screens (scored as ++++ for at least 2/3 independent screens).
b. Genes denoted by (*) are essential

Table 2-2: Summary of Hits from the *ade2-h7.5* SGA Analysis of the Yeast Nonessential Strain Set

Gene	ORF	Gene	ORF	Gene	ORF	Gene	ORF
ACA1	YER045C	*KTI12*	YKL110C	*SDS24*	YBR214W	YGL217C	YGL217C
ACF4	YJR083C	*LCB4*	YOR171C	*SKI8*	YGL213C	YGL230C	YGL230C
ADY4	YLR227C	*LEE1*	YPL054W	*SLK19*	YOR195W	YGR001C	YGR001C
AGP3	YFL055W	*LEU3*	YLR451W	*SNF6*	YHL025W	YGR031W	YGR031W
AIM23	YJL131C	*LIP5*	YOR196C	*SOL3*	YHR163W	YGR051C	YGR051C
ALR2	YFL050C	*MET22*	YOL064C	*SPE1*	YKL184W	YGR149W	YGR149W
APM4	YOL062C	*MON1*	YGL124C	*SPS22*	YCL048W	YGR176W	YGR176W
APS1	YLR170C	*MPC54*	YOR177C	*SRN2*	YLR119W	YGR207C	YGR207C
ARN2	YHL047C	*MRM2*	YGL136C	*SRX1*	YKL086W	YGR266W	YGR266W
ART5	YGR068C	*MRPL22*	YNL177C	*SSH4*	YKL124W	YHL044W	YHL044W
ATO3	YDR384C	*NCE102*	YPR149W	*SWT21*	YNL187W	**YHR022C**	**YHR022C**
AVT3	YKL146W	*NFI1*	YOR156C	*THI72*	YOR192C	YJL049W	YJL049W
BMH2	YDR099W	*NKP1*	YDR383C	*THP1*	YOL072W	YKL070W	YKL070W
BSC1	YDL037C	*NNK1*	YKL171W	*TIM21*	YGR033C	YKL136W	YKL136W
BUD2	YKL092C	*NUP2*	YLR335W	*TMT1*	YER175C	YKL151C	YKL151C
BUD28	YLR062C	*OXP1*	YKL215C	*TPK3*	YKL166C	YKL187C	YKL187C
CAR1	YPL111W	*PAR32*	YDL173W	*TPO2*	YGR138C	YLR125W	YLR125W
COT1	YOR316C	*PDC5*	YLR134W	*TRP4*	YDR354W	YLR225C	YLR225C
CUE2	YKL090W	*PDR12*	YPL058C	*TUM1*	YOR251C	YML053C	YML053C
CYC7	YEL039C	*PFA4*	YOL003C	*UBC11*	YOR339C	YML089C	YML089C
DFG5	YMR238W	*PIR3*	YKL163W	*UTR2*	YEL040W	YMR010W	YMR010W
DGR2	YKL121W	*PLB1*	YMR008C	*VBA4*	YDR119W	YMR085W	YMR085W
DLD1	YDL174C	*PMP2*	YEL017C-A	*VMA21*	YGR105W	YMR090W	YMR090W
EAP1	YKL204W	***PMS1***	**YNL082W**	*VMS1*	YDR049W	YMR258C	YMR258C
EDC3	YEL015W	*PRM4*	YPL156C	*VPS61*	YDR136C	YMR304C-A	YMR304C-A
EFT2	YDR385W	*PSD2*	YGR170W	*VTC1*	YER072W	YOL024W	YOL024W

Gene	ORF	Gene	ORF	Gene	ORF	Gene	ORF
ELC1	YPL046C	*PXL1*	YKR090W	*YAP1801*	YHR161C	YOL079W	YOL079W
FDC1	YDR539W	*QCR10*	YHR001W-A	*YAT2*	YER024W	YOL153C	YOL153C
FIN1	YDR130C	*RDS1*	YCR106W	YBL096C	YBL096C	YOR170W	YOR170W
FOB1	YDR110W	*REC104*	YHR157W	YBR197C	YBR197C	YOR296W	YOR296W
GET2	YER083C	*RGP1*	YDR137W	YBR277C	YBR277C	YPL066W	YPL066W
GIT1	YCR098C	*RNH203*	YLR154C	YCR015C	YCR015C	YPL102C	YPL102C
HIR1	YBL008W	*RPL7B*	YPL198W	YDR109C	YDR109C	YPR078C	YPR078C
HIS6	YIL020C	*RPS25B*	YLR333C	YDR415C	YDR415C	YPR109W	YPR109W
HNT3	YOR258W	*RRD1*	YIL153W	YEL020C	YEL020C	*YPT35*	YHR105W
HOR2	YER062C	*RRT2*	YBR246W	YEL023C	YEL023C	***ZAP1***	**YJL056C**
HSP82	YPL240C	*RSM22*	YKL155C	YER067C-A	YER067C-A	***ZRT1***	**YGL255W**
IRC18	YJL037W	*RUB1*	YDR139C	YER068C-A	YER068C-A		
KES1	YPL145C	*RVS167*	YDR388W	YFH7	YFR007W		
KIN82	YCR091W	*SAP185*	YJL098W	YGL199C	YGL199C		

a. Genes appearing in bold typeface are the strongest hits from the *ade2-h7.5* screen (scored as ++++ for at least 2/3 independent screens).

Table 2-3: Enriched GO Terms of Hits from the *ade2-min3* SGA Analysis of the Yeast Nonessential and Essential Strain Sets

GO Term	Associated Genes
cell cycle [GO:0007049]	*APC11, ASK1, BUB3, CSM3, DBF2, IPL1, MCD1, MCM5, MET30, MMR1, MOB2, NNF1, PDS1, PKC1, RFC2, RFC4, SLG1, SSD1, STU1, TEM1, TOF1*
chromosome [GO:0005694]	*ASK1, CBF2, CEP3, IPL1, MCD1, NNF1, POB3, SLI15, SMC5, STU1*
chromosome, centromeric region [GO:0000775]	*ASK1, CBF2, CEP3, IPL1, MCD1, NNF1, SLI15, STU1*
chromosome segregation [GO:0007059]	*ASK1, CBF2, IPL1, MCD1, NNF1, SLI15*
condensed chromosome kinetochore [GO:0000777]	*ASK1, IPL1, NNF1, SLI15, STU1*
condensed nuclear chromosome kinetochore [GO:0000778]	*ASK1, BUB3, CBF2, CEP3, IPL1*
cytoskeleton [GO:0005856]	*ASK1, CBF2, COF1, IPL1, SLA1, SLI15, STU1, PKC1, USO1*
DNA-directed DNA polymerase activity [GO:0003887]	*DPB3, DPB3, POL31, POL32*
DNA polymerase complex [GO:0042575]	*DPB3, DPB3, POL31, POL32*
DNA replication [GO:0006260]	*DPB3, DPB4, MCM5, MRC1, ORC2, ORC3, POL31, POL32, RAD27, RFC2, RFC4, TOF1*
DNA strand elongation [GO:0022616]	*DPB3, DPB4, POL31, POl32, RAD27, RFC2, RFC4*
intracellular protein transport [GO:0006886]	*COP1, RIC1, SEC17, TLG1, USO1, VPS41*
kinetochore [GO:0000776]	*ASK1, IPL1, NNF1, SLI15, STU1*
leading strand elongation [GO:0006272]	*DPB3, DPB4, POL31, POL32, RFC2, RFC4*
mitosis [GO:0007067]	*APC11, ASK1, MOB2, NNF1, PDS1, SSD1, STU1, TEM1*

GO Term	Associated Genes
nucleus [GO:0005634]	*ASK1, BUB3, CBF2, CEP3, CSM3, COF1, DPB3, DPB4, ERG8, FAL1, IPL1, MCD1, MCM5, MET30, MGA2, MMS21, MOB2, MRC1, NNF1, ORC2, ORC3, PDS1, PKC1, POB3, POL31, POL32, PSE1, RAD27, RFC2, RIC1, RFC4, RPB3, RPT4, RPT6, RRI1, RRS1, RSP5, SLA1, SLI15, SMC5, SNU114, SSA1, STU1, SWH1, TEC1, TOF1, TAF12, ZAP1*
replication fork protection complex [GO:0031298]	*CSM3, MCM5, MRC1, POB3, TOF1*
spindle [GO:0005819]	*ASK1, CBF2, IPL1, PDS1, SLI15, STU1*

Table 2-4: Enriched GO Terms of Hits from the *ade2-min3* SGA Analysis of the Yeast Nonessential and Essential Strain Sets and the *ade2-h7.5* SGA Analysis of the Yeast Nonessential Strain Set

GO Term	Associated Genes
chromosome, centromeric region [GO:0000775]	*ASK1, CBF2, CEP3, HIR1, IPL1, MCD1, NKP1, NNF1, SLI15, SLK19, STU1*
condensed chromosome kinetochore [GO:0000777]	*ASK1, BUB3, CBF2, CEP3, IPL1, NKP1, NNF1, SLI15, SLK19, STU1*
endosome [GO:0005768]	*ARN2, CCZ1, LCB1, MON1, SLA1, SRN2, SSH4, TLG2, VPS41, YPT31, YPT35*
kinetochore [GO:0000776]	*ASK1, IPL1, NKP1, NNF1, SLI15, SLK19, STU1*
leading strand elongation [GO:0006272]	*DPB3, DPB4, POL31, POL32, RFC2, RFC4*
plasma membrane [GO:0005886]	*AGP3, ALR2, ARN2, ATO3, BAP3, DFG5, FDC1, GAS2, GIT1, LCB4, MFA1, NCE102, PDR12, PLB1, PMP2, SLA1, SLG1, SPS22, STT4, TSC11, TPO2, YAP1801,YGR266W, YHL044W*
spindle [GO:0005819]	*ASK1, CBF2, FIN1, IPL1, PDS1, SLI15, SLK19, STU1*

Chapter III

Novel Checkpoint Pathway Organization Promotes Genome Stability in Stationary Phase Yeast Cells

Chapter Summary

Most DNA alterations occur as uncorrected errors during DNA replication in S phase of the cell cycle. However, the majority of eukaryotic cells spend their lifespan in a quiescent state. Currently, little is known about the factors involved in preventing DNA instability within this stationary phase cell population. Previously, we utilized a unique assay system to monitor minisatellite instability in *Saccharomyces cerevisiae*, and found mutations that increased minisatellite alterations specifically in quiescent cells. In Chapter 2, we identified several checkpoint components in our Synthetic Genetic Array (SGA) screen. Here, investigated the role those checkpoint signaling components play in stabilizing minisatellites in stationary phase yeast cells. Our results revealed that a subset of checkpoint components, specifically *MRC1*, *CSM3*, *TOF1*, *DDC1*, *RAD17*, *MEC3*, *TEL1*, *MEC1* and *RAD53,* prevent stationary-phase minisatellite alterations. Further characterization demonstrated that the minisatellite alterations occur within the quiescent cell subpopulation of stationary phase cells. Pathway analysis revealed at least three pathways mediate minisatellite stability, with *MRC1*, *CSM3* and *TOF1* acting in a pathway independent of *MEC1* and *RAD53*. Overall, our data indicate that some well-characterized checkpoint components act to maintain the stability of minisatellites in stationary phase cells but are regulated differently in stationary phase cells compared to actively growing cells.

Introduction

Most eukaryotic cells spend their lifespan in a quiescent or non-dividing state. It is thought that mutations arising within quiescent cells can allow them to escape quiescence, re-entering the cell cycle and initiating tumorigenesis (Kim et al., 2005, Suda et al., 2005, Jin et al., 2009a). Bypass of cellular growth controls results in unregulated cell divisions and the accumulation of genomic instability, two of the major hallmarks of cancer. At present, little is known about the initial mutagenic events that occur within quiescent cells that cause them to become cancerous.

Checkpoints act as guardians of genomic stability, preventing the replication and accumulation of mutated DNA. In the yeast *Saccharomyces cerevisiae*, several checkpoints arrest the cell cycle when DNA damage, replication or mitotic errors occur (Figure 3-1a). During S-phase, the replication checkpoint is activated when replication forks stall (Branzei and Foiani, 2009, Putnam et al., 2009). This allows DNA repair to occur and prevents the formation of single-stranded DNA (ssDNA) which can be used as a template for chromosomal rearrangements. The protein kinase Mec1p is recruited to RPA-coated ssDNA at stalled replication forks, where it phosphorylates signal transducers such as Mrc1p or Rad9p (Emili, 1998, Alcasabas et al., 2001, Naylor et al., 2009). Phosphorylation of Mrc1p or Rad9p results in the recruitment of Rad53p to the replication fork and activation of the replication checkpoint (Vialard et al., 1998, Osborn and Elledge, 2003, Chen and Zhou, 2009).

Intra-S-phase and DNA damage checkpoints utilize similar signal transduction pathways to block cell cycle progression (Figure 3-1a) (Longhese et al., 2003, Putnam et

al., 2009). The DNA damage signal is propagated by the kinases Mec1p and Tel1p, a protein functionally redundant with Mec1p (Weinert et al., 1994, Greenwell et al., 1995, Morrow et al., 1995). Mec1p and Rad24p (a component of the RFC-like complex which loads the PCNA-like clamp composed of Ddc1p, Rad17p and Mec3p onto DNA (Paciotti et al., 1998, Kondo et al., 1999) are independently recruited to the site of DNA damage (Majka and Burgers, 2003, Navadgi-Patil and Burgers, 2009). This localization results in the activation of Mec1p and leads to the activation of Rad53p through the phosphorylation of Rad9p. Alternatively, Mec1p can also phosphorylate the kinase Chk1p to relay the signal and prevent cell cycle progression (Sanchez et al., 1999).

During mitosis, the spindle assembly checkpoint prevents the onset of anaphase until all chromosomes are properly attached to the mitotic spindle (Lew and Burke, 2003). In brief, Mps1p, Mad1p, Mad2p, Mad3p, Bub1p, and Bub3p localize to unattached kinetochores (Hoyt et al., 1991, Li and Murray, 1991). This binding prevents the activation of the anaphase promoting complex (APC) through inhibition of its substrate Cdc20p (Hwang et al., 1998). The inhibition of Cdc20p prevents the degradation of APC substrates, thereby delaying anaphase progression until all sister chromatids are properly aligned. These cell cycle surveillance mechanisms ensure the proper replication of DNA and segregation of chromosomes.

In yeast, stationary phase cells recapitulate the phenotypes of quiescent cells found in other eukaryotic systems (Werner-Washburne et al., 1993, Gray et al., 2004). Recent studies in *S. cerevisiae* have shown that the checkpoint kinase Rad53p is phosphorylated in DNA repair mutants that are in stationary phase (Pawar et al., 2009).

Furthermore, the authors found a dramatic increase in the amount of spontaneous mutability within these cells. Due to the discovery of Rad53p activation in stationary phase cells, we wanted to determine if other well-characterized checkpoint components play a role in maintaining genomic stability once cells have exited the cell cycle.

In Chapter 2, we conducted a modified version of the SGA analysis (Tong et al., 2001, Tong and Boone, 2006) to determine what factors have a role in stabilizing minisatellites during stationary phase. In brief, we mated a query strain containing the *ade2-min3* allele to mutant strains bearing either a complete deletion of a nonessential gene or a temperature-sensitive (ts) allele of an essential gene. We examined the resulting double mutants for the presence of a blebbing phenotype indicative of minisatellite instability. Here, we examine the checkpoint associated genes identified using the SGA analysis in order to determine if these genes have an active role in minisatellite stability in stationary phase cells. Our results reveal that a specific subset of checkpoint components (namely *MRC1*, *CSM3*, *TOF1*, *DDC1*, *RAD17*, *MEC3, TEL1, MEC1* and *RAD53*) prevents minisatellite alterations in quiescent yeast cells in stationary phase.

Interestingly, *CHK1*, *RAD9*, and *BUB3*, despite their major roles in several cell cycle checkpoints, do not stabilize minisatellites in stationary phase cells, implying that checkpoints in stationary phase cells function in novel pathways and are regulated differently. This is supported by our pathway analysis in which we find that the key checkpoint components *MEC1*, *RAD53* and the *MRC1*/*CSM3*/*TOF1* complex function in independent genetic pathways during stationary phase, implying that the latter complex is not part of the Mec1p and Rad53p phosphorylation cascade. We also find that a *RAD9* -

dependent pathway is active in stationary phase cells and prevents minisatellite instability when Mrc1p function is compromised. Our work provides evidence that checkpoint proteins play an active role in maintaining genomic stability in stationary phase cells, and that these proteins interact differently in stationary phase and actively-growing cells.

Results

Components of Several Checkpoint Pathways Mediate Minisatellite Stability during Stationary Phase

For this chapter, we utilized the *ade2-min3* reporter allele (Kelly et al., 2007, Kelly et al., 2011) to determine the effect of mutations in checkpoint genes on minisatellite stability (Figure 3-2a). We previously described the *ade2-min3* reporter assay and its ability to distinguish between minisatellite alterations occurring during log phase growth and those occurring during stationary phase (Kelly et al., 2007, Kelly et al., 2011). Minisatellite alterations that occur specifically during stationary phase result in novel colony morphology called blebbing.

Approximately 100 genes have been annotated in the *Saccharomyces* Genome Database (www.yeastgenome.org) as having checkpoint-related functions (Table 3-1). To determine which of the checkpoint-related genes are important for maintaining minisatellite stability, we analyzed the results of a modified version of the Synthetic Genetic Array (SGA) protocol (Tong et al., 2001, Tong and Boone, 2006) described in Chapter 2. Isolated double mutant strains from this screen containing the *ade2-min3*

allele as well as a deletion or temperature sensitive mutation were analyzed for a blebbing color segregation phenotype.

Our screening of the checkpoint genes revealed a subset that was required for stationary phase minisatellite stability (Table 3-1). Loss of the replication checkpoint genes *MRC1, CSM3* or *TOF1* gave a pronounced blebbing phenotype similar to that of our positive *zrt1*Δ control (Kelly et al., 2007), indicating a role for these genes in maintaining minisatellite stability during stationary phase. Similarly, strains bearing temperature sensitive alleles of the spindle checkpoint gene *IPL1* (Biggins and Murray, 2001, Pinsky et al., 2006), the kinetochore gene *CEP3* (Lechner and Carbon, 1991, Strunnikov et al., 1995) or the S-phase checkpoint gene *RFC4* (Cullmann et al., 1995) produced a strong blebbing phenotype at their corresponding critical temperatures. Additionally, strains containing deletions of *DDC1*, *RAD17*, *MEC3*, or *TEL1* (components of the S-phase and DNA damage checkpoints) exhibited a blebbing phenotype, but at a lower level than the positive control.

To verify the results of our SGA analysis, we deleted several candidate nonessential genes with well-known cell cycle checkpoint roles (Figure 3-1a) in the DTK271 strain background, which has been well-characterized in our previous work (Kelly et al., 2007, Kelly et al., 2011, Kelly et al., 2012). We examined deletions of genes that exhibited stationary phase minisatellite instability (*MRC1*, *CSM3*, *TOF1*, *DDC1*, *RAD17*, *BUB3*, *MEC3* and *TEL1*) and genes that did not (*RAD9* and *CHK1*).

Deletion of *MRC1*, *CSM3* or *TOF1* in DTK271 led to a strong blebbing phenotype (Figure 3-2b). DTK1392 (*mrc1*Δ) displayed an average of 23.9 blebs/colony

(Figure 3-3a). This value is significantly higher than that of DTK271, which had an average of 4.7 blebs/colony. The 95% confidence intervals were calculated for each strain. Lack of overlap between the 95% confidence intervals of DTK1392 and DTK271 indicated that the difference between the blebs quantified for each strain was statistically significant. Similarly, DTK1529 (*csm3*Δ) and DTK1528 (*tof1*Δ) displayed high levels of blebbing (26.2 and 24.4 blebs/colony, respectively). From this data, we conclude that components of the replication checkpoint play an important role in stabilizing minisatellites during stationary phase.

Deletion of the DNA damage checkpoint genes *DDC1*, *RAD17*, *MEC3* or *TEL1* in DTK271 produced an average level of blebbing of 10.5, 12.5, 11.5 and 8.0 blebs/colony, respectively (Figure 3-2b, Figure 3-3a). These values were significantly higher than that of the parental strain DTK271 (4.7 blebs/colony). These results suggest that components of the S-phase and DNA damage checkpoints are also involved in minisatellite stability during stationary phase.

Of the mutants surveyed, DTK1093 (*rad9*Δ), DTK1008 (*chk1*Δ) and DTK1691 (*bub3*Δ) did not exhibit a level of blebbing significantly greater than that of the parental strain (Figure 3-2b, Figure 3-3a). The deletion mutant strains had 3.2, 5.8 and 1.5 blebs/colony, respectively, compared to 4.7 blebs/colony of DTK271, indicating *RAD9*, *CHK1* and *BUB3* do not influence the stability of minisatellites in stationary phase cells.

For most of the genes examined in the two strain backgrounds (DTK271 and the SGA parental strains), deletion of each of the checkpoint genes in our strain background produced results similar to those obtained from the SGA analysis. Interestingly however,

deletion of *BUB3* produced a high level of blebbing in the SGA analysis, but did not bleb significantly in the DTK271 background. This could be due to the presence of an enhancer or suppressor mutation that affect a strain's blebbing phenotype, or due to the possibility that the original strain in the deletion collection was constructed incorrectly.

To verify the deletion of *BUB3* within the nonessential deletion haploid set, we performed PCR analysis across the *BUB3* open reading frame. We found that this strain contained a mixed population of *bub3*Δ and *BUB3* cells. PCR analysis of the *ade2-min3 bub3*Δ strain isolated from the SGA analyses revealed that this $G418^R$ blebbing strain was wild-type at the *BUB3* locus. Deletion of *BUB3* in both the nonessential SGA query strain (DTK1189 5a) and deletion set (BY4742) backgrounds resulted in a suppression of the wild-type blebbing phenotype as seen in the DTK271 background (Figure 3-3b). Our data suggest that the transformation to construct the original *bub3*Δ strain resulted in a mixed population of *bub3*Δ cells and *BUB3* cells in which *KANMX* ($G418^R$) is located elsewhere in the genome, presumably at an area of *BUB3* sequence homology. Future analysis of this strain will be performed to determine the location of the *KANMX* fragment and source of the blebbing phenotype.

To determine if the essential central checkpoint genes *MEC1* and *RAD53* were also involved in maintaining minisatellite stability, we constructed DTK271 derivative strains bearing a hypomorphic allele of *MEC1* (*mec1-21*) or *RAD53* (*rad53-1*) (Sanchez et al., 1996, Raveendranathan et al., 2006). We then calculated the blebbing frequency for each strain. DTK1776 (*mec1-21*) had 14.2 blebs/colony, significantly greater than that of the WT strain. Similarly, DTK1170 (*rad53-1*) had an average of 17.8 blebs/colony,

significantly higher than the 4.7 blebs/colony of DTK271 (Figure 3-3a), demonstrating that loss of *MEC1* or *RAD53* results in a significant increase in minisatellite alterations during stationary phase. We were unable to accurately assess the average number of blebs/colony of a *mec1-21 tel1*Δ strain; in our strain background this double mutant exhibited a severe defect in colony formation.

We observed a sectoring phenotype in both *mec1-21* and *rad53-1* strains (Figure 3-2b), likely resulting from minisatellite alterations that occur during colony formation. This result is consistent with the previously described roles of Mec1p and Rad53p in regulating genome stability during cell cycle growth (Branzei and Foiani, 2006) and indicates that minisatellite alterations in the *mec1-21* and *rad53-1* strains occur in actively dividing cells as well as cells that have entered stationary phase.

Minisatellite Alterations Occur during Stationary Phase in Strains Bearing Mutations of Checkpoint Genes

Previous work by the Werner-Washburne group demonstrated that yeast stationary phase cultures consist of both true quiescent cells as well as nonquiescent cells undergoing slow division (Allen et al., 2006, Aragon et al., 2008). Characterization of these subpopulations of stationary phase cultures showed that each is differentially regulated by a specific set of genes (Aragon et al., 2008). This genetic differentiation allows us to distinguish which cell population gives rise to the blebbing phenotype. Loss of *ETR1*, which encodes for a 2-enoyl thioester reductase, drastically reduces the ability of the quiescent cell population to reenter the cell cycle (Torkko et al., 2001, Aragon et

al., 2008). Similarly, loss of *POR1*, a gene that encodes for mitochondrial porin, reduces the ability of nonquiescent cells to reenter the cell cycle (Sanchez et al., 2001, Aragon et al., 2008). If a cell cannot reenter the cell cycle, it cannot generate a blebbing colony.

To determine if minisatellite alterations in the checkpoint mutants occur in the quiescent or nonquiescent population of stationary phase cells, we deleted *ETR1* or *POR1* in *mrc1*Δ*, csm3*Δ, *tof1*Δ, *mec1-21* or *rad53-1* strains, and quantified the blebbing frequency of the resulting double mutants (Figure 3-4). Strains DTK1587 (*mrc1*Δ *etr1*Δ), DTK1695 (*csm3*Δ *etr1*Δ) or DTK1694 (*tof1*Δ *etr1*Δ) had 0.05, 0.01, and 0.01 blebs/colony, respectively. This is a significant decrease in blebbing compared to each of the single mutants. Similarly, deletion of *ETR1* in a *mec1-21* (DTK1840) or *rad53-1* (DTK1272) background reduced the level of blebbing to 1.6 and 0.01 blebs/colony, respectively. In comparison, deletion of *POR1* in *mrc1*Δ*, csm3*Δ or *tof1*Δ strain backgrounds did not result in a complete loss of blebbing. Double mutants DTK1588 (*mrc1*Δ *por1*Δ), DTK1700 (*csm3*Δ *por1*Δ) or DTK1693 (*tof1*Δ *por1*Δ) had levels of blebbing of 17.7, 18.1 and 13.9 blebs/colony, respectively. These results indicate that minisatellite alterations in *mrc1*Δ*, csm3*Δ or *tof1*Δ strains occur predominantly within the quiescent population rather than the nonquiescent population of stationary phase cells.

Deletion of *POR1* in a *mec1-21* (DTK1827) or *rad53-1* (DTK1270) background however, resulted in a decrease in blebbing from 14.2 blebs/colony (*mec1-21*) to 6.7 blebs/colony and from 17.8 blebs/colony (*rad53-1*) to 3.7 blebs/colony, respectively. We conclude that minisatellite alterations in a *mec1-21* and *rad53-1* background occur within

both quiescent and nonquiescent cells populations, in keeping with phenotypes in actively growing cells.

Independent Pathways Regulate Minisatellite Stability During Stationary Phase

To investigate how many independent pathways regulate stationary phase minisatellite stability, we examined the blebbing of double mutant strains. The strains DTK1551 (*mrc1*Δ *csm3*Δ), DTK1549 (*mrc1*Δ *tof1*Δ) and DTK1554 (*csm3*Δ *tof1*Δ) produced equivalent blebbing levels (data not shown). We interpret this to mean that all three gene products function within the same pathway; therefore, for the remainder of the pathway analysis we only used the *mrc1*Δ strain to construct double mutants.

We previously demonstrated that deletion of the high-affinity zinc transporter gene *ZRT1* results in a dramatic increase in the amount of blebbing in an *ade2-min3* strain (Kelly et al., 2007, Kelly et al., 2011). To determine if *MRC1, RAD17, MEC1* and *RAD53* function within a *ZRT1*-dependent pathway, we constructed *mrc1*Δ *zrt1*Δ, *rad17*Δ *zrt1*Δ, *mec1-21 zrt1*Δ *and rad53-1 zrt1*Δ double mutants. DTK1556 (*mrc1*Δ *zrt1*Δ) had an average of 31.1 blebs/colony, higher than the average number of blebs/colony for each single mutant (*mrc1*Δ = 23.9 and *zrt1*Δ = 24.5 blebs/colony) (Figure 3-5a). However, blebs were difficult to quantify after six days at room temperature with this particular strain due to an enhanced blebbing phenotype of the double mutant. We therefore quantified the average number of blebs at an earlier timepoint (Figure 3-6a). After three days at room temperature, DTK1556 (*mrc1*Δ *zrt1*Δ) produced an average of 28.5 blebs/colony, a value significantly greater than either of the single mutants (*mrc1*Δ = 8.0

and *zrt1*Δ = 15.9 blebs/colony). This additive effect and the enhanced blebbing phenotype of the double mutant indicate that Mrc1p regulates minisatellite stability in a pathway that is at least partially independent of Zrt1p.

To determine if the enhanced blebbing phenotype of the *mrc1*Δ *zrt1*Δ double mutant was due to an increase in the number of early minisatellite alteration events or an increase in the growth rate of the white cells comprising the blebs, we performed a time-course analysis of white cells isolated from blebs of DTK271, DTK1392 (*mrc1*Δ), DTK878 (*zrt1*Δ) and DTK1556 (*mrc1*Δ *zrt1*Δ) strains (Figure 3-6b). We found that blebs from the *mrc1*Δ *zrt1*Δ double mutant did not grow at a significantly faster rate than the wild-type strain or either single mutant. This result, as well as the results of the blebbing quantification, suggests that the enhanced blebbing phenotype of the double mutant is due to an increase in the number of minisatellite alteration events at an earlier timepoint.

The double mutant DTK1762 (*rad17*Δ *zrt1*Δ) produced an average of 16.0 blebs/colony, a value not significantly greater than *rad17*Δ (12.5 blebs/colony) or *zrt1*Δ (24.5 blebs/colony) single mutants, placing *RAD17* in a *ZRT1*-dependent pathway. DTK1832 (*mec1-21 zrt1*Δ) had an average of 24.3 blebs/colony and DTK1171 (*rad53-1 zrt1*Δ) had an average of 23.5 blebs/colony. Both values were not significantly greater than the corresponding single mutants, and, unlike the *MRC1* result, places *MEC1* and *RAD53* in the same pathway as *ZRT1* (Figure 3-5a). These data suggest that Mrc1p functions in a pathway separate from Rad53p and Mec1p during stationary phase. This is in contrast to their S-phase checkpoint roles, in which each gene product functions within

the same checkpoint signaling pathway (Figure 3-1) (Osborn and Elledge, 2003, Chen and Zhou, 2009).

To examine this relationship further, we constructed *mrc1*Δ *mec1-21* (DTK1838), *mrc1*Δ *rad53-1* (DTK1558) and *mec1-21 rad53-1* (DTK1855) double mutants (Figure 3-5b, 3-5c). Analysis of *mrc1*Δ *mec1-21* revealed that while the level of blebbing of the double mutant (29.1 blebs/colony) was not significantly additive when compared to the strains *mrc1*Δ (23.9 blebs/colony) or *mec1-21* (14.2 blebs/colony), the blebbing phenotype of DTK1838 itself was drastically different than the parental strains. Colonies of DTK1838 bore a range of bleb sizes, unlike all other strains in which bleb size is homogeneous. This data suggests that *MRC1* and *MEC1* comprise different pathways, and the minisatellite alterations associated with the double mutant occur at a variety of timepoints during stationary phase.

In keeping with this trend, DTK1558 (*mrc1*Δ *rad53-1*; 38.3 blebs/colony) produced a significantly additive level of blebbing compared to either single mutant, demonstrating that Mrc1p and Rad53p are functioning in separate pathways during stationary phase (Figure 3-5b, 3-5c). Interestingly, while DTK1855 (*mec1-21 rad53-1*; 21.9 blebs/colony) did not have a level of blebbing that was significantly additive when compared to either single mutant at 14.2 (*mec1-21*) or 17.8 (*rad53-1*) blebs/colony, the resulting blebbing phenotype was drastically different. Like DTK1556 (*mrc1*Δ *zrt1*Δ), DTK1855 produced blebs that were significantly larger than those produced by the parental strains, suggesting that the minisatellite alterations in a *mec1-21 rad53-1* strain occur at an earlier timepoint than those in *mec1-21* or *rad53-1* strains. Together, our data

suggests that *MEC1* and *RAD53* comprise different pathways in stationary phase cells. This is in sharp contrast to their roles in actively dividing cells in which Mec1p and Rad53p function together in well-characterized checkpoint signaling pathways (Branzei and Foiani, 2006).

The division of *MEC1* and *RAD53* into different pathways is further supported by the comparison of double mutants DTK1833 (*mec1-21 rad17*Δ) and DTK1765 (*rad53-1 rad17*Δ) (Figure 3-5b). Here, DTK1833 had 34.1 blebs/colony, a value significantly greater than either single mutant at 14.2 (*mec1-21*) or 12.5 (*rad17*Δ) blebs/colony. In contrast, the *rad53-1 rad17*Δ strain (7.0 blebs/colony) produced a level of blebbing significantly lower than either single mutant at 17.8 (*rad53-1*) and 12.5 (*rad17*Δ) blebs/colony, which supports our previous data that *MEC1* and *RAD53* fall into separate pathways during stationary phase. The combination of *mrc1*Δ and *rad17*Δ mutations was synthetically lethal in our strain background; therefore, we are unable to assess the pathway relationship of *MRC1* and *RAD17*.

Our lab has found that *RAD27*, *PKC1* and *END3* represent several distinct pathways that mediate minisatellite instability in stationary phase cells (Kelly et al., 2012). *RAD27* encodes a nuclease involved in processing Okazaki fragments (Liu et al., 2004a). *PKC1* codes for an essential serene/threonine Protein Kinase C homolog, while *END3* encodes a protein involved in endocytosis and actin organization (Levin et al., 1990, Benedetti et al., 1994). DTK1559 (*mrc1*Δ *rad27*Δ) and DTK1839 (*mec1-21 rad27*Δ) produced averages of 59.5 and 46.9 blebs/colony, respectively, values significantly higher than the *mrc1*Δ (23.9 blebs/colony), *rad27*Δ (38.8 blebs/colony) and

mec1-21 (14.2 blebs/colony) single mutants (Figure 3-5d). The strain DTK1217 (*rad53-1 rad27*Δ) had an average of 27.3 blebs/colony. This value was not significantly additive when compared to the parental mutants. DTK1769 (*rad17*Δ *rad27*Δ) had an average of 30.9 blebs/colony, a value that falls between the single mutants at 12.5 (*rad17*Δ) or 38.8 (*rad27*Δ) blebs/colony. From this data we conclude that Rad17p and Rad53p, but not Mrc1p or Mec1p, function in a Rad27p-dependent pathway.

Both DTK1603 (*mrc1*Δ *pkc1-4*; 25.7 blebs/colony), and DTK1777 (*rad17*Δ *pkc1-4*; 15.1 blebs/ colony) produced levels of blebbing that were not significantly elevated when compared to that of the single mutants *mrc1*Δ (23.9 blebs/colony), *pkc1-4* (14.8 blebs/colony) and *rad17*Δ (12.5 blebs/colony) (Figure 3-5e). Similarly, DTK1871 (*mec1-21 pkc1-4*; 13.1 blebs/colony) and DTK1295 (*rad53-1 pkc1-4*; 14.6 blebs/colony) had average levels of blebbing that were not additive when compared to the parental strains (*mec1-21*; 14.2 blebs/colony and *rad53-1*; 17.8 blebs/colony). These data indicate that Mrc1p, Rad17p, Mec1p and Rad53p all function within a Pkc1p-dependent pathway. Similarly, *end3*Δ (8.0 blebs/colony) double mutants DTK1806 (*mrc1*Δ *end3*Δ; 15.9 blebs/colony), DTK1767 (*rad17*Δ *end3*Δ; 7.7 blebs/colony), DTK1883 (*mec1-21 end3*Δ; 12.0 blebs/colony) and DTK1219 (*rad53-1 end3*Δ; 9.8 blebs/colony) did not produce an additive blebbing effect compared to the corresponding single mutants (Figure 3-5f).

Together, our data suggest that checkpoint proteins participate in at least three independent pathways to maintain the stability of minisatellites during stationary phase. One pathway involves Rad53p, Zrt1p, Rad17p and Rad27p, while a second has Mrc1p,

Csm3p and Tof1p. Both pathways contain Pkc1p and End3p. The final pathway utilizes Mec1p, Zrt1p, Pkc1p and End3p but does not contain Rad17p or Rad27p.

Characterization of the Role of Mrc1p in Maintaining Minisatellite Stability in Stationary Phase Cells

In actively dividing cells, Mrc1p promotes Mec1p- and Rad53p- dependent checkpoint signaling as well as maintains proper replicative function (Alcasabas et al., 2001, Osborn and Elledge, 2003, Chen and Zhou, 2009, Naylor et al., 2009). The Elledge group has developed *MRC1* mutants that allow one to study the effects of the checkpoint or replicative functions of Mrc1p separately. These include *mrc1*^{AQ}, a strain bearing mutations at the Mec1p phosphorylation sites, and *mrc1-C14*, a C-terminal truncation mutant that displays a prolonged S-phase (Osborn and Elledge, 2003, Naylor et al., 2009).

To determine if the minisatellite alterations in the *mrc1*Δ strain are due to loss of the checkpoint function of Mrc1p or the replicative function of Mrc1p, we quantified the average number of blebs/colony in strains bearing the *ade2-min3* allele and the *mrc1*^{AQ} or *mrc1-C14* separation of function alleles (Figure 3-6a). DTK1630 (*mrc1*^{AQ}) produced 7.1 blebs/colony, a value that, while greater than that of the WT strain (4.7 blebs/colony), is not a drastic increase such as that seen in the *mrc1*Δ deletion mutant (23.9 blebs/colony). The strain DTK1683 (*mrc1-C14*) had an average of 18.5, a value significantly greater than that of the WT strain. From this data we conclude that minisatellite stability in stationary phase cells is mediated predominantly by the replicative function of Mrc1p,

rather than the checkpoint signaling function. This finding complements our pathway analysis data which showed that *MRC1*, *MEC1* and *RAD53* lie in distinct genetic pathways in stationary phase cells (Figure 3-5b, 3-5c).

Surprisingly, a strain bearing both the AQ and C14 mutations (DTK1766; *mrc1*^{AQ}*-C14*) did not exhibit a level of blebbing equivalent to that of the *mrc1*Δ strain DTK1392 (17.7 versus 23.9 blebs/colony respectively) (Figure 3-6a). This result could be due to the continued presence of the bulk of the Mrc1p protein or to a possible backup checkpoint pathway, either or both of which could contribute to continued minisatellite stability in the absence of the well-characterized functions of Mrc1p.

Mrc1p and Rad9p were previously shown to represent functionally redundant checkpoint pathways (Alcasabas et al., 2001). Further analysis by Alcasabas *et al*., 2001 and Osborn and Elledge, 2003, suggest that Rad9p may act as a backup pathway in actively dividing cells when Mrc1p function is compromised. To determine if Rad9p acts as a backup pathway in stationary phase, we compared the level of blebbing of an *mrc1*^{AQ} *rad9*Δ double mutant to the parental single mutants (Figure 3-6a). The combined mutations in DTK1740 (*mrc1*^{AQ} *rad9*Δ; 13.9 blebs/colony) produced a synergistic blebbing effect when compared to the single mutants *mrc1*^{AQ} (7.1 blebs/colony) and *rad9*Δ (3.2 blebs/colony). Thus, our data suggest that when the checkpoint signaling function of Mrc1p is absent, a Rad9p-dependent checkpoint signaling pathway prevents further minisatellite instability. The *mrc1*Δ *rad9*Δ and *mrc1-C14 rad9*Δ mutation combinations exhibit synthetic lethality in our background. This fits with prior observations that Rad9p is required for cell viability in *mrc1*Δ mutants which accrue

DNA damage due to replication stress (Alcasabas et al., 2001, Osborn and Elledge, 2003).

Our quiescent and nonquiescent population analysis of the *mrc1*Δ strain revealed that the majority of stationary phase minisatellite alterations were specific to quiescent cells. However, we also found that ~25% of alterations appear to occur in nonquiescent cells (Figure 3-4). To determine if the different functions of Mrc1p accounted for these results, we deleted *POR1* and *ETR1* in the *mrc1*^{AQ}, *mrc1-C14* and *mrc1*^{AQ}*-C14* mutant backgrounds (Figure 2-6b). Deletion of *POR1* in both *mrc1*^{AQ} and *mrc1-C14* backgrounds did not result in a decrease in blebbing. DTK1825 (*mrc1*^{AQ} *por1*Δ) and DTK1841 (*mrc1-C14 por1*Δ) had levels of blebbing of 8.2 and 17.1 blebs/colony respectively. A significant decrease in blebbing, however, was observed in DTK1873 (*mrc1*^{AQ}*-C14 por1*Δ; 14.0 blebs/colony). In comparison, deletion of *ETR1* in each of the mutant backgrounds resulted in a dramatic decrease in the level of blebbing compared to each of the single mutants. Strains DTK1826 (*mrc1*^{AQ} *etr1*Δ) and DTK1836 (*mrc1-C14 etr1*Δ) each had levels of blebbing of 0.4 blebs/colony and DTK1882 (*mrc1*^{AQ}*-C14 etr1*Δ) had 0.6 blebs/colony. We conclude that minisatellite alterations associated with the loss of the checkpoint signaling and replication functions of Mrc1p primarily occur within the quiescent population of stationary phase cells.

Dissecting the Mechanism of Minisatellite Alterations in Stationary Phase Yeast Cells

To investigate the mechanism giving rise to the blebbing phenotype in our strains, we quantified the average number of blebs/colony of strains bearing the *ade2-*

min3 minisatellite allele and *rfa1-t11*, a mutant allele of the *RFA1* subunit of Replication Protein A (RPA) (Umezu et al., 1998). RPA is a ssDNA binding protein that is highly conserved eukaryotes and functions to promote effective DNA replication, recombination and repair reviewed in (Fanning et al., 2006). Yeast strains carrying the *rfa1-t11* mutation are defective in recombination during DNA repair and meiosis, but have no measurable defects in DNA replication (Umezu et al., 1998, Soustelle et al., 2002, Kantake et al., 2003). Thus, examination of the *rfa1-t11* allele allows us to separate the effects of repair-associated recombination and DNA replication on minisatellite stability in stationary phase cells.

A strain bearing the *rfa1-t11* and *ade2-min3* alleles (DTK1979) produced a level of blebbing that was not significantly different that of the wild-type strain DTK271 (DTK1979 at 5.2 blebs/colony vs. DTK271 at 4.7 blebs/colony). Thus, the *rfa1-t11* mutation by itself does not appear to have affect minisatellite stability. We then investigated the level of blebbing in strains bearing the *rfa1-t11* and *ade2-min3* alleles as well as a deletion of *MRC1* (DTK1980) or *ZRT1* (DTK1981) (Figure 3-5a). DTK1980 (*mrc1*Δ *rfa1-t11*) produced a level of blebbing of 10.2 blebs/colony, a value approximately 50% of that produced by the single mutant DTK1392 (*mrc1*Δ; 23.9 blebs/colony). A similar result occurred in DTK1981 (*zrt1*Δ *rfa1-t11*) which had an average of 11.3 blebs/colony compared to 24.5 blebs/colony produced by the single *zrt1*Δ mutant DTK878. We conclude that while *rfa1-t11* does not appear to have an effect on the low level of spontaneous minisatellite instability displayed in the wild-type strain,

minisatellite alterations occurring within *mrc1*Δ or *zrt1*Δ mutant strain are at least partially dependent upon the recombination function associated with *RFA1*.

Discussion

For this chapter, we analyzed the results of a modified version of the SGA analysis (Tong et al., 2001, Tong and Boone, 2006) conducted in Chapter 2. The goal was to determine if checkpoint components play an active role in stabilizing minisatellites in stationary phase yeast cells. We find that a specific subset of checkpoint genes, including *MRC1*, *CSM3*, *TOF1*, *DDC1*, *RAD17*, *MEC3, TEL1*, *MEC1* and *RAD53*, act to prevent minisatellite alterations in stationary phase cells. We show that minisatellite alterations within these checkpoint mutant strains occur predominantly in the quiescent cell population of stationary phase colonies. Finally, we demonstrate that *MRC1*, *MEC1* and *RAD53* function in separate pathways in stationary phase cells, a significant difference from the checkpoint pathways characterized in actively dividing cells. Our data suggests that novel checkpoint pathways are in place in stationary phase cells to prevent genomic instability, and that components of these pathways are interacting differently in stationary phase cells compared to actively dividing cells.

The role of checkpoint proteins in actively growing cells is to sense a cellular state and transmit a signal under the appropriate conditions. While quiescent G_0 cells are not actively going through a cell cycle, the stationary phase checkpoint proteins identified in our work likely are still sensing a cellular state and transmitting a signal when problematic conditions are present (possibly ssDNA, as discussed below). This signal

may activate DNA repair activities, for example. In addition, it is possible that the checkpoint proteins in stationary phase cells are establishing a block to progression, as they would in actively growing cells, to prevent the cell from exiting G_0 before the problem has been resolved.

Our SGA screen for genes whose deletion destabilized a minisatellite tract revealed that specific components of checkpoint signaling pathways are active in stationary phase cells. We identified several that are known to function together in well-characterized signaling pathways in actively growing cells. These include *MRC1*, *CSM3* and *TOF1,* whose gene products form a complex that associates with the replication fork and mediates replication checkpoint signaling (Alcasabas et al., 2001, Katou et al., 2003, Osborn and Elledge, 2003, Bando et al., 2009). Also included are the kinase encoded by *TEL1* and PCNA-like clamp complex proteins encoded by *DDC1*, *RAD17* and *MEC3* which mediate DNA damage checkpoint signaling (Kondo et al., 1999, Majka and Burgers, 2003), and are considered to be upstream of Rad9p and Chk1p (Figure 3-1a). However, *CHK1* and *RAD9*, which are central components of the intra-S and DNA damage checkpoint pathways, were not identified as hits in our screen. This surprising result was confirmed by analysis in a separate strain background. *DDC1*, *RAD17*, *MEC3* and *TEL1*, while not strong hits from our SGA screen, were verified to have a significantly elevated level of blebbing when also deleted in this background. Thus, while we have demonstrated that some checkpoint proteins mediate DNA stability in stationary phase cells, our data argue that specific checkpoint pathways, or the interactions between

those checkpoint components, are significantly different in stationary phase cells than in actively growing cells.

A subsequent analysis of essential checkpoint gene mutants reinforced this finding. In actively growing cells, the essential Mec1 protein is upstream of the essential Rad53 protein in the replication checkpoint pathway and in the intra-S and DNA damage pathways (Figure 3-1a) (Branzei and Foiani, 2006). However, our results show that *MEC1* and *RAD53* do not fall within the same genetic pathway, suggesting that Mec1p is not actively signaling a Rad53p checkpoint pathway in stationary phase cells with respect to minisatellite stability (Figure 3-5b, 3-5c). This observation is unlike the previously characterized roles of Mec1p in dividing cells and even in oxidative repair-deficient stationary phase cells in which Mec1p is required to activate Rad53p by phosphorylation (Figure 3-1a) (Branzei and Foiani, 2006, Pawar et al., 2009). Some studies have shown that Rad53p does have a Mec1p-independent role in maintaining genomic stability, in which Rad53p monitors histone levels in order to prevent delays in DNA repair synthesis (Gunjan and Verreault, 2003, Dohrmann and Sclafani, 2006). Our work suggests that Rad53p maintains minisatellite stability in stationary phase cells independently of Mec1p. Therefore, Rad53p could be part of an otherwise unidentified checkpoint signaling pathway in stationary phase cells or it could be monitoring histone levels, either of which then influence minisatellite instability.

Pathway analysis of strains bearing mutations in *MRC1*, *CSM3* or *TOF1* provides evidence that all three genes act within the same genetic pathway. This result was not unexpected, as the protein products of each gene form a heterotrimeric complex that

travels with replication forks (Katou et al., 2003, Bando et al., 2009). Based upon the results from our screen and pathway analysis data, we predict that Mrc1p, Csm3p and Tof1p form a complex that associates with replication forks in stationary phase cells. While bulk DNA synthesis does not occur in stationary phase cells, recent work has demonstrated that discrete areas of DNA replication do occur within the genome of stationary phase yeast cells (de Morgan et al., 2010), presumably at regions of localized DNA repair. Therefore, the Mrc1p/Csm3p/Tof1p complex may associate with replication forks at areas of DNA repair and prevent genomic instability through mediating checkpoint signaling in stationary phase cells. Future co-immunoprecipitation assays will help to establish if these three proteins interact in stationary phase cells.

To address whether or not minisatellites are stabilized by the Mrc1p checkpoint or replication function during stationary phase, we assessed the level of blebbing in strains bearing either the *mrc1*^{AQ} allele or the *mrc1-C14* allele (Figure 3-6a) (Osborn and Elledge, 2003, Naylor et al., 2009). Our data show that the level of blebbing in a strain bearing the Mrc1p checkpoint loss-of-function allele *mrc1*^{AQ} is not drastically higher than that of the WT strain. This indicates that even in the absence of proper checkpoint signaling, the minisatellite is still predominantly stable. In contrast, the level of blebbing in a strain bearing the Mrc1p loss of replicative function allele, *mrc1-C14*, is significantly greater than the WT strain. Together, these results indicate that Mrc1p stabilizes minisatellites in stationary phase cells largely through its replicative function rather than through mediating checkpoint signaling.

In support of this hypothesis, our pathway analysis of *MRC1*, *MEC1* and *RAD53* shows that *MRC1* does not fall within the same genetic pathway as *MEC1* or *RAD53* in stationary phase cells (Figure 3-5b, 3-5c). Similarly, our data demonstrating that *MEC1* and *RAD53* do not lie in the same pathway supports the possibility that the characterized replication checkpoint - in which Mec1p is recruited to the replication fork and activates Rad53p via Mrc1p (Figure 3-1a) (Alcasabas et al., 2001, Osborn and Elledge, 2003, Chen and Zhou, 2009, Naylor et al., 2009) - is not participating in stabilizing minisatellites in stationary phase cells. Therefore, we suggest Mrc1p prevents minisatellite rearrangements in stationary phase cells by maintaining replicative function rather than by promoting checkpoint signaling via a Rad53p signaling pathway (Figure 3-6a); we cannot rule out the possibility that Mrc1p is mediating checkpoint signaling through an as yet unidentified pathway, however.

Interestingly, a strain bearing both the $mrc1^{AQ}$ and *mrc1-C14* deletions did not result in a level of blebbing equivalent to that of the *mrc1*Δ deletion strain (Figure 3-6a). This could be due to either of the following possibilities: 1) The bulk of the Mrc1 protein is still intact and stabilizes the minisatellite through being physically present or 2) A secondary backup pathway is activated when Mrc1p function is aberrant thereby preventing the minisatellite from undergoing further alterations. The second possibility could account for the suppression of minisatellite instability displayed by our strain bearing the $mrc1^{AQ}$ allele.

It was previously demonstrated that Mrc1p and the DNA damage checkpoint protein Rad9p are functionally redundant, suggesting that the Rad9p pathway is activated

in strains bearing mutant Mrc1p (Alcasabas et al., 2001, Osborn and Elledge, 2003). To determine if a Rad9p pathway is initiated in stationary phase cells bearing checkpoint-defective Mrc1p, we assessed the level of blebbing produced by the mutant strain *mrc1*^{AQ} *rad9*Δ. Despite the finding that *RAD9* deletion by itself does not appear to affect minisatellite stability, deletion of *RAD9* in an *mrc1*^{AQ} background results in a synergistic increase in the level of blebbing, demonstrating that a secondary Rad9p - dependent signaling pathway is activated in stationary phase cells to prevent minisatellite instability when Mrc1p checkpoint signaling is compromised.

To determine how many independent pathways regulate minisatellite instability in stationary phase cells, we constructed strains bearing mutations in *MRC1*, *MEC1*, *RAD53* or *RAD17* and several genes we previously identified as stabilizing the *ade2-min3* construct (Kelly et al., 2007, Kelly et al., 2011, Kelly et al., 2012). Our results reveal that there are three distinct pathways that stabilize minisatellites in yeast cells in stationary phase (Figure 3-1b). The first two of these pathways are the *MRC1*/*CSM3*/*TOF1* pathway and the *RAD53*/*ZRT1*/*RAD17*/*RAD27* pathway. Interestingly, *PKC1* and *END3* appear to act in both pathways. The final pathway consists of *MEC1*, *ZRT1*, *PKC1* and *END3* but does not contain *RAD17* or *RAD27*. These data provide further evidence that *MRC1*, *MEC1* and *RAD53* act in separate pathways in stationary phase cells and suggest that Mec1p is not activated through the presence of an intact clamp as in the established checkpoint pathway. Thus, like Rad53p, Mec1p may not be functioning in a checkpoint-dependent signaling pathway or may be participating in an as yet unidentified pathway in stationary phase yeast cells.

A common element of all of the mutants with a strong blebbing phenotype is an involvement in ssDNA metabolism; accumulation of ssDNA could act as a template for minisatellite instability in stationary phase cells. *MRC1*, *CSM3* and *TOF1* promote genomic stability by preventing fork uncoupling and mediating checkpoint signaling in the presence of ssDNA in mitotic cells (Osborn and Elledge, 2003, Bando et al., 2009, Chen and Zhou, 2009, Naylor et al., 2009). *RAD27*, *ZRT1*, *END3*, *RAD53* and *PKC1* are also important in preventing the accumulation of ssDNA. Deletion of *RAD27* results in unprocessed Okazaki fragments and an increase in ssDNA (Kokoska et al., 1998, Lopes et al., 2006). Strains bearing a deletion of *END3* have been shown to produce an increase in ROS (Gourlay and Ayscough, 2006). Similarly, mutations in *RAD53* or *PKC1* result in cells that are susceptible to oxidative stress which can then accumulate ROS (Leroy et al., 2001, Haghnazari and Heyer, 2004, Pujol et al., 2009). Previous studies have shown that an increase in reactive oxygen species (ROS) in yeast cells results in the accumulation of ssDNA and repetitive DNA instability (Jackson et al., 1998, Gourlay and Ayscough, 2006). Our lab recently demonstrated that increased *ade2-min3* blebbing in an *END3* mutant is correlated with an increase in ROS, and a suppressor mutation that reduces the level of blebbing also reduces the level of ROS in the cells (Kelly et al., 2012). Two models are possible from our results – either the *MRC1*/*CSM3*/*TOF1, MEC1/ZRT1* and the *RAD53*/*ZRT1*/*RAD27*/ *RAD17* pathways are independent but acted upon by *PKC1* and *END3* (as shown in Figure 3-1b) or they are branches of a uniform pathway containing *PKC1* and *END3*. In either case, we propose that the primary lesion leading to

minisatellite instability in stationary phase cells is ssDNA formation, and that G_0 cells possess multiple methods for dealing with ssDNA.

To address whether or not an accumulation of ssDNA could be an intermediate of minisatellite instability in stationary phase cells, we quantified the level of blebbing in strains bearing a recombination-defective allele of the ssDNA-binding RPA subunit *RFA1* (*rfa-t11*) (Umezu et al., 1998). We found that the *rfa1-t11* mutation, by itself, does not appear to affect minisatellite instability. However, strains bearing the *rfa1-t11* allele along with deletions of *MRC1* or *ZRT1* displayed a 50% reduction in the level of minisatellite alterations when compared to either single mutant. Thus, loss of the recombination-associated function of *RFA1* results in a partial suppression of the minisatellite alterations in *mrc1*Δ or *zrt1*Δ mutant strains. Based upon our results, we suggest that Rfa1p-initiated recombination mediates a portion of the minisatellite alterations exhibited in strains bearing a deletion of *MRC1* or *ZRT1*. The *rfa1-t11* results support our proposal that stationary phase minisatellite alteration events could result from a failure to repair accumulated ssDNA nicks or gaps. As we have previously discovered that minisatellite alterations are dependent up key recombination factors *RAD52*, *RAD51* and *RAD50* (Kelly et al., 2011), future pathway analysis of the *rfa1-t11* allele in combination with deletions of each recombination factor would provide insight into the mechanism of minisatellite alteration associated with *RPA1*.

A few other checkpoint genes exhibited a moderately strong phenotype in our screens, but have not been analyzed further yet, including *SLI15*, *IPL1*, *CEP3* and *RFC4*. *SLI15* and *IPL1* encode for components of the aurora kinase complex that is involved in

the spindle checkpoint, along with *BIR1* and *NBL1* (reviewed in (Ruchaud et al., 2007)). We note that the essential genes *BIR1* and *NBL1* were not present in our set. The role that *SLI15* and *IPL1* are playing in stationary phase cells is not apparent, although *CEP3* (an essential kinetochore component (Lechner and Carbon, 1991, Strunnikov et al., 1995) may be functioning in a similar manner. As *RFC4* encodes a component of Replication Factor C (Cullmann et al., 1995), it may be involved in a replication step of DNA repair events or it may interact with the *MRC1*/*CSM3*/*TOF1* pathway. Given the outcome of our analysis of *BUB3*, it is possible that any or all of these may be false positives.

Finally, we were interested in the state of the stationary phase cells that were undergoing minisatellite alterations. Stationary phase cultures of yeast cells consist of a non-dividing quiescent cell population and a slow-dividing nonquiescent population of cells (Allen et al., 2006, Aragon et al., 2008). To determine if minisatellite alterations occurred within the true quiescent cell population of stationary phase cells, we constructed double mutants bearing a deletion of *ETR1* or *POR1* in a checkpoint mutant background, as deletion of *ETR1* reduces the reproductive capacity of quiescent cells while deletion of *POR1* has the same effect in nonquiescent cells (Aragon et al., 2008). We found that loss of *ETR1* in all checkpoint strain backgrounds eliminated blebbing in each of these strains, indicating that the majority of the stationary phase alterations are occurring in the quiescent cell population. In comparison, deletion of *POR1* in the majority of strain backgrounds resulted in only a partial decrease in blebbing. The small effect of *POR1* deletion on blebbing in the checkpoint mutants may be explained by the role that checkpoint proteins play in dividing cells – even slowly-dividing nonquiescent

cells that are ostensibly in G_0. Intriguingly, the effect of *POR1* deletion was stronger in the checkpoint mutants *mec1-21* and *rad53-1* in which the level of blebbing was similar to that of the wild-type strain. This result suggests that minisatellite alterations occurring within a *mec1-21* or *rad53-1* strain arise in both non-dividing quiescent cells and dividing cells, consistent with the color segregation phenotype of each strain in which blebbing and sectoring are present together (Figure 3-2b).

In conclusion, our work demonstrates that several checkpoint signaling components may be active during stationary phase and function to prevent the instability of minisatellites. However, the pathways and interactions found in stationary phase cells differ significantly from those found in actively dividing cells. We hypothesize that the stationary-phase checkpoint pathways work to prevent the accumulation of ssDNA that leads to genomic instability in stationary phase cells.

Data Contribution

We thank Dr. Duncan Clarke (pDC369, DCY2556 and DCY2557), Dr. Steve Elledge (Y2298 and Y2544), Dr. Deanna Koepp (DKY2563) and Dr. Richard Kolodner (pKU1-t11) for the corresponding strains listed in parenthesis. We are grateful to Dr. Charlie Boone and Dr. Robin Wright for the yeast haploid strain sets.

We thank Pete Jauert for constructing the SGA query strains and Dr. Katy Kelly for constructing the following strains: DTK271, DTK878, DTK1008, DTK1088, DTK1093, DTK1170, DTK1171, DTK1199, DTK1217, DTK1219, DTK1270 DTK1272, DTK1279, DTK1295, DTK1360 and DTK1361.

Figure 3-1.

Summary of the Arrangement of Checkpoint-Associated Factors in Mitotic and Stationary Phase Pathways.

(a) In *Saccharomyces cerevisiae*, several checkpoints regulate cell cycle progression to ensure that DNA damage or errors made during replication or mitosis can be effectively repaired. These checkpoints include the replication checkpoint, intra-S-phase checkpoint, DNA damage checkpoints and the mitotic checkpoint. Each utilizes several pathways to signal and activate cell cycle arrest. **(b)** In stationary phase G_0 cells, only a subset of checkpoint proteins have roles in maintaining DNA stability. Genes overlaid with an X are not active in G_0 in the indicated pathway. Genes shown in bold exhibit the strongest phenotype. Question marks designate speculative interactions or pathways. The pathway denoted in grey dotted lines represents a Rad9p-dependent back-up pathway that is activated when Mrc1p function is compromised.

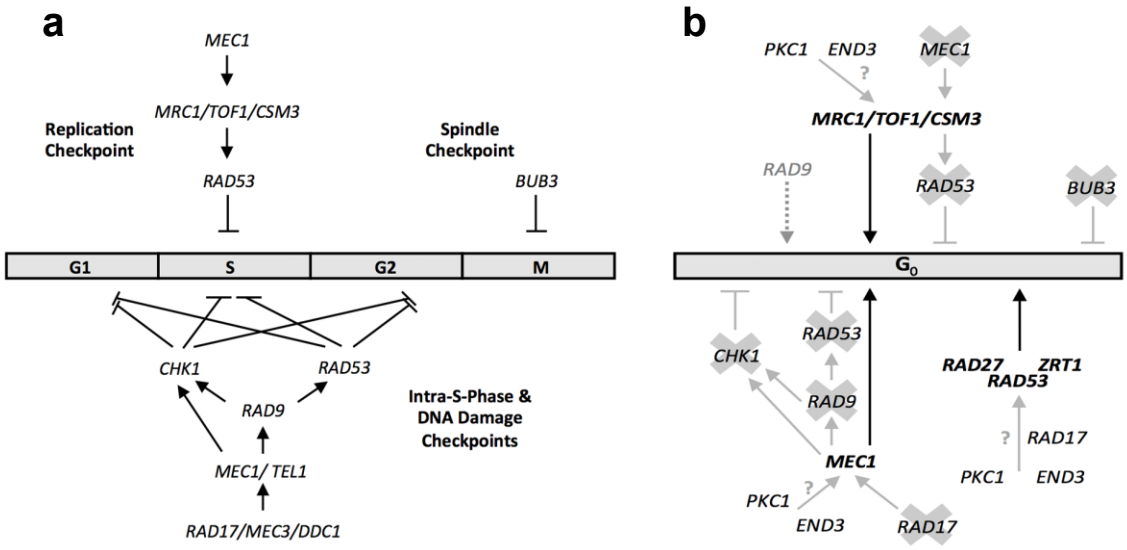

Figure 3-2.

Colony Morphology of Strains Bearing the *ade2-min3* Allele.

Each strain was streaked onto solid YPD media and incubated at 30°C for two days, then left at RT for six days. **(a)** The *ade2-min3* allele consists of three tandem 20bp repeats plus one additional base inserted into the *ADE2* gene at the *Xba*I site, producing a 5bp overhang (ACTAG) at the site of insertion and throwing the *ADE2* gene out of frame. The deletion of one repeat unit or the addition of two repeat units restores the *ADE2* open reading frame (Kelly et al., 2007, Kelly et al., 2011). **(b)** Strains bearing the *ade2-min3* allele display a variety of blebbing phenotype. Strains *mec1-21* and *rad53-1* display both blebbing and sectoring phenotypes.

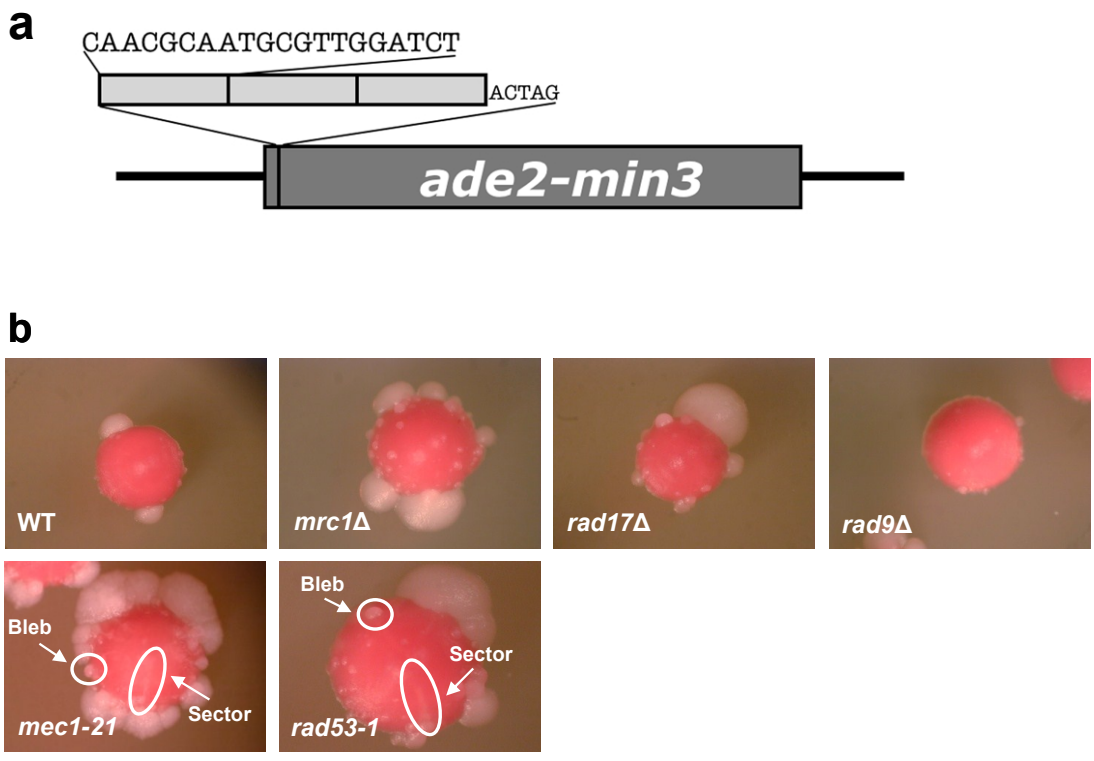

Figure 3-3.

Several Checkpoint Components Stabilize Minisatellites During Stationary Phase. **(a)** YPD cultures inoculated with a single red colony from each strain were grown for four hours at 30°C. Each culture was diluted and plated onto solid YPD media then incubated at 30°C for two days. Strains were then left at RT for six days. Blebs were counted on 100 colonies, and the average number of blebs/colony +/- 95% CI was calculated. This was repeated three times independently. The solid black horizontal line indicates the average number of blebs/colony of the WT strain. **(b)** Blebbing quantification of a *BUB3* deletion in DTK271, DTK11895a and BY4742 strain backgrounds.

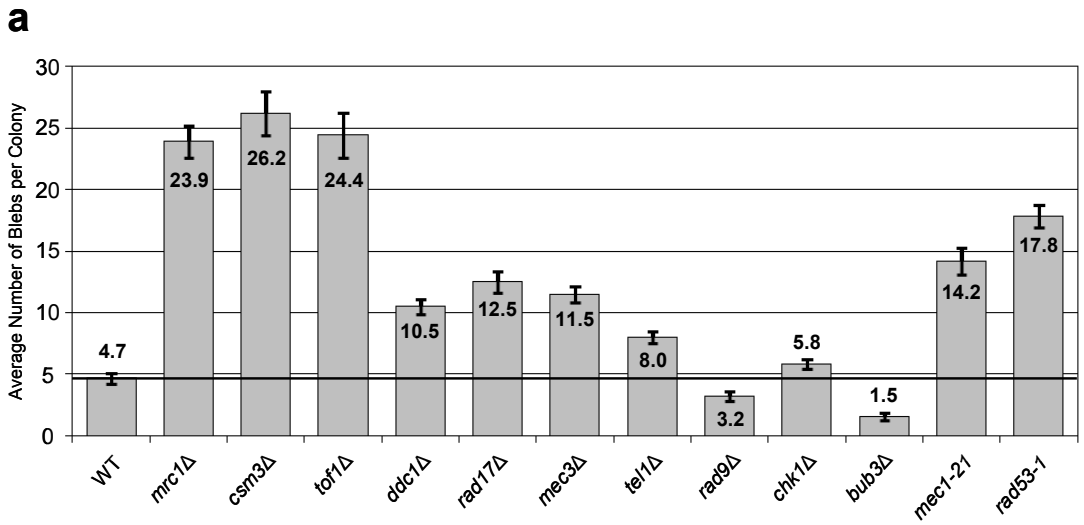

b

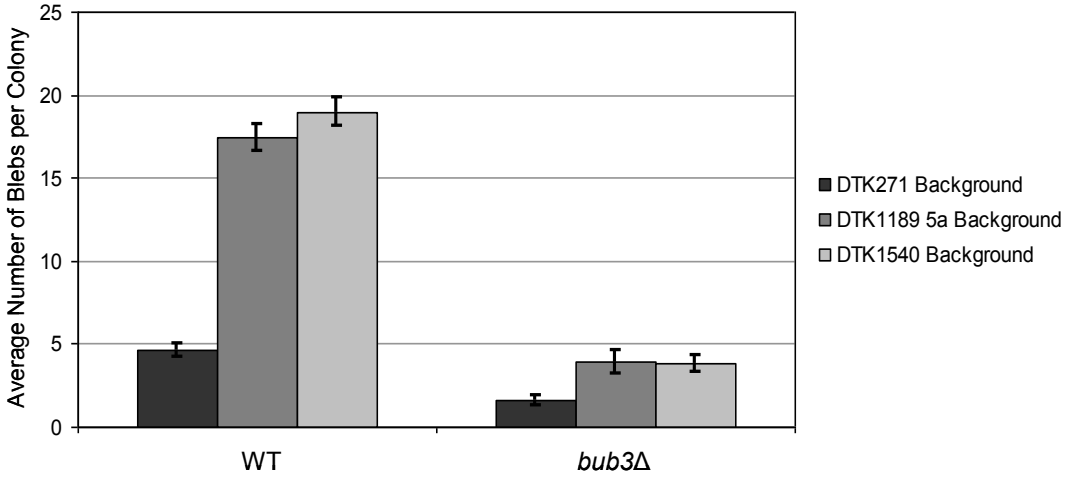
Average Number of Blebs per Colony
25
20
15
10
5
0
WT
bub3Δ
DTK271 Background
DTK1189 5a Background
DTK1540 Background

Figure 3-4.

Minisatellite Alterations Occur in Quiescent Cells in Checkpoint Mutants

Loss of *ETR1* will eliminate blebbing in quiescent G_0 cells, while loss of *POR1* affects non-quiescent G_0 cells. The blebbing frequency was quantified as described in Chapter VII: Materials and Methods and in Figure 2-3.

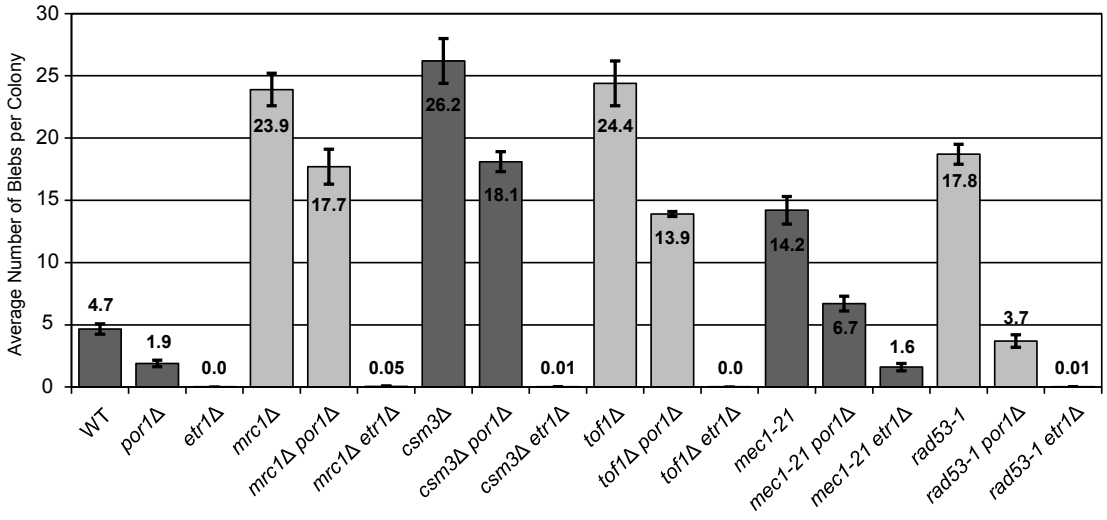

Figure 3-5.

Independent Pathways Regulate Minisatellite Stability During Stationary Phase

The blebbing frequency was scored as described in Chapter VII: Materials and Methods and Figure 3. Strains bearing the *pkc1-4* mutation were grown at 35°C for six days before the number of blebs was counted. **(a)** *ZRT1*-dependent pathway analysis. **(b)** Placement of *MRC1*, *MEC1*, *RAD53* and *RAD17* into pathways. **(c)** The photos depict the blebbing phenotype of single mutants and double mutant strains. **(d)** *RAD27* pathway analysis. **(e)** *PKC1* pathway analysis. **(f)** *END3* pathway analysis. The solid black horizontal line indicates the average number of blebs/colony of the strains *zrt1*Δ (a), *rad27*Δ (d), *pkc1-4* (e) or *end3*Δ (f).

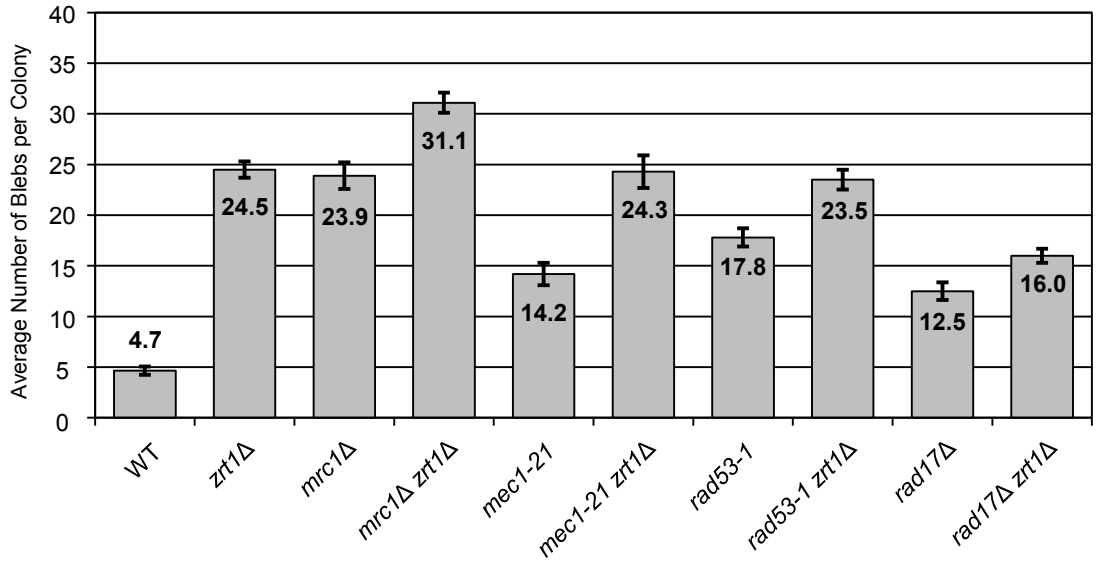

b

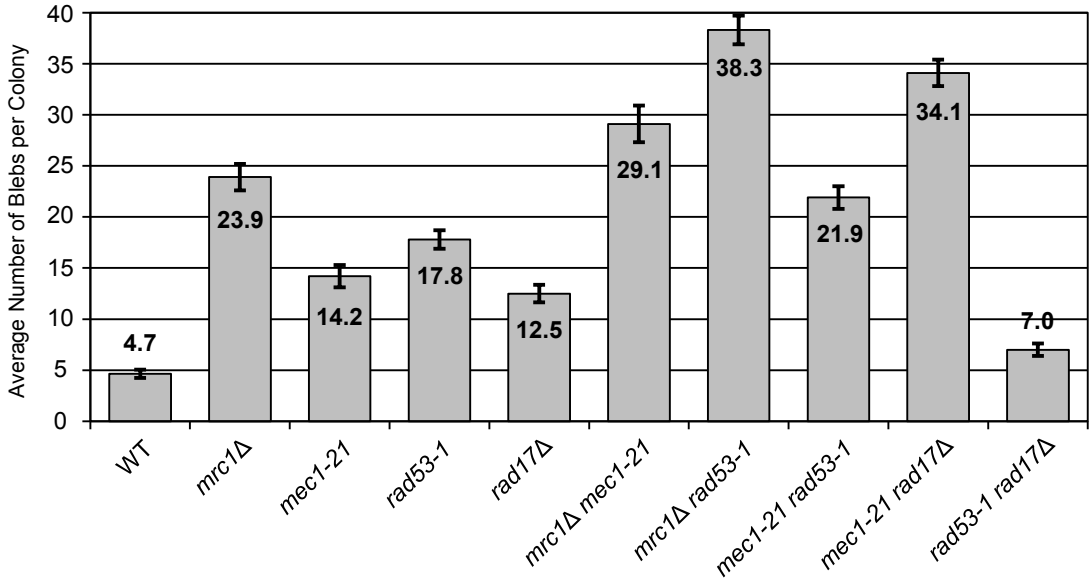
Average Number of Blebs per Colony
40
35
30
25
20
15
10
5
0
4.7
23.9
14.2
17.8
12.5
29.1
38.3
21.9
34.1
7.0
WT
mrc1Δ
mec1-21
rad53-1
rad17Δ
mrc1Δ mec1-21
mrc1Δ rad53-1
mec1-21 rad53-1
mec1-21 rad17Δ
rad53-1 rad17Δ

c

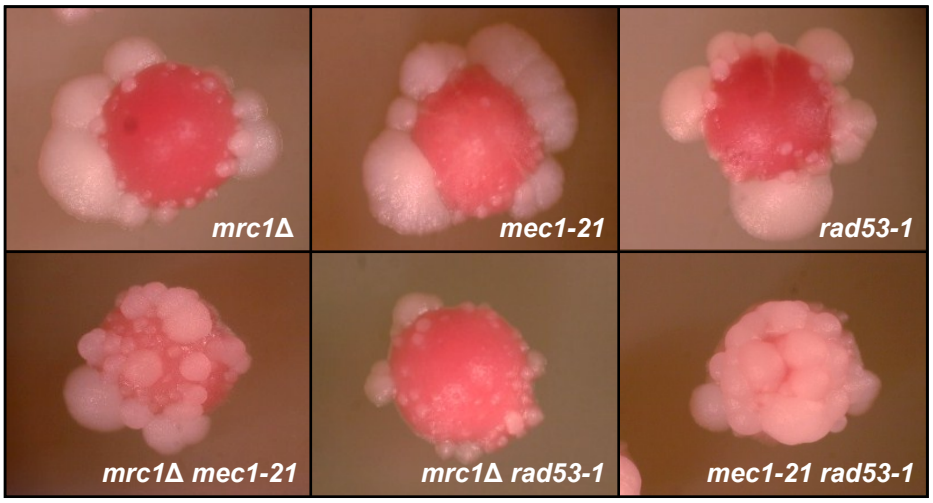
mrc1Δ
mec1-21
rad53-1
mrc1Δ mec1-21
mrc1Δ rad53-1
mec1-21 rad53-1

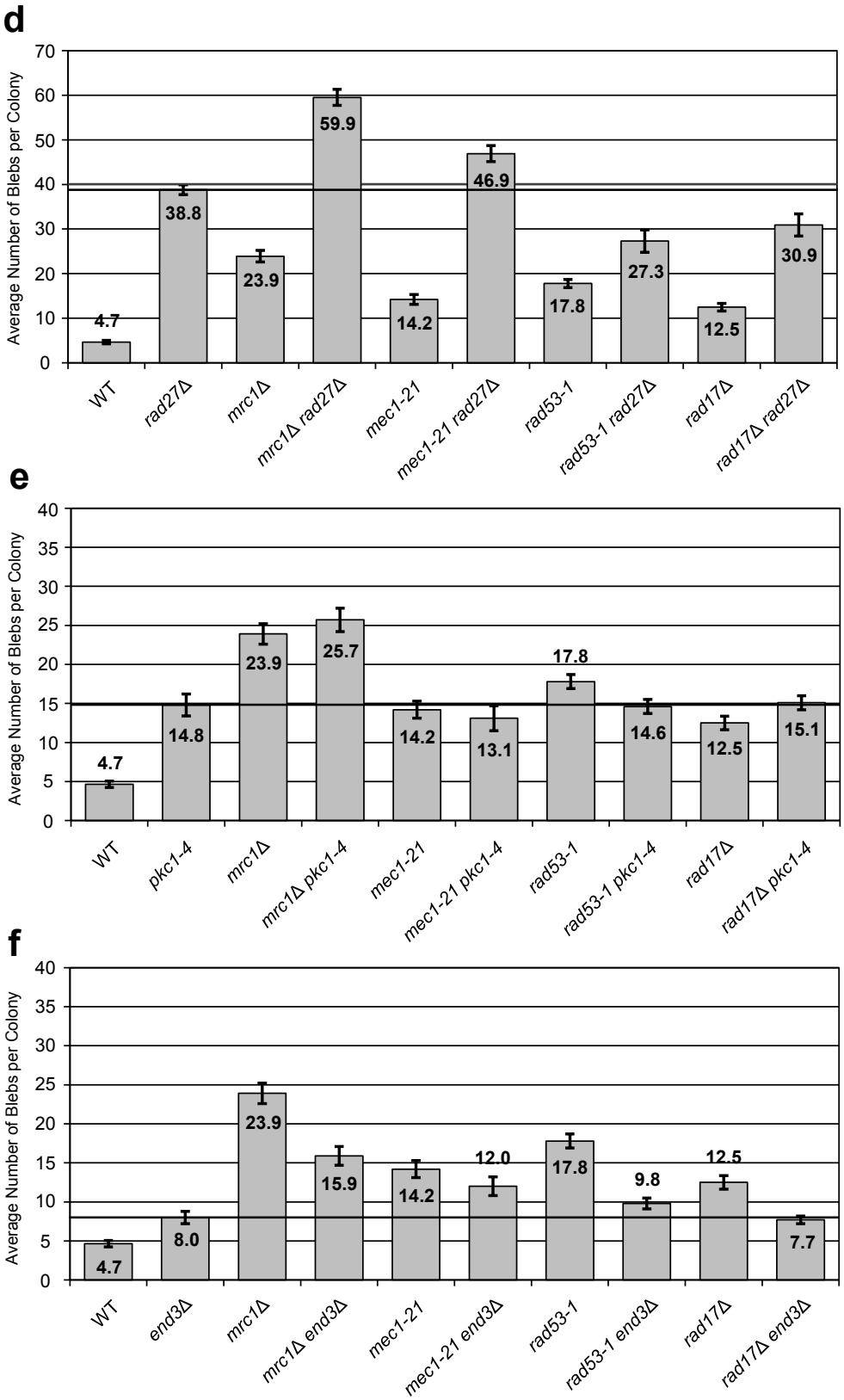
d
Average Number of Blebs per Colony
70
60
50
40
30
20
10
0
4.7
38.8
23.9
59.9
14.2
46.9
17.8
27.3
12.5
30.9
WT
rad27Δ
mrc1Δ
mrc1Δ rad27Δ
mec1-21
mec1-21 rad27Δ
rad53-1
rad53-1 rad27Δ
rad17Δ
rad17Δ rad27Δ
e
Average Number of Blebs per Colony
40
35
30
25
20
15
10
5
0
4.7
14.8
23.9
25.7
14.2
13.1
17.8
14.6
12.5
15.1
WT
pkc1-4
mrc1Δ
mrc1Δ pkc1-4
mec1-21
mec1-21 pkc1-4
rad53-1
rad53-1 pkc1-4
rad17Δ
rad17Δ pkc1-4
f
Average Number of Blebs per Colony
40
35
30
25
20
15
10
5
0
4.7
8.0
23.9
15.9
14.2
12.0
17.8
9.8
12.5
7.7
WT
end3Δ
mrc1Δ
mrc1Δ end3Δ
mec1-21
mec1-21 end3Δ
rad53-1
rad53-1 end3Δ
rad17Δ
rad17Δ end3Δ

Figure 3-6.

Blebbing Characteristics Differ Among Strains Bearing the *ade-min3* Allele

(a) Bleb quantification was performed as described in Chapter VII: Materials and Methods and Figure 3. With the exception that strains were left at RT for three days or six days before the number of blebs were counted. **(b)** Individual blebs were isolated from each mutant strain and used to inoculate a YPD culture. Growth curves were generated for each diluted culture as stated in Materials and Methods. The graph shows the average OD_{600} of bleb culture for each strain taken at 15 minute intervals over the course of 30 hours. Growth rates were generated for each strain by calculating the linear slope of the line of data taken from timepoints 7 - 13 hours. Long Dash/Two Dot Line = DTK271. Dashed Line = DTK878. Solid Line = DTK1392. Dotted Line = DTK1556.

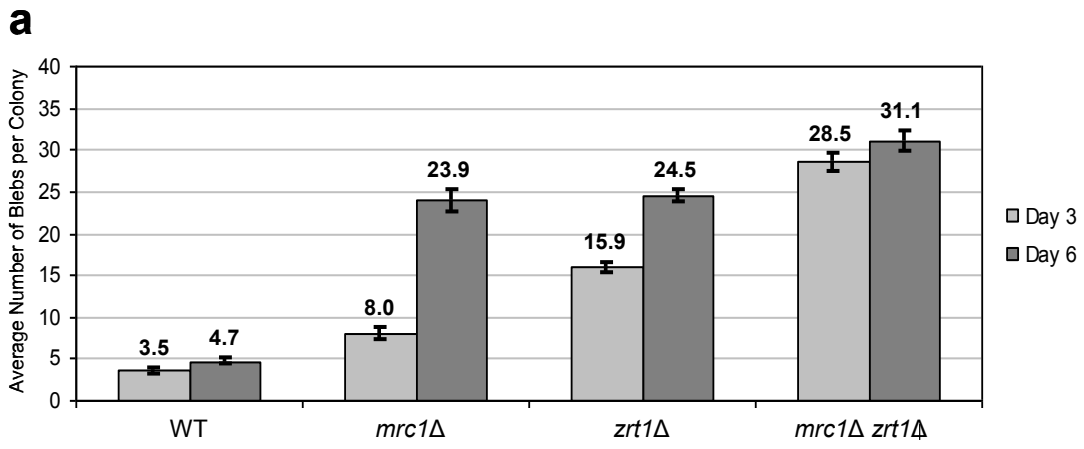

b

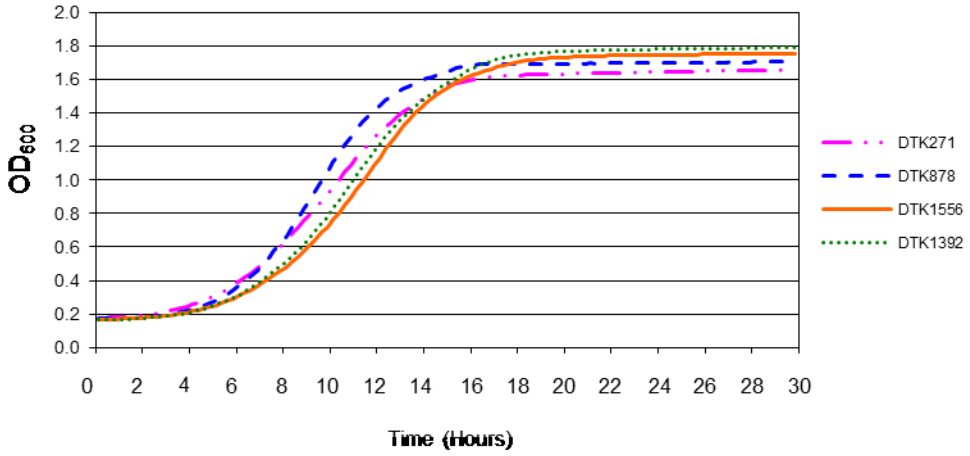

Strain	Growth Rate (OD_{600}/ Hour)
DTK217 (WT)	0.0396
DTK1392 (*mrc1Δ*)	0.0395
DTK878 (*zrt1Δ*)	0.0479
DTK1556 (*mrc1Δ zrt1Δ*)	0.0426

Figure 3-7.

Characterization of the Role of Mrc1p in Stationary Phase Cells

Bleb quantification experiments were performed for each strain as described in Chapter VII: Materials and Methods and Figure 3. **(a)** Analysis of Mrc1p separation-of-function mutant strains bearing *ade2-min3*. **(b)** Stationary phase specificity of Mrc1p separation-of-function mutants.

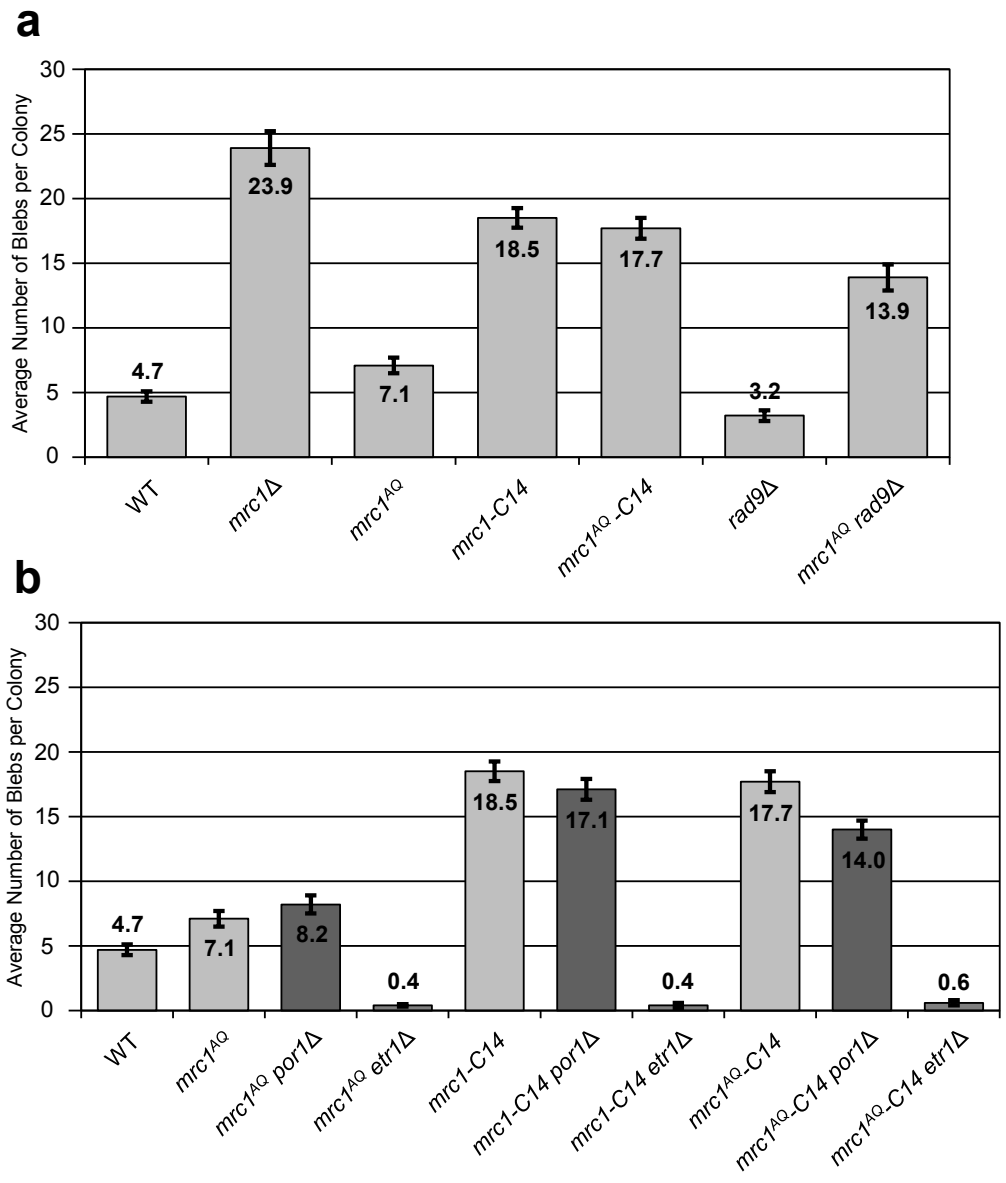

Table 3-1: Blebbing Phenotypes of Checkpoint-Annotated Genes

Gene	ORF	Blebbing Score	Gene	ORF	Blebbing Score	Gene	ORF	Blebbing Score
AME1*	YBR211C	+	*GIN4*	YDR507C	+	*RAD24*	YER173W	++
AMN1	YBR158W	+	***GLC7***	YER133W	+	***RAD53***	YPL153C	NA
BFA1	YJR053W	+	*HHT1*	YBR010W	++	*RAD6*	YGL058W	+
BIR1	YJR089W	NA	*HHT2*	YNL031C	++	*RAD9*	YDR217C	+
BMH1	YER177W	++	*HOP1*	YIL072W	++	*RCK1*	YGL158W	+
BMH2	YDR099W	+	*HSL1*	YKL101W	+	*RCK2*	YLR248W	+
BRE1	YDL074C	+	*HUG1*	YML058W-A	NA	*RED1*	YLR263W	++
BUB1	YGR188C	+	*IBD2*	YNL164C	NA	***RFC4***	YJR068W	+++
BUB2	YMR055C	+	*IES4*	YOR189W	++	*RFX1*	YLR176C	+
BUB3	YOR026W	+++	***IPL1***	YPL209C	+++	*RNR1*	YER070W	no growth
CCR4	YAL021C	+	*KCC4*	YCL024W	++	***RNR2***	YJL026W	NA
CDC25	YLR310C	+	*KEM1*	YGL173C	+	*RNR3*	YIL066C	++
CDC55	YGL190C	NA	*KIN4*	YOR233W	++	*RNR4*	YGR180C	++
CEP3	YMR168C	+++	***LCD1***	YDR499W	NA	*RTS1*	YOR014W	+
CHK1	YBR274W	+	*LTE1*	YAL024C	+	***SDA1***	YGR245C	++
CSM3	YMR048W	+++	*MAD1*	YGL086W	++	*SGO1*	YOR073W	+
CTF18	YMR078C	+	*MAD2*	YJL030W	++	*SGS1*	YMR190C	+
DCR2	YLR361C	+	*MAD3*	YJL013C	++	***SLI15***	YBR156C	+++
DDC1	YPL194W	++	***MEC1***	YBR136W	NA	***SPC105***	YGL093W	+
DDI1	YER143W	++	*MEC3*	YLR288C	++	***SPC24***	YMR117C	+
DMA1	YHR115C	+	*MEK1*	YOR351C	++	***SPC25***	YER018C	+
DMA2	YNL116W	++	***MPS1***	YDL028C	++	*SPC72*	YAL047C	+
DOT1	YDR440W	+	*MRC1*	YCL061C	+++	*SUM1*	YDR310C	+
DPB11	YJL090C	++	***NBL1***	YHR199C	NA	*SWE1*	YJL187C	+
DUN1	YDL101C	++	***NUF2***	YOL069W	+	*TEL1*	YBL088C	++
ELM1	YKL048C	+	*NUP53*	YMR153W	+	***TID3***	YIL144W	+

Gene	ORF	Blebbing Score	Gene	ORF	Blebbing Score	Gene	ORF	Blebbing Score
EOS1	YNL080C	++	*PCH2*	YBR186W	++	*TOF1*	YNL273W	+++
ESC2	YDR363W	++	*PIN4*	YBL051C	+	***TOP2***	YNL088W	NA
FIN1	YDR130C	+	*PPH21*	YDL134C	+	*TSA1*	YML028W	+
FPR3	YML074C	+	*PPH22*	YDL188C	++	***ULP2***	YIL031W	NA
GAC1	YOR178C	+	*PTC2*	YER089C	+	*XRS2*	YDR369C	+
GCN2	YDR283C	+	*PTC3*	YBL056W	+	*ZDS1*	YMR273C	+
GID8	YMR135C	+	*RAD17*	YOR368W	++	*ZDS2*	YML109W	+

* Essential genes are in bold typeface. Blebbing scores ranged from + (little/none) to ++++ (highest level)

NA: These genes were not included in our Nonessential Deletion Haploid Set or our Essential Temperature Sensitive Haploid Set.

Chapter IV

The Mechanism of Stationary Phase Minisatellite Alteration in Replication Checkpoint Mutants is Dependent upon Recombination and Nucleotide Availability

Chapter Summary

Minisatellites are a type of tandem repetitive DNA found within the human genome. Rare alleles of minisatellites have been correlated to an increased risk of several types of human diseases. At present, little is known about how minisatellites undergo alterations within a non-dividing cellular population and become potential pathogenic alleles. We previously developed a color segregation assay to monitor minisatellite instability in the yeast *Saccharomyces cerevisiae*, and found that minisatellite alterations occurring in stationary phase give rise to a blebbing phenotype in which white microcolonies form on the surface of a red colony. In the previous chapters, we found that the deletion of the replication-associated genes *MRC1*, *CSM3* and *TOF1* resulted in a high level of blebbing indicating their presence is required to prevent minisatellite instability in stationary phase cells. Here, we utilize the color segregation assay to study potential mechanisms that give rise to repeat instability in stationary phase cells. We find that tract alterations within an *mrc1*Δ strain are primarily mediated by recombination-dependent mechanisms. We further show that depletion of nucleotide pools results in a high level of stationary phase minisatellite instability. Thus, our work implicates recombination as well as aberrant replication - through loss of nucleotide availability - as mechanisms for repeat tract alterations in non-dividing cells.

Introduction

A specific type of repetitive element within the human genome is known as a minisatellite. Of particular interest is gaining an understanding of the mechanisms that drive minisatellite instability. This is due to previous studies identifying a correlation between rare alleles of these repetitive sequences and an increased risk of developing several diseases such as myoclonus epilepsy (Lafreniere et al., 1997, Virtaneva et al., 1997), coronary artery disease (Wu et al., 1996, Rebhi et al., 2008) and many different forms of cancer (Krontiris, 1995, Calvo et al., 1998, Rosell et al., 1999, Weitzel et al., 2000, Vega et al., 2001). Currently, we and others hypothesize that disease-associated minisatellite alleles are derived from common alleles that are established within the human population.

Several mechanisms of minisatellite alteration have been identified in meiotic and mitotic cells. Hypermutable germline mutations have been shown to occur when minisatellites are adjacent to recombination hotspots (Monckton et al., 1994, Buard et al., 2000). Complex inter- and intra-allelic recombination events were observed within germ cell minisatellites (Jeffreys et al., 1998) (reviewed in (Richard et al., 2008)). In contrast, the majority of mitotic alterations are thought to occur as a result of replication slippage (Jeffreys and Neumann, 1997). At present, little is known about how repeat alteration events are generated within non-dividing cells.

To study minisatellite alterations, we previously developed a color segregation assay utilizing the yeast *S. cerevisiae* (Kelly et al., 2007, Kelly et al., 2011, Kelly et al., 2012). For this assay, a minisatellite consisting of three identical repeats with a 5bp linker

has been inserted into the *ADE2* (the *ade2-min3* allele) resulting in red Ade^- cells. Alterations occurring within the minisatellite during stationary phase result in the change of red to white Ade^+ cells that form blebs.

Previously, we identified that the blebbing phenotype produced by several mutant strains was dependent upon homologous recombination pathways (Kelly et al., 2011). We found that *ade2-min3* minisatellite alterations within a wild-type strain or a zinc homeostasis mutant, *zrt1*Δ, were mediated by *RAD2*-dependent and *RAD52*-independent recombination pathways. A dependence upon recombination pathways was also found in the previously characterized blebbing strains bearing a deletion of the actin organization and endocytosis gene, *END3* , or a temperature-sensitive allele of *PKC1*, a gene that encodes for a serene/threonine Protein Kinase C homolog (Levin et al., 1990, Kelly et al., 2012). Therefore, we predict that a recombination-dependent mechanism gives rise to stationary phase specific minisatellite alterations mediated by the recombination factors Rad50p, Rad51p or Rad52p.

In Chapter 2, we identified over 100 factors that prevent minisatellite alterations from taking place in stationary phase cells using a whole-genome screen known as the Synthetic Genetic Array (SGA) analysis. Included were several genes associated with DNA replication. Further characterization of the replication pausing complex genes, *MRC1*, *CSM3* and *TOF1*, in Chapter 3 revealed that these genes prevent minisatellite instability primarily through maintaining proper replicative function. Our results suggest that aberrant replication could act as an additional mechanism for minisatellite alterations in stationary phase yeast cells.

For this chapter, we investigate the mechanism of minisatellite alterations occurring within stationary phase cells of the mutant strain *ade2-min3 mrc1*Δ. We begin by showing that *MRC1*, C*SM3* and *TOF1* are expressed within quiescent yeast cells. We also show that the tract alterations occurring within an *mrc1*Δ strain are mediated primarily by *RAD52*-dependent recombination pathways and that a portion of these alterations occur through single strand annealing (SSA). Finally, we demonstrate that minisatellite instability in the *mrc1*Δ mutant strain is increased when nucleotide pools are depleted. Therefore, our work shows that stationary phase minisatellite stability depends upon nucleotide availability and proper replication, and that tract alterations occur through recombination-based mechanisms.

Results

Components of the Replication Checkpoint Complex are Expressed in Quiescent Stationary Phase Cells

As described in Chapters 2 and 3, we identified several components associated with the replication checkpoint as factors that stabilize the *ade2-min3* minisatellite in stationary phase cells. These included the replication checkpoint complex genes *MRC1*, *CSM3* and *TOF1* (Katou et al., 2003, Osborn and Elledge, 2003, Bando et al., 2009) which, when mutated, were found to result in a high level of minisatellite instability. We further demonstrated that minisatellite alterations associated with each strain occurred predominantly within the quiescent cell subpopulation of stationary phase cells. Here, we characterize the expression of Mrc1p, Csm3p and Tof1p in stationary phase cells.

Previously, the Werner-Washburne group discovered that stationary phase cultures of yeast are composed of true non-dividing, or quiescent (Q) cells as well as a slowly dividing population of nonquiescent (NQ) cells (Allen et al., 2006, Aragon et al., 2008). For this chapter, we utilized a modified Percoll density-gradient centrifugation assay developed by the Werner-Washburne laboratory to separate stationary phase quiescent and nonquiescent cells of the wild-type strain, DTK1657, bearing the *ade2-min3* allele. Centrifugation of stationary phase cultures produced upper and lower bands of cells which, according to Allen et al., 2006 and Aragon, et al. 2008, represent nonquiescent and quiescent cells, respectively (Figure 4-1a). To verify the cellular composition of each fraction, we monitored the cell-cycle re-entry of cells from upper and lower fractions by counting the number of budding cells over the course of time (Figure 4-1b). A characteristic of quiescent cells is their synchronous re-entry from G_0 into the cell cycle (Allen et al., 2006). We found that the lower fraction re-entered the cell cycle and began budding in a homogeneous fashion while that of the upper fraction did not. Thus, the lower fraction consists of quiescent cells while the upper is comprised of nonquiescent cells. We also performed whole cell counts of upper and lower fractions collected after 48 hours (hrs.) and 120 hrs. (Figure 4-1c). These timepoints corresponded to the diauxic shift and stationary phase, respectively. We found that in our strain background, stationary phase cultures primarily consist of quiescent cells (a ratio of 100:1; Q:NQ). Finally, cells from both upper and lower fractions were collected after 120 hrs. and incubated on YPD plates. Both fractions consisted of red cells.

To further characterize each cellular fraction, we monitored the expression of a 3HA-tagged acetyl-coA synthetase (Acs1p) in the DTK1657 strain background after harvesting cells via Percoll density-gradient centrifugation at timepoints 18 hrs., 48 hrs., and 120 hrs. (De Virgilio et al., 1992). Acs1p was previously characterized by the Werner-Washburne group as being primarily expressed in quiescent cells of stationary phase cultures (Davidson et al., 2011). As expected, we found that Acs1p-3HA was not expressed until cells had entered the diauxic shift at 48 hrs. (We note that a very faint upper band is present at 48 hrs. after density-gradient centrifugation; however, the amount of cells in this fraction was too low to harvest (Figure 4-1a).) The expression of Acs1p-3HA was predominantly in the lower fractions harvested at 48 and 120 hrs. Our results suggest that cell cultures differentiate into quiescent and nonquiescent cells at the diauxic shift (48 hrs.) and that the lower fraction of cells is quiescent.

To determine if Mrc1p, Csm3p and Tof1p are expressed in stationary phase cells, we tagged each protein with 3HA in the DTK1657 strain background (Figure 4-1e). Cells were harvested at the timepoints 18 hrs., 48 hrs. and 120 hrs., subjected to Percoll density-gradient centrifugation and then western blot analysis as above. As expected, each protein is expressed in mitotic cells (18 hrs.) in keeping with the role of Mrc1p, Csm3p and Tof1p in S-phase DNA replication (Katou et al., 2003, Osborn and Elledge, 2003, Bando et al., 2009). We find that each protein is expressed in quiescent cells that are present at the 48 hr. timepoint. Mrc1p and Tof1p bands are present at the 120 hr timepoint that corresponds to stationary phase. We did not see a Csm3p band at the 120 hr. timepoint; however, the Csm3p expression level could be too low to detect using our

current methods. Together our results show that Mrc1p, Csm3p and Tof1p are expressed in quiescent cells, potentially at different timepoints after cells have exited mitotic growth.

Minisatellite Alterations in an ade2-min3 mrc1Δ *Strain are Dependent Upon Homologous Recombination*

In the preceding chapters, we described a novel color segregation assay that allows us to monitor minisatellite alterations within stationary phase cells. Minisatellite tract alterations that occur within stationary phase cells can be detected by monitoring cells for the presence of a blebbing phenotype. As described in Chapters 2 and 3, deletion of *MRC1* resulted in a high level of blebbing compared to the wild-type parental strain indicating that Mrc1p has a role in stationary phase minisatellite stability.

In *S. cerevisiae*, homologous recombination is the primary mechanism of DNA strand exchange and is a source of sequence alteration. Homologous recombination is regulated by a *RAD52*-dependent pathway and a *RAD52*-independent pathway comprised of *RAD50* and *RAD51* (Coic et al., 2008). We previously demonstrated that *ade2-min3* tract alterations occurring in a wild-type or *zrt1*Δ, *end3*Δ or *pkc1-4* mutant strains were dependent upon the recombination genes *RAD50*, *RAD51* or *RAD52* (Kelly et al., 2011, Kelly et al., 2012). In this chapter, we investigate if minisatellite instability in an *mrc1*Δ strain is also dependent upon recombination.

To determine if recombination mediates *ade2-min3* alterations in the *mrc1*Δ mutant, we quantified the number of blebs/colony in strains bearing deletions of *RAD50*,

RAD51 or *RAD52* (Figure 4-2). For each strain, we counted the number of blebs on at least 100 individual colonies and quantified the average number of blebs/colony +/- 95% confidence intervals (CI). Overlapping confidence intervals indicated that the level of blebbing between strains was not significantly different. Deletion of *RAD50* (DTK1594), *RAD51* (DTK1589) or *RAD52* (DTK1621) in the *mrc1*Δ background resulted in a significant decrease in blebbing from 23.9 to 6.4, 11.9 and 2.3 blebs/colony, respectively. Thus, *mrc1*Δ minisatellite alterations are dependent upon each recombination gene with *RAD52* playing a significant role.

To study the independent contributions of *RAD50*, *RAD51* or *RAD52* on *ade2-min3* tract alteration, we constructed pair-wise deletion mutant combinations of each gene in the *mrc1*Δ background. The level of blebbing in a *mrc1*Δ *rad50*Δ *rad52*Δ triple mutant (DTK1646) was reduced to 1.3 blebs/colony, a value significantly lower than either double mutant strain (*mrc1*Δ *rad50*Δ at 6.4 bleb/colony; *mrc1*Δ *rad52*Δ at 2.3blebs/colony). Therefore, both *RAD52*-dependent and *RAD52*-independent mechanisms requiring *RAD50* contribute to tract alterations. Blebbing in a *mrc1*Δ *rad51*Δ *rad52*Δ strain (DTK1647) resulted in 6.8 blebs/colony, a value between that of the double mutants *mrc1*Δ *rad51*Δ 11.9 (blebs/colony) and *mrc1*Δ *rad52*Δ (2.3 blebs/colony). The triple mutant *mrc1*Δ *rad50*Δ *rad51*Δ (DTK1650) produced a level of blebbing significantly lower than either corresponding double mutant at 1.7 blebs/colony vs. 6.4 (*mrc1*Δ *rad50*Δ) and 11.9 (*mrc1*Δ *rad51*Δ) blebs/colony. Finally, blebbing produced by the quadruple mutant, *mrc1*Δ *rad50*Δ *rad51*Δ *rad52*Δ (DTK1648), remained at 1.7 blebs/colony. Together, our results suggest that a *RAD52*-independent pathway featuring

RAD51 does not contribute to *ade2-min3* tract alterations in the presence of wild-type *RAD50*.

Single-Strand Annealing and Nonhomologous End-Joining Contribute to Tract Alterations in an mrc1Δ *Mutant Strain*

Single-strand annealing (SSA) represents an additional *RAD52*-dependent recombination pathway (reviewed in (Symington, 2002)). We previously found that SSA has a role in *ade2-min3* alteration in a *zrt11*Δ mutant strain (Kelly et al., 2011). A major component of the SSA pathway is the DNA repair protein, Rad59p (Petukhova et al., 1999, Davis and Symington, 2001). To determine if *RAD52*-dependent tract alterations in the *mrc1*Δ deletion mutant were influenced by a SSA mechanism, we deleted *RAD59* in the *mrc1*Δ strain background (DTK1739) and quantified the average number of blebs/colony (Figure 4-3). Deletion of *RAD59* resulted in a 50% reduction in the level of blebbing compared to the *mrc1*Δ single mutant, DTK1392 (*mrc1*Δ at 23.9 blebs/colony vs. *mrc1*Δ *rad59*Δ at 13.4 blebs/colony). Therefore, at least some of the *RAD52*-dependent minisatellite alterations in an *mrc1*Δ strain are mediated by SSA.

A second *RAD52*-independent pathway in yeast is known as nonhomologous end-joining (NHEJ) (reviewed in (Symington, 2002)). This DNA repair pathway utilizes the required DNA ligase Dnl4p (Schar et al., 1997, Wilson et al., 1997). To determine if NHEJ mediates *ade2-min3* minisatellite alterations, we deleted *DNL4* in the *mrc1*Δ background (Figure 4-3). The *mrc1*Δ *dnl4*Δ double mutant (DTK1770) showed a 50% decrease in the level of blebbing when compared to the *mrc1*Δ parent strain (*mrc1*Δ at

23.9 blebs/colony vs. *mrc1*Δ *dnl4*Δ at 15.9 bleb/colony). A *mrc1*Δ *dnl4*Δ *rad59*Δ strain (DTK1935) exhibited a level of blebbing overlapping that of both *mrc1*Δ *dnl4*Δ and *mrc1*Δ *rad59*Δ double mutants. Our results suggest that NHEJ partially facilitates minisatellite tract alterations in the *mrc1*Δ strain. This is in contrast to our previous work in which we discovered that NHEJ does not influence *zrt1*Δ *ade2-min3* tract changes (Kelly et al., 2011), suggesting that different mechanisms contribute to minisatellite alterations in different genetic pathways.

Interestingly, a *mrc1*Δ *dnl4*Δ *rad52*Δ triple mutant (DTK1928) exhibited a significant decrease in the level of blebbing to 2.1 blebs/colony compared to the *mrc1*Δ *dnl4*Δ double mutant at 15.9 blebs/colony. This value is equivalent to that produced by the *mrc1*Δ *rad52*Δ strain. These results suggest that the *RAD52*-dependent pathway mediates tract alterations in the *mrc1*Δ strain when the NHEJ pathway has been compromised.

In Chapter 3, we demonstrated that *MEC1* represented an independent pathway in stationary phase cells. To determine if the minisatellite alterations within a *mec1-21* strain were dependent upon *RAD50*, *RAD51* or *RAD52*, we deleted each recombination gene in the *MEC1* mutant background. The following strains each produced a level of blebbing that was significantly lower than that of the parental *mec1-21* strain (DTK1776 at 14.2 blebs/colony): *mec1-21 rad52*Δ (DTK1986) at 2.4 +/- 0.4 blebs/colony, *mec1-21 rad51*Δ (DTK1987) at 2.8 +/- 0.5 blebs/colony and *mec1-21 rad51*Δ *rad52*Δ (DTK1988) at 2.6 +/- 0.4 blebs/colony. We were unable to assess the level of blebbing of *mec1-21 rad50*Δ mutants as the deletion of *RAD50* resulted in strains with a severe growth defect.

From our data, we conclude that alterations in the *mec1-21* strain are mediated by *RAD52*-dependent and *RAD52*-independent pathways.

The Availability of Nucleotide Pools Affects ade2-min3 *Minisatellite Tract Stability*

In Chapter 2 and Chapter 3, we identified several replication checkpoint genes as factors that maintain the stability of the *ade2-min3* minisatellite allele in stationary phase cells. These included the replication complex genes *MRC1*, *CSM3* and *TOF1* as well as the checkpoint kinase genes *MEC1* and *RAD53* (Branzei and Foiani, 2006). Further characterization of Mrc1p revealed that minisatellite stability was primarily regulated by the replicative function of Mrc1p, with the checkpoint-associated function of Mrc1p playing a minor role (Osborn and Elledge, 2003, Naylor et al., 2009). This result was supported by the observation that *MRC1*, *MEC1* and *RAD53* function in pathways that are at least partially independent of each other.

Preliminary studies performed in our laboratory suggested a link between *RAD53* minisatellite stability and nucleotide levels in stationary phase cells. Previous research has demonstrated a correlation between replication inhibition and nucleotide depletion (Frenkel et al., 1964, Slater, 1973, Desany et al., 1998) indicating that altering dNTP levels within a cell disrupts DNA replication. To further investigate the role of nucleotide availability in stationary phase minisatellite stability, we constructed strains bearing deletions of the genes *SML1* or *DUN1* and quantified the average number of blebs/colony (Figure 4-4). *SML1* encodes for a ribonucleotide reductase (RNR) inhibitor that suppresses production of dNTPs (Zhao et al., 1998, Chabes et al., 1999). *DUN1* encodes

for a serine threonine kinase that induces RNR transcription and phosphorylates Sml1p resulting in its degradation and dNTP production (Zhao and Rothstein, 2002). Both genes are regulated by *MEC1* and *RAD53* (Zhao et al., 1998, Zhao et al., 2001, Zhao and Rothstein, 2002).

Deletion of *SML1* in the *mrc1*Δ strain background (DTK1771) resulted in a reduction in the level of blebbing from 23.9 blebs/colony (*mrc1*Δ) to 14.2 blebs/colony, thus suggesting that an increase in dNTPs corresponded to a decrease in tract instability. We were unable to assess the level of blebbing of an *mrc1*Δ *dun1*Δ strain as colony formation was severely reduced. The deletion of *DUN* in the *mrc1*Δ *sml1*Δ strain background (DTK1831) resulted in significant increase in blebbing to 22.9 blebs/colony, a value that matches that of *mrc1*Δ single mutant. Therefore, a decrease in dNTP levels correlated with an increase in minisatellite instability. Our data suggest that nucleotide availability greatly impacts minisatellite stability in the *mrc1*Δ strain.

We next studied the effect of nucleotide availability on the stability of the *ade2-min3* allele in strains bearing hypomorphic alleles of *MEC1* or *RAD53* (Figure 4-4) (Sanchez et al., 1996, Raveendranathan et al., 2006). Deletion of *SML1* in a *mec1-21* strain background (DTK1808) resulted in a decrease in the level of blebbing from 14.4 +/- 1.1 blebs/colony (*mec1-21*) to 11.4 +/- 0.8 blebs/colony. The lack of overlapping confidence intervals indicates that these two averages are significantly different. This correlates with previous studies in which the authors found that a *mec1-21 sml1*Δ mutant had increased levels of dNTPs and suppressed levels of spontaneous sister chromatid exchange and hyper-recombination when compared to the WT parental strain (Fasullo et

al., 2010). Deletion of *SML1* in a *rad53-1* background (DTK1726) similarly produced a level of blebbing that was significantly decreased when compared to the single mutant (*rad53-1* at 17.8 blebs/colony vs. *rad53-1 sml1*Δ at 5.4 blebs/colony). We conclude that tract alterations in *mec1-21* and *rad53-1* strains are suppressed upon deletion of *SML1* and we predict that this corresponds to an increase in intracellular dNTP pools.

The deletion of *DUN1* in *mec1-21 sml1*Δ or *rad53-1 sml1*Δ strain backgrounds produced contrasting results. The *mec1-21 sml1*Δ *dun1*Δ triple mutant (DTK1814) produced 11.6 blebs/colony, a value not significantly different from that of the *mec1-21 sml1*Δ double mutant (11.4 blebs/colony). Deletion of *DUN1* in the *rad53-1 sml1*Δ background (DTK1811) resulted in a significant increase in the level of blebbing compared to the double mutant parental strain (*rad53-1 sml1*Δ at 5.4 blebs/colony vs. *rad53-1 sml1*Δ *dun1*Δ at 26.7 blebs/colony). We were unable to construct *mec1-21 dun1*Δ or *rad53-1 dun1*Δ double mutants as this combination was synthetically lethal in our strain background. From this data we conclude that the deletion of *DUN1* results in tract instability in a *rad53-1* strain but does not appear to affect minisatellite instability in a *mec1-21* strain.

Deletion of *SML1* in the wild-type strain background (DTK1729) did not result in a significant decrease in blebbing. The deletion of *DUN1* (DTK1821), however, resulted in a significant increase in the number of blebs when compared to the WT parental strain. The *dun1*Δ *sml1*Δ double mutant (DTK1859) also displayed a significant increase in the level of blebbing compared to the WT and *sml1*Δ strains, but not to the extent of that produced by the *dun1*Δ single mutant. This suggests that a decrease in the level of dNTPs

results in an increase in minisatellite instability within the WT strain and that the level of basal minisatellite instability inherently present within the WT strain is not further stabilized by increasing dNTP pools.

Discussion

For this chapter, we investigated the mechanisms associated with minisatellite instability in stationary phase cells bearing mutations in several replication-associated genes. Importantly, we show that the replication complex genes *MRC1*, *TOF1* and *CSM3* are expressed within quiescent cells. We find that tract alterations within the *ade2-min3* allele of a *mrc1*Δ strain are dependent upon recombination-based mechanisms that primarily utilize *RAD52*. Finally, we provide evidence that nucleotide availability is associated with stationary phase minisatellite stability. Specifically, we find that the loss of nucleotide availability results in tract alterations within the *ade2-min3* allele. Therefore, our work establishes two mechanisms that contribute to minisatellite alterations within stationary phase cells.

Previous work has shown that stationary phase cultures of yeast consist of a heterogeneous population of cells composed of both quiescent (non-dividing) and non-quiescent (slowly dividing) cells (Allen et al., 2006, Aragon et al., 2008). Here, we show that the replication proteins Mrc1p, Csm3p and Tof1p are expressed in both nonquiescent and quiescent cells that are present at the diauxic shift. We find that Mrc1p and Tof1p are expressed in stationary phase quiescent cells as well, lending further evidence to the hypothesis that these proteins are involved in regulating minisatellite stability in G_0 cells.

We were unable to detect Csm3p in quiescent stationary phase cells. However, this could be due to a very low level of expression; expression of both Mrc1p and Tof1p in this population of cells was also low compared to other timepoints. Characterization of each population in our strain background demonstrated that stationary phase cultures were primarily composed of quiescent cells. Thus, while the expression level of each gene is low in the quiescent population, deletion of these genes would have a much more drastic effect on colonies as a whole. This is in agreement with the results discussed in Chapter 3 in which we demonstrate that the majority of minisatellite alteration events occur primarily within the quiescent cell population of *mrc1*Δ, *csm3*Δ and *tof1*Δ strains.

We previously demonstrated that *ade2-min3* minisatellite alterations in wild-type (WT), *zrt1*Δ, *end3*Δ and *pkc1-4* strains were dependent upon the recombination genes *RAD50*, *RAD51* or *RAD52* (Kelly et al., 2011, Kelly et al., 2012). Deletion of *RAD50* or *RAD51* in a *mrc1*Δ strain background resulted in a 50% reduction in the level of blebbing compared to the single mutant parental strain, whereas the loss of *RAD52* resulted in a 90% reduction of blebbing in the *mrc1*Δ mutant, a level indistinguishable from the WT strain. Thus, each recombination gene product facilitates a portion of the minisatellite alterations that occur within the replication mutant *mrc1*Δ strain, with the most dramatic contribution from that of Rad52p.

Deletion of both *RAD50* and *RAD52* in the *mrc1*Δ background resulted in a further decrease in the number of blebs/colony when compared to the parental double mutant strains *rad50*Δ *mrc1*Δ and *rad52*Δ *mrc1*Δ. In contrast, no additional decrease in blebbing was observed in the triple mutant strain bearing deletions of *RAD51*, *RAD52*

and *MRC1* when compared to the parental strains. These results indicate that both *RAD52*-dependent recombination and *RAD52*-independent recombination mechanisms requiring *RAD50* contribute to minisatellite alterations in the *mrc1*Δ strain.

Deletion of *RAD50* and *RAD51* in the *mrc1*Δ strain background resulted in a significant decrease in blebbing compared to the parental double mutants *rad50*Δ *mrc1*Δ and *rad51*Δ *mrc1*Δ. This level of blebbing did not further decrease in a strain bearing deletions of *RAD50*, *RAD51*, *RAD52* and *MRC1*. Therefore, *RAD51* does not appear to contribute to minisatellite alterations in an *mrc1*Δ strain in the presence of wild-type *RAD50*. Interestingly, we found that the *RAD52*-dependent recombination pathway of single-strand annealing (SSA) and the *RAD50*-dependent pathway of nonhomologous end-joining contributed to minisatellite alterations within the *mrc1*Δ strain. These results correspond to the observation that *RAD52*-dependent and *RAD52*-independent mechanisms requiring *RAD50* are necessary for *ade2-min3* minisatellite alterations within the *mrc1*Δ mutant strain.

Previous work has indicated that the predominate mechanism of minisatellite alteration within meiotic germline cells is homologous recombination (Jeffreys et al., 1998, Jeffreys et al., 1999). Similarly, recombination has also been implicated in mitotic minisatellite tract alterations in somatic cells (Jeffreys and Neumann, 1997). Together our results suggest that recombination is a mode of repeat tract instability within stationary phase cells as well. As stationary phase cells consist of both quiescent and nonquiescent cells (Allen et al., 2006, Aragon et al., 2008), we are interested in determining if the

recombination - dependent and - independent mechanisms of minisatellite alteration are specific to one population or the other.

In Chapter 2 and Chapter 3 we discovered that mutations of several replication-associated genes resulted in a high degree of minisatellite instability, thereby implicating aberrant DNA replication as a source of tract alteration. In accordance with our data, mitotic minisatellite instability in yeast has been linked to mutations in the flap endonuclease *RAD27* (Lopes et al., 2002, Maleki et al., 2002) or the PCNA clamp (Kokoska et al., 1999). Here, we studied the effect of depleting nucleotide levels on minisatellite stability by deleting the ribonucleotide reductase inhibitor (RNR) gene *SML1*, in *MRC1*, *MEC1* or *RAD53* mutant strain backgrounds (Zhao et al., 1998). The deletion of *SML1* resulted in a significant decrease in the level of blebbing when compared to the parental strains suggesting that increasing nucleotide pools stabilizes minisatellites in stationary phase. Due to the strong association of replication mutants and increased minisatellite instability as well as previous research that suggests a link between nucleotide depletion and aberrant replication, we predict that a reduction in nucleotide availability in stationary phase cells results in aberrant replication that can give rise to genomic mutations, such as minisatellite alterations.

In a parallel experiment, we deleted the gene *DUN1* which encodes for a kinase that upregulates RNR expression and increases nucleotide pools (Zhao and Rothstein, 2002). We found that the deletion of *DUN1* in *mrc1*Δ *sml1*Δ or *rad53-1 sml1*Δ strain backgrounds resulted in a dramatic increase in minisatellite instability indicating that nucleotide depletion results in tract alterations. Interestingly, we did not see an increase

in minisatellite instability in a *mec1-21 sml1*Δ *dun1*Δ strain. However, previous work characterizing dNTP levels within *mec1-21* strains revealed that dNTPs are increased 2-fold in both *mec1-21 sml1*Δ and *mec1-21 sml1*Δ *dun1*Δ mutants when compared to the WT strain (Fasullo et al., 2010). This provides an explanation as to why we see the same level of blebbing in both of these mutant strains. Future blebbing quantification and pathway analysis utilizing an *RNR1* over-expression plasmid would complement these experiments.

Several studies have identified links between stationary phase, recombination and DNA replication. In *Escherichia coli*, expression of the DNA polymerase III gene *dnaN* and the gene *recF* – involved in DNA repair, recombination and fork recovery – have been shown to be induced in stationary phase cells (Villarroya et al., 1998). Furthermore, others have shown that stationary phase mutations in *E. coli* were the result of recombination and DNA polymerase errors (Harris et al., 1994, Strathern et al., 1995, Harris et al., 1997a). Recent work has also identified areas of DNA replication in stationary phase yeast, which the authors speculated were sites of DNA repair (de Morgan et al., 2010). Our results suggest that stationary phase minisatellite alterations are the result of insufficient or incorrect repair mechanisms that occur at sites of DNA damage. Mutations in replication-associated genes or the lack of abundant nucleotides within this population of cells could result in polymerase slippage events during DNA repair resulting in ssDNA. This model is further supported by the experiments discussed in Chapter 3 in which we demonstrated that minisatellite alterations in *mrc1*Δ and *zrt1*Δ mutants were partially dependent upon the recombination and repair-associated function

of the ssDNA binding protein Replication Protein A (RPA) (Umezu et al., 1998, Fanning et al., 2006). Thus, replication and recombination genes are important in stationary phase cells to prevent potentially harmful genomic instability.

In summary, our lab has shown that recombination and aberrant replication through loss of nucleotide availability are mechanisms of minisatellite alteration within stationary phase cells. Through our previous work, we have identified several independent pathways that mediate minisatellite stability of the *ade2-min3* tract (summarized in Figure 4-5) (Kelly et al., 2007, Kelly et al., 2011, Kelly et al., 2012). These pathways are separated by the individual components that contribute to minisatellite stability and are represented by the genes *ZRT1*, *MEC1*, *RAD53*, *RAD27*, *END3* and *MRC1*. Each pathway is further sub-divided by a dependence on which recombination factors mediate tract alterations. Pathways that are stabilized by the presence of nucleotides are indicated. Thus, our laboratory has established a model of factors and associated mechanisms that regulate stationary phase minisatellite stability.

Data Contribution

We are grateful to Dr. Anja Bielinsky's lab for technical assistance with protein isolation and western blotting techniques. We greatly appreciate the use of reagents and equipment from the labs of Dr. Anja Bielinsky and Dr. Duncan Clarke.

Dr. Katy Kelly constructed the strains DTK271, DTK1170, DTK1316 and the parental strains DTK1056, DTK1074, DTK1230 and DTK1253 used to construct the

mutants for this chapter. The final figure was constructed in cooperation with work performed by Dr. Katy Kelly.

Figure 4-1.

Protein Expression in Yeast Cells Bearing the *ade2-min3* Minisatellite Allele.

(a) Cells from DTK1657 (wild-type) cultures were harvested at timepoints 18hrs., 48hrs. and 120hrs. Individual populations of stationary phase yeast cells were isolated by overlaying harvested cells onto Percoll density gradients. Cells were centrifuged and upper and lower fractions were collected, washed and pelleted. The arrows indicate the position of cells after centrifugation. Entrance into stationary phase was monitored by OD_{600} measurements at each timepoint. **(b)** The average percentage of budding cells was determined by counting the total number of cells with buds for at least 300 cells per timepoint. This experiment was repeated and the error bars represent the standard deviation. **(c)** The total number of cells in each fraction was determined by whole-cell counts of both upper and lower fractions. The experiment was repeated twice, and the error bars are the standard deviation. **(d)** Expression of Quiescent - Associated Acs1p. Cells from Acs1p-3HA cultures were harvested at timepoints 18hrs., 48hrs. and 120hrs as described in (a) and Chapter VII: Materials and Methods. For western blot analysis, trichloroacetic acid protein purification was performed as stated in Chapter VII: Materials and Methods. Protein samples were subjected to SDS-PAGE and then transferred to a nitrocellulose membrane. Expression of Acs1p-3HA was detected by anti-3HA-conjugated antibody. **(e)** Expression of Mrc1p-3HA, Csm3p-3HA and Tof1p-3HA. Cell fractionation and western blot expression was performed as described in (a) and in Chapter VII: Materials and Methods.

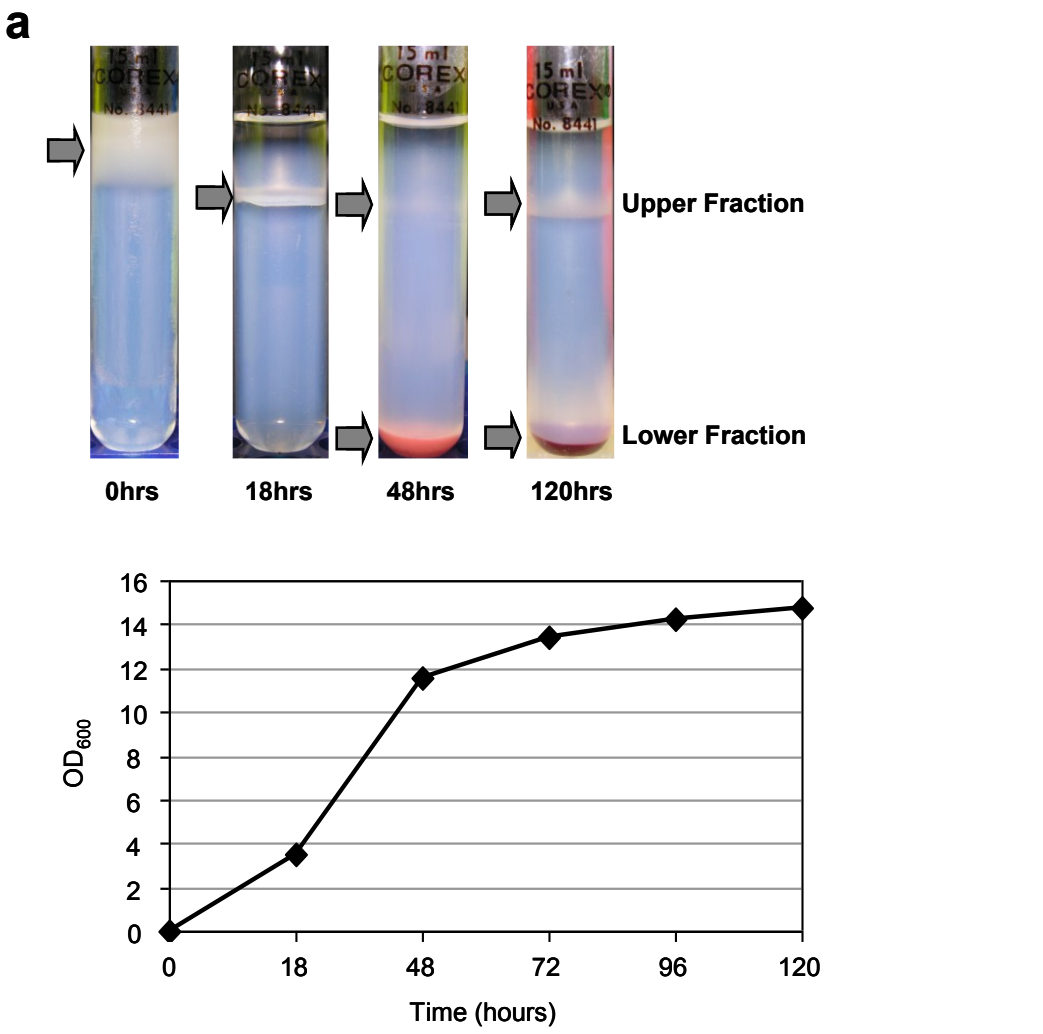
a
Upper Fraction
Lower Fraction
0hrs
18hrs
48hrs
120hrs
OD600
Time (hours)
b
Average % of Budded Cells
Time (minutes)
Upper Fraction
Lower Fraction

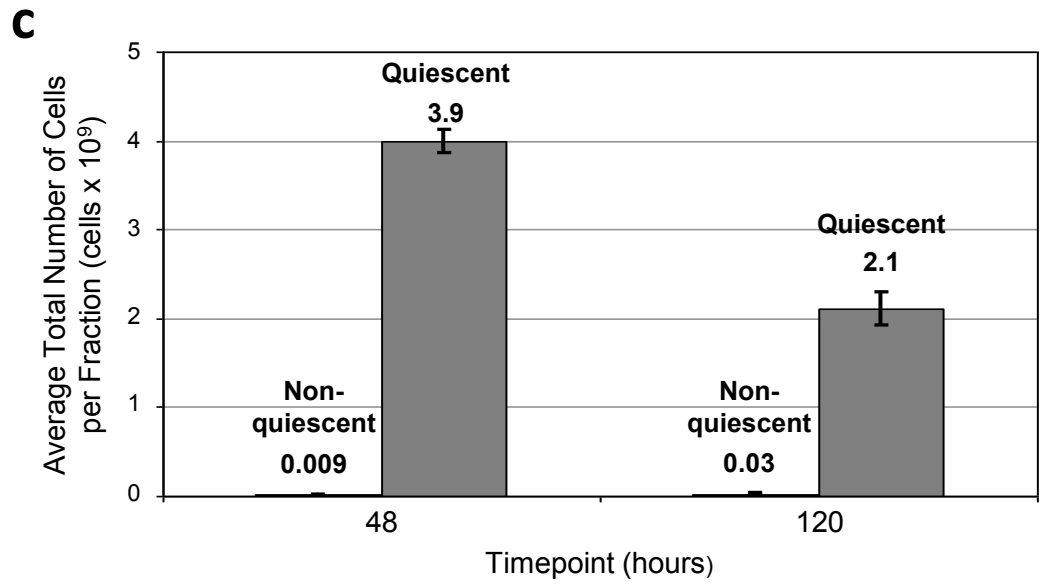
c
Average Total Number of Cells per Fraction (cells x 10^9)
5
4
3
2
1
0
Quiescent
3.9
Quiescent
2.1
Non-quiescent
0.009
Non-quiescent
0.03
48
120
Timepoint (hours)

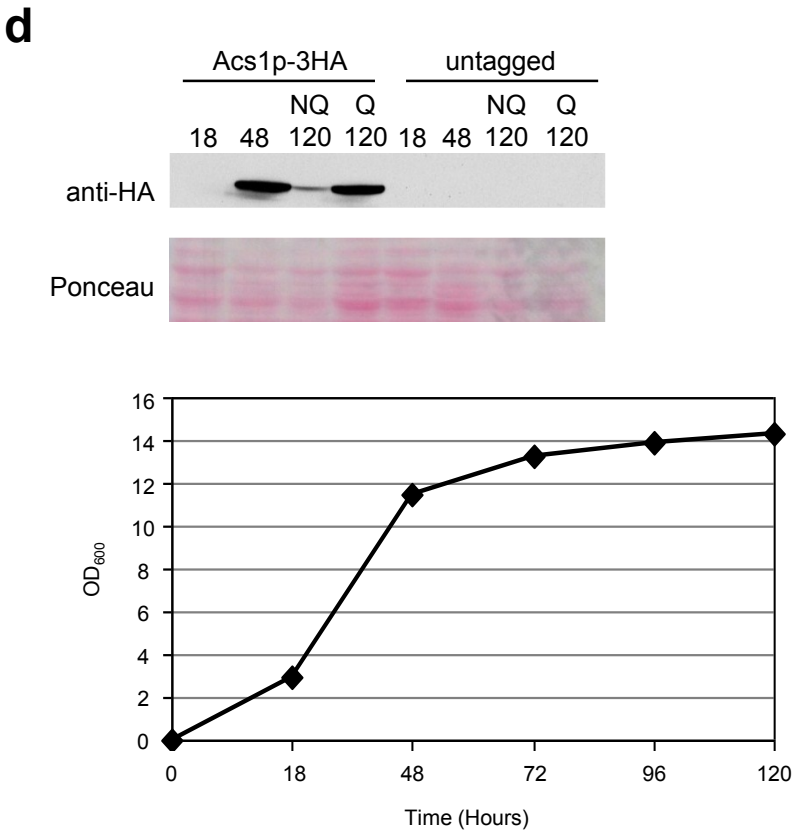
d
Acs1p-3HA
untagged
NQ Q
NQ Q
18 48 120 120 18 48 120 120
anti-HA
Ponceau
OD600
16
14
12
10
8
6
4
2
0
0 18 48 72 96 120
Time (Hours)

e

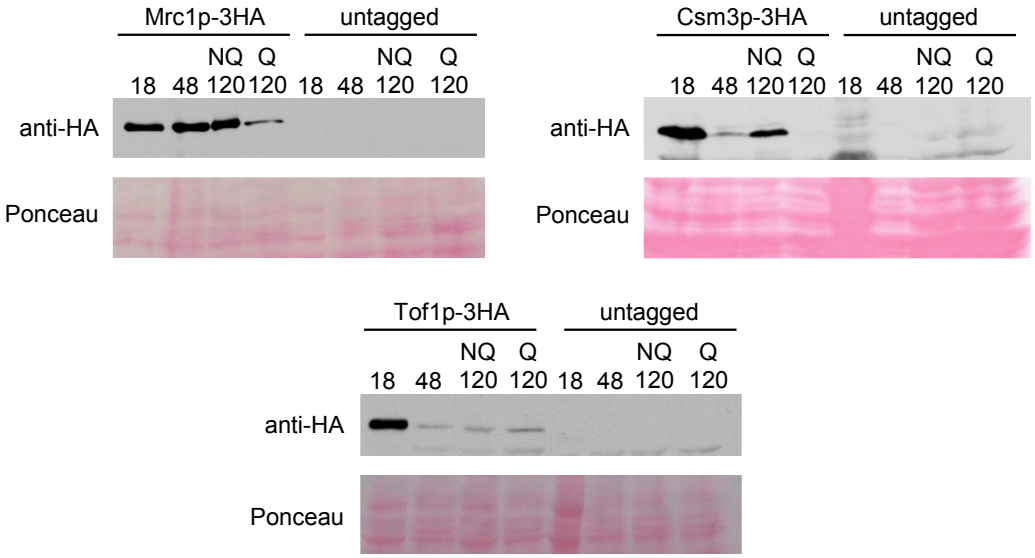
Mrc1p-3HA
untagged
NQ Q
18 48 120 120 18 48 120 120
anti-HA
Ponceau
Csm3p-3HA
untagged
NQ Q
18 48 120 120 18 48 120 120
anti-HA
Ponceau
Tof1p-3HA
untagged
NQ Q
18 48 120 120 18 48 120 120
anti-HA
Ponceau

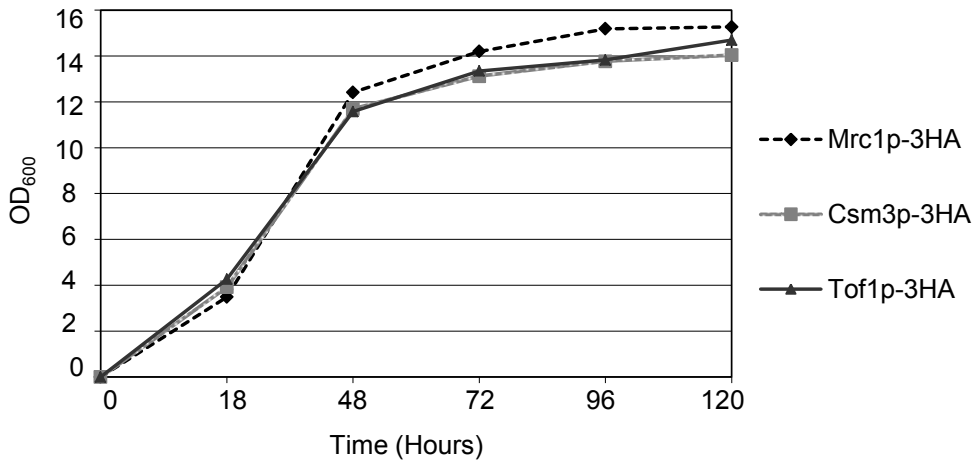
16
14
12
10
8
6
4
2
0
OD600
0
18
48
72
96
120
Time (Hours)
Mrc1p-3HA
Csm3p-3HA
Tof1p-3HA

Figure 4-2.

Minisatellite Tract Alterations in an *mrc1*Δ Strain are Mediated by Homologous Recombination.

For blebbing quantification analysis, a single red colony was used to inoculate 5mL of liquid YPD media for each strain. The cultures were incubated at 30°C for four hours., diluted and then plated onto solid YPD media. Each strain was incubated for two days at 30°C and then at RT for six days. Individual blebs were counted on at least 100 colonies for each strain. Only colonies ranging in size from 1.26 to 1.32 mm in diameter were included. The blebbing quantification assay was repeated three independent times, and the average number of blebs/colony +/- 95% confidence interval was calculated for each strain.

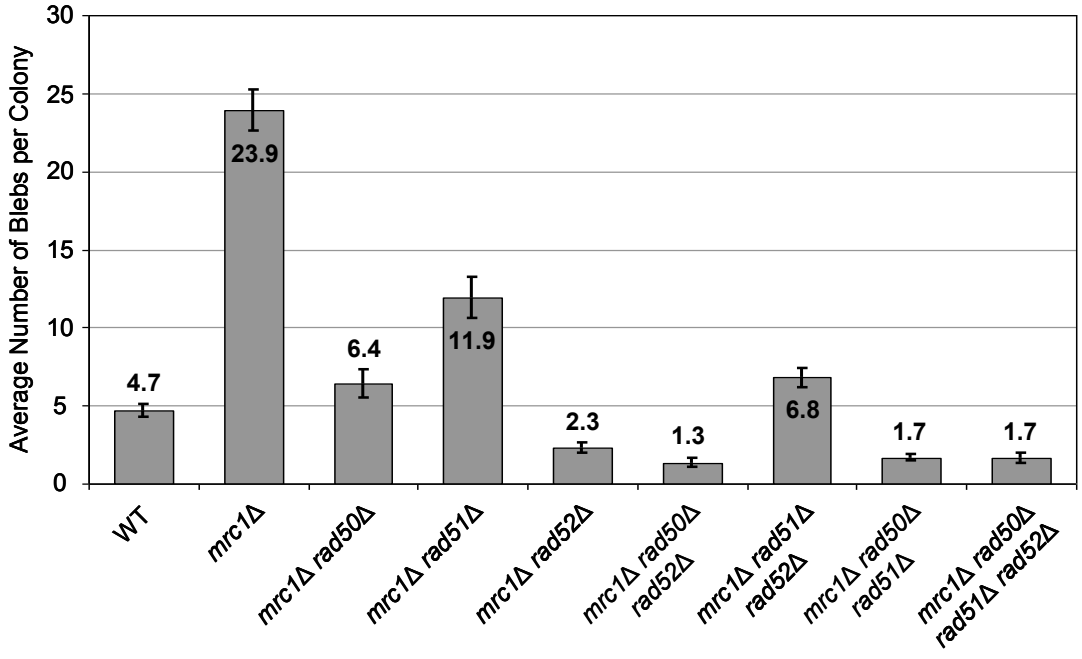

Figure 4-3.

Minisatellite Alterations in an *mrc1*Δ Strain are Partially Dependent Upon Single Strand Annealing and Non-Homologous End Joining.

Blebbing quantifications were performed for each strain as described in Figure 4-1 and Chapter VII: Materials and Methods.

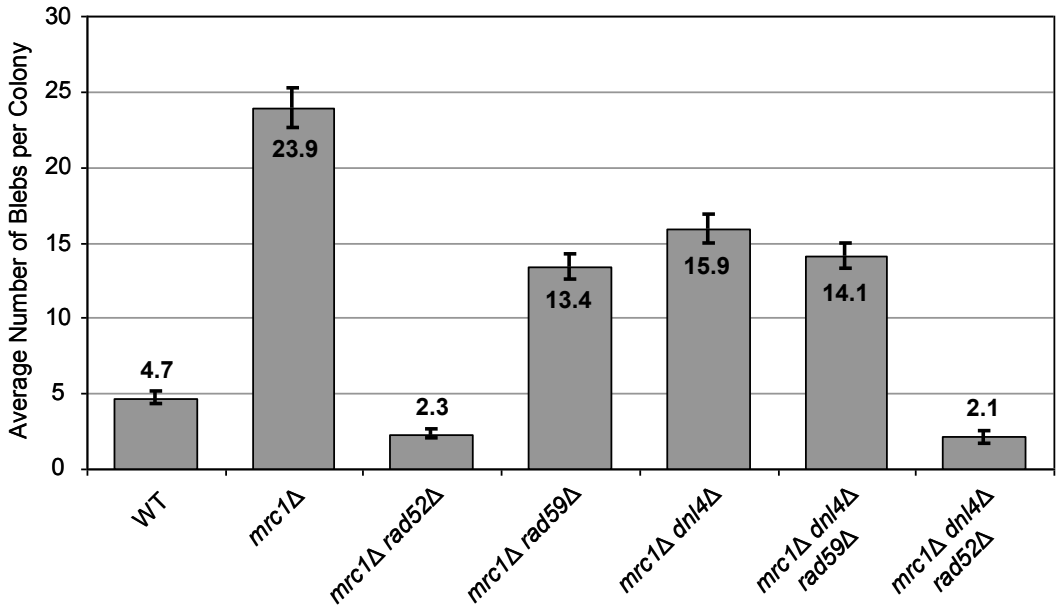

Figure 4-4.

Nucleotide Pool Availability Affects the Stability of the *ade2-min3* Minisatellite.

For each strain, blebbing quantification was performed as in Figure 4-1 and in Chapter VII: Materials and Methods.

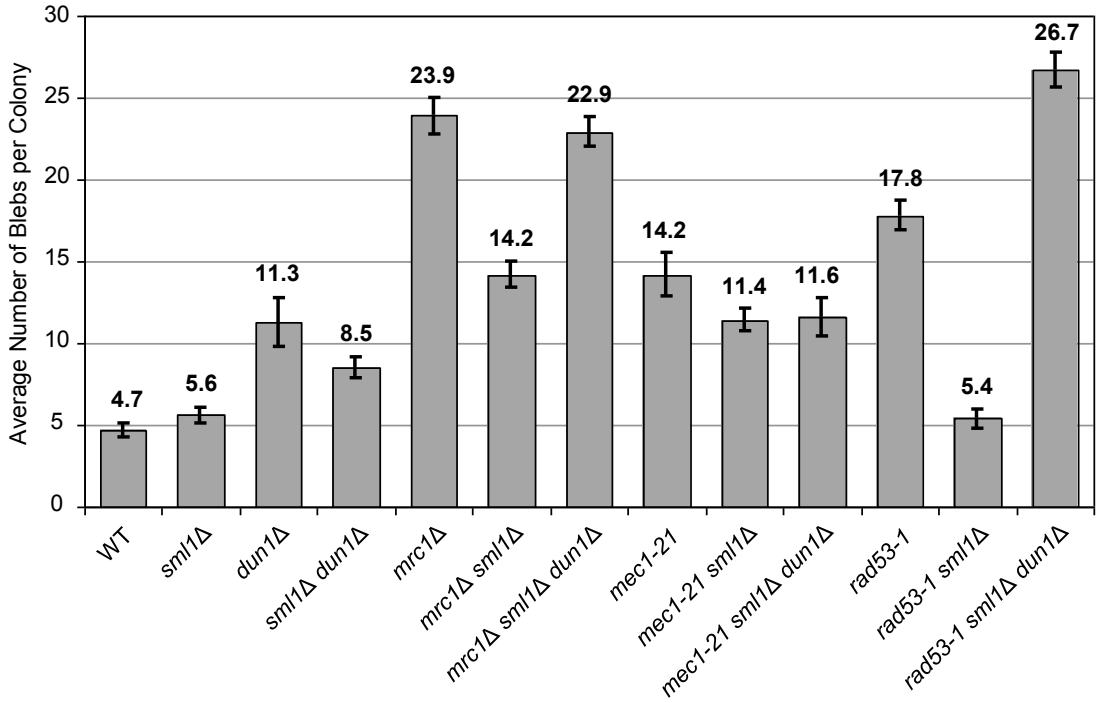

Figure 4-5.

Summary of Pathways that Mediate Minisatellite Stability in Stationary Phase Yeast. Several independent pathways mediate stationary phase minisatellite stability of the *ade2-min3* allele. These include the *ZRT1*, *MEC1*, *RAD53*, *END3*, *RAD27* and *MRC1* pathways. Components of each pathway are represented by labeled squares. Each pathway is subdivided by the recombination pathway that contributes to tract alterations in mutant strains. Minisatellite alterations within the *MEC1*, *RAD53* and the *MRC1* pathways are stabilized by the availability of plentiful nucleotide pools.

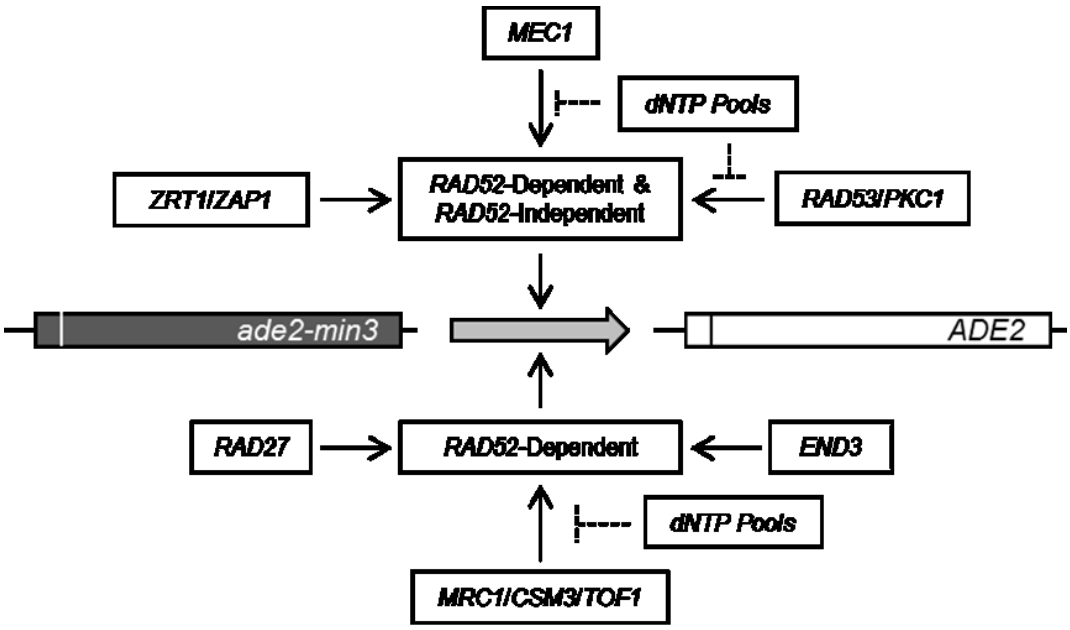

Chapter V

The Influence of Replication Checkpoint Components on the Stability of the Human *HRAS1* Oncogene - associated Minisatellite

Chapter Summary

Numerous studies have identified links between alterations in non-coding repetitive elements known as minisatellites and several types of diseases ranging from cancer to diabetes. However, little is known about the factors that contribute to minisatellite alterations. Previously, we identified that strains bearing the *ade2-min3* minisatellite as well as a deletion of the replication checkpoint genes *MRC1*, *CSM3* or *TOF1* resulted in a high degree of stationary phase minisatellite instability. Here, we examine the effect of the genes *MRC1*, *CSM3* and *TOF1* on the stability of the human *HRAS1*-associated minisatellite. We find that each gene regulates *HRAS1* minisatellite stability in stationary phase yeast cells. Analysis of the specific tract alterations giving rise to blebs in *mrc1*Δ, *csm3*Δ and *tof1*Δ strains revealed that the majority of alterations consisted of the loss of one repeat unit from the center of the minisatellite allele. Finally, we demonstrate that minisatellite alterations in an *ade2-h7.5 mrc1*Δ strain occur primarily through a *RAD52*-independent pathway that utilizes both *RAD50* and *RAD51*. Together, our results show an important link between components of the replication checkpoint and the preservation of human minisatellite stability.

Introduction

Minisatellites are a class of tandem repetitive DNA composed of variable repeat units (Vergnaud and Denoeud, 2000). Rare altered minisatellite alleles have been shown to correlate with an increased risk or development of disease. Correspondingly, rare alleles of the *HRAS1* oncogene-associated minisatellite allele were found to act as enhancers of *HRAS1* transcription suggesting a mechanism for cancer development (Trepicchio and Krontiris, 1992, Green and Krontiris, 1993, Krontiris, 1995). It is currently thought that rare minisatellite alleles are derived from alterations that have occurred within common alleles of the human population. To date, little is known about what factors prevent minisatellites from altering and becoming disease-associated alleles.

To study the stability of a human minisatellite, we inserted a minisatellite composed of seven-and-a-half variable repeats of the *HRAS1*-associated minisatellite into the *ADE2* gene of *S. cerevisiae* (*ade2-h7.5* allele) (Figure 5-1). This minisatellite consists of four different repeat units which vary in C or G content at positions +14nt and +22nt. We previously demonstrated that *ade2-h7.5* alterations occurring within stationary phase cells give rise to a blebbing phenotype (Kelly et al., 2011).

In Chapter 2 and Chapter 3, we identified and characterized several components associated with the replication checkpoint that were involved in the maintenance of *ade2-min3* minisatellite stability in stationary phase cells. These included the components of the replication pausing complex, *MRC1*, *CSM3* and *TOF1* (Alcasabas et al., 2001, Katou et al., 2003, Osborn and Elledge, 2003, Bando et al., 2009). In Chapters 3 and 4 we further demonstrated that minisatellite stability is mediated by the replicative function

rather than the checkpoint function of Mrc1p and that tract alterations in an *mrc1*Δ strain are dependent upon the recombination gene *RAD52*. While these replication genes were not identified as hits in our *ade2-h7.5* SGA analysis discussed in Chapter 2, it is possible that *MRC1*, *CSM3* and *TOF1* are associated with *ade2-h7.5* minisatellite stability. Due to the high level of stringency we established for scoring each strain as a hit, strains that produced a mid-level of blebbing in comparison to our positive control would have been discarded during our screen.

In this chapter, we investigate if *MRC1*, *CSM3* and *TOF1* are involved with mediating the stability of the *ade2-h7.5* allele. Deletion of each gene resulted in a high level of blebbing compared to the parental wild-type strain, indicating that components of the replication checkpoint prevent alterations of a human-associated minisatellite. Characterization of minisatellite alterations occurring within *mrc1*Δ, *csm3*Δ and *tof1*Δ mutant strains revealed that the majority of tract alterations consisted of the loss of one repeat unit from the center of the allele. Finally, we show that *ade2-h7.5 mrc1*Δ minisatellite alterations are primarily dependent upon a *RAD52*-independent mechanism that utilizes the recombination factors *RAD50* and *RAD51*. Our work establishes the importance of *MRC1*, *CSM3* and *TOF1* in the maintenance of human-associated minisatellites and demonstrates that components of the replication checkpoint regulate repeat stability regardless of tract size or sequence composition.

Results

Components of the Replication Checkpoint Affect the Stability of the ade2-h7.5 *Minisatellite Allele*

For this chapter, we utilized the *ade2-h7.5* allele to monitor minisatellite alterations using an *ADE2*-dependent color segregation assay (Kelly et al., 2011, Kelly et al., 2012). As described in Chapter 2, the *ade2-h7.5* allele is comprised of seven-and-a-half repeat units plus flanking sequence of the human *HRAS1*-associated minisatellite (Figure 5-1). Stationary phase minisatellite alterations occurring within the *ade2-h7.5* allele give rise to a blebbing phenotype (Kelly et al., 2011, Kelly et al., 2012).

In Chapters 2 and 3, we found that the replication checkpoint genes *MRC1*, *CSM3* and *TOF1* (Alcasabas et al., 2001, Katou et al., 2003, Osborn and Elledge, 2003, Bando et al., 2009) regulated the stability of the *ade2-min3* allele. The composition of *ade2-min3* allele - only three identical repeat units - is in stark contrast to that of the more complex human-associated *ade2-h7.5* minisatellite allele, and as discussed in Chapter 2, the stability of both alleles is largely regulated by a different set of factors. Here, we ask if genes associated with the replication checkpoint are involved in preventing the instability of the *ade2-h7.5* minisatellite.

To determine if *MRC1*, *CSM3* and *TOF1* regulate the stability of the *HRAS1*-assocated minisatellite, we constructed strains bearing the *ade2-h7.5* allele as wells as a deletion of each checkpoint gene and quantified the average number of blebs/colony +/- 95% confidence intervals (CI) for each strain (Figure 5-2). Non-overlapping 95% CI indicated that the level of blebbing between strains was significantly different. Deletion

of each gene resulted in an enhanced blebbing phenotype. DTK1533 (*mrc1*Δ) produced 8.6 blebs/colony, a significant increase in blebbing compared to the wild-type strain at 2.0 blebs/colony. Similar phenotypes were observed in both DTK1543 (*csm3*Δ) and DTK1560 (*tof1*Δ) mutants. Deletion of *CSM3* or *TOF1* resulted in 11.7 and 10.9 blebs/colony, respectively; both values significantly greater than the wild-type strain. Our data suggest that the replication complex genes *MRC1*, *CSM3* and *TOF1* are important for maintaining the stability of the *ade2-h7.5* minisatellite allele in stationary phase cells.

We examined the tract alterations occurring within the strains DTK271 (wild-type), DTK1533 (*mrc1*Δ), DTK1543 (*csm3*Δ) and DTK1560 (*tof1*Δ) by performing whole cell PCR across the *ade2-h7.5* minisatellite tract of at least 100 individual blebs and analyzing the results using gel electrophoresis. The majority of tract alterations occurring in each strain consisted of a contraction of the minisatellite allele. The most common contraction for all strains was the loss of one repeat unit (DTK1188 (WT) = 95/104, 91%; DTK1533 (*mrc1*Δ) = 95/104, 91%; DTK1543 (*csm3*Δ) = 106/114, 93%; DTK1560 (*tof1*Δ) = 99/104, 95%). Loss of four repeat units was observed at a low frequency for each deletion mutant (DTK1188 (WT) = 5/104, 5%; DTK1533 (*mrc1*Δ) = 5/104, 5%; DTK1543 (*csm3*Δ) = 7/114, 6%; DTK1560 (*tof1*Δ) = 3/104, 3%). We also observed tract contractions consisting of the gain of one repeat unit (DTK1188 (WT) = 1/104, 1%; DTK1543 (*csm3*Δ) = 1/114, 1%) or two repeat units (DTK1188 (WT) = 3/104, 3%; DTK1533 (*mrc1*Δ) = 3/104, 3%; DTK1560 (*tof1*Δ) = 2/104, 2%), however expansions were not observed in all strains. Interestingly, loss of the entire repeat tract was observed in 1/104 (1%) analyzed blebs in the strain DTK1533 (*mrc1*Δ).

To identify the location of the *ade2-h7.5* tract alterations, we sequenced across the minisatellite tract of 25 individual blebs isolated from each replication checkpoint mutant strain (Figure 5-3). Tract contractions consisting of the loss of one repeat primarily occurred within the center of the minisatellite allele at the fourth or fifth repeat unit. Expansions of the tract consisted of the addition of repeat units at the center of the minisatellite, predominantly between the third and fourth repeat.

Alterations of the ade2-h7.5 *Minisatellite Allele in an* mrc1Δ *Strain are Dependent upon Recombination Factors*

To date, the minisatellite alterations in each mutant strain studied within our lab have consisted of the loss or gain of whole repeat units (Chapter 2 and Chapter 4) (Kelly et al., 2007, Kelly et al., 2011). Based upon these findings, we hypothesize that tract alterations giving rise to the blebbing phenotype are dependent upon recombination. In *S. cerevisiae*, two pathways regulate recombination-mediated genomic rearrangements. These include the *RAD52*-dependent pathway and the *RAD52*-independent pathway that utilizes the recombination factors *RAD50* and *RAD51* (Coic et al., 2008). We previously demonstrated that minisatellite alterations occurring within an *ade2-min3 zrt1*Δ strain and an *ade2-h7.5 zrt1*Δ strain were dependent upon both pathways and utilized the recombination factors *RAD50*, *RAD51* or *RAD52* (Kelly et al., 2007, Kelly et al., 2011). This finding was also observed in wild-type parental strains. In Chapter 4, we found that *ade2-min3* minisatellite alterations in an *mrc1*Δ strain were primarily dependent upon

RAD52. Here, we examine which recombination pathways mediate *ade2-h7.5* tract alterations in the *mrc1*Δ deletion strain.

To determine if recombination factors were associated with minisatellite alterations in the *ade2-h7.5 mrc1*Δ strain, we deleted the recombination genes *RAD50*, *RAD51* or *RAD52* in an *mrc1*Δ mutant background. We then quantified the average number of blebs/colony for each strain (Figure 5-4). Deletion of *RAD50* (DTK1672; *mrc1*Δ *rad50*Δ) significantly reduced the level of blebbing of the parental *mrc1*Δ (DTK1533) strain from 8.6 to 2.0 blebs/colony, a suppression of approximately 76% of the total number of blebs. This value was not significantly different from that of the wild-type strain, DTK1188, at 2.0 blebs/colony. Similarly, deletion of *RAD51* (DTK1658; *mrc1*Δ *rad51*Δ) reduced the level of blebbing by 74% to 2.2 blebs/colony. In contrast, deletion of the recombination gene *RAD52* resulted in only a 16% decrease in the number of blebs to 7.2 blebs/colony (DTK1664; *mrc1*Δ *rad52*Δ). Our results suggest that the majority of minisatellite alterations in DTK1533 (*ade2-h7.5 mrc1*Δ) are predominantly dependent upon *RAD50* and *RAD51* with only a partial dependence upon *RAD52*.

To study the individual contributions of each recombination gene, we constructed strains bearing the *mrc1*Δ deletion mutation as well as pair-wise combinations of deletions of each recombination gene. Deletion of both *RAD50* and *RAD51* in the *mrc1*Δ background (DTK1773; *mrc1*Δ *rad50*Δ *rad51*Δ) reduced the level of blebbing produced by either double mutant (*mrc1*Δ *rad50*Δ at 2.0 blebs/colony; *mrc1*Δ *rad51*Δ at 2.2 blebs/colony) to 1.4 blebs/colony. Thus, both *RAD50* and *RAD51* greatly contribute to *MRC1* - dependent minisatellite alterations. The triple mutant strain DTK1734 (*mrc1*Δ

*rad50*Δ *rad52*Δ) displayed a 50% reduction in blebbing compared to the double mutant DTK1664 (*mrc1*Δ *rad52*Δ) (*mrc1*Δ *rad50*Δ *rad52*Δ at 7.2 blebs/colony; *mrc1*Δ *rad52*Δ at 4.4 blebs/colony). However, this value was still greater than the number of blebs produced by the strain DTK1672 (*mrc1*Δ *rad50*Δ) at 2.0 blebs/colony. This result suggests that minisatellite alterations occurring via a *RAD52*-independent pathway utilize *RAD50*. DTK1733 (*mrc1*Δ *rad51*Δ *rad52*Δ; 2.1 blebs/colony) produced a level of blebbing corresponding to a 71% reduction in the number of blebs produced by the double mutant DTK1664 (*mrc1*Δ *rad52*Δ at 7.2 blebs/colony) yet indistinguishable from that of the double mutant DTK1658 (*mrc1*Δ *rad51*Δ at 2.1 blebs/colony). Thus, *RAD52*-independent tract alterations are also dependent upon *RAD51*. We did not observe a further decrease in blebbing in the quadruple mutant DTK1663 (*mrc1*Δ *rad50*Δ *rad51*Δ *rad52*Δ at 2.1 blebs/colony). Together, our results suggest that *MRC1*-dependent minisatellite alterations are predominantly mediated by a *RAD52*-independent pathway utilizing *RAD50* and *RAD51*.

Discussion

In this chapter, we studied the effect of the replication checkpoint components - *MRC1*, *CSM3* and *TOF1* (Alcasabas et al., 2001, Katou et al., 2003, Osborn and Elledge, 2003, Bando et al., 2009) - on the stability of the human *HRAS1*-associated minisatellite allele, *ade2-h7.5*. We find that each independent gene prevents minisatellite alterations in stationary phase cells. Characterization of the *ade2-h7.5* tract isolated from individual blebs revealed that the majority of tract alterations associated with the deletion of each

gene consisted of contractions, primarily at the center of the minisatellite. Finally, we find that tract alterations within an *mrc1*Δ deletion strain are primarily mediated by a *RAD52*-independent pathway consisting of both *RAD50* and *RAD51* recombination genes.

Deletion of the genes *MRC1*, *CSM3* and *TOF1* resulted in dramatic increase in *ade2-h7.5* minisatellite instability when compared to the WT strain (Figure 5-2) indicating that the presence of these genes is required to prevent alterations within a human-derived minisatellite. This finding is similar to that discussed in Chapters 2 and 3 in which we identify *MRC1*, *CSM3* and *TOF1* as genes that are important for maintaining the stability of the simple minisatellite allele, *ade2-min3*. In yeast cells, *MRC1*, *CSM3* and *TOF1* form a heterotrimeric complex, known as the replication pausing complex, which associates with replication forks (Katou et al., 2003, Bando et al., 2009). The purpose of this complex hinges on maintaining replication by: 1) mediating the replication checkpoint signal through kinases *MEC1* and *RAD53* and 2) maintaining proper replicative function (Alcasabas et al., 2001, Osborn and Elledge, 2003, Naylor et al., 2009). Each function prevents the accumulation of ssDNA, a known precursor to genomic instability.

The question remains as to why replication-associated factors are active in stationary phase cells. Previous work has discovered that while bulk DNA synthesis does not occur in this cell population, isolated regions of replication are present (de Morgan et al., 2010). The authors argue that these regions correspond to patches of DNA repair.

Thus, absent or reduced DNA replication in stationary phase cells could result in genomic instability by giving rise to incorrectly repaired regions of DNA.

In the preceding chapters, we demonstrated that Mrc1p prevents *ade2-min3* minisatellite instability primarily by mediating accurate replication rather than checkpoint signaling. We also showed that Mrc1p, Csm3p and Tof1p are expressed within quiescent yeast cells. Based upon these results, we hypothesize that *MRC1*, *CSM3* and *TOF1* prevent *ade2-h7.5* minisatellite alterations by maintaining proper replicative function at sites of DNA repair. Future analysis of Mrc1p separation of function mutants in which either the replication signaling function of Mrc1p is compromised (Osborn and Elledge, 2003) or the replication function of Mrc1p is deviant (Naylor et al., 2009) will give insight into the mechanism of *MRC1*-associated *ade2-h7.5* minisatellite stability.

In yeast, DNA alterations are mediated by *RAD52*-dependent or *RAD52*-independent homologous recombination pathways (Coic et al., 2008). We previously demonstrated that *ade2-h7.5* minisatellite alterations in several mutant strains were dependent upon recombination-associated mechanisms (Kelly et al., 2011, Kelly et al., 2012). Here, we investigated the dependence of *ade2-h7.5* tract alterations within an *mrc1*Δ deletion mutant and characterized the specific tract alterations giving rise to the blebbing phenotype (Figure 5-4). Loss of the recombination factors *RAD50* and *RAD51* dramatically reduced the level of *mrc1*Δ minisatellite alterations by over 70%. Only a modest decrease in tract alterations (~16%) was observed in an *mrc1*Δ strain lacking *RAD52*. Minisatellite alterations in the *mrc1*Δ *rad52*Δ strain were further suppressed upon deletion of *RAD50* or *RAD51*. Together, our data show that *ade2-h7.5 mrc1*Δ

minisatellite alterations are predominantly mediated by a *RAD52*-independent pathway that utilizes *RAD50* and *RAD51*. This finding is in contrast to that discussed in Chapter 4 in which minisatellite alterations in the *ade2-min3 mrc1*Δ strain were primarily mediated by *RAD52*. Thus, with respect to *mrc1*Δ mutant strains, differences in minisatellite composition appear to affect which recombination pathways facilitate tract alterations. Future pathway analysis dissecting *RAD52*-independent mechanisms, such as nonhomologous end-joining, will give further insight into *ade2-h7.5* alteration.

Characterization of the specific repeat alterations within *mrc1*Δ, *csm3*Δ or *tof1*Δ strains revealed that the majority of tract alterations consisted of the loss of one repeat unit from the center of the minisatellite. This finding is in contrast to that associated with highly mutable minisatellites within the human genome in which tract alterations are polar - specifically localizing to the periphery of the minisatellite (reviewed in (Bois, 2003)). However, this observation has been linked to the presence of meiotic recombination hotspots that are often located within the sequence surrounding the minisatellite (Jeffreys et al., 1998, Jeffreys et al., 1999, Buard et al., 2000). For our analyses, we monitored minisatellite alterations in unreplicated haploid stationary phase cells in which sister chromatids or homologs are not present to facilitate strand exchange.

We previously proposed a model in which intramolecular repair events could account for the minisatellite alterations observed in *ade2-h7.5* strains (Kelly et al., 2011). This model is dependent upon DNA polymerase slippage at repair sites - due to the limited nucleotide availability in quiescent cells - resulting in tract contractions or expansions. Our work, discussed here and in preceding chapters, identifying replication-

associated factors and nucleotide abundance as important for stabilizing minisatellite sequences supports this model. Thus, our data provides insight into the mechanism of human-associated minisatellite alterations that occur within non-dividing cells.

Intriguingly, the replication checkpoint genes *MRC1*, *CSM3* and *TOF1* are highly conserved in eukaryotes. Human orthologs of each gene are Claspin, Tipin and Tim1 (Gotter et al., 2007, Yoshizawa-Sugata and Masai, 2007), respectively. Similar to their homologous role in yeast, Claspin (Chini and Chen, 2003), Tipin and Tim1 have been shown to form a stable complex which mediates replication checkpoint signaling as well as maintains proper replicative function (Chini and Chen, 2003, Gotter et al., 2007, Yoshizawa-Sugata and Masai, 2007, Sercin and Kemp, 2011, Uno and Masai, 2011). Due to the conservation of function of Mrc1p, Csm3p and Tof1p in higher order eukaryotes, our findings are directly applicable to minisatellite repeat stability in human cells and suggest a potential mechanism of tract alteration that could give rise to disease associated alleles.

Data Contribution

We thank Laura Brosnan and Dr. Katy Kelly for constructing the strain DTK1188. Laura Brosnan constructed and performed blebbing quantification on the following strains: DTK1533, DTK1543 and DTK1560. PCR, gel electrophoresis and sequencing across the minisatellite tract of blebs isolated from DTK1188, DTK1533, DTK1543 and DTK1560 was performed in cooperation with Laura Brosnan and Pete Jauert.

Figure 5-1.

The *ade2-h7.5* Minisatellite Allele.

The *ade2-h7.5* minisatellite allele is composed of seven-and-a-half 28bp repeats of the minisatellite sequence associated with the *HRAS1* oncogene. The minisatellite plus flanking sequence is inserted into the *Xba*I site of the yeast gene *ADE2*. The minisatellite is composed of variable repeat sequence. Each repeat unit, numbered 1-4, differ at positions +14nt and + 22nt in either a C or a G content. Insertion of the minisatellite disrupts the *ADE2* open reading frame; the loss of one repeat unit from the minisatellite restores the *ADE2* reading.

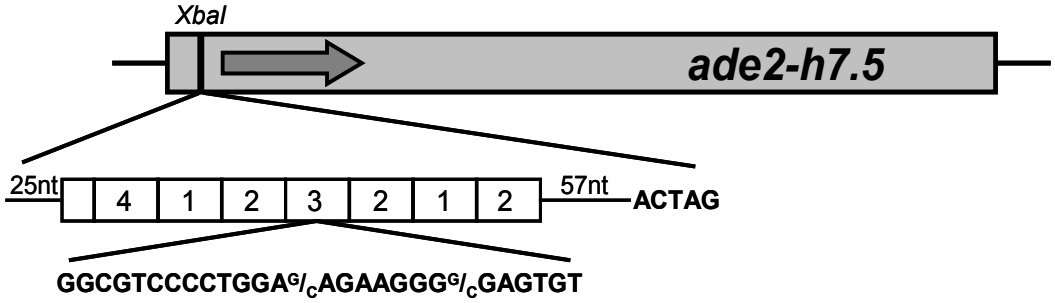

Figure 5-2.

Replication Checkpoint Components are Required for *ade2-h7.5* Minisatellite Stability. Pictures depict single colonies of the wild-type (WT) and deletion mutant strains. Blebbing quantification was performed on strains bearing the *ade2-h7.5* allele. YPD cultures of red cells were grown for four hours at 30°C. Cultures were diluted, plated onto solid YPD and incubated at 30°C for two days. The resulting colonies were then incubated at RT for six days. Blebs were counted on 100 individual colonies for each strain and the average number of blebs +/- the 95% confidence interval was calculated. This experiment was repeated three independent times. The solid horizontal black line indicates the average number of blebs of the WT strain.

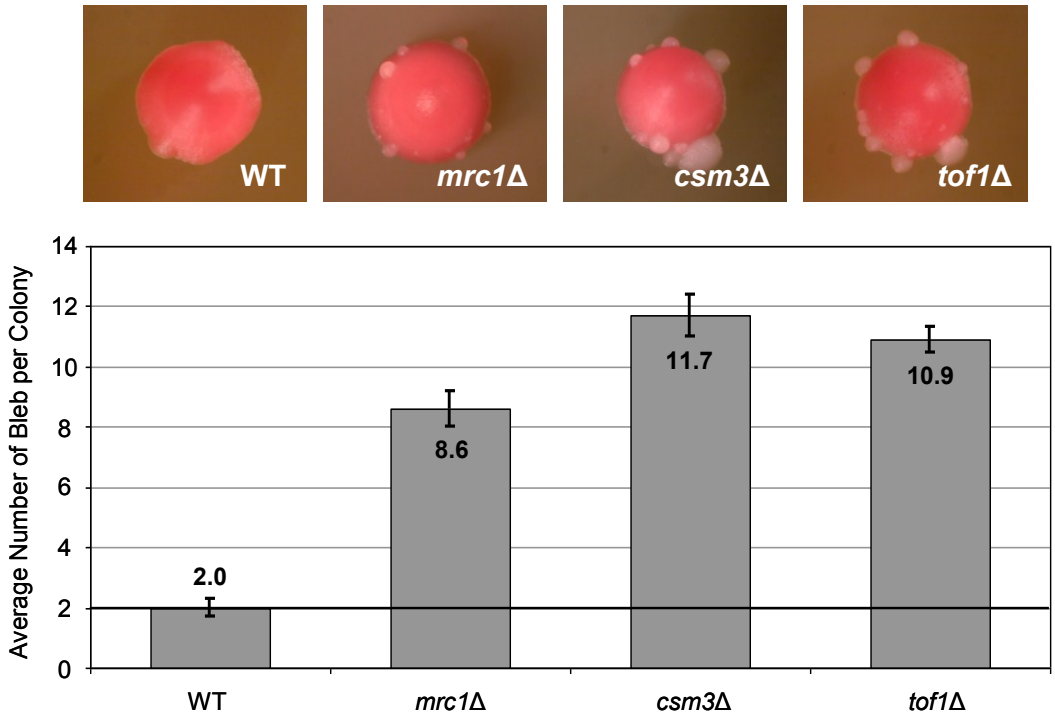

Figure 5-3.

Summary of the *ade2-h7.5* Tract Alterations Observed in Replication Checkpoint Strains. Genomic DNA was isolated from 25 independent blebs for *mrc1*Δ, *csm3*Δ or *tof1*Δ strains. PCR was performed across the minisatellite tract and the resulting product was analyzed by sequencing. The parental *ade2-h7.5* allele is given as a reference. The location of a lost repeat unit is indicated by a break within the minisatellite tract. The grey squares represent the location of gene conversion events.

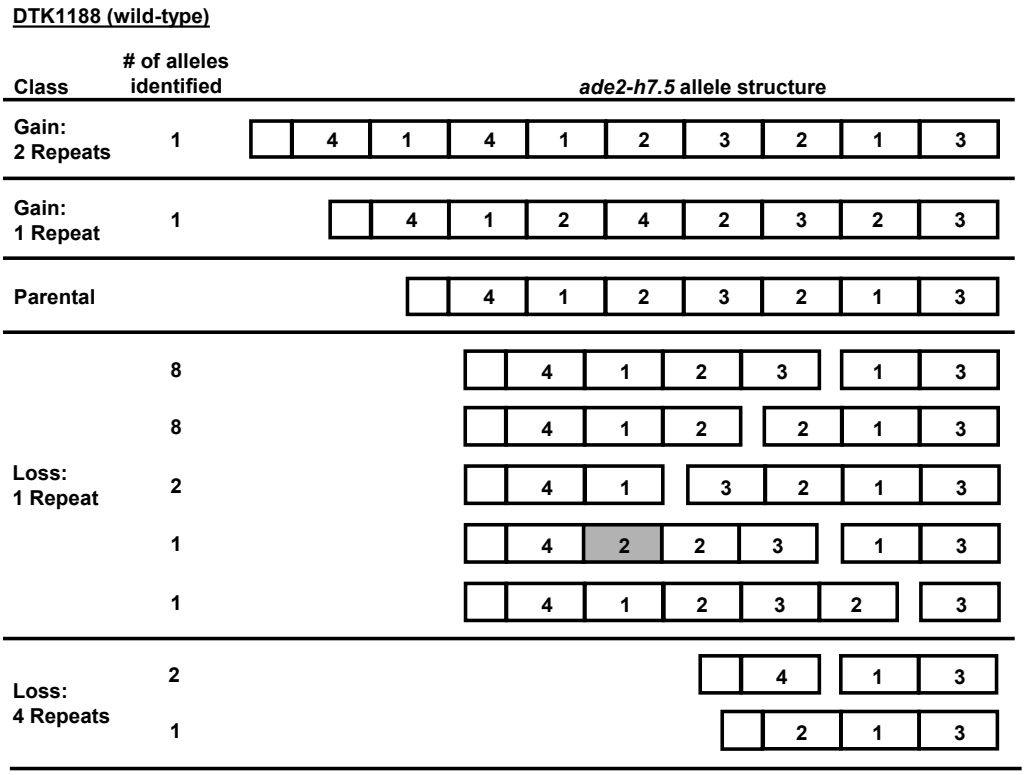

DTK1533 (*mrc1*Δ)

Class	# of alleles identified	*ade2-h7.5* allele structure
Gain: 2 Repeats	1	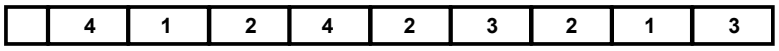
	1	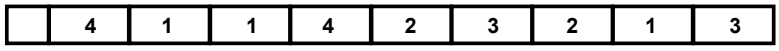
Parental		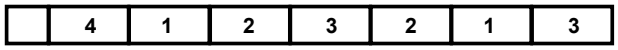
Loss: 1 Repeat	10	
	5	
	3	
	1	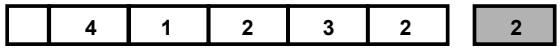
	1	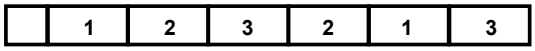
Loss: 4 Repeats	2	
Loss: Repeat Tract	1	

DTK1543 (*csm3*Δ)

Class	# of alleles identified	*ade2-h7.5* allele structure
Parental		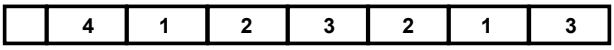
Loss: 1 Repeat	8	
	6	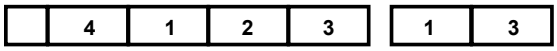
	3	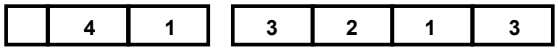
	1	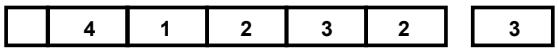
Loss: 4 Repeats	6	
	1	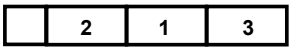

DTK1560 (*tof1*Δ)

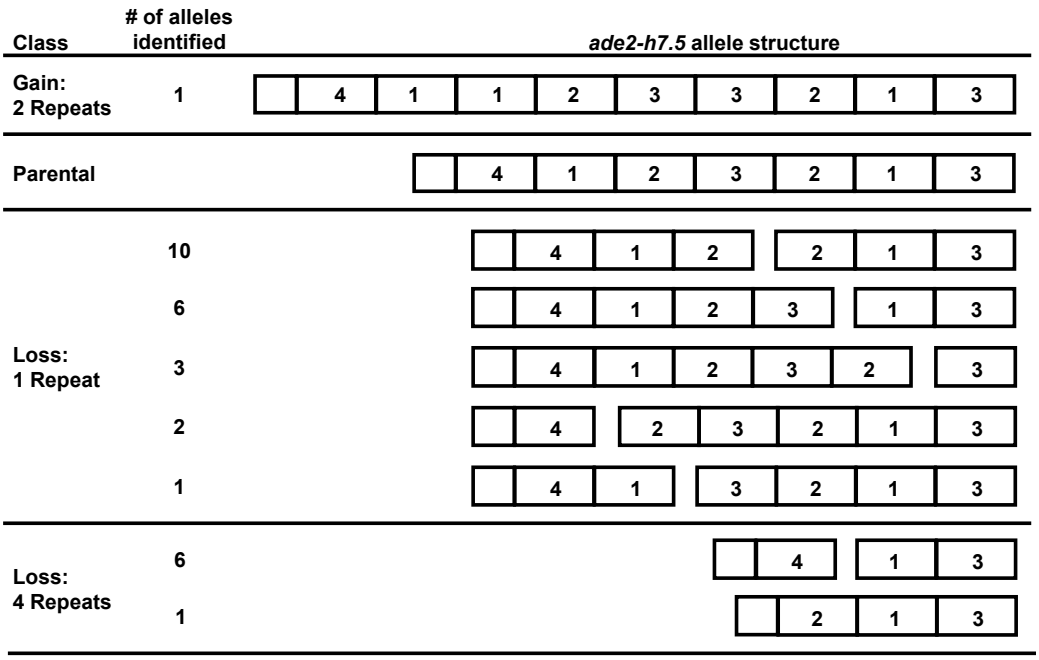

Figure 5-4.

Minisatellite Alterations in an *mrc1*Δ Strain are Mediated by Recombination Factors. Bleb quantification was performed on all strains as described in Figure 5-2 and Chapter VII: Materials and Methods.

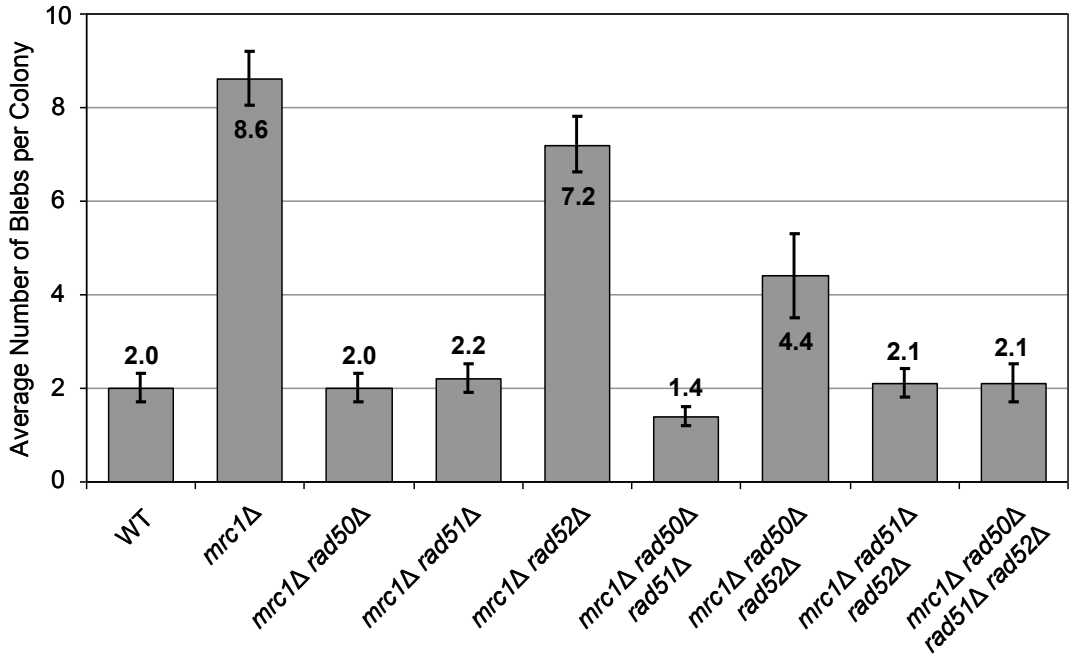

Chapter VI

Final Discussion

In the preceding chapters, we investigated several factors that are important for preventing minisatellite alterations in stationary phase cells of the yeast *Saccharomyces cerevisiae*. We began by conducting a modified version of the Synthetic Genetic Array (SGA) analysis to screen the yeast genome for genes that, when mutated, resulted in a high level of minisatellite instability. Our screen implicated over 200 candidate genes that regulate the stability of a simple minisatellite (the *ade2-min3* allele) or a human-derived minisatellite (the *ade2-h7.5* allele). GO term analyses of our candidate hits revealed an enrichment of DNA replication - and repair - associated genes, suggesting potential regulatory mechanisms for stationary phase minisatellite stability.

In chapter 3, we discussed the characterization of several strong hits identified in our *ade2-min3* SGA screen as well as genes that expressed functionally related gene products that represented components of DNA damage and replication checkpoints. We found that a specific subset of these genes prevented stationary phase minisatellite instability. Pathway analysis revealed that the genetic relationships of each gene previously established in actively dividing cells were not conserved in stationary phase cells. For example, components of the well-characterized replication checkpoint, *MRC1*, *MEC1* and *RAD53*, were found to comprise at least partially independent pathways. We found that this result was, in part, due to the replicative function of Mrc1p rather than its checkpoint function being the primary mode of Mrc1p-dependent minisatellite stability. Importantly, we demonstrated that tract alterations occur within the quiescent population of stationary phase cells in *mrc1*Δ, *csm3*Δ, *tof1*Δ, *mec1-21* and *rad53-1* strains. Thus, we

find that checkpoint components are active in stationary phase quiescent cells and facilitate genomic minisatellite stability.

Our work described in chapter 4 explored the potential mechanisms associated with stationary phase minisatellite instability. We found that *ade2-min3* tract alterations occurring in a *mrc1*Δ mutant strain were primarily mediated by *RAD52*-dependent recombination pathways. Additionally, we demonstrated that minisatellite alterations in *mrc1*Δ, *mec1-21* and *rad53-1* strains were suppressed by increasing nucleotide availability and conversely antagonized by decreasing nucleotide pools. These data demonstrate that mechanisms associated with repetitive tract alterations in stationary phase cells include recombination and nucleotide depletion. Due to the relationship between nucleotide levels and replication, we predict that polymerase slippage may account for the increase in minisatellite stability when dNTPs are depleted.

In Chapter 5, we examined the effect of *MRC1*, *CSM3* and *TOF1* on the stability of a human-derived minisatellite, the *ade2-7.5* allele. We found that the deletion of each gene resulted in an increase in *ade2-h7.5* minisatellite instability. Furthermore, tract alterations in an *mrc1*Δ strain were mediated primarily by the recombination factor genes, *RAD50* and *RAD51*. Our work provides a mechanistic explanation as to how minisatellites alter and give rise to disease-associated alleles in non-dividing human cells.

Minisatellite Composition and the Factors that Regulate Repeat Stability in Stationary Phase Cells

In chapter 2, we identified numerous factors that regulated the stability of the *ade2-min3* or the *ade2-h7.5* minisatellite allele in stationary phase cells. Interestingly, only seven candidate genes overlapped both screens, suggesting that the *ade2-min3* and *ade2-h7.5* minisatellites are regulated by different gene products in stationary phase. Because this assay directly monitors the effect of trans-acting factors rather than surrounding cis-acting sequences on minisatellite stability, we predict that the tract sequence and size of the minisatellite influences which factors regulate repeat stability.

Previous studies have established a link between the composition of the minisatellite and repeat tract stability (Desmarais et al., 1993, Buard et al., 1998, Jauert and Kirkpatrick, 2005), while the effect of tract length on repeat stability is controversial. Several studies have indicated that tract length impacts the mutation rate of a minisatellite (Buard et al., 1998, Berg et al., 2003, Jauert and Kirkpatrick, 2005) while others have claimed that there is little correlation (Jeffreys et al., 1994). Based upon our analyses, we cannot distinguish between the individual contributions of either the repeat sequence or the tract length in terms of the stability of each minisatellite allele. This controversy could be further addressed by introducing minisatellites differing in either repeat length or sequence composition into mutant strains identified as hits in our screen and then quantifying the level of blebbing for each strain.

Of the seven overlapping hits identified in our screens, three are specifically associated with regulating intracellular zinc levels and include the genes *COT1*, *ZRT1* and *ZAP1* (Conklin et al., 1992, Zhao and Eide, 1996, Zhao and Eide, 1997). The data presented here support our previous hypothesis that maintaining zinc homeostasis within

cells stabilizes minisatellite tracts regardless of the repeat composition or size (Kelly et al., 2007, Kelly et al., 2011). Zinc is an important cofactor for DNA binding proteins, such as those associated with DNA repair (Asahina et al., 1994, Cho et al., 1994, Wiltzius et al., 2005, Ahel et al., 2008) and functions, together with the enzyme superoxide dismutase, in preventing cells from accumulating reactive oxygen species (ROS) that can cause DNA damage (Ho and Ames, 2002, Ho, 2004, Clegg et al., 2005). Studies have also demonstrated a link between zinc deficiency and several diseases such as cancer (Ho, 2004, Han et al., 2009, Alder et al., 2012), diabetes (Kinlaw et al., 1983, Blostein-Fujii et al., 1997) and kidney disease (Lobo et al., 2010). We hypothesize that the deletion of *COT1*, *ZRT1* or *ZAP1* disrupts zinc levels within the cell. As a result, minisatellite instability through zinc depletion could occur by: 1) the aberrant function of DNA binding proteins that require zinc as a cofactor and 2) the accumulation of ROS resulting in DNA damage that is incorrectly repaired at the minisatellite locus. Based upon our results discussed above and in the preceding chapters, we conclude that either of these mechanisms are possible.

In chapter 2 and chapter 3, we discussed the identification of several hits that were false positives. These included the hits YLR125W and *BUB3*. PCR analysis of the parental YLR125W and *BUB3* deletion strains from the nonessential deletion collection revealed that each strain was wild-type at the target locus. As both strains were $G418^R$, we predict that the *KANMX* PCR fragments used to construct the parental strains are located elsewhere in the yeast genome at areas of sequence homology. To determine the location of the *KANMX* fragments, we propose performing complementation tests using a

plasmid library in which we select transformants with a suppressed blebbing phenotype. Based upon the results of each SGA analysis and the high level of blebbing observed in both mutant strains, it would be interesting to see if the location of the *KANMX* fragments in each strain overlaps the open reading frames of genes associated with maintaining intracellular zinc levels.

Due to the discovery of incorrect strains that gave rise to strong blebbing phenotypes, we interpret the results from our SGA screens with caution. As we continue to study the hits identified in each screen, we will verify the mutations of the parental strains by PCR and sequencing, and verify the blebbing phenotype in our laboratory strain background. Interestingly, an investigation into the laboratories that produced the haploid deletion collection revealed that only three out of a total of 16 labs constructed the parental strains that gave rise to false positives. This suggests the potential for common secondary mutations within these strain backgrounds that could affect minisatellite stability. It would be interesting to determine if the strains giving rise to false positives in our SGA analyses were also identified in whole-genome yeast screens performed by other laboratories.

DNA Replication Factors and ade2-min3 *Minisatellite Stability*

Independent analyses of the candidate genes identified in each screen revealed a correlation between stationary phase minisatellite stability, DNA replication and DNA repair. GO term analyses of the 100 hits identified in our *ade2-min3* screen revealed that genes associated with DNA replication were greatly enriched within our data set. These

included the replication checkpoint genes *MRC1*, *CSM3* and *TOF1* (Alcasabas et al., 2001, Katou et al., 2003, Osborn and Elledge, 2003, Bando et al., 2009), the flap endonuclease gene *RAD27* (Liu et al., 2004a), the PCNA clamp loader genes *RFC2* and *RFC4* (Cullmann et al., 1995, Yao et al., 2003, Chilkova et al., 2007) and genes that encode for subunits of Polδ (*POL31* & *POL32*) or Polε (*DPB3* & *DPB4*) (Araki et al., 1991, Araki, 1994, Hashimoto et al., 1998, Ohya et al., 2000). Previous studies have demonstrated that mutations in the replication gene *RAD27,* the PCNA processivity factor, the essential catalytic subunit of Polδ (*POL3*) or the *PIF1* helicase result in mitotic minisatellite instability (Kokoska et al., 1998, Kokoska et al., 1999, Lopes et al., 2002, Maleki et al., 2002, Ribeyre et al., 2009). Furthermore, characterization of *MRC1* in Chapter 3 demonstrated that *ade2-min3* minisatellite stability is primarily mediated by the replicative function associated with Mrc1p. Thus, replication is strongly associated with *ade2-min3* repeat tract stability.

As bulk DNA synthesis does not occur in stationary phase cells, the question remains as to what role DNA replication factors could have within a non-dividing cell population. Interestingly, several genes listed above have been shown to be associated with DNA repair. For example, Polδ has been implicated in base excision repair (BER) (Blank et al., 1994) and the repair of UV-damaged DNA (Torres-Ramos et al., 1997). Polε, a second replicative polymerase, functions in BER (Wang et al., 1993), nucleotide excision repair (NER) (Shivji et al., 1995), as well as double strand break repair (Holmes and Haber, 1999). Furthermore, inhibition of the exonuclease activity of either

polymerase in stationary phase yeast cells results in a mutator phenotype (Babudri et al., 2001) indicating that both polymerases enhance genomic stability in non-dividing cells.

In Chapter 3, we demonstrated that *ade2-min3* stationary phase alterations within *mrc1*Δ and *zrt1*Δ strains were partially dependent upon the recombination function of the ssDNA binding protein, replication protein A (RPA) (Umezu et al., 1998). RPA is a highly conserved protein essential for DNA replication and repair (reviewed in (Fanning et al., 2006)). Based upon our data, we hypothesize that gene products associated with DNA replication are actively preventing *ade-min3* minisatellite instability by facilitating proper replication during DNA repair in stationary phase cells. The role of mismatch repair in mediating stationary phase minisatellite stability is discussed below.

To determine what types of DNA damage affect stationary phase minisatellite stability, we are determining the level of blebbing in *ade2-min3* strains that have been exposed to different DNA damaging reagents or UV (see Chapter 9: Appendices). We are also monitoring the accumulation of RPA foci in log phase and stationary phase cells bearing the *ade2-min3* minisatellite. These experiments will give us insight into the type of DNA damage and DNA repair mechanisms that could contribute to genome instability within stationary phase cells.

Finally, one of our goals is to conduct experiments that address if DNA replication is physically occurring in stationary phase cells. While previous studies in *Escherichia coli* have established that DNA replication is active in stationary phase cells (Bridges, 1996, Harris et al., 1997a), the evidence of DNA replication occurring during stationary phase in higher order eukaryotes is lacking. To our knowledge, only one

published study in yeast has identified areas of DNA replication in stationary phase cells (de Morgan, 2010). However, this study fails to address whether this replication is occurring within the previously characterized nonquiescent (slowly-dividing) or quiescent (non-dividing) cell subpopulations associated with stationary phase cultures of yeast (Allen et al., 2006, Aragon et al., 2008). We propose addressing this issue by monitoring DNA replication using bromodeoxyuridine (BrdU) labeling. BrdU incorporation in nonquiescent and quiescent cells can be studied by separating stationary phase cultures into fractions of each subpopulation using the Percoll density-gradient centrifugation assay described in Chapter 4.

Mismatch Repair and the Stability of the HRAS1*-associated* ade2-h7.5 *Allele*

We discovered that the human-derived *ade2-h7.5* minisatellite allele, and not the *ade2-min3* allele, was regulated by mismatch repair in stationary phase. This finding is significant because until now, mismatch repair has been used as a defining characteristic of microsatellite stability rather than minisatellite stability (Sia et al., 1997). As we discussed in Chapter 2, this could be due to the authors utilizing a minisatellite identical to that of the *ade2-min3* allele in their studies rather than an allele of more complexity. Our work demonstrates that the composition of the minisatellite can greatly affect which factors regulate the stability of the repeat tract and suggest that studies utilizing human-associated minisatellite alleles would be more relevant with respect to human health and disease.

Mismatch repair has previously been shown to have an active role in stationary phase cells. Studies conducted in stationary phase *E. coli* cells have shown that a depletion of mismatch repair components resulted in an increase the rate of genomic mutations (Longerich et al., 1995, Harris et al., 1997b). The deletion of mismatch repair genes in stationary phase cells of the yeast *S. cerevisiae* has also been shown to result in a mutator phenotype (Halas et al., 2002). These studies, together with our findings discussed in Chapter 2, suggest that the mismatch repair system is active in stationary phase cells as a mechanism to prevent genome instability. We propose following up on this finding by determining which subpopulation of stationary phase cells mismatch repair is active in.

The mechanisms associated with mismatch repair are largely dependent upon the type of DNA substrate to be repaired. A complex consisting of Mlh1p, Pms1p, Msh2p and Msh6p recognize base:base mismatches and small loops generated from misalignment during replication, while a second complex containing Mlh1p, Pms1p, Msh2p and Msh3p identify and repair large loop structures (Habraken et al., 1996, Johnson et al., 1996, Marsischky et al., 1996). In Chapter 2, we found that deletion of *MLH1*, *PMS1*, *MSH2* or *MSH6* resulted in a high level of *ade2-h7.5* tract alteration implicating this complex in repeat stability. Our results suggest that this complex prevents minisatellite instability in stationary phase cells by correcting mispaired bases and loops generated through the misalignment of *ade2-h7.5* repeat units. Future pathway analysis utilizing each of the mutant mismatch repair yeast strains will help to establish the relationships between each gene.

Aberrant mismatch repair has been identified as a source of cancer formation in humans. Mutations in the human mismatch repair genes *MLH1*, *MSH2*, *MSH6* and *PMS2* (homologs of yeast *MLH1*, *MSH2*, *MSH6* and *PMS1*, respectively) have been shown to give rise to Lynch Syndrome – an inherited defect in which individuals have an increased susceptibility to the development of hereditary non-polyposis colorectal cancer (HNPCC) (Fishel et al., 1993, Bronner et al., 1994, Nicolaides et al., 1994, Bonadona et al., 2011). Furthermore, the presence of altered microsatellites is a hallmark of HNPCC (Umar, 2004, Sheng et al., 2006, Geiersbach and Samowitz, 2011). Mutations in mismatch repair genes are predicted to give rise to microsatellite instability due to the accumulation of uncorrected replication errors. Microsatellite instability is thought to result in the abnormal expression of genes associated with cell proliferation, further promoting disease (reviewed in (Boland and Goel, 2010)). Similar mechanisms have been proposed for the association of rare altered alleles of the *HRAS1* minisatellite and cancer formation (Devlin et al., 1993, Ding et al., 1999, Weitzel et al., 2000, Vega et al., 2001) described in the preceding chapters. Our results extend these studies and identify a new link between *HRAS1*- associated minisatellite stability and mismatch repair in non-dividing cells thereby establishing a potential mechanism of human disease formation.

The Role of Checkpoint Components in Stationary Phase Minisatellite Stability

In Chapter 3, we investigated the association of mitotic checkpoint factors and *ade2-min3* minisatellite stability in stationary phase cells. Due to the high level of blebbing produced by the *mrc1*Δ, *csm3*Δ and *tof1*Δ strains during our SGA analysis

(Chapter 2), we specifically focused on studying checkpoint components that have known associations with these genes. These included components of the replication checkpoint and the intra-S-phase DNA damage checkpoint – *DDC1*, *RAD17*, *MEC3*, *CHK1*, *RAD9*, *MEC1* and *RAD53* (Branzei and Foiani, 2005, 2006). We found that despite the characterized relationships established between each checkpoint gene in mitotic cells, only a specific subset of these genes were involved in stationary phase minisatellite stability. Our results suggest that complex differences exist between the interactions of and regulation of checkpoint pathway components in stationary phase cells compared to actively dividing cells.

Little is known about the role checkpoint signaling factors could have in a non-dividing cell. Previous research in yeast has demonstrated that the kinase Rad53p is activated in repair deficient stationary phase cells in the presence of reactive oxygen species (ROS) (Evert et al., 2004, Pawar et al., 2009). ROS accumulate at high levels in stationary phase cells due to mitochondrial metabolism (Herker et al., 2004, Allen et al., 2006, Drakulic et al., 2006). Oxidative stress due to the presence of ROS can result in damage to DNA as well as cellular proteins and lipids (reviewed in (Jamieson, 1998)). Our laboratory has recently reported that an increase in ROS in an *end3*Δ strain correlated with an increase in stationary phase minisatellite instability (Kelly et al., 2012), suggesting a link between oxidative damage and repeat alterations in non-dividing cells. We propose that checkpoint components and regulatory pathways are in place in stationary phase cells to prevent the accumulation of ROS, thus preventing genomic instability that could accrue through oxidative damage. To determine if an increase in

ROS is present in each of our checkpoint mutants, we propose monitoring the level of H2DCF-DA stained ROS in cells using flow cytometry as described in Kelly et al., 2012. Furthermore, we can expand this experiment to determine the level of ROS in nonquiescent and quiescent cell fractions of each strain using the Percoll density-gradient centrifugation assay described in Chapter 4.

Intriguingly, we discovered that *MEC1*, *MRC1* and *RAD53* fell within separate pathways in stationary phase cells despite their established roles in the replication checkpoint pathway of mitotic cells (Chapter 3) (Alcasabas et al., 2001, Osborn and Elledge, 2003, Branzei and Foiani, 2006). As discussed in Chapter 3, one possible explanation for this was that we found that Mrc1p mediates minisatellite stability in stationary phase by maintaining proper replication function rather than through mediating Mec1p/Rad53p-dependent checkpoint signaling. Previous work has also identified a Mec1p-independent role for Rad53p in which Rad53p regulates histone levels in actively dividing cells by mediating the degradation of histones that are not bound to chromatin (Gunjan and Verreault, 2003, Dohrmann and Sclafani, 2006). In keeping with our DNA replication and repair model of minisatellite stability proposed above, Rad53p could have an active role in stationary phase cells by monitoring histone levels during repair synthesis. It would be interesting to determine if there is a connection between Rad53p and histone repair complexes that modify chromatin to facilitate DNA repair mechanisms at sites of DNA damage (Tsukuda et al., 2005).

A Rad53p-independent role for Mec1p was previously identified in mitotic cells in which Mec1p activated the spindle assembly checkpoint (SAC) after DNA damage

(Kim and Burke, 2008). Several components of the spindle checkpoint were identified in our SGA screen. Future pathway analysis utilizing the *mec1-21* allele in combination with mutant SAC genes identified in our screen will help determine if Mec1p activates the spindle checkpoint in stationary phase cells. As the SAC monitors chromosomal attachment during mitosis, we have yet to discern what role these proteins could have in non-dividing cells. Finally, it is possible that *MEC1* or *RAD53* are associated with other hits identified in our SGA analysis that were not discussed here. Further investigation into these potential relationships might identify new roles for both Mec1p and Rad53p.

The Mechanisms of Minisatellite Alteration in Stationary Phase Cells

In Chapter 4 and Chapter 5, we established that minisatellite alterations in an *mrc1*Δ strain bearing either the *ade2-min3* allele or the *ade2-h7.5* alleles were dependent upon recombination mechanisms. Previous work performed in our laboratory also demonstrated that the blebbing phenotype associated with the deletion of *ZRT1*, *END3* or a mutation in *PKC1* in strains bearing either minisatellite allele was recombination-dependent (Kelly et al., 2011, Kelly et al., 2012) suggesting a universal role for recombination pathways in stationary phase cells.

Homologous recombination is an important repair mechanism associated with DNA damage and has been implicated in meiotic as well as mitotic minisatellite alterations (Jeffreys and Neumann, 1997, Jeffreys et al., 1998, Jeffreys et al., 1999). We previously described a recombination-associated mechanism for minisatellite alterations in haploid stationary phase cells (see Chapter 9: Appendices) (Kelly et al., 2011) and

predict that tract alterations occur through *RAD52*-dependent single strand annealing (SSA) or intra-molecular repair pathways. Both mechanisms can lead to strand misalignment and generate tract expansions or contractions (Klein, 1995). In our previous work and Chapter 4, we demonstrated that minisatellite alterations in *zrt1*Δ and *mrc1*Δ strains were partially mediated by SSA. Our current model for intramolecular repair events involves the generation of ssDNA and DNA repair synthesis. Briefly, after the generation of a ssDNA gap, DNA is synthesized, at which point polymerase slippage events and strand misalignment could result in the expansion or contraction of the repeat.

Finally, we investigated the correlation between nucleotide pools and stationary phase minisatellite stability (Chapter 4). We found that the depletion of dNTPs in mutant strains bearing the *ade2-min3* allele resulted in a dramatic increase in the level of stationary phase tract alterations. In a complimentary experiment, we demonstrated that increased levels of dNTPs resulted in repeat tract stabilization. Therefore, our results demonstrate a link between nucleotide availability and stationary phase minisatellite stability.

Prior work has shown that limiting dNTPs corresponds to an inhibition of DNA replication (Frenkel et al., 1964, Slater, 1973, Desany et al., 1998). As described above, we have identified and characterized several replication and repair associated factors as having a role in stationary phase minisatellite stability. Areas of DNA replication could correspond to repair mechanisms taking place at sites of DNA damage. We hypothesize that limited availability of nucleotide pools in stationary phase cells can result in

polymerase slippage at areas of DNA replication giving rise to alterations within the minisatellite tract.

Revisiting the Formation of the Blebbing Phenotype in Yeast Stationary Phase Cells

Our laboratory has established a correlation between minisatellite alterations occurring in stationary phase cells and a color segregation phenotype known as blebbing in which white microcolonies form on the surface of a predominate red colony. This phenotype is in sharp contrast to the sectoring phenotype observed in mitotic cells in which colonies consist of alternating red and white wedges.

As described in Chapter 3, stationary phase cells are composed of both nonquiescent and quiescent cells. Using mutational pathway analysis, we have been able to distinguish which population of cells gives rise to the blebbing phenotype (Kelly et al., 2011, Kelly et al., 2012). In Chapter 4, we described a density-centrifugation protocol that allows us to separate nonquiescent and quiescent stationary phase cells and monitor the expression levels of proteins within each of these subpopulations over the course of time. Using these two approaches, we have shown that the blebbing phenotype, and hence minisatellite alterations, occur within the quiescent subpopulation in each of our mutant strains discussed here and in previous work (Kelly et al., 2011, Kelly et al., 2012).

We have recently discovered a limitation to using these approaches to verify stationary phase-specificity of minisatellite tract alterations. By characterizing nonquiescent and quiescent stationary phase cells, the Werner-Washburne lab has suggested a model in which yeast cells differentiate into these subpopulations at the

diauxic shift rather than at a later timepoint in stationary phase (Allen et al., 2006, Werner-Washburne et al., 2012). Correspondingly, through using a stationary phase centrifugation assay, discussed in Chapter 4, we detected the presence of quiescent and nonquiescent cells at the 48 hour timepoint which, in our strain background, correlated with the diauxic shift. Thus, while we can show that minisatellite alterations occur within quiescent cells, we are unable to fully distinguish between tract alterations that take place at or after the diauxic shift in stationary phase.

Through our work, we have discovered that minisatellite alterations occurring in different mutant strain backgrounds give rise to a variety of blebbing phenotypes. For example, as discussed in Chapter 3, deletion of the replication checkpoint gene *MRC1* resulted in blebs that were only approximately 1/8 the size of that produced by our well characterized *zrt1*Δ strain. We demonstrated that differences in bleb size corresponded to the timing of the minisatellite alteration event. Small blebs are indicative of events that happened at a later timepoint whereas large blebs indicate events that happened at an earlier timepoint. Our results suggest that the timing of these events correspond to later stationary phase and diauxic shift/early stationary phase, respectively. To determine at what timepoint the actual minisatellite alteration events occur, we propose an assay in which we monitor GFP expression over the course of time. Briefly, the *min3* minisatellite will be tagged with the GFP reporter construct. An intact minisatellite will not result in GFP expression; however, alterations to the minisatellite will result in GFP expression and can be readily detected using fluorescence microscopy. As these events are rare, it is possible that they will be difficult to detect initially.

In summary, we propose the following updated model of blebbing formation within yeast cells (Figure 6-1): In (a), the sectoring phenotype is specific to minisatellite alterations that take place during log phase growth. Several red cells within the yeast colony experience minisatellite tract alterations that result in the production of white cells. As the colony continues to grow, the resulting color segregation phenotype is that of white and red sectioning. At the diauxic shift, cells differentiate into nonquiescent and quiescent cells. Based upon our data, stationary phase cells are predominately composed of the quiescent cells subpopulation. In (b), the blebbing phenotype is specific to cells in which the minisatellite alteration occurs at or after the diauxic shift. Bleb size is indicative of when the alteration event occurred with large blebs corresponding to early events and small blebs corresponding to later events. In some mutant strains, such as *rad53-1* and *mec1-21* mutants, blebbing occurs in both nonquiescent and quiescent cells.

Conclusions

Our lab is the first lab to conduct a whole-genome high-throughput screen to identify factors that regulate minisatellite stability in stationary phase. Through our work, we have identified over 100 different factors that regulate minisatellite stability in stationary phase. Furthermore, we establish that the composition of the minisatellite affects which factors stabilize the repeat tract. Investigation into replication and checkpoint associated factors identified as hits in our screen suggest that minisatellite alterations occur in stationary phase cells due to uncorrected or improperly repaired sites of DNA damage. This conjecture is supported by the observation that minisatellite

alterations in mutant strains are mediated by recombination repair pathways and antagonized by an increase in nucleotide availability. Thus, our work provides novel insight into the regulatory mechanisms of minisatellite stability in quiescent cells and provides an explanation of how minisatellites can undergo alterations and become potentially pathogenic alleles.

Figure 6-1.

Model of Minisatellite Tract Alterations in Mitotic and Stationary Phase Cells (based upon a model presented in Kelly et al., 2007).

(a) Minisatellite alterations in log phase cells result in the transformation of red Ade^- cells to white Ade^+ cells. As the colony increases in size, the red and white cells produce alternating wedges. Adenine depletion in the media results in a shift from log phase to stationary phase. The blocks indicate cells that have differentiated into nonquiescent and quiescent cells. This event occurs at the diauxic shift, which is indicated by a vertical dotted line. **(b)** Minisatellite alterations in red Ade^- cells occurring during the diauxic shift or in stationary phase cells give rise to white Ade^+ cells that form blebs. Blebs can continue to grow in the adenine depleted media. Tract alterations may occur in both nonquiescent and quiescent cells depending upon the mutant strain. The size of the bleb is dependent upon the timepoint at which the minisatellite alteration took place; a large bleb is indicative of an early tract alteration event whereas a small bleb indicates a tract alteration that occurred at a later point in time.

a. Sectoring

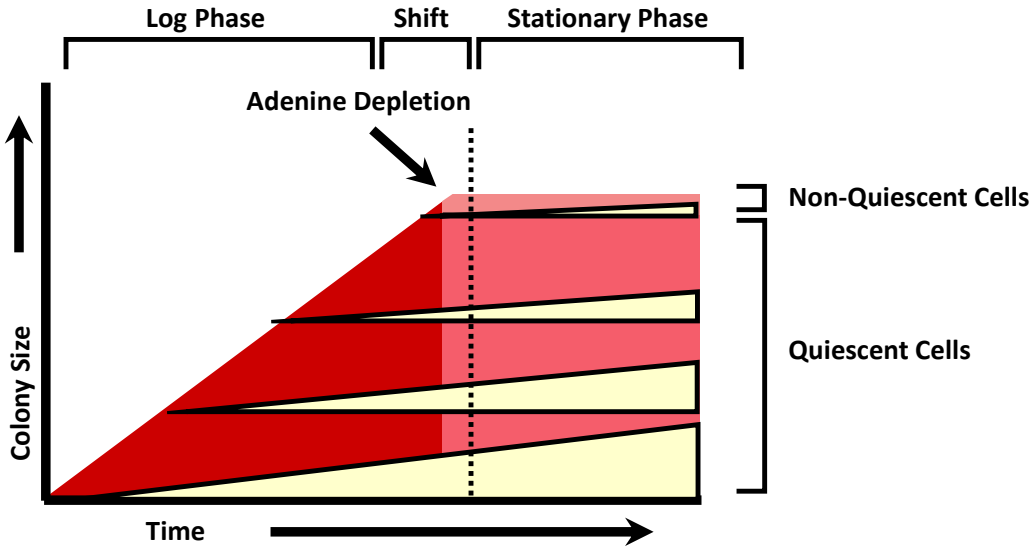

b. Blebbing

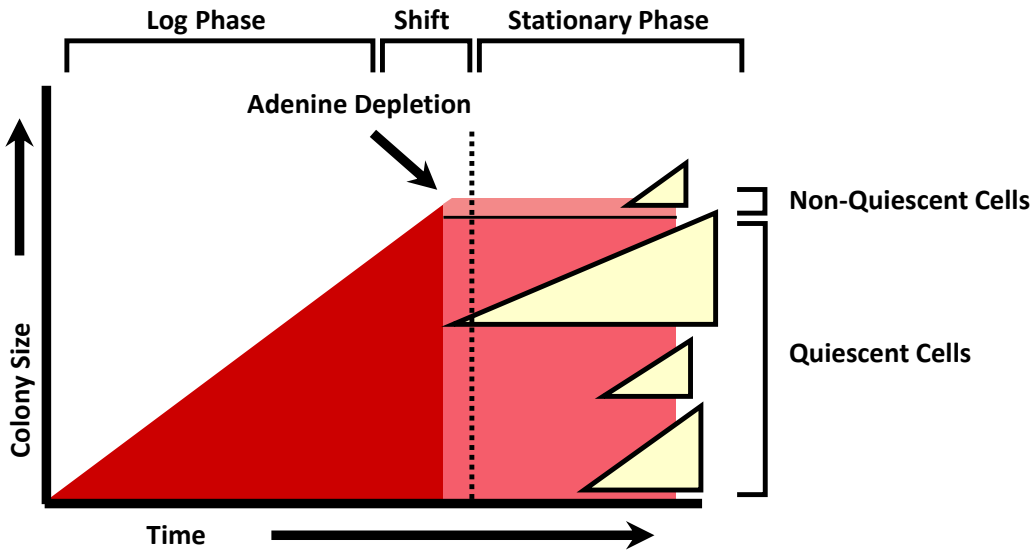

Chapter VII

Materials and Methods

Media, Plasmids and Yeast Strains

Solid and liquid media used in this work were prepared as stated in(Guthrie and Fink, 1991). All media used for the SGA analysis was prepared as described in (Tong et al., 2001, Tong and Boone, 2006). Pre-sporulation solid media consisted of 2% Agar, 5% Dextrose, 1% Difco Yeast Extract, and 3% Difco Nutrient Broth. Selective YPD media was made at the following concentrations: 1) 300mg/L Hygromycin B (Invitrogen) or 2) 200mg/L geneticin sulfate (G418) (Cellgro).

Saccharomyces cerevisiae strains used in this study are listed in Table 8-1. Each strain was derived from DTK264 (*MAT*a *his7-2 leu2::HisG trp1-289 ura3-52 ade2-min3*) or DTK271 (*MAT*α *his7-2 leu2::HisG trp1-289 ura3-52 ade2-min3*) (Kelly et al., 2007). Yeast strains bearing deletions of non-essential genes were constructed by isolating corresponding genomic DNA from the non-essential Yeast Deletion Strain Haploid Set. In brief, PCR products containing the *KANMX4* gene (G418 resistance) were generated from the genomic DNA using 5' and 3' flanking primers listed in Table 8-2. Parental strains were transformed with the *KANMX* PCR product and grown for four hours at 30°C in liquid YPD media. Transformants were selected on YPD + G418 solid media. Strains transformed with a *URA3* marker were constructed using the plasmid pRS316 as a PCR template. Transformants were selected on media lacking uracil. All isolates were verified by PCR.

Strains constructed by mating are listed in Table 8-1. Parental strains were mated, sporulated and dissected as described in (Jauert et al., 2002). Spores bearing the desired phenotypes were selected for using auxotrophic markers, temperature sensitivity or

sensitivity to a specific DNA damage reagent. Strains bearing the *pkc1-4* allele were selected based on lack of growth at 37°C. Strains containing the *mec1-21* or *rad53-1* allele were isolated by sensitivity to 50mM hydroxyurea (HU). Yeast strains with the *rfa1-t11* allele were isolated by sensitivity to 0.02% methyl methanesulfonate (MMS).

Yeast strains constructed from parental strains of two different genetic backgrounds were constructed by backcrossing to DTK271 for a total of three times. DTK1630, bearing the *ade2-min3* allele and a checkpoint defective allele of *MRC1* (*mrc1*^{AQ}), was constructed by mating DTK271 with Y2298 (from S. Elledge, Harvard Medical School) (Osborn and Elledge, 2003). Spores were isolated by red colony color and growth on media lacking histidine. The strain DTK1683, bearing the *ade2-min3* and a replication defective allele of *MRC1* (*mrc1-C14*) was constructed by mating DTK271 with Y2544 (S. Elledge, Harvard Medical School) (Naylor et al., 2009). Spores were isolated by resistance to G418 and red colony color. The strain DTK1776, bearing a point mutation in *MEC1*, was constructed by mating DTK271 with the *mec1-21* strain DKY2563 (from D. Koepp, University of Minnesota); this strain was originally from Y663 (Sanchez et al., 1996). The resulting diploid was sporulated and dissected, and a spore bearing the *ade2-min3* allele as well as the *mec1-21* mutation was isolated by colony color and sensitivity to 100mM HU.

DTK1766, a strain bearing the C14 C-terminal truncation of Mrc1p combined with the AQ point mutations, was constructed by transforming a *KANMX* PCR product into DTK1630. The *KANMX* PCR product, bearing *MRC1* flanking sequence to delete residues 844 - 1096, was generated using pFAKANMX6 as template and primers

78415868 and 78415869. Transformants were selected by resistance to G418 and the resulting strain was sequenced.

The strain DTK1979 bearing the *rfa1-t11* allele was constructed using the "pop-in/pop-out" method described in (Boeke et al., 1984). Here, the *rfa1-tll* open reading frame was excised from pKU1-t11 (from R. Kolodner, University of California San Diego) (Umezu et al., 1998) with *Sal*I and *Hind*III. The resulting fragment was gel purified. The purified *rfa1-t11* fragment was cloned into the multiple cloning site of pRS306 resulting in plasmid pBMA105. Insertion of the *rfa1-t11* open reading was confirmed by sequencing. pBMA105 was then linearized with *Mfe*I. The digested plasmid was gel purified and transformed into DTK271. Transformants bearing an integrated *rfa1-t11* allele were selected on solid media lacking uracil. Ura^+ transformants were patched onto YPD media and incubated at 30°C, then replica-plated to 5-FOA media. Single papillae were patched onto YPD, incubated at 30°C overnight, then replica-plated to media lacking uracil. DTK1979 was isolated as a red Ura^- transformant bearing the *rfa1-t11* allele as verified by sequencing and sensitivity to 0.02% MMS.

The parental yeast strain, DTK1657, used for protein isolation of stationary phase cells and western blot analysis was constructed by deleting the *TRP1* ORF in the strain DTK271 using primers 54969732 and 54969733. DTK1872, bearing a C-terminally 3HA tagged Tof1p, was constructed according to (Longtine et al., 1998). In brief, a 3HA-*TRP1* PCR product containing 51bp of 3' *TOF1* coding sequence ending just before the stop codon (forward primer 82966884) and 51bp of 3'UTR sequence (reverse primer 82966884) was generated using the plasmid pFA6a-3HA-TRP1 (from J. Berman,

University of Minnesota) as a template. Transformants were selected on solid synthetic media lacking tryptophan. This protocol was used to generate DTK1889, DTK1931 and DTK1933 using the primers listed in Table 8-2. We were unable to successfully tag Mrc1p at the C-terminus; therefore, we constructed an N-terminally tagged strain utilizing the plasmid pCMF022 (from D. Koepp, University of Minnesota). In brief, pCMF022 was digested with *Nde*I and gel purified. The linearized plasmid was transformed into DTK1920 and transformants were selected on media lacking leucine. Transformants were verified by growth on 200mM HU. All tagged strains were verified by sequencing.

For the *ade2-min3* SGA analysis, we constructed the query strain DTK893 (*MAT*a *his3-1 ura3-0 can1::MFA1pr-spHIS5 ade2-min3 - URA3MX*) using a two-step PCR process. Here, pDC369 (from D. Clarke, University of Minnesota) was used to generate a *URA3MX* PCR product, flanked by a 5' TEF promoter site and a 3' TEF terminator site, using primers 14193004 and 14193005. DTK281 genomic DNA was used as a PCR template to isolate the *ade2-min3* allele using primers 14193006 and 14193007. To combine the *URA3MX* and *ade2-min3* PCR products, we performed PCR using primers 14193007 and 14193008 resulting in the *ade2-min3 URA3MX*-linked cassette. The cassette was transformed into DCY2556 (from D. Clarke, University of Minnesota). Transformants were selected on solid synthetic media lacking uracil, yielding DTK893. DTK893 was crossed to DCY2557 (from D. Clarke, University of Minnesota) to generate the strain DTK1175. The DTK1175 diploid was sporulated and dissected. Red spores were selected on solid synthetic media lacking uracil. Query strains for the SGA analyses

were isolates of DTK1175: DTK1189 5a = *MAT*a derivative for the nonessential SGA and DTK1189 2b = *MAT*α derivate for the essential SGA.

To construct the *ade2-h7.5* query strain, DTK1624 (*MAT*a *his3-1 ura3-0 can1::MFA1pr-spHIS5 ade2-h7.5 - URA3MX*), we generated an *ade2-h7.5 URA3MX*-linked cassette using a two-step PCR process. In brief, we obtained a *URA3MX* PCR product, bearing a 5' TEF promoter site and a 3' TEF terminator site from pDC369 using primers 14193004 and 14193005. We isolated an *ade2-h7.5* PCR product from DTK1188 genomic DNA using primers 14193006 and 14193007. The two PCR products (*URA3MX* and *ade2-h7.5*) were combined using primers 14193007 and 14193008. The complete *ade2-h7.5 URA3MX*-linked cassette was transformed into DCY2556. Red Ura^+ cells were selected on solid synthetic media lacking uracil, yielding DTK1624.

Synthetic Genetic Array Analysis

Nonessential SGA

We conducted a modified version of the Synthetic Genetic Array analysis (Tong et al., 2001, Tong and Boone, 2006). For this screen, we inoculated liquid YPD media with a single red colony of the DTK1189 5a (*ade2-min3*) or the DTK1624 (*ade2-h7.5*) query strain. After incubation at 30°C overnight with agitation, the culture was plated onto solid YPD media. Once these plates were dry, strains from the *MAT*α non-essential Yeast Deletion Strain Haploid Set (from R. Wright, University of Minnesota) (Invitrogen) were manually pinned onto the query strain in a 96-well format and incubated at 30°C overnight. Zygotes were pinned to SD-Ura + G418 solid media and

incubated at 30°C overnight. To enhance the level of sporulation, we pinned the diploids to pre-sporulation solid media and incubated the diploids at 30°C overnight. Strains were sporulated at room temperature (RT) for 6 days. *MAT*a progeny were selected on SD-His/Arg/Ura + Canavanine (Can) (US Biological) solid media and incubated at 30°C overnight. This step was repeated. Double mutants containing the *ade2-min3* or *ade2-h7.5* allele were isolated by pinning the strains to SD-His/Arg/Ura + Can + G418 solid media. This selection step was repeated. After selection, the haploids were left at RT on YPD for 5 days to assay for the blebbing phenotype. Each strain was pinned in duplicate. The screen was repeated three independent times. A *MAT*α *zrt1*Δ haploid mutant, which has a strong degree of blebbing, was used as a positive control for our screen (Kelly et al. 2007). Mutants producing a high degree of blebbing (+++ or ++++ on a qualitative scale of + to ++++; blebbing of the *zrt1*Δ control = ++++) were considered hits. Strains were characterized as having the "strongest" level of blebbing if ranked as ++++ for 2 out of the 3 screens.

Essential SGA

For this screen, we followed a protocol similar to the Nonessential SGA protocol described above (Tong et al. 2001; Tong and Boone 2009; Li et al 2011). The *ade2-min3* query strain used for the essential SGA was DTK1189 2b. Strains to be examined that were part of a *MAT*a Essential Temperature Sensitive (ts) Strain Set (from C. Boone, University of Toronto) containing 455 ts alleles were manually pinned onto the query strain in a 96-well format and incubated at RT for 2 days. Zygotes were pinned to SD-Ura + G418 solid media and incubated at RT overnight. Diploids were pinned to pre-

sporulation solid media and incubated at RT overnight. Strains were then sporulated at RT for 6 days. *MAT*a progeny were selected on SD-His/Arg/Ura + Can solid media and incubated at RT for 2 days. This step was repeated. Double mutants containing the *ade2-min3* allele as well as a temperature sensitive allele were isolated by pinning the strains to SD-His/Arg/Ura + Can + G418 solid media and incubating at RT for 2 days. This selection step was repeated. After selection, the haploids were pinned to 5 separate YPD solid media plates. Each plate was left at 26°C, 30°C, 32°C, 34°C or 37°C for 5 days. Each strain was pinned in duplicate, and the screen was repeated three independent times. Blebbing for each plate was scored as stated above. A *MAT*a *zrt1*Δ haploid mutant was used as a positive control for this screen. We defined a hit as: 1) a strain that produced a steady increasing level of blebbing only reaching +++ or ++++ when the critical temperature of the ts allele is reached for all 3 screens or 2) a strain that produced a level of blebbing of +++ to ++++ only when the critical temperature of the ts allele is reached for all 3 screens (blebbing of the *zrt1*Δ control = ++++). Any hits ranked with a level of blebbing of ++++ for 2 out of 3 screens was considered to have the "strongest" blebbing phenotype.

GO Term Analysis

The following data bases were used to identify enriched GO terms associated with the 100 hits from the *ade2-min3* SGA screen, the 157 hits from the *ade2-h7.5* SGA screen or the strongest blebbing hits for each screen: Generic Gene Ontology Term Finder (http://go.princeton.edu/cgi-bin/GOTermFinder), Funcassociate 2.0

(http://llama.mshri.on.ca/ funcassociate_ client/html/), Fun Spec (http://funspec.med. utoronto.ca/), Profiling of Complex Functionality (ProfCom) (http://webclu.bio.wzw. tum.de/profcom/) and Database for Annotation, Visualization and Integrated Discovery v6.7 (DAVID) (http://david.abcc.ncifcrf.gov/). Default parameters were used for all databases. Significant GO terms were characterized as terms that were represented in at least three out of the five databases. The background list for GO term analysis incorporated all genes in the *S. cerevisiae* genome. All analyses were performed in September, 2012.

Blebbing Quantification Assay

Yeast strains used for this assay were streaked onto solid YPD media and incubated at 30°C for 48 hours for single colony formation. A single red colony was used to inoculate 5mL of liquid YPD media. Cultures were incubated at 30°C for 4 hours with agitation. Suitable dilutions of each culture were plated onto solid YPD media, incubated at 30°C for 2 days and then left at RT for 6 days. Blebs lying on the surface of 30 - 50 individual colonies were then counted. The protocol was repeated for 3 independent experiments for each strain resulting in a total of at least 100 colonies analyzed in the assay. Only colonies ranging from 1.26 to 1.32 mm in diameter were included in the quantification analysis. We then calculated the average number of blebs/colony and the 95% confidence interval (CI) for each strain. Strains bearing the *pkc1-4* mutation were grown at 35°C for 6 days, and then the number of blebs was counted.

Analysis of the ade2-h7.5 Minisatellite Tract

Yeast strains bearing the *ade2-h7.5* were struck onto YPD for single colonies and incubated at 30°C for 3 days. Strains were then kept at RT for 6 days after which at least 100 individual blebs were picked and patched onto solid YPD media. After 2 days of growth at 30°C, whole cell PCR was performed on the patches of isolated blebs using primers 14193007 and 14193008. Gel electrophoresis was used to visualize the minisatellite allele tract size. To characterize the specific tract alterations, sequencing was carried out for 20 independent blebs from each strain.

Growth Curve Analysis

YPD cultures, inoculated with a single red colony from strains DTK271, DTK1392, DTK878 or DTK1556, were grown for 4 hours at 30°C. Cultures were then diluted, plated onto solid YPD media and incubated at 30°C for 2 days. Strains were then left at RT for 6 days. Individual blebs were isolated from each strain, patched onto YPD solid media and incubated at 30°C overnight. For each strain, 3 white patches were streaked onto YPD solid media for single colonies and incubated at 30°C for 48 hours. A single white colony from each bleb was used to inoculate YPD cultures that were incubated at 30°C overnight. Cultures were diluted 1:1000 in liquid YPD, and 350µL of each dilution were added to a round bottom 96 well plate. Growth curves were generated for each diluted culture using the TECAN Sunrise™ microplate reader and Magellan™ data analysis software (TECAN Group Ltd). Timepoints were taken every 15 minutes over the course of 48 hours. The average OD_{600} was calculated for each culture at each

timepoint. The growth rates were generated for each strain by calculating the linear slope of the line of data taken from timepoints 7 - 13 hours.

Fractionation of Stationary Phase Cellular Populations

To isolate the individual cellular populations of stationary phase yeast cells, we performed a modified version of the Percoll gradient centrifugation experiment described in (Allen et al., 2006). The strains DTK1657, DTK1872, DTK1889, DTK1930, DTK1931 and DTK1933 were struck onto solid YPD media and grown at 30°C for 48 hours. Single red colonies from each strain were used to inoculate 60mL of liquid YPD. Cultures were grown in a 30°C incubator shaker for a total of 120 hours. Cells were harvested from each culture at the following timepoints: 18 hours (log phase), 48 hours (diauxic shift) and 120 hours (stationary phase). The following number of cells was harvested from each timepoint: $1.20x10^9$ cells at 18 hours, $3.61x10^9$ at 48 hours, and $3.61x10^9$ cells at 120 hours. The total number of cells harvested was increased for the 48 and 120 hour timepoints in order to obtain enough cells for analysis from the upper cell fraction after gradient centrifugation. Harvested cells were pelleted and resuspended in 1mL of 50mM Tris Base, pH 7.5. The OD_{600} of each culture were taken at 0, 18, 48 and 120 hours.

To form the density gradients, the Percoll gradient solution (GE Healthcare) and 1.5M NaCl were mixed together in a 9:1 ratio. A total of 10mL of this mixture was added to a 15mL Corex tube and centrifuged at 10,000 g_{av} to form the gradient. Centrifugation was performed in a Sorvall RC 5B Plus centrifuge with rotor SA-600 at 4°C. After

centrifugation, 1mL of the harvested cell suspension solution was overlaid onto the pre-formed gradient. The cells were then centrifuged at 400 g_{av} in a tabletop centrifuge with swinging buckets at RT for 45 minutes. To remove the Percoll, upper and lower cell fractions were collected, washed in 25mL of 50mM Tris Base, pH7.5 and pelleted. This washing step was repeated twice more.

Protein Isolation of Stationary Phase Cell Populations and Western Blotting

Trichloroacetic acid (TCA) preps for protein isolation were performed on the washed upper and lower cell fractions collected by Percoll gradient centrifugation as stated in (Ricke and Bielinsky, 2006). In brief, cell fractions were washed in 1mL of 20% TCA, pelleted and resuspended in 250µL of 20% TCA. Acid-washed glass beads (Sigma Aldrich) were added to the cell suspensions. The suspensions were then put into a cell disruptor for 2 minutes at 4°C. Cell lysates were centrifuged at 4,000 rpm for 3 minutes and separated from the glass beads. For each collected fraction, the resulting supernatant was removed and the pellet was resuspended in approximately 100µL of 1x SDS-PAGE buffer containing dithiothreitol (DTT). [The 1x buffer solution was prepared by combining 400µL of a 2X SDS-PAGE stock (4% SDS, 20% glycerol, 120mM Tris pH 6.8, and 0.1% bromophenol blue), 100µL of 1M DTT and 500µL H2O.] The pH of each sample was adjusted by adding 30-50µL of 1M Tris, pH 9.5. Resuspended pellets were boiled for 5 minutes and centrifuged at 3,000 rpm for 10 minutes.

Western blotting protocol was performed as stated in (Ricke and Bielinsky, 2006). Briefly, protein concentrations of each TCA prep were determined using the RC DC

Protein Assay (Bio-Rad). The total amount of protein loaded per well for each the strains DTK1657, DTK1930 and DTK1931 were normalized to an absorbance of 0.4. Protein loaded for DTK1872 and DTK1889 were normalized to an absorbance of 0.8 to account for the low level of HA expression. Samples were subjected to SDS-PAGE and transferred to a nitrocellulose membrane. Blots bearing 3HA-tagged proteins were probed using the anti-HA- Peroxidase High Affinity primary antibody (Roche).

Budding Index of Stationary Phase Cell Fractions

Stationary phase cultures of DTK1657 were harvested using Percoll gradient centrifugation as stated above after 120 hours. The total amount of cells loaded per gradient equaled $3.61x10^9$ cells. Isolated upper or lower fractions were used to inoculate 3mL liquid YPD to an OD_{600} of 0.1. Cultures were then incubated at 30°C with agitation. For each timepoint, 300 cells were examined microscopically for the presence of buds. Timepoints were taken every 30 minutes over the course of 4 hours. The percentage of budding cells along with the standard deviation was calculated for each timepoint by comparing the number of cells with buds to the total number of cells (% Budding Cells = (Number of Cells with Buds/Total Number of Cells)*100). This experiment was repeated and the average percentages of budding cells and standard deviations were calculated.

Whole Cell Counts of Stationary Phase Cell Fractions

Cultures of DTK1657 were harvested after 120 hours growth using gradient centrifugation as stated above with the total amount of cells loaded onto the gradient

totaling $3.61x10^9$ cells. Hemocytometer cell counts were performed for both upper and lower fractions. This experiment was performed 2 independent times. The average number of cells comprising the upper or lower fraction was then calculated along with the standard deviation.

Table 8-1: Plasmids and Yeast Strains used in this study

Strain	Relevant genotype	Construction details
pCMF022	*MRC1-3HA-LEU2*	Gift from D. Koepp
pDC369	*URA3MX*	Gift from D. Clarke; originally from M. Tyers (p*URAMX*)
pKU1-t11	*rfa1-t11*	Umezu *et al*., 1998
Y2298	$mrc1^{AQ}$	Osborn and Elledge, 2003
Y2544	*mrc1-C14*	Naylor *et al.,* 2009
DCY1793	*rad53-1*	Raveendranathan *et al*., 2006
DCY2556	*his3-1 ura3-0 can1::MFA1pr-spHIS5*, *MAT*a	gift from D. Clarke; originally from M. Tyers (2446-14-2)
DCY2557	*his3-1 ura3-0 can1:: MFA1pr-spHIS5*, *MAT*α	gift from D. Clarke; originally from M. Tyers (3172-50-4)
DKY2563	*mec1-21*	gift from D. Koepp; originally from S. Elledge (Y663)
DTK264	*ade2-min3*, *MAT*a	Kelly *et al.*, 2007
DTK271	*ade2-min3*, *MAT*α	Kelly *et al.*, 2007
DTK284	*ade2-min3*	Kelly *et al.*, 2007
DTK878	*ade2-min3*, *zrt1*Δ*::KANMX*	Kelly *et al.*, 2007
DTK893	*ade2-min3 - URA3MX his3-1 ura3-0 can1::MFA1pr-spHIS5*, *MAT*a	DCY2556 with *ade2-min3 - URA3MX* linked cassette
DTK902	*ade2-min3 zap1*Δ	Kelly *et al*., 2007
DTK904	*ade2-min3*, *zrt1*Δ*::LEU2*	Kelly *et al*., 2011
DTK1008	*ade2-min3*, *chk1*Δ*::KANMX*	DTK271 with $chk1\Delta::KANMX^{a}$
DTK1012	*ade2-min3*, *zrt1*Δ*::LEU2*, *rad27*Δ*::KANMX*	DTK904 with $rad27\Delta::KANMX^{a}$

Strain	Relevant genotype	Construction details
DTK1056	*ade2-min3*, *rad50*Δ::*KANMX*	Kelly *et al*., 2011
DTK1057	*ade2-min3*, *zrt1*Δ::*LEU2*, *rad50*Δ::*KANMX*	Kelly *et al*., 2011
DTK1074	*ade2-min3*, *rad51*Δ::*KANMX*	Kelly *et al*., 2011
DTK1076	*ade2-min3*, *zrt1*Δ::*LEU2*, *rad51*Δ::*KANMX*	Kelly *et al*., 2011
DTK1082	*ade2-min3*, *cot1*Δ::*KANMX*	Kelly *et al*., 2011
DTK1088	*ade2-min3*, *end3*Δ*::KANMX*	DTK271 with *end3*Δ*::KANMX*[a]
DTK1093	*ade2-min3*, *rad9*Δ*::KANMX*	DTK271 with *rad9*Δ*::KANMX*[a]
DTK1170	*ade2-min3*, *rad53-1*	DTK271 x DCY1793, isolated spore
DTK1171	*ade2-min3*, *rad53-1*, *zrt1*Δ*::KANMX*	DTK878 x DCY1793, isolated spore
DTK1175	*ade2-min3 - URA3MX his3-1 ura3-0 can1:: MFA1pr-spHIS5*	DCY2557 x DTK893
DTK1188	*ade2-h7.5*	Kelly *et al*., 2011
DTK1189 2b	*ade2-min3 - URA3MX his3-1 ura3-0 can1:: MFA1pr-spHIS5*, *MAT*α	*MAT*α DTK1175
DTK1189 5a	*ade2-min3 - URA3MX his3-1 ura3-0 can1:: MFA1pr-spHIS5*, *MAT*a	*MAT*a DTK1175
DTK1191	*ade2-min3*, *zrt1*Δ::*LEU2*, *rad52*Δ::*URA3*	Kelly *et al*., 2011
DTK1199	*ade2-min3*, *rad27*Δ*::KANMX*	DTK271 x DTK1012, isolated spore
DTK1200	*ade2-h7.5 zrt1*Δ	Kelly *et al*., 2011
DTK1217	*ade2-min3*, *rad53-1*, *rad27*Δ*::KANMX*	DTK1170 x DTK1199, isolated spore
DTK1219	*ade2-min3*, *rad53-1*, *end3*Δ*::KANMX*	DTK1088 x DTK1170, isolated spore
DTK1230	*ade2-min3*, *rad59*Δ::*KANMX*	Kelly *et al*., 2011
DTK1253	*ade2-min3*, *rad52*Δ::*URA3*	Kelly *et al*., 2011
DTK1268	*ade2-min3*, *zrt1*Δ::*LEU2*, *rad50*Δ::*KANMX*, *rad52*Δ::*URA3*	Kelly *et al*., 2011

Strain	Relevant genotype	Construction details
DTK1269	*ade2-min3*, *zrt1*Δ::*LEU2*, *rad51*Δ::*KANMX*, *rad52*Δ::*URA3*	Kelly *et al*., 2011
DTK1270	*ade2-min3*, *rad53-1*, *por1*Δ*::KANMX*	DTK1170 with *por1*Δ*::KANMX*[a]
DTK1272	*ade2-min3*, *rad53-1*, *etr1*Δ*::KANMX*	DTK1170 with *etr1*Δ*::KANMX*[a]
DTK1279	*ade2-min3*, *pkc1-4*	DTK271 x YKH27, isolated spore
DTK1289	*ade2-min3*, *rad50*Δ::KANMX, *rad52*Δ::URA3	Kelly *et al*., 2011
DTK1290	*ade2-min3*, *rad51*Δ::KANMX, *rad52*Δ::URA3	Kelly *et al*., 2011
DTK1295	*ade2-min3*, *rad53-1, pkc1-4*	DTK1170 x DTK1279, isolated spore
DTK1299	*ade2-min3*, *rad50*Δ::*KANMX*, *rad51*Δ::*KANMX*	Kelly *et al*., 2011
DTK1316	*ade2-min3*, *dnl4*Δ*::KANMX*	Kelly *et al*., 2011
DTK1320	*ade2-min3*, *rad50*Δ::KANMX, *rad51*Δ::KANMX, *rad52*Δ::URA3	Kelly *et al*., 2011
DTK1360	*ade2-min3*, *etr1*Δ*::KANMX*	Kelly *et al*., 2011
DTK1361	*ade2-min3*, *por1*Δ*::KANMX*	Kelly *et al*., 2011
DTK1392	*ade2-min3*, *mrc1*Δ*::KANMX*	DTK271 with *mrc1*Δ*::KANMX*[a]
DTK1400	*ade2-h7.5, rad50*Δ::*KANMX*	Kelly *et al*., 2011
DTK1401	*ade2-h7.5*, *rad51*Δ::*KANMX*	Kelly *et al*., 2011
DTK1406	*ade2-h7.5, zrt1*Δ*::KANMX, rad50*Δ::*KANMX*	Kelly *et al*., 2011
DTK1407	*ade2-h7.5, zrt1*Δ*::LEU2 , rad50*Δ*::KANMX, rad52*Δ::*URA3*	Kelly *et al*., 2011
DTK1427	*ade2-h7.5, rad52*Δ::*URA3*	Kelly *et al*., 2011
DTK1426	*ade2-h7.5, rad50*Δ*::KANMX, rad52*Δ::*URA3*	Kelly *et al*., 2011
DTK1521	*ade2-min3*, *csm3*Δ*::KANMX*	DTK264 with *csm3*Δ*::KANMX*[a]
DTK1526	*ade2-min3*, *ddc1*Δ*::KANMX*	DTK271 with *ddc1*Δ*::KANMX*[a]

Strain	Relevant genotype	Construction details
DTK1527	*ade2-min3*, *rad17Δ::KANMX*	DTK271 with *rad17Δ::KANMX*[a]
DTK1528	*ade2-min3*, *tof1Δ::KANMX*	DTK271 with *tof1Δ::KANMX*[a]
DTK1529	*ade2-min3*, *csm3Δ::KANMX*	DTK271 with *csm3Δ::KANMX*[a]
DTK1530	*ade2-min3*, *mec3Δ::KANMX*	DTK271 with *mec3Δ::KANMX*[a]
DTK1532	*ade2-min3*, *tof1Δ::KANMX*	DTK264 with *tof1Δ::KANMX*[a]
DTK1533	*ade2-h7.5, mrc1Δ::KANMX*	DTK1188 *mrc1Δ::KANMX*[a]
DTK1539	*ade2-min3*, *mrc1Δ::KANMX*	DTK264 with *mrc1Δ::KANMX*[a]
DTK1543	*ade2-h7.5, csm3Δ::KANMX*	DTK1188 *csm3Δ::KANMX*[a]
DTK1549	*ade2-min3*, *mrc1Δ::KANMX*, *tof1Δ::KANMX*	DTK1392 x DTK1532, isolated spore
DTK1551	*ade2-min3*, *mrc1Δ::KANMX*, *csm3Δ::KANMX*	DTK1392 x DTK1521, isolated spore
DTK1554	*ade2-min3*, *tof1Δ::KANMX*, *csm3Δ::KANMX*	DTK1528 x DTK1521, isolated spore
DTK1556	*ade2-min3*, *mrc1Δ::KANMX*, *zrt1Δ::KANMX*	DTK1539 x DTK878, isolated spore
DTK1558	*ade2-min3*, *mrc1Δ::KANMX*, *rad53-1*	DTK1392 x DTK1170, isolated spore
DTK1559	*ade2-min3*, *mrc1Δ::KANMX*, *rad27Δ::KANMX*	DTK1392 x DTK1199, isolated spore
DTK1560	*ade2-h7.5, tof1Δ::KANMX*	DTK1188 *tof1Δ::KANMX*[a]
DTK1587	*ade2-min3*, *mrc1Δ::KANMX*, *etr1Δ::KANMX*	DTK1539 x DTK1360, isolated spore
DTK1588	*ade2-min3*, *mrc1Δ::KANMX*, *por1Δ::KANMX*	DTK1539 x DTK1361, isolated spore
DTK1589	*ade2-min3*, *mrc1Δ::KANMX*, *rad51Δ::KANMX*	DTK1392 x DTK1074, isolated spore
DTK1594	*ade2-min3*, *mrc1Δ::KANMX*, *rad50Δ::KANMX*	DTK1539 x DTK1056, isolated spore
DTK1603	*ade2-min3*, *mrc1Δ::KANMX*, *pkc1-4*	DTK1392 x DTK1279, isolated spore
DTK1621	*ade2-min3*, *mrc1Δ::KANMX*, *rad52Δ::URA3*	DTK1392 x DTK1289, isolated spore

Strain	Relevant genotype	Construction details
DTK1624	*ade2-h7.5 - URA3MX his3-1 ura3-0 can1:: MFA1pr-spHIS5, MAT*a	DCY2556 with *ade2-h7.5 - URA3MX* linked cassette
DTK1630	*ade2-min3*, $mrc1^{AQ}$	DTK271 x Y2298, isolated spore
DTK1646	*ade2-min3*, *mrc1Δ::KANMX*, *rad50Δ::KANMX, rad51Δ::KANMX*	DTK1594 x DTK1621, isolated spore
DTK1647	*ade2-min3*, *mrc1Δ::KANMX*, *rad51Δ::KANMX, rad52Δ::URA3*	DTK1299 x DTK1621, isolated spore
DTK1648	*ade2-min3*, *mrc1Δ::KANMX*, *rad50Δ::KANMX, rad51Δ::KANMX, rad52Δ::URA3*	DTK1299 x DTK1621, isolated spore
DTK1650	*ade2-min3*, *mrc1Δ::KANMX*, *rad50Δ::KANMX, rad52Δ::URA3*	DTK1299 x DTK1621, isolated spore
DTK1657	*ade2-min3*, *trp1Δ::KANMX*	DTK271 with *trp1*Δ::KANMX[a]
DTK1658	*ade2-h7.5, mrc1*Δ::*KANMX , rad51Δ::KANMX*	DTK1533 x DTK1401, isolated spore
DTK1663	*ade2-h7.5, mrc1*Δ::*KANMX , rad50Δ::KANMX, rad51Δ::KANMX, rad52Δ::URA3*	DTK1533 x DTK1438, isolated spore
DTK1664	*ade2-h7.5, mrc1*Δ::*KANMX , rad52Δ::URA3*	DTK1533 x DTK1427, isolated spore
DTK1672	*ade2-h7.5, mrc1*Δ::*KANMX , rad50Δ::KANMX*	DTK1533 x DTK1406, isolated spore
DTK1683	*ade2-min3*, *mrc1-C14*	DTK271 x Y2544, isolated spore
DTK1691	*ade2-min3*, *bub3Δ::KANMX*	DTK271 with *bub3Δ::KANMX*[a]
DTK1693	*ade2-min3*, *tof1Δ::KANMX*, *por1Δ::KANMX*	DTK1532 x DTK1361, isolated spore
DTK1694	*ade2-min3*, *tof1Δ::KANMX*, *etr1Δ::KANMX*	DTK1532 x DTK1360, isolated spore
DTK1695	*ade2-min3*, *csm3Δ::KANMX*, *etr1Δ::KANMX*	DTK1521 x DTK1360, isolated spore
DTK1697	*ade2-min3*, *rad17Δ::KANMX*	DTK264 with *rad17Δ::KANMX*[a]
DTK1699	*ade2-min3*, *mon1Δ::KANMX*	DTK271 with *mon1Δ::KANMX*[a]
DTK1700	*ade2-min3*, *csm3Δ::KANMX*, *por1Δ::KANMX*	DTK1521 x DTK1361, isolated spore

Strain	Relevant genotype	Construction details
DTK1708	*ade2-h7.5, rad50Δ::KANMX,rad51Δ::KANMX,rad52Δ::URA3*	DTK1401 x DTK1407, isolated spore
DTK1710	*ade2-min3*, *rad17Δ::KANMX*, *etr1Δ::KANMX*	DTK1527 x DTK1360, isolated spore
DTK1711	*ade2-min3*, *rad17Δ::KANMX*, *por1Δ::KANMX*	DTK1527 x DTK1361, isolated spore
DTK1726	*ade2-min3, rad53-1*, *sml1Δ::KANMX*	DTK1170 with *sml1Δ::KANMX*[a]
DTK1729	*ade2-min3, sml1Δ::KANMX*	DTK271 with *sml1Δ::KANMX*[a]
DTK1733	*ade2-h7.5, mrc1Δ::KANMX , rad51Δ::KANMX, rad52Δ::URA3*	DTK1658 *rad52Δ::URA3*[a]
DTK1734	*ade2-h7.5, mrc1Δ::KANMX , rad50Δ::KANMX, rad52Δ::URA3*	DTK1672 *rad52Δ::URA3*[a]
DTK1739	*ade2-min3*, *mrc1Δ::KANMX*, *rad59Δ::KANMX*	DTK1539 x DTK1230, isolated spore
DTK1740	*ade2-min3*, *mrc1*^{AQ}, *rad9Δ::KANMX*	DTK1630 with *rad9Δ::KANMX*[a]
DTK1762	*ade2-min3*, *rad17Δ::KANMX*, *zrt1Δ::KANMX*	DTK1697 x DTK878, isolated spore
DTK1763	*ade2-min3*, *tel1Δ::KANMX*	DTK271 with *tel1Δ::KANMX*[a]
DTK1765	*ade2-min3*, *rad17Δ::KANMX*, *rad53-1*	DTK1697 x DTK1170, isolated spore
DTK1766	*ade2-min3*, *mrc1*^{AQ}*-C14*	DTK1630 with *mrc1-C14::KANMX*[a]
DTK1767	*ade2-min3*, *rad17Δ::KANMX*, *end3Δ::KANMX*	DTK1697 x DTK1088, isolated spore
DTK1769	*ade2-min3*, *rad17Δ::KANMX*, *rad27Δ::KANMX*	DTK1697 x DTK1199, isolated spore
DTK1770	*ade2-min3, mrc1Δ::KANMX*, *dnl4Δ::KANMX*	DTK1539 x DTK1316, isolated spore
DTK1771	*ade2-min3, mrc1Δ::KANMX*, *sml1Δ::KANMX*	DTK1539 x DTK1729; spore isolated
DTK1773	*ade2-h7.5, mrc1Δ::KANMX , rad50Δ::KANMX, rad51Δ::KANMX*	DTK1658 x DTK1672, isolated spore
DTK1776	*ade2-min3*, *mec1-21*	DTK271 x DKY2563, isolated spore
DTK1777	*ade2-min3*, *rad17Δ::KANMX, pkc1-4*	DTK1697 x DTK1279, isolated spore
DTK1781	*ade2-min3, tel1Δ::KANMX*, *sml1Δ::KANMX*	DTK1764 x DTK1729, isolated spore

Strain	Relevant genotype	Construction details
DTK1806	*ade2-min3*, *mrc1Δ::KANMX*, *end3Δ::KANMX*	DTK1539 x DTK1088, isolated spore
DTK1808	*ade2-min3, mec1-21*, *dun1Δ::URA3*	DTK1776 with *dun1Δ::URA3*[a]
DTK1809	*ade2-min3*, *rad53-1, rad9Δ::KANMX*	DTK1170 with *rad9*Δ::KANMX[a]
DTK1811	*ade2-min3, rad53-1*, *sml1Δ::KANMX*, *dun1Δ::URA3*	DTK1726 with *dun1Δ::URA3*[a]
DTK1814	*ade2-min3, mec1-21*, *dun1Δ::URA3*, *sml1Δ::KANMX*	DTK1808 with *sml1Δ::KANMX*[a]
DTK1815	*ade2-min3, mrc1Δ::KANMX*, *dun1Δ::URA3*	DTK1392 with *dun1Δ::URA3*[a]
DTK1821	*ade2-min3, dun1Δ::URA3*	DTK271 with *dun1Δ::URA3*[a]
DTK1825	*ade2-min3*, *mrc1*^{AQ}, *por1Δ::KANMX*	DTK1630 with *por1Δ::KANMX*[a]
DTK1826	*ade2-min3*, *mrc1*^{AQ}, *etr1Δ::KANMX*	DTK1630 with *etr1Δ::KANMX*[a]
DTK1827	*ade2-min3*, *mec1-21*, *por1Δ::KANMX*	DTK1776 with *por1Δ::KANMX*[a]
DTK1831	*ade2-min3, mrc1Δ::KANMX*, *sml1Δ::KANMX*, *dun1Δ::URA3*	DTK1771 with *dun1Δ::URA3*[a]
DTK1832	*ade2-min3*, *mec1-21*, *zrt1Δ::LEU2*	DTK1776 with *zrt1Δ::LEU2*[a]
DTK1833	*ade2-min3*, *mec1-21*, *rad17Δ::KANMX*	DTK1776 with *rad17Δ::KANMX*[a]
DTK1836	*ade2-min3*, *mrc1-C14*, *etr1Δ::KANMX*	DTK1683 with *etr1Δ::KANMX*[a]
DTK1838	*ade2-min3*, *mec1-21*, *mrc1Δ::KANMX*	DTK1776 with *mrc1Δ::KANMX*[a]
DTK1839	*ade2-min3*, *mec1-21*, *rad27Δ::KANMX*	DTK1776 with *rad27Δ::KANMX*[a]
DTK1840	*ade2-min3*, *mec1-21*, *etr1Δ::KANMX*	DTK1776 with *etr1Δ::KANMX*[a]
DTK1841	*ade2-min3*, *mrc1-C14*, *por1Δ::KANMX*	DTK1683 with *por1Δ::KANMX*[a]
DTK1842	*ade2-min3*, *mec1-21*, *rad9Δ::KANMX*	DTK1776 with *rad9Δ::KANMX*[a]
DTK1855	*ade2-min3*, *mec1-21*, *rad53-1*	DTK1776 x DTK1170, isolated spore
DTK1859	*ade2-min3, sml1Δ::KANMX*, *dun1Δ::URA3*	DTK1729 with *dun1Δ::URA3*[a]

Strain	Relevant genotype	Construction details
DTK1862	*ade2-min3*, *mec1-21, tel1Δ::KANMX*	DTK1776 with *tel1*Δ::KANMX[a]
DTK1871	*ade2-min3*, *mec1-21*, *pkc1-4*	DTK1776 x DTK1603, isolated spore
DTK1872	*ade2-min3*, *TOF1-3HA-TRP1*	DTK1657 with *3HA-TRP1*
DTK1873	*ade2-min3*, *mrc1^{AQ}-C14*, *por1Δ::URA3*	DTK1766 with *por1*Δ::*URA3*[a]
DTK1882	*ade2-min3*, *mrc1^{AQ}-C14*, *etr1Δ::URA3*	DTK1766 with *etr1*Δ::*URA3*[a]
DTK1883	*ade2-min3*, *mec1-21*, *end3Δ::KANMX*	DTK1776 with *end3Δ::KANMX*[a]
DTK1889	*ade2-min3*, *CSM3-3HA-TRP1*	DTK1657 with *3HA-TRP1*
DTK1900	*ade2-h7.5, mlh1Δ::KANMX*	DTK1188 *mlh1*Δ::*KANMX*[a]
DTK1901	*ade2-h7.5, mlh3Δ::KANMX*	DTK1188 *mlh3*Δ::*KANMX*[a]
DTK1902	*ade2-h7.5, pms1Δ::KANMX*	DTK1188 *pms1*Δ::*KANMX*[a]
DTK1903	*ade2-h7.5, msh2Δ::KANMX*	DTK1188 *msh2*Δ::*KANMX*[a]
DTK1904	*ade2-h7.5, mlh3Δ::KANMX*	DTK1188 *mlh3*Δ::*KANMX*[a]
DTK1905	*ade2-h7.5, mlh2Δ::KANMX*	DTK1188 *mlh2*Δ::*KANMX*[a]
DTK1906	*ade2-h7.5, exo1Δ::KANMX*	DTK1188 *exo1*Δ::*KANMX*[a]
DTK1907	*ade2-h7.5, msh6Δ::KANMX*	DTK1188 *msh6*Δ::*KANMX*[a]
DTK1920	*ade2-min3, mrc1Δ::KANMX*	DTK1657 with *mrc1*Δ::KANMX[a]
DTK1921	*ade2-h7.5*, *rad53-1*	DTK1188 x DTK1765, isolated spore
DTK1922	*ade2-h7.5*, *mec1-21*	DTK1188 x DTK1776, isolated spore
DTK1928	*ade2-min3*, *mrc1Δ::KANMX*, *dnl4Δ::KANMX, rad52Δ::KANMX*	DTK1770 x DTK1621, isolated spore

Strain	Relevant genotype	Construction details
DTK1930	*ade2-min3*, *MRC1-3HA-LEU2*	DTK1920 with *MRC1-3HA-LEU2* from pCMF022
DTK1931	*ade2-min3*, *ACS1-3HA-TRP1*	DTK1657 with *3HA-TRP1*
DTK1933	*ade2-min3*, *GND1-3HA-TRP1*	DTK1657 with *3HA-TRP1*
DTK1935	*ade2-min3*, *mrc1*Δ*::KANMX*, *dnl4*Δ*::KANMX, rad59*Δ*::KANMX*	DTK1770 x DTK1230, isolated spore
DTK1973	*ade2-h7.5*, *cot1*Δ*::KANMX*	DTK1188 with *cot1*Δ*::KANMX*[a]
DTK1975	*ade2-h7.5*, *zap1*Δ*::KANMX*	DTK1188 with *zap1*Δ*::KANMX*[a]
DTK1979	*ade2-min3*, *rfa1-t11*	DTK271 with *rfa1-t11* from pKU1-t11
DTK1980	*ade2-min3*, *rfa1-t11*, *mrc1*Δ*::KANMX*	DTK1979 with *mrc1*Δ*::KANMX*[a]
DTK1981	*ade2-min3*, *rfa1-t11*, *zrt1*Δ*::KANMX*	DTK1979 with *zrt1*Δ*::KANMX*[a]
DTK1986	*ade2-min3*, *mec1-21*, *rad52*Δ*::URA3*	DTK1776 x DTK1290, isolated spore
DTK1987	*ade2-min3*, *mec1-21*, *rad51*Δ*::KANMX*	DTK1776 x DTK1299, isolated spore
DTK1988	*ade2-min3*, *mec1-21*, *rad51*Δ*::KANMX*, *rad52*Δ*::URA3*	DTK1776 x DTK1290, isolated spore
DTK1990	*ade2-h7.5*, *mon1*Δ*::KANMX*	DTK1188 with *mon1*Δ*::KANMX*[a]
DTK1991	*ade2-min3*, *rpl22a*Δ*::KANMX*	DTK271 with *rpl22a*Δ*::KANMX*[a]
DTK1992	*ade2-h7.5*, *rpl22a*Δ*::KANMX*	DTK1188 with *rpl22a*Δ*::KANMX*[a]
DTK1993	*ade2-min3*, YGL217CΔ*::KANMX*	DTK271 with YGL217CΔ*::KANMX*[a]
DTK1994	*ade2-h7.5*, YGL217CΔ*::KANMX*	DTK1188 with YGL217CΔ*::KANMX*[a]

[a] Indicates that the strain was made using a PCR-generated construct.

Table 8-2: Primers

Primer	Reference Number	Sequence
Acs1/3HA F	84742698	ACATTGTCAAACCCTGGCATTGTTAGACATCTAATTGATTCGGTCAAGTTGCGGATCCCCG GGTTAATTAA
Acs1/3HA R	84742699	GAAATAATAATAAGTAAGCAGCTCGGTTATAAGAGAACAAAAACACACGAGAATTCGAG CTCGTTTAAAC
Ade2 F	14193008	GGGTTAGCTATTTCGCCCAATG
Ade2 F + Tag	14193006	TCCAGTTTAAACGAGCTCGAATTCGAAGCCGAGAATTTTGTAACACC
Ade2 R	14193007	TCGCCTTAAGTTGAACGGAGTC
Bub3 F	56555516	TACGAACTGCCCAGGGGATTGATA
Bub3 R	56555517	TCGAGATCGCCAAGACCTAAGT
Chk1 F	23094597	GAGGCCTGCCGAAGTTAATA
Chk1 R	23094598	CGATGACACACTAGAAATCGAC
Csm3 F	46100595	CGCCACGGCTAACTCCAAACATAA
Csm3 R	46100596	CGAGGGAAGCTTGGCTGTTTTCT
Csm3/3HA F	83197164	GAGTTTGGCGTAGATCAAGATGAGTTGGATGCTATGAAGGAAATGGGCTTTCGGATCCCC GGGTTAATTAA
Csm3/3HA R	83197165	TTGAAGTAGATATTGTATAATAACGCCCAAGAAGAAAAAATCAAACACTCGGAATTCGAG CTCGTTTAAAAC
Ddc1 F	49746409	CTTCGAGACCAAAGCACTGA
Ddc1 R	49746410	AGTCCATGTCGCAATAAGC
Dun1 F	81393356	TAACAAGTAAAGGGGCTTAACATACAGTAAAAAAGGCAATTATAGTGAAGGATTGTACTG AGAGTGCACC
Dun1 R	81393357	TTGGAAAAATCCAGATTCAAACAATGTTTTTGAAATAATGCTTCTCATGTCTGTGCGGTAT TTCACACCG

Primer	Reference Number	Sequence
End3 F	28278222	GAGTTAGTGGGTATTGGAAAGGC
End3 R	28278223	CCACACCGTTACTGGATAGA
Etr1 F	37616573	TGTACCCAGGGGTGGTTTCCAT
Etr1 R	37616572	TTGAAGGGTCGACGTCCCCTTTTA
Exo1 F	48201622	CGTCTTTAGCAAAGGCGGGAAGTA
Exo1 R	48201623	GCATTGTTCATAGCGGGGCAAA
Gnd1/3HA F	84742696	ATCAACTGGACTGGCCACGGTGGTAATGTTTCTTCCTCTACATACCAAGCTCGGATCCCCG GGTTAATTAA
Gnd1/3HA R	84742697	CATTTGGATTTATTTATCTATTTATTATTATGATTACTTTTACTATAACTGAATTCGAGCTC GTTTAAAC
Mec3 F	49746407	TAACTTCTGTGCAGGGGTAGTCGT
Mec3 R	49746408	TGCAACATACCGTTCGTAAGGCT
Mlh1 F	36803545	CGGTGTTTAGTAATCGCGCTAGCA
Mlh1 R	36803546	CTCGGGTCTTTGGTACCGTTGAAT
Mlh2 F	49451839	GCTATATTGCCCTGGCACAATG
Mlh2 R	49451840	TGCAACCTCACAGAATCAGAT
Mlh3 F	49451841	GCGCAAATTCAACCCCATTGAT
Mlh3 R	49451842	CGGTAATGCAACAGTGGAGCAGT
Mon1 F	56866461	GGCTAGTATGCGTACCTTTATCCC
Mon1 R	56866462	GTGTTTGGTTAACACCCCTTCT
Mrc1 F	46100597	ACACCAACTCTACTGGCTCTCA

Primer	Reference Number	Sequence
Mrc1 R	46100598	TGCCTCCTTTACCTAACCTACTC
Mrc1/KanMX/ C14 F	78415868	AGAAAAAGGAGATTAGAAATTGGCGATGATGCAAAGCTTGTTAAAAACCCACGTACGCT GCAGGTCGAC
Mrc1/KanMX/ C14 R	78415869	AAGACAGCTTCTGGAGTTCAATCAACTTCTTCGGAAAAGATAAAAAACCAATCGATGAAT TCGAGCTCG
Msh2 F	48201624	CGCACTCCATCAAGTGAACCTCAA
Msh2 R	48201625	CCGGAGATACTCTTTCCAGTGGT
Msh3 F	48774856	AGTGTTTCCCCGACTCACCTTT
Msh3 R	48774857	TGTACAAGGCCAAGGCATAACAGT
Msh6 F	48774858	AATAAACGCGTGAGCAGTAGCTGA
Msh6 R	48774859	CTTGCCCAAGATGCGGTAAAAGA
Pms1 F	2694460	TAGAAAGCACAGATTAATAC
Pms1 R	2694461	ACATATATCCATCAAGCATC
Por1 F	37616575	CCAATCAAACACCGCCATTTCG
Por1 R	37616574	TTCTCACTGCCAAGCAACCA
Psd2 F	83065163	TGAGGGGTCTTTAACTGGAA
Psd2 R	83065164	GGTTGCAAGAGGAACAAACG
Rad17 F	49746405	AAGGTGCATCTCAGGCTACTGAAG
Rad17 R	49746406	TAGGTGAATGGGCTGGTTTGGGTA
Rad27 F	23094593	GCGTAACATCGCGCAAATGAAG
Rad27 R	23094594	TCCACGTTCAAGTTCCCAGAAA

Primer	Reference Number	Sequence
Rad9 F	28611970	ACGATGAGCAATGTGAAGTGAGCA
Rad9 R	28611971	CGTGTGGGAGGATGTTCTTAGACT
Rpl22a F	88529802	TTTTCCTTTCCACCTCAGTGCG
Rpl22a R	88529803	GGCAAAGCGTCTCATAAGCAAC
Sml1 F	58828328	TCGCCATTTTGGGAAGTCATCCGT
Sml1 R	58828329	GGACAATGTTGGCGCTAGCGATA
Tef/Ura3 F	14193004	GGGTTAGCTATTTCGCCCAATGTGTCCATCTGACATTACTATTTTGCATTTTAATTTAATAG ATCTGTTTAGCTTGCCTCGT
Tef/Ura3 R	14193005	GGTGTTACAAAATTCTCGGCTTCGAATTCGAGCTCGTTTAAACTGGA
Tel1 F	78479079	TATGAGCGTGATAGGAGGGTCT
Tel1 R	78479080	GGTAGCTTCACTATCAGCGATTGT
Tof1 F	46100599	TGGGTAGTGCCCTGTATGAATTGC
Tof1 R	46100600	GACGATAGGCGACAAAACCCAAGA
Tof1/3HA F	82966884	TTTTTGGCAAAAAGTCTAGAGTTGTTTTGAGCCAAGGTGATAGTGATGATCGGATCCCCGG GTTAATTAA
Tof1/3HA R	82966885	TTGTTTTAATATTATGTCAATACTTTGAACTTAAAAACAGAGTAAAGAAGGAATTCGAGCT CGTTTAAAAC
Trp1 F	54969732	ATTGGTGACTATTGAGCACGTGAGTATACGTGATTAAGCACACAAAGGCAGCTTGGAGTG ATTGTACTGAGAGTGCACC
Trp1 R	54969733	CAAAAGGCCTGCAGGCAAGTGCACAAACAATACTTAAATAAATACTACTCAGTAATAACC TGTGCGGTATTTCACACCG
YGL217C F	88529806	TGAAGGTGTGCCACTCACAGTA
YGL217C F	88529807	TCCCTTAGCTAGCCGTGTTT

Primer	Reference Number	Sequence
Zap1 F	14767981	ACTTGCCGCCTACTTGGC
Zap1 R	14767982	AATGTCCTTCCCCCCCAC
Zrt1 F	12966370	TACGCACGGCATTAGCTC
Zrt1 R	12966371	ACTCGTAGATGGCACGGTC

Chapter VIII

References

Abou-Khalil R, Brack AS (2010) Muscle stem cells and reversible quiescence: the role of sprouty. Cell Cycle 9:2575-2580.
Ahel I, Ahel D, Matsusaka T, Clark AJ, Pines J, Boulton SJ, West SC (2008) Poly(ADP-ribose)-binding zinc finger motifs in DNA repair/checkpoint proteins. Nature 451:81-85.
Alani E (1996) The Saccharomyces cerevisiae Msh2 and Msh6 proteins form a complex that specifically binds to duplex oligonucleotides containing mismatched DNA base pairs. Mol Cell Biol 16:5604-5615.
Alcasabas AA, Osborn AJ, Bachant J, Hu F, Werler PJ, Bousset K, Furuya K, Diffley JF, Carr AM, Elledge SJ (2001) Mrc1 transduces signals of DNA replication stress to activate Rad53. Nat Cell Biol 3:958-965.
Alder H, Taccioli C, Chen H, Jiang Y, Smalley KJ, Fadda P, Ozer HG, Huebner K, Farber JL, Croce CM, Fong LY (2012) Dysregulation of miR-31 and miR-21 induced by zinc deficiency promotes esophageal cancer. Carcinogenesis 33:1736-1744.
Allen C, Buttner S, Aragon AD, Thomas JA, Meirelles O, Jaetao JE, Benn D, Ruby SW, Veenhuis M, Madeo F, Werner-Washburne M (2006) Isolation of quiescent and nonquiescent cells from yeast stationary-phase cultures. J Cell Biol 174:89-100.
Aragon AD, Rodriguez AL, Meirelles O, Roy S, Davidson GS, Tapia PH, Allen C, Joe R, Benn D, Werner-Washburne M (2008) Characterization of differentiated quiescent and nonquiescent cells in yeast stationary-phase cultures. Mol Biol Cell 19:1271-1280.
Arai F, Hirao A, Ohmura M, Sato H, Matsuoka S, Takubo K, Ito K, Koh GY, Suda T (2004) Tie2/angiopoietin-1 signaling regulates hematopoietic stem cell quiescence in the bone marrow niche. Cell 118:149-161.
Araki H (1994) [Function of DNA polymerases in budding yeast]. Tanpakushitsu Kakusan Koso 39:1579-1583.
Araki H, Hamatake RK, Morrison A, Johnson AL, Johnston LH, Sugino A (1991) Cloning DPB3, the gene encoding the third subunit of DNA polymerase II of Saccharomyces cerevisiae. Nucleic Acids Res 19:4867-4872.
Armour JA, Harris PC, Jeffreys AJ (1993) Allelic diversity at minisatellite MS205 (D16S309): evidence for polarized variability. Hum Mol Genet 2:1137-1145.
Asahina H, Kuraoka I, Shirakawa M, Morita EH, Miura N, Miyamoto I, Ohtsuka E, Okada Y, Tanaka K (1994) The XPA protein is a zinc metalloprotein with an ability to recognize various kinds of DNA damage. Mutat Res 315:229-237.
Ashley T (1994) Mammalian meiotic recombination: a reexamination. Hum Genet 94:587-593.
Babudri N, Pavlov YI, Matmati N, Ludovisi C, Achilli A (2001) Stationary-phase mutations in proofreading exonuclease-deficient strains of the yeast Saccharomyces cerevisiae. Mol Genet Genomics 265:362-366.
Bando M, Katou Y, Komata M, Tanaka H, Itoh T, Sutani T, Shirahige K (2009) Csm3, Tof1, and Mrc1 form a heterotrimeric mediator complex that associates with DNA replication forks. J Biol Chem 284:34355-34365.

Benedetti H, Raths S, Crausaz F, Riezman H (1994) The END3 gene encodes a protein that is required for the internalization step of endocytosis and for actin cytoskeleton organization in yeast. Mol Biol Cell 5:1023-1037.
Berg I, Neumann R, Cederberg H, Rannug U, Jeffreys AJ (2003) Two modes of germline instability at human minisatellite MS1 (locus D1S7): complex rearrangements and paradoxical hyperdeletion. Am J Hum Genet 72:1436-1447.
Biggins S, Murray AW (2001) The budding yeast protein kinase Ipl1/Aurora allows the absence of tension to activate the spindle checkpoint. Genes & development 15:3118-3129.
Blank A, Kim B, Loeb LA (1994) DNA polymerase delta is required for base excision repair of DNA methylation damage in Saccharomyces cerevisiae. Proc Natl Acad Sci U S A 91:9047-9051.
Blostein-Fujii A, DiSilvestro RA, Frid D, Katz C, Malarkey W (1997) Short-term zinc supplementation in women with non-insulin-dependent diabetes mellitus: effects on plasma 5'-nucleotidase activities, insulin-like growth factor I concentrations, and lipoprotein oxidation rates in vitro. The American journal of clinical nutrition 66:639-642.
Boeke JD, LaCroute F, Fink GR (1984) A positive selection for mutants lacking orotidine-5'-phosphate decarboxylase activity in yeast: 5-fluoro-orotic acid resistance. Mol Gen Genet 197:345-346.
Bois P, Jeffreys AJ (1999) Minisatellite instability and germline mutation. Cell Mol Life Sci 55:1636-1648.
Bois PR (2003) Hypermutable minisatellites, a human affair? Genomics 81:349-355.
Boland CR, Goel A (2010) Microsatellite instability in colorectal cancer. Gastroenterology 138:2073-2087 e2073.
Bonadona V, Bonaiti B, Olschwang S, Grandjouan S, Huiart L, Longy M, Guimbaud R, Buecher B, Bignon YJ, Caron O, Colas C, Nogues C, Lejeune-Dumoulin S, Olivier-Faivre L, Polycarpe-Osaer F, Nguyen TD, Desseigne F, Saurin JC, Berthet P, Leroux D, Duffour J, Manouvrier S, Frebourg T, Sobol H, Lasset C, Bonaiti-Pellie C, French Cancer Genetics N (2011) Cancer risks associated with germline mutations in MLH1, MSH2, and MSH6 genes in Lynch syndrome. JAMA : the journal of the American Medical Association 305:2304-2310.
Branzei D, Foiani M (2005) The DNA damage response during DNA replication. Curr Opin Cell Biol 17:568-575.
Branzei D, Foiani M (2006) The Rad53 signal transduction pathway: Replication fork stabilization, DNA repair, and adaptation. Exp Cell Res 312:2654-2659.
Branzei D, Foiani M (2009) The checkpoint response to replication stress. DNA repair 8:1038-1046.
Bridges BA (1996) Elevated mutation rate in mutT bacteria during starvation: evidence for DNA turnover? J Bacteriol 178:2709-2711.
Bronner CE, Baker SM, Morrison PT, Warren G, Smith LG, Lescoe MK, Kane M, Earabino C, Lipford J, Lindblom A, et al. (1994) Mutation in the DNA mismatch repair gene homologue hMLH1 is associated with hereditary non-polyposis colon cancer. Nature 368:258-261.

Brook JD, McCurrach ME, Harley HG, Buckler AJ, Church D, Aburatani H, Hunter K, Stanton VP, Thirion JP, Hudson T, et al. (1992) Molecular basis of myotonic dystrophy: expansion of a trinucleotide (CTG) repeat at the 3' end of a transcript encoding a protein kinase family member. Cell 69:385.

Buard J, Bourdet A, Yardley J, Dubrova Y, Jeffreys AJ (1998) Influences of array size and homogeneity on minisatellite mutation. EMBO J 17:3495-3502.

Buard J, Shone AC, Jeffreys AJ (2000) Meiotic recombination and flanking marker exchange at the highly unstable human minisatellite CEB1 (D2S90). Am J Hum Genet 67:333-344.

Buard J, Vergnaud G (1994) Complex recombination events at the hypermutable minisatellite CEB1 (D2S90). EMBO J 13:3203-3210.

Calvo R, Pifarre A, Rosell R, Sanchez JJ, Monzo M, Ribera JM, Feliu E (1998) H-RAS 1 minisatellite rare alleles: a genetic susceptibility and prognostic factor for non-Hodgkin's lymphoma. J Natl Cancer Inst 90:1095-1098.

Capon DJ, Chen EY, Levinson AD, Seeburg PH, Goeddel DV (1983) Complete nucleotide sequences of the T24 human bladder carcinoma oncogene and its normal homologue. Nature 302:33-37.

Chabes A, Domkin V, Thelander L (1999) Yeast Sml1, a protein inhibitor of ribonucleotide reductase. J Biol Chem 274:36679-36683.

Chandley AC (1989) Asymmetry in chromosome pairing: a major factor in de novo mutation and the production of genetic disease in man. J Med Genet 26:546-552.

Chen SH, Zhou H (2009) Reconstitution of Rad53 activation by Mec1 through adaptor protein Mrc1. The Journal of biological chemistry 284:18593-18604.

Chilkova O, Stenlund P, Isoz I, Stith CM, Grabowski P, Lundstrom EB, Burgers PM, Johansson E (2007) The eukaryotic leading and lagging strand DNA polymerases are loaded onto primer-ends via separate mechanisms but have comparable processivity in the presence of PCNA. Nucleic Acids Res 35:6588-6597.

Chini CC, Chen J (2003) Human claspin is required for replication checkpoint control. J Biol Chem 278:30057-30062.

Cho Y, Gorina S, Jeffrey PD, Pavletich NP (1994) Crystal structure of a p53 tumor suppressor-DNA complex: understanding tumorigenic mutations. Science 265:346-355.

Clegg MS, Hanna LA, Niles BJ, Momma TY, Keen CL (2005) Zinc deficiency-induced cell death. IUBMB life 57:661-669.

Cohen R, Yokoi T, Holland JP, Pepper AE, Holland MJ (1987) Transcription of the constitutively expressed yeast enolase gene ENO1 is mediated by positive and negative cis-acting regulatory sequences. Mol Cell Biol 7:2753-2761.

Coic E, Feldman T, Landman AS, Haber JE (2008) Mechanisms of Rad52-independent spontaneous and UV-induced mitotic recombination in Saccharomyces cerevisiae. Genetics 179:199-211.

Conklin DS, McMaster JA, Culbertson MR, Kung C (1992) COT1, a gene involved in cobalt accumulation in Saccharomyces cerevisiae. Mol Cell Biol 12:3678-3688.

Cottingham FR, Hoyt MA (1997) Mitotic spindle positioning in Saccharomyces cerevisiae is accomplished by antagonistically acting microtubule motor proteins. J Cell Biol 138:1041-1053.
Cullmann G, Fien K, Kobayashi R, Stillman B (1995) Characterization of the five replication factor C genes of Saccharomyces cerevisiae. Mol Cell Biol 15:4661-4671.
Davidson GS, Joe RM, Roy S, Meirelles O, Allen CP, Wilson MR, Tapia PH, Manzanilla EE, Dodson AE, Chakraborty S, Carter M, Young S, Edwards B, Sklar L, Werner-Washburne M (2011) The proteomics of quiescent and nonquiescent cell differentiation in yeast stationary-phase cultures. Mol Biol Cell 22:988-998.
Davis AP, Symington LS (2001) The yeast recombinational repair protein Rad59 interacts with Rad52 and stimulates single-strand annealing. Genetics 159:515-525.
Davis BM, McCurrach ME, Taneja KL, Singer RH, Housman DE (1997) Expansion of a CUG trinucleotide repeat in the 3' untranslated region of myotonic dystrophy protein kinase transcripts results in nuclear retention of transcripts. Proc Natl Acad Sci U S A 94:7388-7393.
de Morgan A, Brodsky L, Ronin Y, Nevo E, Korol A, Kashi Y (2010) Genome-wide analysis of DNA turnover and gene expression in stationary-phase Saccharomyces cerevisiae. Microbiology 156:1758-1771.
Desmarais E, Vigneron S, Buresi C, Cambien F, Cambou JP, Roizes G (1993) Variant mapping of the Apo(B) AT rich minisatellite. Dependence on nucleotide sequence of the copy number variations. Instability of the non-canonical alleles. Nucleic Acids Res 21:2179-2184.
De Virgilio C, Burckert N, Barth G, Neuhaus JM, Boller T, Wiemken A (1992) Cloning and disruption of a gene required for growth on acetate but not on ethanol: the acetyl-coenzyme A synthetase gene of Saccharomyces cerevisiae. Yeast 8:1043-1051.
Debrauwere H, Gendrel CG, Lechat S, Dutreix M (1997) Differences and similarities between various tandem repeat sequences: minisatellites and microsatellites. Biochimie 79:577-586.
Denoeud F, Vergnaud G, Benson G (2003) Predicting human minisatellite polymorphism. Genome Res 13:856-867.
Desany BA, Alcasabas AA, Bachant JB, Elledge SJ (1998) Recovery from DNA replicational stress is the essential function of the S-phase checkpoint pathway. Genes Dev 12:2956-2970.
Devlin B, Krontiris T, Risch N (1993) Population genetics of the HRAS1 minisatellite locus. Am J Hum Genet 53:1298-1305.
Ding S, Larson GP, Foldenauer K, Zhang G, Krontiris TG (1999) Distinct mutation patterns of breast cancer-associated alleles of the HRAS1 minisatellite locus. Hum Mol Genet 8:515-521.
Dohrmann PR, Sclafani RA (2006) Novel role for checkpoint Rad53 protein kinase in the initiation of chromosomal DNA replication in Saccharomyces cerevisiae. Genetics 174:87-99.

Drakulic T, M.D.Temple, Guido R, Jarolim S, Breitenbach M, Attfield PV, Dawes IW (2006) Involvement of oxidative stress response genes in redox homeostasis, the level of reactive oxygen species, and ageing in Saccharomyces cerevisiae. FEMS Yeast Research 5:1215-1228.

Emili A (1998) MEC1-dependent phosphorylation of Rad9p in response to DNA damage. Molecular cell 2:183-189.

Evert BA, Salmon TB, Song B, Jingjing L, Siede W, Doetsch PW (2004) Spontaneous DNA damage in Saccharomyces cerevisiae elicits phenotypic properties similar to cancer cells. J Biol Chem 279:22585-22594.

Fanning E, Klimovich V, Nager AR (2006) A dynamic model for replication protein A (RPA) function in DNA processing pathways. Nucleic Acids Res 34:4126-4137.

Faraone SV, Doyle AE, Mick E, Biederman J (2001) Meta-analysis of the association between the 7-repeat allele of the dopamine D(4) receptor gene and attention deficit hyperactivity disorder. Am J Psychiatry 158:1052-1057.

Fasullo M, Tsaponina O, Sun M, Chabes A (2010) Elevated dNTP levels suppress hyper-recombination in Saccharomyces cerevisiae S-phase checkpoint mutants. Nucleic Acids Res 38:1195-1203.

Fishel R, Lescoe MK, Rao MR, Copeland NG, Jenkins NA, Garber J, Kane M, Kolodner R (1993) The human mutator gene homolog MSH2 and its association with hereditary nonpolyposis colon cancer. Cell 75:1027-1038.

Frenkel EP, Skinner WN, Smiley JD (1964) Studies on a Metabolic Defect Induced by Hydroxyurea (Nsc-32065). Cancer chemotherapy reports Part 1 40:19-22.

Geiersbach KB, Samowitz WS (2011) Microsatellite instability and colorectal cancer. Arch Pathol Lab Med 135:1269-1277.

Giot L, Chanet R, Simon M, Facca C, Faye G (1997) Involvement of the yeast DNA polymerase delta in DNA repair in vivo. Genetics 146:1239-1251.

Gotter AL, Suppa C, Emanuel BS (2007) Mammalian TIMELESS and Tipin are evolutionarily conserved replication fork-associated factors. J Mol Biol 366:36-52.

Gourlay CW, Ayscough KR (2006) Actin-induced hyperactivation of the Ras signaling pathway leads to apoptosis in Saccharomyces cerevisiae. Molecular and cellular biology 26:6487-6501.

Gray JV, Petsko GA, Johnston GC, Ringe D, Singer RA, Werner-Washburne M (2004) "Sleeping beauty": quiescence in Saccharomyces cerevisiae. Microbiol Mol Biol Rev 68:187-206.

Green M, Krontiris TG (1993) Allelic variation of reporter gene activation by the HRAS1 minisatellite. Genomics 17:429-434.

Greenwell PW, Kronmal SL, Porter SE, Gassenhuber J, Obermaier B, Petes TD (1995) TEL1, a gene involved in controlling telomere length in S. cerevisiae, is homologous to the human ataxia telangiectasia gene. Cell 82:823-829.

Gunjan A, Verreault A (2003) A Rad53 kinase-dependent surveillance mechanism that regulates histone protein levels in S. cerevisiae. Cell 115:537-549.

Guthrie C, Fink G (eds.) (1991) Guide to Yeast Genetics and Molecular Biology: Academic Press.

Habraken Y, Sung P, Prakash L, Prakash S (1996) Binding of insertion/deletion DNA mismatches by the heterodimer of yeast mismatch repair proteins MSH2 and MSH3. Current biology : CB 6:1185-1187.
Haghnazari E, Heyer WD (2004) The Hog1 MAP kinase pathway and the Mec1 DNA damage checkpoint pathway independently control the cellular responses to hydrogen peroxide. DNA repair 3:769-776.
Halas A, Baranowska H, Policinska Z (2002) The influence of the mismatch-repair system on stationary-phase mutagenesis in the yeast Saccharomyces cerevisiae. Curr Genet 42:140-146.
Han CT, Schoene NW, Lei KY (2009) Influence of zinc deficiency on Akt-Mdm2-p53 and Akt-p21 signaling axes in normal and malignant human prostate cells. American journal of physiology Cell physiology 297:C1188-1199.
Harfe BD, Jinks-Robertson S (2000) Mismatch repair proteins and mitotic genome stability. Mutat Res 451:151-167.
Harris RS, Bull HJ, Rosenberg SM (1997a) A direct role for DNA polymerase III in adaptive reversion of a frameshift mutation in Escherichia coli. Mutat Res 375:19-24.
Harris RS, Feng G, Ross KJ, Sidhu R, Thulin C, Longerich S, Szigety SK, Winkler ME, Rosenberg SM (1997b) Mismatch repair protein MutL becomes limiting during stationary-phase mutation. Genes Dev 11:2426-2437.
Harris RS, Longerich S, Rosenberg SM (1994) Recombination in adaptive mutation. Science 264:258-260.
Hashimoto K, Nakashima N, Ohara T, Maki S, Sugino A (1998) The second subunit of DNA polymerase III (delta) is encoded by the HYS2 gene in Saccharomyces cerevisiae. Nucleic Acids Res 26:477-485.
Herker E, Jungwirth H, Lehmann KA, Maldener C, Frohlich KU, Wissing S, Buttner S, Fehr M, Sigrist S, Madeo F (2004) Chronological aging leads to apoptosis in yeast. J Cell Biol 164:501-507.
Ho E (2004) Zinc deficiency, DNA damage and cancer risk. J Nutr Biochem 15:572-578.
Ho E, Ames BN (2002) Low intracellular zinc induces oxidative DNA damage, disrupts p53, NFkappa B, and AP1 DNA binding, and affects DNA repair in a rat glioma cell line. Proc Natl Acad Sci U S A 99:16770-16775.
Holmes AM, Haber JE (1999) Double-strand break repair in yeast requires both leading and lagging strand DNA polymerases. Cell 96:415-424.
Hoyt MA, Totis L, Roberts BT (1991) S. cerevisiae genes required for cell cycle arrest in response to loss of microtubule function. Cell 66:507-517.
Hwang LH, Lau LF, Smith DL, Mistrot CA, Hardwick KG, Hwang ES, Amon A, Murray AW (1998) Budding yeast Cdc20: a target of the spindle checkpoint. Science (New York, NY 279:1041-1044.
Jackson AL, Chen R, Loeb LA (1998) Induction of microsatellite instability by oxidative DNA damage. Proceedings of the National Academy of Sciences of the United States of America 95:12468-12473.
Jamieson DJ (1998) Oxidative stress responses of the yeast Saccharomyces cerevisiae. Yeast 14:1511-1527.

Jauert PA, Edmiston SN, Conway K, Kirkpatrick DT (2002) RAD1 controls the meiotic expansion of the human HRAS1 minisatellite in Saccharomyces cerevisiae. Mol Cell Biol 22:953-964.
Jauert PA, Kirkpatrick DT (2005) Length and sequence heterozygosity differentially affect HRAS1 minisatellite stability during meiosis in yeast. Genetics 170:601-612.
Jeffreys AJ, Barber R, Bois P, Buard J, Dubrova YE, Grant G, Hollies CR, May CA, Neumann R, Panayi M, Ritchie AE, Shone AC, Signer E, Stead JD, Tamaki K (1999) Human minisatellites, repeat DNA instability and meiotic recombination. Electrophoresis 20:1665-1675.
Jeffreys AJ, Murray J, Neumann R (1998) High-resolution mapping of crossovers in human sperm defines a minisatellite-associated recombination hotspot. Mol Cell 2:267-273.
Jeffreys AJ, Neumann R (1997) Somatic mutation processes at a human minisatellite. Hum Mol Genet 6:129-132; 134-126.
Jeffreys AJ, Tamaki K, MacLeod A, Monckton DG, Neil DL, Armour JA (1994) Complex gene conversion events in germline mutation at human minisatellites. Nat Genet 6:136-145.
Jin K, Ewton DZ, Park S, Hu J, Friedman E (2009a) Mirk regulates the exit of colon cancer cells from quiescence. The Journal of biological chemistry 284:22916-22925.
Jin K, Ewton DZ, Park S, Hu J, Friedman E (2009b) Mirk regulates the exit of colon cancer cells from quiescence. J Biol Chem 284:22916-22925.
Johnson RE, Kovvali GK, Prakash L, Prakash S (1996) Requirement of the yeast MSH3 and MSH6 genes for MSH2-dependent genomic stability. J Biol Chem 271:7285-7288.
Johnston LH, Thomas AP (1982) The isolation of new DNA synthesis mutants in the yeast Saccharomyces cerevisiae. Mol Gen Genet 186:439-444.
Kanadia RN, Shin J, Yuan Y, Beattie SG, Wheeler TM, Thornton CA, Swanson MS (2006) Reversal of RNA missplicing and myotonia after muscleblind overexpression in a mouse poly(CUG) model for myotonic dystrophy. Proc Natl Acad Sci U S A 103:11748-11753.
Kantake N, Sugiyama T, Kolodner RD, Kowalczykowski SC (2003) The recombination-deficient mutant RPA (rfa1-t11) is displaced slowly from single-stranded DNA by Rad51 protein. The Journal of biological chemistry 278:23410-23417.
Kataoka T, Powers S, McGill C, Fasano O, Strathern J, Broach J, Wigler M (1984) Genetic analysis of yeast RAS1 and RAS2 genes. Cell 37:437-445.
Katou Y, Kanoh Y, Bando M, Noguchi H, Tanaka H, Ashikari T, Sugimoto K, Shirahige K (2003) S-phase checkpoint proteins Tof1 and Mrc1 form a stable replication-pausing complex. Nature 424:1078-1083.
Kelly MK, Alver B, Kirkpatrick DT (2011) Minisatellite alterations in ZRT1 mutants occur via RAD52-dependent and RAD52-independent mechanisms in quiescent stationary phase yeast cells. DNA Repair (Amst) 10:556-566.

Kelly MK, Brosnan L, Jauert PA, Dunham MJ, Kirkpatrick DT (2012) Multiple Pathways Regulate Minisatellite Stability During Stationary Phase in Yeast. G3 (Bethesda) 2:1185-1195.
Kelly MK, Jauert PA, Jensen LE, Chan CL, Truong CS, Kirkpatrick DT (2007) Zinc regulates the stability of repetitive minisatellite DNA tracts during stationary phase. Genetics 177:2469-2479.
Kennedy GC, German MS, Rutter WJ (1995) The minisatellite in the diabetes susceptibility locus IDDM2 regulates insulin transcription. Nat Genet 9:293-298.
Kenyon J, Gerson SL (2007) The role of DNA damage repair in aging of adult stem cells. Nucleic Acids Res 35:7557-7565.
Kim CF, Jackson EL, Woolfenden AE, Lawrence S, Babar I, Vogel S, Crowley D, Bronson RT, Jacks T (2005) Identification of bronchioalveolar stem cells in normal lung and lung cancer. Cell 121:823-835.
Kim EM, Burke DJ (2008) DNA damage activates the SAC in an ATM/ATR-dependent manner, independently of the kinetochore. PLoS Genet 4:e1000015.
Kinlaw WB, Levine AS, Morley JE, Silvis SE, McClain CJ (1983) Abnormal zinc metabolism in type II diabetes mellitus. The American journal of medicine 75:273-277.
Kirkbride HJ, Bolscher JG, Nazmi K, Vinall LE, Nash MW, Moss FM, Mitchell DM, Swallow DM (2001) Genetic polymorphism of MUC7: allele frequencies and association with asthma. Eur J Hum Genet 9:347-354.
Klein HL (1995) Genetic control of intrachromosomal recombination. Bioessays 17:147-159.
Kokoska RJ, Stefanovic L, Buermeyer AB, Liskay RM, Petes TD (1999) A mutation of the yeast gene encoding PCNA destabilizes both microsatellite and minisatellite DNA sequences. Genetics 151:511-519.
Kokoska RJ, Stefanovic L, Tran HT, Resnick MA, Gordenin DA, Petes TD (1998) Destabilization of yeast micro- and minisatellite DNA sequences by mutations affecting a nuclease involved in Okazaki fragment processing (rad27) and DNA polymerase delta (pol3-t). Mol Cell Biol 18:2779-2788.
Kondo T, Matsumoto K, Sugimoto K (1999) Role of a complex containing Rad17, Mec3, and Ddc1 in the yeast DNA damage checkpoint pathway. Molecular and cellular biology 19:1136-1143.
Krontiris TG (1995) Minisatellites and human disease. Science 269:1682-1683.
Lafreniere RG, Rochefort DL, Chretien N, Rommens JM, Cochius JI, Kalviainen R, Nousiainen U, Patry G, Farrell K, Soderfeldt B, Federico A, Hale BR, Cossio OH, Sorensen T, Pouliot MA, Kmiec T, Uldall P, Janszky J, Pranzatelli MR, Andermann F, Andermann E, Rouleau GA (1997) Unstable insertion in the 5' flanking region of the cystatin B gene is the most common mutation in progressive myoclonus epilepsy type 1, EPM1. Nat Genet 15:298-302.
Lechner J, Carbon J (1991) A 240 kd multisubunit protein complex, CBF3, is a major component of the budding yeast centromere. Cell 64:717-725.
Legendre M, Pochet N, Pak T, Verstrepen KJ (2007) Sequence-based estimation of minisatellite and microsatellite repeat variability. Genome Res 17:1787-1796.

Leroy C, Mann C, Marsolier MC (2001) Silent repair accounts for cell cycle specificity in the signaling of oxidative DNA lesions. The EMBO journal 20:2896-2906.
Levin DE, Fields FO, Kunisawa R, Bishop JM, Thorner J (1990) A candidate protein kinase C gene, PKC1, is required for the S. cerevisiae cell cycle. Cell 62:213-224.
Lew DJ, Burke DJ (2003) The spindle assembly and spindle position checkpoints. Annual review of genetics 37:251-282.
Li R, Murray AW (1991) Feedback control of mitosis in budding yeast. Cell 66:519-531.
Li Z, Vizeacoumar FJ, Bahr S, Li J, Warringer J, Vizeacoumar FS, Min R, Vandersluis B, Bellay J, Devit M, Fleming JA, Stephens A, Haase J, Lin ZY, Baryshnikova A, Lu H, Yan Z, Jin K, Barker S, Datti A, Giaever G, Nislow C, Bulawa C, Myers CL, Costanzo M, Gingras AC, Zhang Z, Blomberg A, Bloom K, Andrews B, Boone C (2011) Systematic exploration of essential yeast gene function with temperature-sensitive mutants. Nat Biotechnol 29:361-367.
Liu Y, Barlowe C (2002) Analysis of Sec22p in endoplasmic reticulum/Golgi transport reveals cellular redundancy in SNARE protein function. Mol Biol Cell 13:3314-3324.
Liu Y, Elf SE, Asai T, Miyata Y, Liu Y, Sashida G, Huang G, Di Giandomenico S, Koff A, Nimer SD (2009a) The p53 tumor suppressor protein is a critical regulator of hematopoietic stem cell behavior. Cell Cycle 8:3120-3124.
Liu Y, Elf SE, Miyata Y, Sashida G, Liu Y, Huang G, Di Giandomenico S, Lee JM, Deblasio A, Menendez S, Antipin J, Reva B, Koff A, Nimer SD (2009b) p53 regulates hematopoietic stem cell quiescence. Cell stem cell 4:37-48.
Liu Y, Kao HI, Bambara RA (2004a) Flap endonuclease 1: a central component of DNA metabolism. Annu Rev Biochem 73:589-615.
Liu Y, Zhang H, Veeraraghavan J, Bambara RA, Freudenreich CH (2004b) Saccharomyces cerevisiae flap endonuclease 1 uses flap equilibration to maintain triplet repeat stability. Mol Cell Biol 24:4049-4064.
Lobo JC, Torres JP, Fouque D, Mafra D (2010) Zinc deficiency in chronic kidney disease: is there a relationship with adipose tissue and atherosclerosis? Biological trace element research 135:16-21.
Longerich S, Galloway AM, Harris RS, Wong C, Rosenberg SM (1995) Adaptive mutation sequences reproduced by mismatch repair deficiency. Proc Natl Acad Sci U S A 92:12017-12020.
Longhese MP, Clerici M, Lucchini G (2003) The S-phase checkpoint and its regulation in Saccharomyces cerevisiae. Mutation research 532:41-58.
Longtine MS, McKenzie A, 3rd, Demarini DJ, Shah NG, Wach A, Brachat A, Philippsen P, Pringle JR (1998) Additional modules for versatile and economical PCR-based gene deletion and modification in Saccharomyces cerevisiae. Yeast 14:953-961.
Lopes J, Debrauwere H, Buard J, Nicolas A (2002) Instability of the human minisatellite CEB1 in rad27Delta and dna2-1 replication-deficient yeast cells. EMBO J 21:3201-3211.
Lopes J, Ribeyre C, Nicolas A (2006) Complex minisatellite rearrangements generated in the total or partial absence of Rad27/hFEN1 activity occur in a single generation

and are Rad51 and Rad52 dependent. Molecular and cellular biology 26:6675-6689.
Lou H, Komata M, Katou Y, Guan Z, Reis CC, Budd M, Shirahige K, Campbell JL (2008) Mrc1 and DNA polymerase epsilon function together in linking DNA replication and the S phase checkpoint. Mol Cell 32:106-117.
Lukusa T, Fryns JP (2008) Human chromosome fragility. Biochim Biophys Acta 1779:3-16.
MacDiarmid CW, Gaither LA, Eide D (2000) Zinc transporters that regulate vacuolar zinc storage in Saccharomyces cerevisiae. EMBO J 19:2845-2855.
Majka J, Burgers PM (2003) Yeast Rad17/Mec3/Ddc1: a sliding clamp for the DNA damage checkpoint. Proceedings of the National Academy of Sciences of the United States of America 100:2249-2254.
Maleki S, Cederberg H, Rannug U (2002) The human minisatellites MS1, MS32, MS205 and CEB1 integrated into the yeast genome exhibit different degrees of mitotic instability but are all stabilised by RAD27. Curr Genet 41:333-341.
Mankodi A, Takahashi MP, Jiang H, Beck CL, Bowers WJ, Moxley RT, Cannon SC, Thornton CA (2002) Expanded CUG repeats trigger aberrant splicing of ClC-1 chloride channel pre-mRNA and hyperexcitability of skeletal muscle in myotonic dystrophy. Mol Cell 10:35-44.
Marsischky GT, Filosi N, Kane MF, Kolodner R (1996) Redundancy of Saccharomyces cerevisiae MSH3 and MSH6 in MSH2-dependent mismatch repair. Genes Dev 10:407-420.
Marti TM, Kunz C, Fleck O (2002) DNA mismatch repair and mutation avoidance pathways. J Cell Physiol 191:28-41.
Meiling-Wesse K, Barth H, Voss C, Barmark G, Muren E, Ronne H, Thumm M (2002) Yeast Mon1p/Aut12p functions in vacuolar fusion of autophagosomes and cvt-vesicles. FEBS Lett 530:174-180.
Miller JW, Urbinati CR, Teng-Umnuay P, Stenberg MG, Byrne BJ, Thornton CA, Swanson MS (2000) Recruitment of human muscleblind proteins to (CUG)(n) expansions associated with myotonic dystrophy. EMBO J 19:4439-4448.
Monckton DG, Neumann R, Guram T, Fretwell N, Tamaki K, MacLeod A, Jeffreys AJ (1994) Minisatellite mutation rate variation associated with a flanking DNA sequence polymorphism. Nat Genet 8:162-170.
Montelone BA, Koelliker KJ (1995) Interactions among mutations affecting spontaneous mutation, mitotic recombination, and DNA repair in yeast. Curr Genet 27:102-109.
Morrow DM, Tagle DA, Shiloh Y, Collins FS, Hieter P (1995) TEL1, an S. cerevisiae homolog of the human gene mutated in ataxia telangiectasia, is functionally related to the yeast checkpoint gene MEC1. Cell 82:831-840.
Napierala M, Krzyzosiak WJ (1997) CUG repeats present in myotonin kinase RNA form metastable "slippery" hairpins. J Biol Chem 272:31079-31085.
Navadgi-Patil VM, Burgers PM (2009) A tale of two tails: activation of DNA damage checkpoint kinase Mec1/ATR by the 9-1-1 clamp and by Dpb11/TopBP1. DNA repair 8:996-1003.

Naylor ML, Li JM, Osborn AJ, Elledge SJ (2009) Mrc1 phosphorylation in response to DNA replication stress is required for Mec1 accumulation at the stalled fork. Proc Natl Acad Sci U S A 106:12765-12770.
Ni L, Snyder M (2001) A genomic study of the bipolar bud site selection pattern in Saccharomyces cerevisiae. Mol Biol Cell 12:2147-2170.
Nicolaides NC, Papadopoulos N, Liu B, Wei YF, Carter KC, Ruben SM, Rosen CA, Haseltine WA, Fleischmann RD, Fraser CM, et al. (1994) Mutations of two PMS homologues in hereditary nonpolyposis colon cancer. Nature 371:75-80.
Nitiss J, Wang JC (1988) DNA topoisomerase-targeting antitumor drugs can be studied in yeast. Proc Natl Acad Sci U S A 85:7501-7505.
Noskov V, Maki S, Kawasaki Y, Leem SH, Ono B, Araki H, Pavlov Y, Sugino A (1994) The RFC2 gene encoding a subunit of replication factor C of Saccharomyces cerevisiae. Nucleic Acids Res 22:1527-1535.
Ohya T, Maki S, Kawasaki Y, Sugino A (2000) Structure and function of the fourth subunit (Dpb4p) of DNA polymerase epsilon in Saccharomyces cerevisiae. Nucleic Acids Res 28:3846-3852.
Orgel LE, Crick FH (1980) Selfish DNA: the ultimate parasite. Nature 284:604-607.
Osborn AJ, Elledge SJ (2003) Mrc1 is a replication fork component whose phosphorylation in response to DNA replication stress activates Rad53. Genes Dev 17:1755-1767.
Paciotti V, Lucchini G, Plevani P, Longhese MP (1998) Mec1p is essential for phosphorylation of the yeast DNA damage checkpoint protein Ddc1p, which physically interacts with Mec3p. The EMBO journal 17:4199-4209.
Palmieri L, Agrimi G, Runswick MJ, Fearnley IM, Palmieri F, Walker JE (2001) Identification in Saccharomyces cerevisiae of two isoforms of a novel mitochondrial transporter for 2-oxoadipate and 2-oxoglutarate. J Biol Chem 276:1916-1922.
Pawar V, Jingjing L, Patel N, Kaur N, Doetsch PW, Shadel GS, Zhang H, Siede W (2009) Checkpoint kinase phosphorylation in response to endogenous oxidative DNA damage in repair-deficient stationary-phase Saccharomyces cerevisiae. Mech Ageing Dev 130:501-508.
Petukhova G, Stratton SA, Sung P (1999) Single strand DNA binding and annealing activities in the yeast recombination factor Rad59. J Biol Chem 274:33839-33842.
Pinsky BA, Kung C, Shokat KM, Biggins S (2006) The Ipl1-Aurora protein kinase activates the spindle checkpoint by creating unattached kinetochores. Nature cell biology 8:78-83.
Planta RJ, Mager WH (1998) The list of cytoplasmic ribosomal proteins of Saccharomyces cerevisiae. Yeast 14:471-477.
Prakash S, Prakash L (1977) Increased spontaneous mitotic segregation in MMS-sensitive mutants of Saccharomyces cerevisiae. Genetics 87:229-236.
Prolla TA, Christie DM, Liskay RM (1994a) Dual requirement in yeast DNA mismatch repair for MLH1 and PMS1, two homologs of the bacterial mutL gene. Mol Cell Biol 14:407-415.

Prolla TA, Pang Q, Alani E, Kolodner RD, Liskay RM (1994b) MLH1, PMS1, and MSH2 interactions during the initiation of DNA mismatch repair in yeast. Science 265:1091-1093.
Pujol N, Bonet C, Vilella F, Petkova MI, Mozo-Villarias A, de la Torre-Ruiz MA (2009) Two proteins from Saccharomyces cerevisiae: Pfy1 and Pkc1, play a dual role in activating actin polymerization and in increasing cell viability in the adaptive response to oxidative stress. FEMS yeast research 9:1196-1207.
Putnam CD, Jaehnig EJ, Kolodner RD (2009) Perspectives on the DNA damage and replication checkpoint responses in Saccharomyces cerevisiae. DNA repair 8:974-982.
Raveendranathan M, Chattopadhyay S, Bolon YT, Haworth J, Clarke DJ, Bielinsky AK (2006) Genome-wide replication profiles of S-phase checkpoint mutants reveal fragile sites in yeast. EMBO J 25:3627-3639.
Rebhi L, Omezzine A, Kchok K, Belkahla R, Ben Hadjmbarek I, Rejeb J, Ben Rejeb N, Nabli N, Bibi A, Massoud T, Abdelaziz A, Boughzala E, Bouslama A (2008) 5' ins/del and 3' VNTR polymorphisms in the apolipoprotein B gene in relation to lipids and coronary artery disease. Clin Chem Lab Med 46:329-334.
Resnick MA, Setlow JK (1972) Repair of pyrimidine dimer damage induced in yeast by ultraviolet light. J Bacteriol 109:979-986.
Reya T, Morrison SJ, Clarke MF, Weissman IL (2001) Stem cells, cancer, and cancer stem cells. Nature 414:105-111.
Ribeyre C, Lopes J, Boule JB, Piazza A, Guedin A, Zakian VA, Mergny JL, Nicolas A (2009) The yeast Pif1 helicase prevents genomic instability caused by G-quadruplex-forming CEB1 sequences in vivo. PLoS Genet 5:e1000475.
Richard GF, Kerrest A, Dujon B (2008) Comparative genomics and molecular dynamics of DNA repeats in eukaryotes. Microbiol Mol Biol Rev 72:686-727.
Richards RI, Sutherland GR (1994) Simple repeat DNA is not replicated simply. Nat Genet 6:114-116.
Ricke RM, Bielinsky AK (2006) A conserved Hsp10-like domain in Mcm10 is required to stabilize the catalytic subunit of DNA polymerase-alpha in budding yeast. J Biol Chem 281:18414-18425.
Rosell R, Calvo R, Sanchez JJ, Maurel J, Guillot M, Monzo M, Nunez L, Barnadas A (1999) Genetic susceptibility associated with rare HRAS1 variable number of tandem repeats alleles in Spanish non-small cell lung cancer patients. Clin Cancer Res 5:1849-1854.
Rosenberg SM (2001) Evolving responsively: adaptive mutation. Nature reviews Genetics 2:504-515.
Royle NJ, Clarkson RE, Wong Z, Jeffreys AJ (1988) Clustering of hypervariable minisatellites in the proterminal regions of human autosomes. Genomics 3:352-360.
Ruchaud S, Carmena M, Earnshaw WC (2007) Chromosomal passengers: conducting cell division. Nature reviews Molecular cell biology 8:798-812.

Sanchez NS, Pearce DA, Cardillo TS, Uribe S, Sherman F (2001) Requirements of Cyc2p and the porin, Por1p, for ionic stability and mitochondrial integrity in Saccharomyces cerevisiae. Arch Biochem Biophys 392:326-332.
Sanchez Y, Bachant J, Wang H, Hu F, Liu D, Tetzlaff M, Elledge SJ (1999) Control of the DNA damage checkpoint by chk1 and rad53 protein kinases through distinct mechanisms. Science (New York, NY 286:1166-1171.
Sanchez Y, Desany BA, Jones WJ, Liu Q, Wang B, Elledge SJ (1996) Regulation of RAD53 by the ATM-like kinases MEC1 and TEL1 in yeast cell cycle checkpoint pathways. Science 271:357-360.
Schar P, Herrmann G, Daly G, Lindahl T (1997) A newly identified DNA ligase of Saccharomyces cerevisiae involved in RAD52-independent repair of DNA double-strand breaks. Gene Dev 11:1912-1924.
Schlotterer C, Tautz D (1992) Slippage synthesis of simple sequence DNA. Nucleic Acids Res 20:211-215.
Sercin O, Kemp MG (2011) Characterization of functional domains in human Claspin. Cell Cycle 10:1599-1606.
Sheng JQ, Chan TL, Chan YW, Huang JS, Chen JG, Zhang MZ, Guo XL, Mu H, Chan AS, Li SR, Yuen ST, Leung SY (2006) Microsatellite instability and novel mismatch repair gene mutations in northern Chinese population with hereditary non-polyposis colorectal cancer. Chinese journal of digestive diseases 7:197-205.
Shivji MK, Podust VN, Hubscher U, Wood RD (1995) Nucleotide excision repair DNA synthesis by DNA polymerase epsilon in the presence of PCNA, RFC, and RPA. Biochemistry 34:5011-5017.
Sia EA, Kokoska RJ, Dominska M, Greenwell P, Petes TD (1997) Microsatellite instability in yeast: dependence on repeat unit size and DNA mismatch repair genes. Mol Cell Biol 17:2851-2858.
Slater ML (1973) Effect of reversible inhibition of deoxyribonucleic acid synthesis on the yeast cell cycle. J Bacteriol 113:263-270.
Smirnov MN, Smirnov VN, Budowsky EI, Inge-Vechtomov SG, Serebrjakov NG (1967) Red pigment of adenine-deficient yeast Saccharomyces cerevisiae. Biochem Biophys Res Commun 27:299-304.
Soustelle C, Vedel M, Kolodner R, Nicolas A (2002) Replication protein A is required for meiotic recombination in Saccharomyces cerevisiae. Genetics 161:535-547.
Spandidos DA, Holmes L (1987) Transcriptional enhancer activity in the variable tandem repeat DNA sequence downstream of the human Ha-ras 1 gene. FEBS Lett 218:41-46.
Stone JR, Yang S (2006) Hydrogen peroxide: a signaling messenger. Antioxid Redox Signal 8:243-270.
Strahl T, Thorner J (2007) Synthesis and function of membrane phosphoinositides in budding yeast, Saccharomyces cerevisiae. Biochim Biophys Acta 1771:353-404.
Strand M, Earley MC, Crouse GF, Petes TD (1995) Mutations in the MSH3 gene preferentially lead to deletions within tracts of simple repetitive DNA in Saccharomyces cerevisiae. Proc Natl Acad Sci U S A 92:10418-10421.

Strand M, Prolla TA, Liskay RM, Petes TD (1993) Destabilization of tracts of simple repetitive DNA in yeast by mutations affecting DNA mismatch repair. Nature 365:274-276.
Strathern JN, Shafer BK, McGill CB (1995) DNA synthesis errors associated with double-strand-break repair. Genetics 140:965-972.
Strunnikov AV, Kingsbury J, Koshland D (1995) CEP3 encodes a centromere protein of Saccharomyces cerevisiae. The Journal of cell biology 128:749-760.
Suda T, Arai F, Hirao A (2005) Hematopoietic stem cells and their niche. Trends Immunol 26:426-433.
Sugimoto K, Sakamoto Y, Takahashi O, Matsumoto K (1995) HYS2, an essential gene required for DNA replication in Saccharomyces cerevisiae. Nucleic Acids Res 23:3493-3500.
Symington LS (2002) Role of RAD52 epistasis group genes in homologous recombination and double-strand break repair. Microbiol Mol Biol Rev 66:630-670, table of contents.
Tautz D, Renz M (1984) Simple sequences are ubiquitous repetitive components of eukaryotic genomes. Nucleic Acids Res 12:4127-4138.
Tong AH, Boone C (2006) Synthetic genetic array analysis in Saccharomyces cerevisiae. Methods Mol Biol 313:171-192.
Tong AH, Evangelista M, Parsons AB, Xu H, Bader GD, Page N, Robinson M, Raghibizadeh S, Hogue CW, Bussey H, Andrews B, Tyers M, Boone C (2001) Systematic genetic analysis with ordered arrays of yeast deletion mutants. Science 294:2364-2368.
Torkko JM, Koivuranta KT, Miinalainen IJ, Yagi AI, Schmitz W, Kastaniotis AJ, Airenne TT, Gurvitz A, Hiltunen KJ (2001) Candida tropicalis Etr1p and Saccharomyces cerevisiae Ybr026p (Mrf1'p), 2-enoyl thioester reductases essential for mitochondrial respiratory competence. Mol Cell Biol 21:6243-6253.
Torres-Ramos CA, Prakash S, Prakash L (1997) Requirement of yeast DNA polymerase delta in post-replicational repair of UV-damaged DNA. J Biol Chem 272:25445-25448.
Trepicchio WL, Krontiris TG (1992) Members of the rel/NF-kappa B family of transcriptional regulatory proteins bind the HRAS1 minisatellite DNA sequence. Nucleic Acids Res 20:2427-2434.
Tseng HM, Tomkinson AE (2004) Processing and joining of DNA ends coordinated by interactions among Dnl4/Lif1, Pol4, and FEN-1. J Biol Chem 279:47580-47588.
Tsukuda T, Fleming AB, Nickoloff JA, Osley MA (2005) Chromatin remodelling at a DNA double-strand break site in Saccharomyces cerevisiae. Nature 438:379-383.
Turri MG, Cuin KA, Porter AC (1995) Characterisation of a novel minisatellite that provides multiple splice donor sites in an interferon-induced transcript. Nucleic Acids Res 23:1854-1861.
Umar A (2004) Lynch syndrome (HNPCC) and microsatellite instability. Disease markers 20:179-180.

Umezu K, Sugawara N, Chen C, Haber JE, Kolodner RD (1998) Genetic analysis of yeast RPA1 reveals its multiple functions in DNA metabolism. Genetics 148:989-1005.
Uno S, Masai H (2011) Efficient expression and purification of human replication fork-stabilizing factor, Claspin, from mammalian cells: DNA-binding activity and novel protein interactions. Genes Cells 16:842-856.
Vanoli F, Fumasoni M, Szakal B, Maloisel L, Branzei D (2010) Replication and recombination factors contributing to recombination-dependent bypass of DNA lesions by template switch. PLoS Genet 6:e1001205.
Vega A, Sobrido MJ, Ruiz-Ponte C, Barros F, Carracedo A (2001) Rare HRAS1 alleles are a risk factor for the development of brain tumors. Cancer 92:2920-2926.
Vergnaud G, Denoeud F (2000) Minisatellites: mutability and genome architecture. Genome Res 10:899-907.
Vialard JE, Gilbert CS, Green CM, Lowndes NF (1998) The budding yeast Rad9 checkpoint protein is subjected to Mec1/Tel1-dependent hyperphosphorylation and interacts with Rad53 after DNA damage. The EMBO journal 17:5679-5688.
Videla LA, Fernandez V (1988) Biochemical aspects of cellular oxidative stress. Arch Biol Med Exp (Santiago) 21:85-92.
Villarroya M, Perez-Roger I, Macian F, Armengod ME (1998) Stationary phase induction of dnaN and recF, two genes of Escherichia coli involved in DNA replication and repair. EMBO J 17:1829-1837.
Virtaneva K, D'Amato E, Miao J, Koskiniemi M, Norio R, Avanzini G, Franceschetti S, Michelucci R, Tassinari CA, Omer S, Pennacchio LA, Myers RM, Dieguez-Lucena JL, Krahe R, de la Chapelle A, Lehesjoki AE (1997) Unstable minisatellite expansion causing recessively inherited myoclonus epilepsy, EPM1. Nat Genet 15:393-396.
Wang CW, Stromhaug PE, Shima J, Klionsky DJ (2002) The Ccz1-Mon1 protein complex is required for the late step of multiple vacuole delivery pathways. J Biol Chem 277:47917-47927.
Wang Z, Wu X, Friedberg EC (1993) DNA repair synthesis during base excision repair in vitro is catalyzed by DNA polymerase epsilon and is influenced by DNA polymerases alpha and delta in Saccharomyces cerevisiae. Mol Cell Biol 13:1051-1058.
Weinert TA, Kiser GL, Hartwell LH (1994) Mitotic checkpoint genes in budding yeast and the dependence of mitosis on DNA replication and repair. Genes Dev 8:652-665.
Weitzel JN, Ding S, Larson GP, Nelson RA, Goodman A, Grendys EC, Ball HG, Krontiris TG (2000) The HRAS1 minisatellite locus and risk of ovarian cancer. Cancer Res 60:259-261.
Werner-Washburne M, Braun E, Johnston GC, Singer RA (1993) Stationary phase in the yeast Saccharomyces cerevisiae. Microbiol Rev 57:383-401.
Werner-Washburne M, Roy S, Davidson GS (2012) Aging and the Survival of Quiescent and Non-quiescent Cells in Yeast Stationary-Phase Cultures. Sub-cellular biochemistry 57:123-143.

Wilson TE, Grawunder U, Lieber MR (1997) Yeast DNA ligase IV mediates non-homologous DNA end joining. Nature 388:495-498.
Wiltzius JJ, Hohl M, Fleming JC, Petrini JH (2005) The Rad50 hook domain is a critical determinant of Mre11 complex functions. Nat Struct Mol Biol 12:403-407.
Wintersberger U, Karwan A (1987) Retardation of cell cycle progression in yeast cells recovering from DNA damage: a study at the single cell level. Mol Gen Genet 207:320-327.
Wu JH, Chern MS, Lo SK, Wen MS, Kao JT (1996) Apolipoprotein B 3' hypervariable repeat genotype: association with plasma lipid concentration, coronary artery disease, and other restriction fragment polymorphisms. Clin Chem 42:927-932.
Wu X, Wilson TE, Lieber MR (1999) A role for FEN-1 in nonhomologous DNA end joining: the order of strand annealing and nucleolytic processing events. Proc Natl Acad Sci U S A 96:1303-1308.
Yang B, Chan RC, Jing J, Li T, Sham P, Chen RY (2007) A meta-analysis of association studies between the 10-repeat allele of a VNTR polymorphism in the 3'-UTR of dopamine transporter gene and attention deficit hyperactivity disorder. Am J Med Genet B Neuropsychiatr Genet 144B:541-550.
Yao N, Coryell L, Zhang D, Georgescu RE, Finkelstein J, Coman MM, Hingorani MM, O'Donnell M (2003) Replication factor C clamp loader subunit arrangement within the circular pentamer and its attachment points to proliferating cell nuclear antigen. J Biol Chem 278:50744-50753.
Yoshizawa-Sugata N, Masai H (2007) Human Tim/Timeless-interacting protein, Tipin, is required for efficient progression of S phase and DNA replication checkpoint. J Biol Chem 282:2729-2740.
Yu S, Mangelsdorf M, Hewett D, Hobson L, Baker E, Eyre HJ, Lapsys N, Le Paslier D, Doggett NA, Sutherland GR, Richards RI (1997) Human chromosomal fragile site FRA16B is an amplified AT-rich minisatellite repeat. Cell 88:367-374.
Zhao H, Eide D (1996) The yeast ZRT1 gene encodes the zinc transporter protein of a high-affinity uptake system induced by zinc limitation. Proc Natl Acad Sci U S A 93:2454-2458.
Zhao H, Eide DJ (1997) Zap1p, a metalloregulatory protein involved in zinc-responsive transcriptional regulation in Saccharomyces cerevisiae. Mol Cell Biol 17:5044-5052.
Zhao X, Chabes A, Domkin V, Thelander L, Rothstein R (2001) The ribonucleotide reductase inhibitor Sml1 is a new target of the Mec1/Rad53 kinase cascade during growth and in response to DNA damage. EMBO J 20:3544-3553.
Zhao X, Muller EG, Rothstein R (1998) A suppressor of two essential checkpoint genes identifies a novel protein that negatively affects dNTP pools. Mol Cell 2:329-340.
Zhao X, Rothstein R (2002) The Dun1 checkpoint kinase phosphorylates and regulates the ribonucleotide reductase inhibitor Sml1. Proc Natl Acad Sci U S A 99:3746-3751.

Chapter IX

Appendices

The Effect of DNA Damaging Agents and UV

on Stationary Phase Minisatellite Stability

Background

In Chapter 2, we described our lab's unique color segregation assay for detecting alterations that occurred within the minisatellite allele *ade2-min3* (Kelly et al., 2007, Kelly et al., 2011, Kelly et al., 2012). A novel colony phenotype known as blebbing was indicative of minisatellite alterations that had occurred within stationary phase cells. In Chapter 2 and Chapter 3, we identified and characterized several genes that when mutated, gave rise to strong blebbing phenotypes. A common function of each gene product is the direct or indirect prevention of single-stranded DNA (ssDNA), a known precursor to genomic instability. We hypothesize that minisatellite alterations occurring in stationary phase cells are the result of unrepaired or incorrectly repaired DNA damage sites that lead to the accumulation of ssDNA. Thus, an ongoing goal is to determine what, if any, type of DNA damage contributes to minisatellite alterations. Here, we analyzed the effect of various DNA damaging reagents and UV exposure on stationary phase minisatellite stability in strains bearing the *ade2-min3* allele. This analysis was performed on the following strains discussed in Chapters 2 and 3: DTK271 (wild-type, WT), DTK878 (*zrt1*Δ), DTK1088 (*end3*Δ), DTK1170 (*rad53-1*), DTK1199 (*rad27*Δ), DTK1392 (*mrc1*Δ), DTK1630 ($mrc1^{aq}$), DTK1683 (*mrc1-C14*) and DTK1766 ($mrc1^{aq}$-*C14*).

Materials and Methods

Solid YPD media was prepared according to (Guthrie and Fink, 1991). For the stationary phase disk assay, the following concentrations of DNA damaging reagents

were used: 1) camptothecin = 0.05mM and 0.10mM; 2) ethyl methanesulfonate (EMS) = 2% and 4%; 3) methyl methanesulfonate (MMS) = 0.5% and 1%; 4) hydroxyurea (HU) = 1.0M and 2.5M; 5) UV = 5 seconds and 10 seconds. Yeast Strains used for this experiment were: DTK271 (wild-type (WT)), DTK878 (*zrt1*Δ), DTK1056 (*rad50*Δ), DTK1088 (*end3*Δ), DTK1170 (*rad53-1*), DTK1199 (*rad27*Δ), DTK1392 (*mrc1*Δ), DTK1630 ($mrc1^{aq}$), DTK1683 (*mrc1-C14*) and DTK1766 ($mrc1^{aq}$-*C14*). Construction for these strains is described in Chapter VII: Materials and Methods.

DNA Damage Reagent Stationary Phase Disk Assay

Prior to this assay, control experiments were performed to determine the concentrations of DNA damaging reagents to use for this assay. In brief, DTK271 (WT) and compound sensitive strains DTK1056 (*rad50*Δ) or DTK1170 (*rad53-1*) were exposed to each compound listed above at a range of 0x, 1x, 2x, 10x, or 50x the published concentrations of each compound using the disk assay methods listed below. Bleb quantification and cell viability assays were performed as list below. Concentrations of each reagent were chosen if the reagent affected the blebbing phenotype and did not affect cell lethality.

All yeast strains used for this assay were streaked onto solid YPD media and incubated at 30°C for 48 hours. A single red colony was used to inoculate 5mL of liquid YPD media. Cultures were incubated at 30°C for 4 hours with agitation. Appropriate dilutions of each culture were plated onto solid YPD media using a modified lid that prevented cells from being spread onto the very center of the plate. The cell free zone

was circular in shape and approximately 1.9cm in diameter. The plates were then incubated at 30°C for 2 days after which 3/4 inch filter paper disks (Fischer Scientific) soaked in the specified DNA damaging reagent were added to the cell free zone in the center of the plate. For UV treatment, cells were exposed to UV light for the time indicated above. The colonies were then left at RT for 6 days. Blebs were then counted on approximately 30 - 50 colonies located within a diameter of 1.4cm with respect to the filter disk. Colonies ranging from 1.26 to 1.32mm in diameter were included in the analysis. This experiment was repeated 3 independent times for a total of at least 100 individual colonies. We calculated the average number of blebs/colony as well as the 95% CI for each strain. Non-overlapping 95% CI's between strains was indicative of significantly different levels of blebbing. When applicable, a *rad50*Δ strain (known to be sensitive to most DNA damaging compounds) was used as a control.

Cell Viability Assay

To determine the cell viability of colonies exposed to the various DNA damaging reagents, we performed FACS analysis on whole colonies using propidium iodide (PI) to identify dead cells. At least 3 whole colonies analyzed for bleb quantification and lying closest to the filter disk were isolated, resuspended in a solution of 1mL of 1X phosphate buffered saline (PBS) and 1.5µL of 10X PI and then sonicated. FACS was performed on the instrument BD FACSCalibur and data was analyzed using Flow Jo software. At least 5 independent colonies were analyzed for each strain. The average %PI labeled cells was calculated +/- standard deviation.

Results

For each strain and DNA damaging reagent, we performed the DNA Damage Reagent Stationary Phase Disk Assay described above. In brief, diluted cultures of each strain were plated onto YPD in such a way that the center of the plate was left free of cells. Strains were then grown until colonies had reached the end of the diauxic shift or had exited the diauxic shift. At this point, a filter disk containing a DNA damaging reagent was added to the center of the plate or the plate was exposed to UV. After six days of exposure, blebs were counted on at least 100 individual colonies. The average number of blebs +/- the 95% confidence interval (CI) was then calculated for each strain and compound. Cell viability was monitored using a propidium iodide (PI)-dependent FACS cell sorting assay described below. The average number of blebs/colony as well as the % PI cell viability for each compound are depicted in the figures below.

Figure 9-1. Camptothecin: topoisomerase I inhibitor (Nitiss and Wang, 1988)

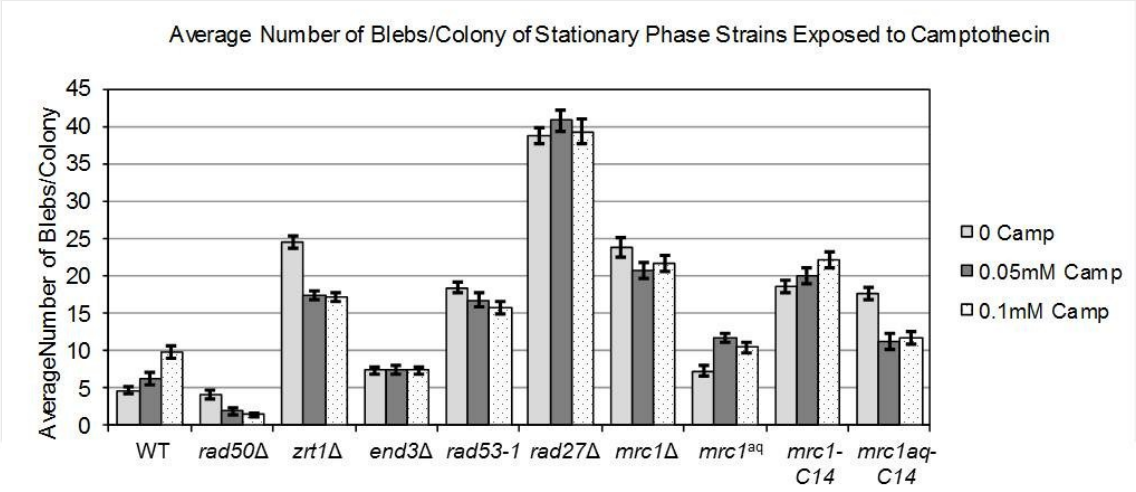

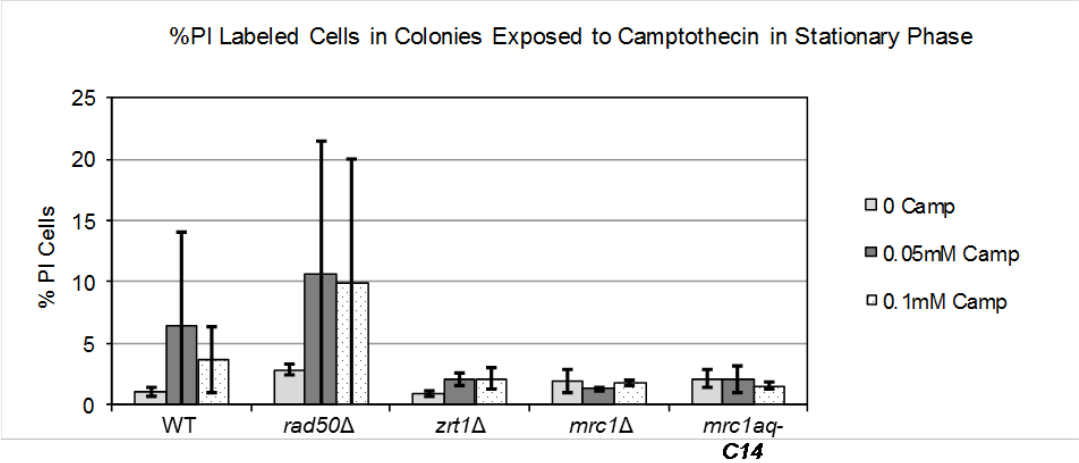

Figure 9-2. EMS: alkylating agent (Wintersberger and Karwan, 1987)

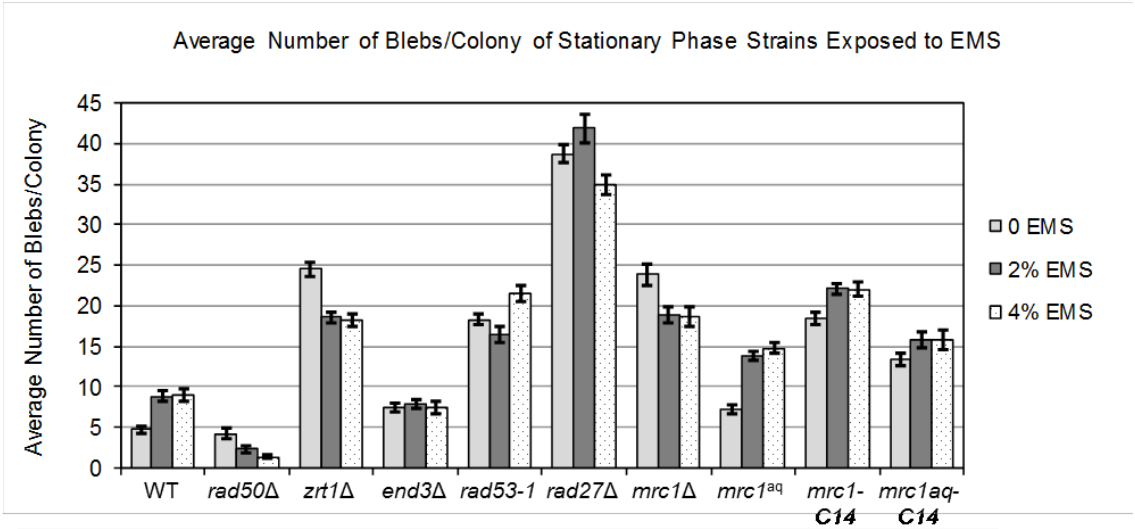

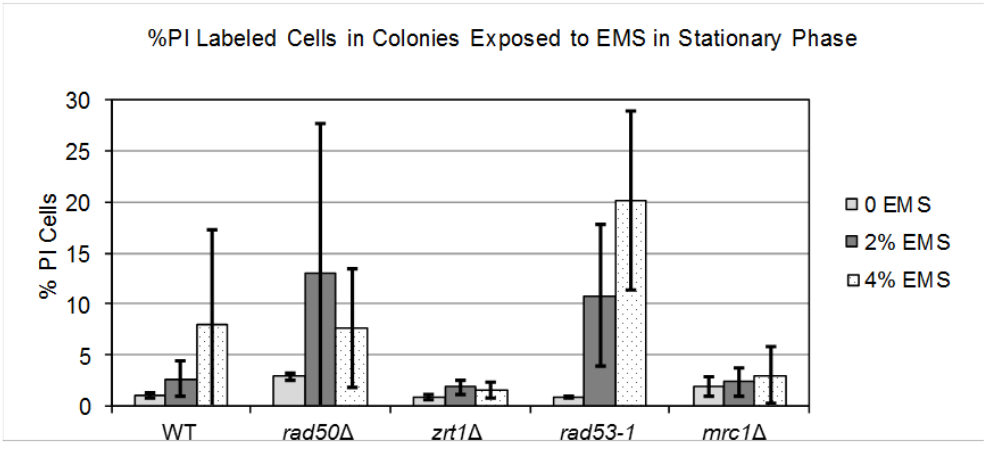

Figure 9-3. MMS: alkylating agent (Wintersberger and Karwan, 1987)

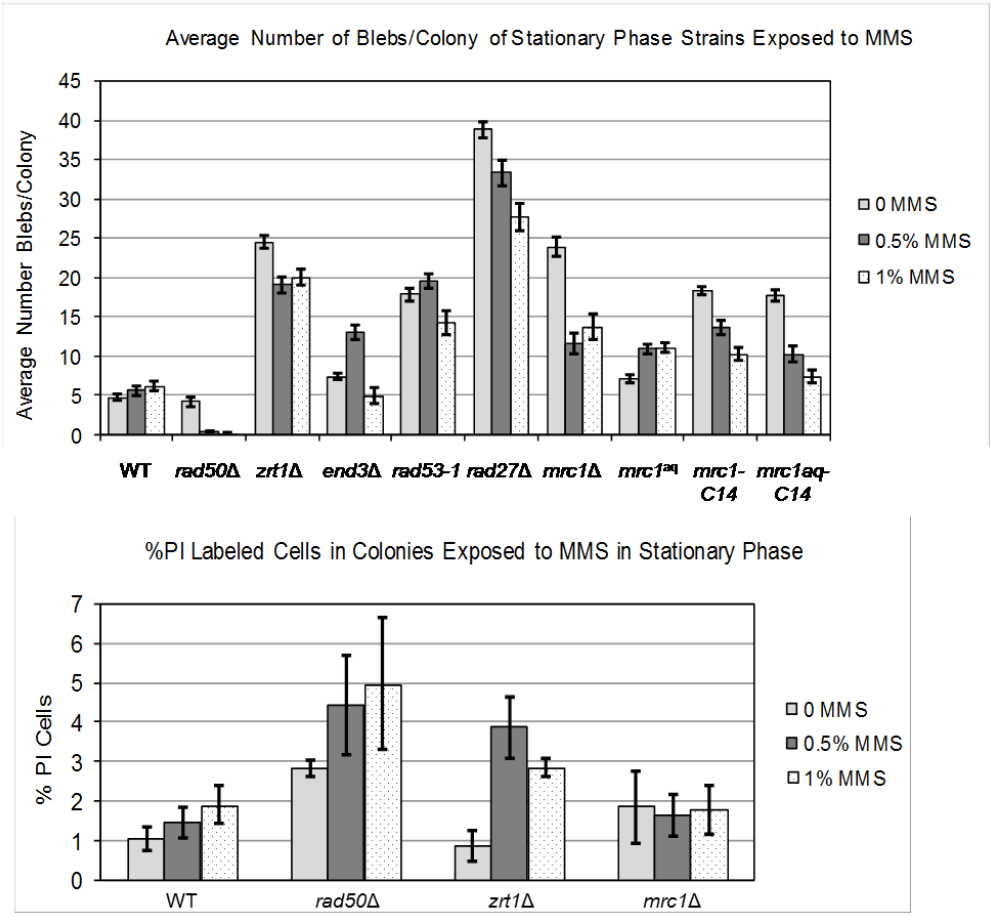

Figure 9-4. HU: arrests DNA replication (Slater, 1973)

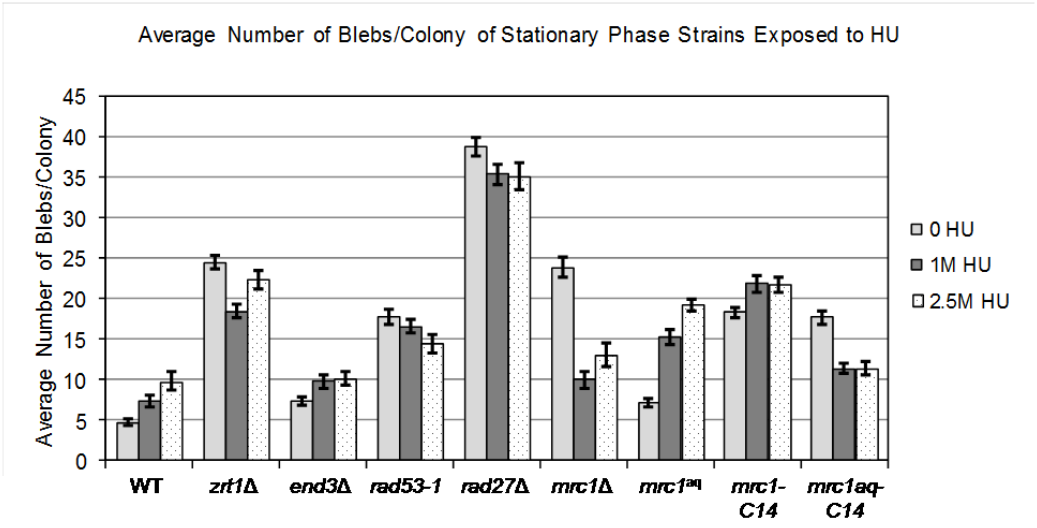

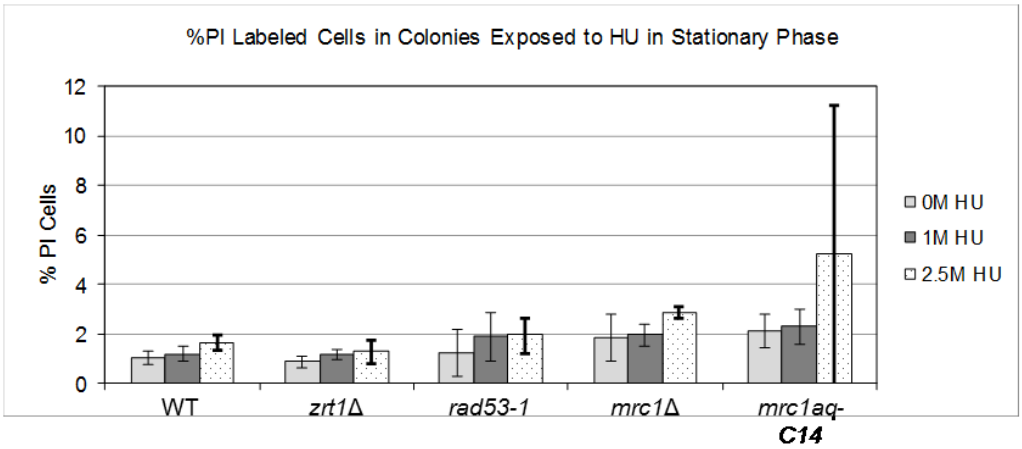

Figure 9-5. UV: creates pyrimidine dimers (Resnick and Setlow, 1972)

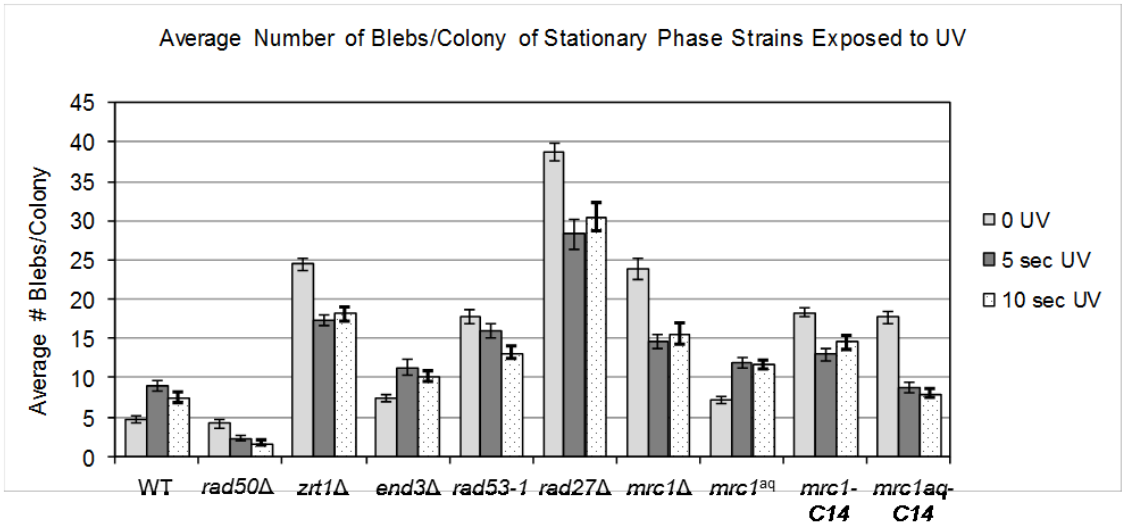

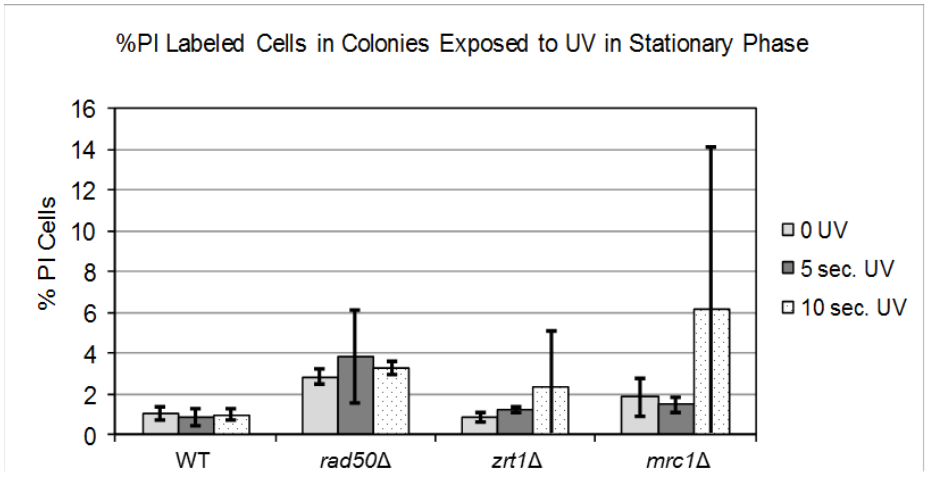

Conclusions and Future Experiments

With the exception of MMS, exposure to all other reagents as well as UV were found to result in a significant increase in the number of blebs produced by the WT strain (summary Table 9-1). These results indicate many types of DNA damage - topoisomerase I inhibition, DNA alkylation, fork stalling and dimer formation - increase *ade2-min3* minisatellite instability in WT stationary phase cells.

Interestingly, we observed a wide variety of phenotypes produced by several mutant strains upon exposure to each reagent at stationary phase (summary Table 9-1). For example, DTK878 (*zrt1*Δ) displayed a significant decrease in the number of blebs/colony after exposure to each type of DNA damaging reagent as well as UV. This effect was also found in strains DTK1199 (*rad27*Δ) and DTK1392 (*mrc1*Δ), with the exception of camptothecin. The decrease in blebbing did not correspond to a significant increase in cell death. (However, we note that *zrt1*Δ mutants are unexpectedly sensitive to MMS and will be following up on this finding.) Based upon our results, we predict that checkpoint activity and DNA repair functions are elevated in the mutant strains. Thus, exposure to various DNA damaging factors does not result in an increase in minisatellite instability as these cells are poised to readily repair and prevent genomic rearrangements.

As discussed in Chapter 3, one possibility of checkpoint activation in these strains could include the *RAD9*-dependent backup pathway that was found to suppress minisatellite instability in cells with aberrant Mrc1p function. However, minisatellite instability was significantly increase in the Mrc1p separation of function mutants DTK1630 ($mrc1_{AQ}$) and DTK1683 (*mrc1-C14*) for almost all DNA damaging reagents

suggesting that this may not be the case - at least with respect to *MRC1* mutant strains. We have yet to measure the cell lethality for the separation of function mutants exposed to each condition to determine if cell death is affecting minisatellite stability.

The strain DTK1088 (*end3*Δ) was one of the few strains that showed a significant increase in the level of blebbing upon exposure to almost all DNA damaging reagents and UV, with the exception of camptothecin and EMS. We have recently demonstrated that DTK1088 produces a high level of reactive oxygen species (ROS) (Kelly et al., 2012). It is possible that the level of damage and genomic instability arising as a result of intracellular ROS is compounded when cells are exposed to additional sources of DNA damage. This could, in effect, overload cellular repair mechanisms resulting in an increase in minisatellite instability. We have recently shown that ROS are greatly reduced in an *end3*Δ *ras2*Δ double mutant (Kelly et al., 2012). *RAS2* encodes for GTP-binding protein involved in stress response (Kataoka et al., 1984). To determine if the increased levels of ROS act synergistically with DNA damaging compounds, it would be interesting to study the level of blebbing produce by the *end3*Δ *ras2*Δ strain after exposure to each DNA damaging compound and UV.

Each reagent and UV exposure we analyzed had an effect on DNA replication, typically through means of fork stalling. Therefore, we plan to investigate the effect of the double strain break and single strand nick - inducing compound Phleomycin (Moore, 1989) on minisatellite stability using the methods described here. We would also like to perform this assay using compounds that induce ROS such as hydrogen peroxide (H_2O_2) (reviewed in (Stone and Yang, 2006)) or *tert*-Butyl hydroperoxide (TBHP) (reviewed in

(Videla and Fernandez, 1988). Based upon the relationship of each mutant and the production of intracellular ROS (described in Chapter 2), we predict that exposure of each strain to these compounds will greatly increase the level of minisatellite alterations. These future experiments will give us further insight into the types of DNA damage that could contribute to stationary phase genomic instability as well as help us to determine a potential cause of minisatellite alterations.

Table 9-1. Summary of Exposure to DNA Damaging Reagents and UV*

	0.05 mM Camp	0.1 mM Camp	2% EMS	4% EMS	0.5% MMS	1% MMS	1M HU	2.5M HU	5 sec. UV	10 sec. UV
DTK271 (WT)	+	+	+	+	NC	+	+	+	+	+
DTK1056 (*rad50*Δ)	-	-	-	-	-	-	NA	NA	-	-
DTK878 (*zrt1*Δ)	-	-	-	-	-	-	-	-	-	-
DTK1088 (*end3*Δ)	NC	NC	NC	NC	+	-	+	+	+	+
DTK1170 (*rad53-1*)	NC	-	NC	+	NC	-	NC	-	NC	-
DTK1199 (*rad27*Δ)	NC	NC	+	-	-	-	-	-	-	-
DTK1392 (*mrc1*Δ)	-	NC	-	-	-	-	-	-	-	-
DTK1630 (*mrc1^{aq}*)	+	+	+	+	+	+	+	+	+	+
DTK1683 (*mrc1-C14*)	NC	+	+	+	-	-	+	+	-	-
DTK1766 (*mrc1^{aq}-C14*)	-	-	+	+	-	-	-	-	-	-

* Camp = Camptothecin; (+) = Significant Increase in Blebbing; (-) = Significant Decrease in Blebbing; NC = No Change; NA = Not Applicable

Data Contribution

Dr. Katy Kelly constructed the strains DTK271, DTK878, DTK1056, DTK1088, DTK1170 and DTK1199. We are grateful to Pete Jauert who performed the cell viability PI assays for all strains described above.

References

Kataoka T, Powers S, McGill C, Fasano O, Strathern J, Broach J, Wigler M (1984) Genetic analysis of yeast RAS1 and RAS2 genes. Cell 37:437-445.

Kelly MK, Jauert PA, Jensen LE, Chan CL, Truong CS, Kirkpatrick DT (2007) Zinc regulates the stability of repetitive minisatellite DNA tracts during stationary phase. Genetics 177:2469-2479.

Kelly MK, Alver B, Kirkpatrick DT (2011) Minisatellite alterations in ZRT1 mutants occur via RAD52-dependent and RAD52-independent mechanisms in quiescent stationary phase yeast cells. DNA Repair (Amst) 10:556-566.

Kelly MK, Brosnan L, Jauert PA, Dunham MJ, Kirkpatrick DT (2012) Multiple Pathways Regulate Minisatellite Stability During Stationary Phase in Yeast. G3 (Bethesda) 2:1185-1195.

Moore CW (1989) Cleavage of cellular and extracellular Saccharomyces cerevisiae DNA by bleomycin and phleomycin. Cancer Res 49:6935-6940.

Nitiss J, Wang JC (1988) DNA topoisomerase-targeting antitumor drugs can be studied in yeast. Proc Natl Acad Sci U S A 85:7501-7505.

Resnick MA, Setlow JK (1972) Repair of pyrimidine dimer damage induced in yeast by ultraviolet light. J Bacteriol 109:979-986.

Slater ML (1973) Effect of reversible inhibition of deoxyribonucleic acid synthesis on the yeast cell cycle. J Bacteriol 113:263-270.

Stone JR, Yang S (2006) Hydrogen peroxide: a signaling messenger. Antioxid Redox Signal 8:243-270.

Videla LA, Fernandez V (1988) Biochemical aspects of cellular oxidative stress. Arch Biol Med Exp (Santiago) 21:85-92.

Wintersberger U, Karwan A (1987) Retardation of cell cycle progression in yeast cells recovering from DNA damage: a study at the single cell level. Mol Gen Genet 207:320-327.